Development of a Novel Multi-Parameter Monitoring Tool for Optimisation and Environmental Compliance of Anaerobic Digestion Technology

A submission presented in partial fulfilment of the requirements of the University of South Wales / Prifysgol De Cymru for the degree of Doctor of Philosophy

This research program was carried out in collaboration with Bryn Group

Ângela Patrícia Gonçalves de Oliveira

February 2021

Ysgoloriaethau Sgiliau Economi Gwybodaeth
Knowledge Economy Skills Scholarships

UNDEB EWROPEAIDD
EUROPEAN UNION

Llywodraeth Cymru
Welsh Government

Cronfa Gymdeithasol Ewrop
European Social Fund

Acknowledgements

Knowledge Economy Skills Scholarships (KESS) is a pan-Wales higher level skills initiative led by Bangor University on behalf of the HE sector in Wales. It is part funded by the Welsh Government's European Social Fund convergence programme for West Wales and the Valleys and co-sponsored by Bryn Group and the University of South Wales (Wales Centre of Excellence for Anaerobic Digestion). The GC-IMS unit used in this study was funded via the A4B KTC Project funded by the European Regional Development Funding 2010-2015 and the Welsh Government. Firstly, I would like to acknowledge my director of studies, Prof. Sandra Esteves for believing in me and in my skills. I will always be grateful to her for this significant opportunity. I also want to thank the other members of my supervision team, Dr. James Reed and Dr. Tim Patterson. Without this amazing team and all their support, this project could not have developed and move forward in the way it has. I want to manifest my gratitude to Dr. Alex Chong that worked with me during my research. Jennifer Price is an amazing company partner. I appreciate all her patience in replying to all my questions, her willingness to always help and the supply of process samples. I would like to acknowledge the technical support provided by Dr. Philemon Kumi, Dr. Savvas Savvas and Dr. Rajkumar Gangappa (supported by the ERDF/WG SMART Circle project). I would also like to thank Dr. Angelo Iannetelli, Michael Darke, Melanie Johnson, Ruggero Bellini, Sky Redhead, Ciaran Burns and Joanne Donnelly for all their help in my research and for sharing expertise elated to laboratory setups and analytical methodologies. In addition, thanks to Simon Thomas, Chamilka Thilakaratne, Dr. Amandeep Kaur, and the other SERC team members for all the happy moments that we have shared together. I would like to acknowledge the operation teams at various anaerobic digestion plants, which due to confidentiality agreements is not possible to be mentioned here. Related with GC-IMS, I want to show my appreciation for the help from Dr. Kristie Goggin, Sheri Murrell, Dr. Emma Brodrick (from Imspex) and Prof. Antony Davies. Your help has improved my research. Acknowledgements are also due to the KESS and GRO teams, in particular to Alison Evans, Clare Naylor, Llinos Spargo, Chloe Hexter, and Penny Dowdney who have supported me.

To my Portuguese friends in the UK, my initial group Tiago Luso, Dr. João Ramos, and Pedro Couto, and also to Rita Luso, Margarida Luso, Claudio Couto, Frederico Rocha, Pritt Jurimae, João Moutinho and Ana Oliveira. Also, all my USW friends, especially to Lukas Buchall, Eduard-Andrei Incze and Katherine Humphrey. To my Welsh family that is the best that I could have. Also, my old friend since 2009, Dr. Leo Popov for his help in securing my place here. And last but not the least, all my friends and my family back home for their support, especially Marisa Santos, Marta Cordeiro, Fernanda Ferreira, Nuno Abreu, Carla Sousa, Miguel Rocha, Joaninha Nogueira, Maria Rocha, Laurinda Oliveira, Isabel Maia Mendes, João Oliveira, and Iasmin Dabbeni. My love and deepest gratitude go to my lovely Jabr Massoud who demonstrated an immense patience during good and not so good times. Always pushing me to go to the lab or to write my thesis. To finish, my last acknowledgement goes to my very special ones: my mum and my sister. Your love keeps me following my dreams. Papá, where you are, you are my lovely star. Without you all, I could not be doing this.

Abstract

Anaerobic Digestion (AD) technology is used to treat a range of organic feedstocks (e.g. sewages, animal manures, food wastes, industrial organic wastes, and energy crops). It has seen a significant increase in deployment in the last two decades around the world. Due to the wide and sometimes difficult feedstocks range, the process can suffer from instability. Therefore, AD is particularly sensitive to process disturbances by irregular feeding with the potential for microbial toxicity from an accumulation of process intermediates or the presence of inhibitory compounds. This instability can lead to lower conversion efficiencies and reduced biogas production. Another challenge for AD plants is related to the fact that they can be a source of odours, which can lead to complaints from neighbours living close by or close to digestate land spreading areas. Except for gaseous measurements (CH_4, CO_2, H_2S and gas flow), AD plants typically rely on single off-line measurements for solids, total acids and buffering capacity. There is therefore a need to develop monitoring tools that are reliable, that can be used in real-time and that can provide multi-parameter identification and quantification to support plant operations. Besides monitoring strategies can enhance process performance, reduce odour complains, and support environmental compliance and evidence gathering. Here a novel approach using Gas Chromatography-Ion Mobility Spectrometry (GC-IMS) as a multi-parameter monitoring tool to measure volatile organic compounds (VOCs) has been investigated. To enable the development of the tool, a number of samples were sourced from a variety of full-scale AD plants, environmental samples and samples generated from laboratory operated digesters. The majority of samples were sourced from a novel full-scale AD plant that treats food wastes and cattle slurry and was occasionally co-fed with maize silage. The reactor design for this AD plant was based on a plug flow system with gas mixing. The AD plant was chosen due to the diversity of feedstocks, the presence of a homogenisation tank, the type of reactor enabling process intermediates to be sampled, and the existence of a pasteurisation process, and the storage of digestates. Work included the development of an analytical methodology using GC-IMS suitable for AD process related samples. It was the first time that GC-IMS was utilised within this biotechnology industry, except for siloxane measurements in the biogas. Parameters evaluated to optimise peak separations were flows for drift and carrier gas, time for headspace equilibrium, temperatures, and sample preparation (e.g. dilutions, addition of salts). The tool's performance was evaluated in terms of accuracy, precision, and reliability for identification of several compounds including terpenes, aromatics, ketones, volatile fatty acids (VFAs) and ammonia. The method error was lower than 5% in the repeatability study and 7% in the intermediate precision study. The analytical method was found to be highly robust and the system performed well. In addition to the identification of

several key volatiles for AD samples, a preliminary quantification performance was conducted. Initially a 2nd order polynomial equation was used for ammonia hydroxide, limonene, VFAs (acetic, propionic and butyric acids), and several ketones and later a Boltzmann function was used for ketones and limonene. Limits of detection and quantification (LOD and LOQ) were calculated for VFAs using a linear equation, between 0 – 500 mg/L. Acetic acid had the highest LOD of 13 mg/L and the LOQ of 40 mg/L. In the case of digestates, which can feature high concentrations of ammonia (in excess of 204 mg/L), an impact was felt in terms of carry-over of ammonia. This impact includes loss of the RIP, the creation of extra peaks for terpenes and ketones, and a reduction of detection for aromatics. A solution was established for minimizing ammonia impact, which was based on the addition of an acidifying salt, $NaHSO_4$, which proved to be efficient for concentrations lower than 2.5 g/L of ammonia. For greater ammonia concentrations, a sample dilution would be necessary with the addition of the salt. The tool has enabled the establishment of the fate of volatiles through the AD process (by measuring intermediates and final compounds at full scale as well as a lab scale), and the type and load of odorous compounds within the various samples. In addition, the GC-IMS based spectra analysed by an artificial intelligence based self-organising map (SOM) for classification was found to enable an effective sample comparison identifying the sources of contamination rapidly. With an increase in diversity of samples analysed by GC-IMS associated with a more effective pattern recognition tool, the fingerprinting of environmental contaminants would likely be able to be established rapidly, facilitating the identification of sources of environmental pollutants by regulators enabling the halting accidental spillages. AD plants can have their typical matrices characterised by GC-IMS and in case of a local environmental pollution event, AD plants could protect themselves from being wrongly identified as the source of local incidents that could have been generated by other agricultural or industrial activities and discharges. Finally, this research conducted a preliminary investigation of a laboratory based multi-stage and one-stage reactor setup performance, which concluded that a number of volatiles were reduced in both systems with the multi-stage reactor performing slightly better than the single stage reactors (in particular in the case of terpenes). This study concluded that GC-IMS is a promising analytical tool for multi-parameter diagnosis and control of AD technology. Its ability to analyse a wide range of matrices (gas, liquid and solid), ability to provide rapid measurements with a reduced analytical tool footprint, and the relatively low operator training required can all facilitate its integration as a process analyser for in-situ real-time plant monitoring and control for this industry. Other biotechnologies and biorefining plants could also benefit from the use of this analytical tool (e.g. biochemical and biopolymer factories). Areas of positive impact are expected to relate to feedstock conversions and improved energy/production yields, improved odour management, and environmental compliance.

Table of Contents

List of Tables

List of Figures

List of Equations

Nomenclature

ABP	Animal by product
AD	Anaerobic digestion
ADBA	Anaerobic Digestion and Bioresources Association
AI	Artificial intelligence
ARI	Alternative reactant ions
Avg.	Average
A4B KTC	Academic expertise for business knowledge transfer centres
BTEX	Benzene, toluene, ethylbenzene, and xylene
CD	Corona discharge
COD	Chemical oxygen demand
R^2	Correlation coefficient
CSTR	Continuous stirred-tank reactor
CSV	Comma-separated values
CWAs	Chemical warfare agents
DAPI-PIMS	Dopant-assisted photoionization positive ion mobility spectrometry
DDT	Dichlorodiphenyltrichloroethane
DI	Deionised water
Dr.	Doctor
DTBP	Di-tert-butylpyridine
DW	Dry weight
EBA	European Biogas Association
ELISA	Enzyme-linked-immuno-sorbent-assay
EN	European norm
EO	Essential oils
ESF	European Social Fund
ESI-IMS	Electrospray ionization-ion mobility spectrometry
EPA	Environmental Protection Agency
EQUIP.	Equipment
EU	European Union
FT-NIR	Fourier Transform Near-Infrared Spectroscopy
FW	Food waste
G.A.S.	Gesellschaft Für Analytische Sensorsysteme
GC	Gas chromatography
GC-FID/PFPD	Gas chromatography with flame ionization detection/pulsed flame photometric detection
GC-IMS	Gas Chromatograph-Ion Mobility Spectrometry
GC-MS	Gas Chromatography-Mass Spectrometry
GC–MS/O	Gas Chromatography-Mass Spectrometry-Olfactometry
GRO	Graduate Research Office
HF-LPME	Hollow fibre microextraction technique
HMX	1,3,5,7-Tetranitro-1,3,5,7-tetrazocine
HPLC	High Performance Liquid Chromatography
HRMS	High resolution mass-spectrometry
HRT	Hydraulic retention time
HS-SPME-MIR-IMS	Head-space solid phase microextraction with modified ionization region ion mobility spectrometry
HTF	Heat transfer fluid
IEC	Installed electric capacity
IL-SDME	Ionic liquid single-drop microextraction
IMS–TOF−MS	Ion mobility spectrometry time-of-flight mass spectrometry
KESS	Knowledge Economy Skills Scholarship
kg	Kilogram
LAV	Laboratory Analytical Viewer
LD-GC-IMS	Laser desorption with gas chromatography and ion mobility spectrometry
LOD	Limit of detection
LOQ	Limit of quantification
MCC-IMS	Multi-capillary column with Ion Mobility Spectrometry
ms	millisecond
MSW	Municipal solid waste
Mt	Million tonnes
MTBE	Methyl tert butyl ether
MW	Megawatt
ND	No dilution
NH_3	Ammonia
NIR	Near infrared spectroscopy
NIST	National Institute of Standards and Technology
NPS	New psychoactive substance
NTO	2,4-Dihydro-5-nitro-3H-1,2,4-triazol-3-one
OFMSW	Organic fraction of municipal solid waste
OLR	Organic loading rate
Optical density	OD_{540nm}
OPLS-DA	Orthogonal partial least squares discriminant analysis
PA	Proton affinity
PACs	Polycyclic aromatic compounds

PBB	Polybrominated biphenyls
PCA	Principal Component Analysis
PCBs	Polychlorinated biphenyls
PCR	Polymerase chain reaction
PETN	Pentaerythritol tetranitrate
PF reactor	Plug flow reactor
pH	Potential of Hydrogen
PLS-R	Partial least squares regression
µg/L	Parts per billion
Prof.	Professor
PTFE	Polytetrafluoroethylene
pVOCs	Plant volatile organic compounds
RDX	Cyclo-1,3,5-Trimethylene-2,4,6-Trinitramine
RIP	Reaction Ion Peak
RSD	Relative Standard Deviation
SD	Standard deviation
SERC	Sustainable Environment Research Centre
SHS-MCC- GC-IMS	Headspace multi capillary column gas chromatography ion mobility spectrometry
SOM	Self-organization map
SP1-SP8	Sample Point 1–Sample Point 8
Sparse-PLS-DA	Sparse-partial least squares-discriminant analysis
SPME	Solid phase micro extraction
SPME-GC-FID	Gas chromatography and flame ionization detection preceded by solid phase micro-extraction
Stand. Dev.	Standard deviation
TD	Thermal desorption
TD-GC-MS	Thermal Desorption and Gas Chromatography-Mass Spectrometry
TD-IMS	Thermal desorption-ion mobility spectrometry
TDS	Temporal dominance of sensations
TICs	Toxic industrial chemicals
TMA	Trimethylamine
TNT	2,4,6-Trinitrotoluene
TOF-MS	Time-of-flight mass spectrometer
TS	Total Solids
TWh	Terawatt-hour
USA	United States of America
USW	University of South Wales
UK	United Kingdom
UV	Ultraviolet radiation
VDI	The German standard Olfactometry Determination of Odour Intensity
VFAs	Volatile Fatty Acids
VOCs	Volatile Organic Compounds
VS	Volatile Solids
WRAP	Waste and Resources Action Programme
WW	Wet weight
µSPE	Micro-solid-phase extraction
(2,4,6-TCA)	2,4,6-tricholoroanisole

1. INTRODUCTION

1.1 BACKGROUND

According to the European report “Estimates of European food waste (FW) levels”, approximately 88 Mt of food are wasted annually in the European Union (EU). This represents approximately 20% of all of the food produced (Stenmark *et al.*, 2016) and the major source is households which generate 47 Mt of FW, equating to 92 kg / person / year (Stenmark *et al.*, 2016). As a result of the Landfill Directive 1999 implementation across European countries, a significant shift of recovery of food wastes has taken place from landfill to recycling processes such as anaerobic digestion (AD) and composting. Challenges still exist in terms of optimisation of these facilities.

In addition to FW, agricultural wastes and wastewater sludges are also produced and require appropriate treatment. In the United Kingdom (UK) alone, approximately 90 Mt of animal slurries are produced annually (ADBA, 2017) and resources exist across Europe where more than 1500 Mt per year of animal manure and slurries are produced from cattle and pig production units (Holm-Nielsen *et al.*, 2009). Sigurnjak *et al.* (2017) suggested only 7.8% of livestock manure is currently processed and treated (Sigurnjak *et al.*, 2017).

Animal slurries have been associated with greenhouse gas emissions, environmental nutrient overloads (of particular concern are excesses of nitrogen and phosphorus in environmental receptors) and the release of pathogens (Bonetta *et al.*, 2011; Hjorth *et al.*, 2009; Holm-Nielsen *et al.*, 2009). Whilst targets for the treatment of these agricultural wastes are not defined, countries aim to minimise the impact of the agricultural sector and its related environmental pollution (Alvarenga *et al.*, 2015).

An environmental concern related to organic wastes and their treatment is related to odours released through the degradation of organics. Odour emissions are a significant issue for the waste and wastewater treatment sector due to complaints from neighbours and therefore the characterization of the sources of volatile odour emissions from these infrastructures is very important (Rappert and Müller, 2005). However, this has been difficult to achieve, as it has been a challenge to detect, measure and quantify these odours (Littarru, 2007). Similarly, little knowledge exists about the potential ways to reduce the emissions of these compounds by either improving their conversion, entrapment or recovery (Agler *et al.*, 2011).

At waste treatment plant level, it is important to understand if conversions can be improved to degrade the odorous compounds, or if any existing odour abatement equipment requires maintenance (e.g. biofilters). At a more macro scale, numerous sources of odours can occur in a common location, and it is important to identify if odours are generated from a specific waste treatment plant or a nearby farm or another waste treatment infrastructure (ADBA, 2012). The industry has adopted systems such as biofilters, bioscrubbers, or suspended growth reactors and membrane bioreactors to reduce odour emissions (Schlegelmilch *et al.*, 2005a). However, these technologies may not be sufficient across all operating conditions or may even be inappropriately designed or managed, and odours can continue to be released to the environment (Talaiekhozani *et al.*, 2016). In addition to the odour related nuisance caused, in severe cases of environmental permitting infringements a loss of permit to operate can occur with a significant economic impact for the plant owner or operator and the related supply chain of companies or local authorities providing the feedstocks for treatment. It is therefore imperative for the industry to be able to access a fast odour diagnosis tool developed to measure the chemical signatures of source compounds, which can be applied to help minimise the impact of odour by enhancing the conversion or recovery of these compounds.

The waste management hierarchy emphasizes a reduction of waste generation, reutilization of products, recycling of materials, production of energy from waste and, as a last resort, landfilling. The demand for sustainable options is rising, especially for options that combine waste treatment with the production of non-fossil energy. AD is a biochemical process that occurs in sealed vessels, in which organic matter is degraded to mainly methane and carbon dioxide and trace elements through a series of reactions mediated by several groups of microorganisms in one or more digesters of various types. AD is an environmentally attractive technology that can deliver waste treatment, pollution reduction, renewable energy generation and improvement of agricultural practices by recycling of nutrients (Mao *et al.*, 2015; Singhania *et al.*, 2013). Furthermore, it can help to achieve the EU's 2020 and 2030 decarbonisation and renewable energy targets because the EU intends to increase at least 32% share for renewable energy, increase at least 32.5% the improvement in energy efficiency and reduce at least 40% the greenhouse gas emissions (from 1990 levels) by 2030 (European Union, 2014; Verbeeck *et al.*, 2018).

Europe currently has 18,202 biogas installations in operation (Germany 11,084 plants, Italy 1,655 plants, France 837 plants, UK 715 plants, and Switzerland 634 plants), with an installed electric capacity (IEC) of 11,082 MW. The deployment is continuing to grow

in some regions with the focus of delivering waste treatment and, in many cases, bioenergy production (EBA, 2017). Since 2005, the United States of America (USA) added a total of 255 AD plants for treating cattle waste (mainly dairy), either as a single feedstock or mixed with other organic substrates. This had been deployed to begin to address the issue of slurry and manure management in the agriculture sector (Edwards *et al.*, 2015).

Typically, monitoring in AD plants relates to biogas flowrate and composition (sometimes performed online) as well as solids loading and conversion, pH and alkalinity and total VFAs, which are present in digester matrices (performed off-line) (Esteves *et al.*, 2012). However, these limited number of parameters and frequency of sampling does not provide operators with the necessary knowledge to diagnose and optimise plant performance. Process disturbances can typically be caused by organic or hydraulic overloads, the presence of toxic or inhibitory compounds, the lack of nutrients or trace elements essential for microorganisms' maintenance and growth, and the deviation from optimum operating temperatures (Esteves *et al.*, 2012). Process success relates to an appropriate balance between the growth rates of the principal metabolic groups of bacteria and *archaea* (i.e. acid-forming bacteria, acetogens, and methanogens), which is also challenging to achieve. Therefore the development of a multi-parameter tool for monitoring intermediate compounds from within these stages that remain undigested within the digester matrix or digestates is critical.

In addition to gaseous discharges, the AD companies operating environmental permitted sites require appropriate management of their solids and liquid discharges to the environment both in the case of the planned use of digestates on land as well as accidental discharges (Holm-Nielsen *et al.*, 2009; Li *et al.*, 2018). Related to this, and in addition to the need to bring about tighter plant construction standards and the implementation of robust plant design and operation best practices (Scottish Environment Agency, 2015), there is also a need to develop a fast detection and chemical fingerprinting tool for various plant matrices. This tool could help diagnose the source of discharge and avoid significant environmental pollution from accidental spillages from AD plants to neighbouring environmental receptors (Studer *et al.*, 2017; Wang, 2014).

AD has the versatility to degrade a multitude of organic feedstocks, however, this can bring some challenges as the process is required to cope with feedstocks with a wide range of physical and chemical composition and the possibility that feedstocks contain or break down to chemical compounds that may inhibit the digestion process (Chen *et*

al., 2008). In addition, the AD process is delivered by complex and dynamic systems where mechanical, microbiological and physical-chemical aspects ultimately influence the process performance and stability. Due to the complexities and the multiple requirements in the design and operation of the plants, performance optimisation of AD plants is often still required from a number of perspectives:

- Improvements in conversion efficiencies and footprint size reduction with greater stabilisation of wastes as well as an increased biogas yield (Zhang *et al.*, 2014);
- Increased robustness even when feedstocks and loading are variable (Wang, 2014);
- Increased environmental performance and regulatory compliance in terms of reduced greenhouse emissions, odours and any unplanned environmental discharge or spillages (Studer *et al.*, 2017).

1.2 AIM OF THE PROJECT

The aim of the research presented in this thesis is to investigate and develop a novel multiparameter analytical tool that can be used to identify and quantify volatile compounds present within various matrices relevant to AD plants, and to help investigate the potential for its utilisation for optimisation of AD technology performance in terms of energy production, odour management, and environmental compliance.

1.3 OBJECTIVES OF THE PROJECT

To deliver the aim of this project, the following objectives have been defined:

- **Objective 1:** Undertake a critical literature review and determine available methodologies to detect and quantify volatile compounds typically found in gaseous, solid, and liquid matrices of similar nature as in AD plants. Ascertain the challenges and limitations of currently used techniques and enable a comparison with the technique being proposed.
- **Objective 2:** To develop a novel methodology based on GC-IMS for fingerprinting chemical signatures as well as quantifying volatile compounds present in AD plants (feedstocks, digester matrices, biogas, and digestates) and being able to match their source and characteristics.

- **Objective 3:** Investigate the performance of GC-IMS in identification of volatile compounds in AD relevant matrices. Establish LOD, LOQ, robustness, repeatability and reproducibility of the analytical tool for numerous analytes. Investigate the tool's ability to quantify compounds relevant to AD operations and support plant optimisation.
- **Objective 4:** Conduct a preliminary investigation of the "fate" of volatile (including odorous) compounds throughout the AD process including feedstock storage, digester vessel, and digestate storage.
- **Objective 5:** To use monitoring results to understand and demonstrate the impact of changes to process configurations on the production/degradation of volatile compounds and suggest strategies to increase process efficiency and to reduce volatile emissions.

1.4 NOVELTY

This research brings several aspects of novelty:

- There is a lack of research relating directly to the production and/or degradation of volatile (odorous) compounds within the AD process (as demonstrated in the literature review). This research, therefore, represents the first study to document in depth the presence and degradation of such compounds.
- The research is expected to lead to the development of innovative analytical techniques to fingerprint and quantify volatile compounds present in a full-scale AD plant, including the development of new analytical methodologies. This is the first time that the techniques have been developed specifically for the AD sector.
- The method development associated with applying the novel monitoring technique to the waste management sector involves several novel findings.
- The techniques developed will be utilised to inform potential changes to plant design, configuration, and operational procedures to reduce plant inefficiencies and potential nuisance. This is the first time that this approach to the management of an AD facility has been investigated and documented.
- The methodology developed has also been applied in the field and has been shown to be capable of distinguishing between several potential organic pollutants. This is the first time that this technique has been applied in this way.

Figure 1 depicts the research conducted. AD monitoring is typically inadequate to understand what is happening with the AD process such as the input of feedstocks or the organic loading rate (OLR) and this lack of knowledge can lead to system design

choices that result in oversized digesters for stability or the use of inadequate scrubbers for treating odours. What is actually important to identify, as well, is the actual cause of these disturbances (e.g. why were these odours produced, what is the source of the odours).

Equally is also important to control intermediate residual products such as VFAs, which reduce process efficiency, and control the quality of final products such as the amount of limonene within the biomethane stream when this is to be injected into the gas network. Therefore, an adequate analytical tool is required to help the industry and the regulators to understand and control the causes of these symptoms and to reduce the impacts on the environment and local communities.

Past approaches for monitoring have been explored, largely as a single parameter analysis, without the potential to deliver real-time analysis and without the potential to characterise odours and improve digester performance. A monitoring approach based on GC-IMS has the potential to characterise odours and improve reactors' performance having the advantage to identify compounds and be used for real-time and online monitoring and even support regulatory performance.

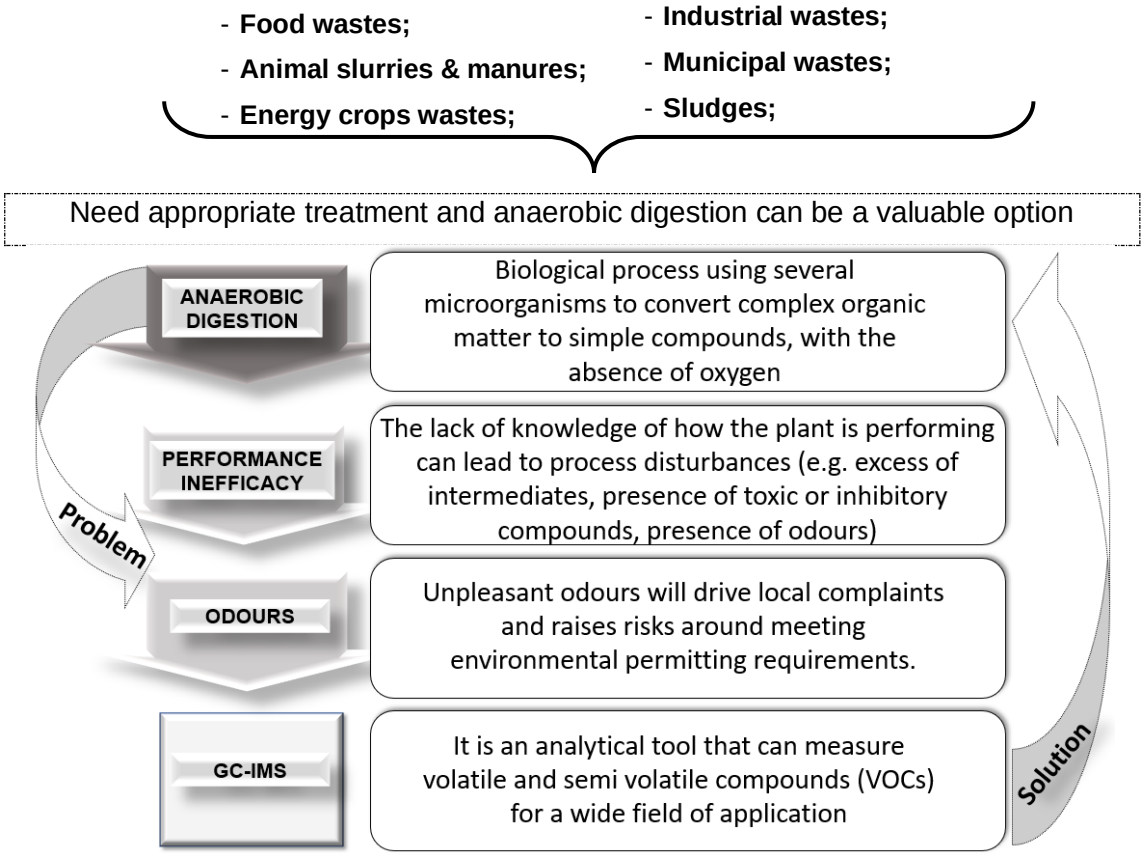

Figure 1: Schematic summarising the need for the project

2. LITERATURE REVIEW

2.1 ANAEROBIC DIGESTION

AD is a naturally occurring biological process where a consortium of bacteria and *archaea* convert complex organic matter to simple compounds, without the presence of oxygen (O_2). The process has been industrialised for the treatment of organic wastes and energy recovery from crops. This process allows the recycling of nutrients and the final products are digestate and biogas. Most of the gases present in biogas are methane (CH_4) (about 40-75%), carbon dioxide (CO_2) (about 25-50%), with trace amounts of compounds such as hydrogen sulphide (H_2S) (about 0.005-2%), ammonia (NH_3) (less 1%), water vapour (H_2O), siloxanes, and mercaptans (in some cases) (Toledo-Cervantes *et al.*, 2016). The digestate is a nutrient-rich substance and the biogas can be used for heating, power production, or, following upgrading, can be used as a transport fuel, or production of chemicals or replacement for natural gas (Verbeeck *et al.*, 2018).

2.1.1 Process of Anaerobic Digestion

The process can be described by the following four phases: hydrolysis, acidogenesis, acetogenesis and methanogenesis (Appels *et al.*, 2008). Figure 2 represents a schematic of the AD process. In the hydrolysis phase, high molecular weight compounds such as carbohydrates, lipids, and proteins are hydrolysed to soluble organic substrates such as amino acids from proteins, glucose from carbohydrates and fatty acids from lipids (Mata-Alvarez, 2003). Hydrolysis can be the rate-limiting step because the hydrolytic enzymes are required to be primarily adsorbed on the surface of the solid substrates (Zhang *et al.*, 2014). In the acidogenesis phase, VFAs, NH_3, CO_2, H_2S, and other by-products are produced (Appels *et al.*, 2008; Zhang *et al.*, 2014).

In the acetogenesis phase, the organic acids and alcohols are further degraded to produce acetate, formate, CO_2, H_2 (hydrogen) (Alvarado *et al.*, 2014). Two groups of methanogenic bacteria will either produce methane from acetate (aceticlastic) or use hydrogen as an electron donor and carbon dioxide as acceptor (hydrogenotrophic) (Appels *et al.*, 2008). Hydrogenotrophic methanogens and hydrogen-producing acetogenic bacteria grow in syntrophic associations because hydrogenotrophic methanogens bacteria keep the amount of hydrogen low to allow acetogenesis to become thermodynamically favourable (Angenent *et al.*, 2004).

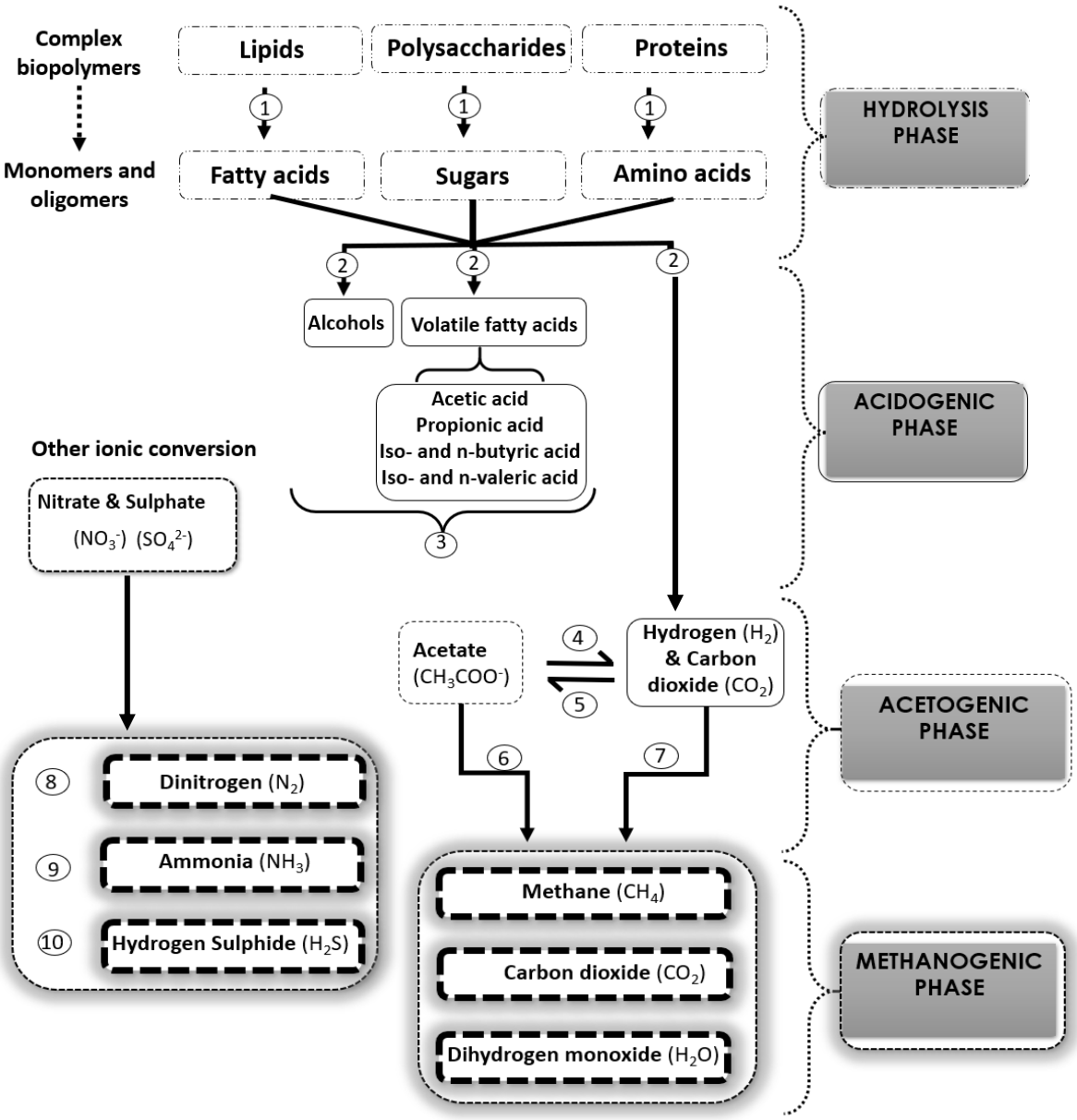

1 – **Hydrolytic Bacteria**
2 – **Fermentative Bacteria**
3 – **Obligate Hydrogen producing Bacteria**
4 – **Homoacetogenic Bacteria**
5 – **Syntrophic acetate oxidizing Bacteria**
6 – **Acetoclastic Methanogens**
7 – **Hydrogenotrophic Methanogens**
8 – **Denitrifying Methanogens**
9 – **Dissimilative Nitrate-reducing Bacteria**
10 – **Sulphate-reducing Bacteria**

Figure 2: AD Process adapted from *(*Alvarado *et al.,* 2014)

The production of methane has been stated to be the most sensitive step in AD and the presence of viable methanogens can be the most effective indicator of a stable and effective digestion process (Alvarado *et al.*, 2014; Wallace *et al.*, 2011; Williams *et al.*, 2013). According to Cook *et al.* (2017) key monitoring parameters (biogas composition, pH, VFAs, alkalinity, long chain VFAs, free ammonia and ammonium) are indicators to measure the process stability for real-time monitoring. Having an assessment tool for anaerobic codigestion (digestion of two or more substrates) to improve the performance

and stability in the reactors, provide insight to design engineers to avoid challenges such as ammonia inhibition or nutrient imbalances during the process and the reduce the number of experiments / test to do (Cook *et al.*, 2017). The feedstocks conversion can be measured by chemical demand of oxygen (COD) and total and volatile solids (TS and VS). The presence of intermediate substances accumulation can be done by VFA, pH, alkalinity analysis or measure the amount of H_2 or CO_2. To see the product formation can be done by measuring the gas production rate, amount of CH_4, CO_2, and H_2S (Mesquita *et al.*, 2017). Compounds such as bicarbonate, VFAs, and ammonia affect the buffer capacity in a digester (Mata-Alvarez, 2003). A typically indicator values for a stable reactor would between 6.1 – 8.3 for pH, 2 – 20 g $CaCO_3$/L for alkalinity, free ammonia maximum 200 mg NH_3-N/L, total VFAs maximum 3250 mg COD/L, ammonium maximum 3250 mg NH_4^+-N/L, long chain fatty acids maximum 1400 mg COD/L and methane composition 55% or above in the biogas (Cook *et al.*, 2017).

2.1.2 Volatile compounds related to AD systems

Volatile compounds emanating from the various solid, liquid and gaseous matrices in AD plants are of interest, as quantification of these may be able to provide a:

a) means of evaluating characteristics of feedstocks and digestates including stability;

b) means of identifying and quantifying intermediate compounds within the various stages of the AD process, which may indicate a shift in metabolic pathways, accumulation of inhibitors or non-degradation of certain compounds;

c) rapid mechanism to identify any source of unwanted spillages;

d) means to minimise and control odour emissions by enabling alterations to degradation efficiencies, detecting odour emission sources or by supporting ancillary odour removal mechanisms and strategies.

Odour emissions bring a significant challenge for the waste management industry, (e.g. landfills), and for competent authorities for a long time. Odours are becoming a major reason why exist public complaints and these odorous emissions can affect the quality of life of next-door neighbour (Fang *et al.*, 2012; Sironi *et al.*, 2010). This situation is forcing countries and local regulatory agencies to create odour regulations, especially for agricultural operations and food industries and waste management facilities (Rappert *et al.*, 2005).

AD technology, as compared to composting or landfill, minimises odour emissions by being performed in enclosed tanks and through processing and utilisation of the biogas

streams (Mata-Alvarez *et al.*, 2000) rather than releasing to the atmosphere. However, care is required in particular when handling feedstocks at reception buildings / tanks and when the digestate is stored or is being utilised. In terms of odour emissions, in addition to odours related to specific feedstocks, anaerobic metabolisms would encourage the generation of odorous metabolic products such as VFAs, reduced sulphur compounds, amines, thiols and final products such as NH_3 and H_2S (Alvarado *et al.*, 2014; Wallace *et al.*, 2011).

A reduction of odours will likely impact positively on the deployment and operation of the waste management industry and on the communities living in the surroundings of AD sites. As indicated above, odour emissions can be indicators of the instability of the AD process or identify degradation inefficiencies (Rappert and Müller, 2005). Being able to monitor these compounds may enable the implementation of improved plant designs or operations and an increase in plant efficiencies.

2.1.2.1 Volatile compounds found in feedstocks

Numerous correlations of specific organic feedstocks composition with odours have been attempted. For example, Zhang *et al.* (2012) recommended that controlling the lipid and protein contents in Municipal Solid Waste (MSW) can reduce the odour from landfills and the effect of lipids lasts longer than that of protein (Zhang *et al.*, 2012). According to Sundberg *et al.* (2012), the effect of low pH and microbial composition on odour in FW composting has been correlated. The authors concluded that the odour was much stronger when the compost was acidic than when it was neutral or alkaline and *Lactobacteria* and *Clostridia* were present, which are known to produce odorous substances (Sundberg *et al.*, 2013). Therefore, the same principle can be applied to AD as the odour can be much stronger when the compost was acidic due the presence of VFAs, for example.

Nimmermark studied the influence of odour concentration and individual odour thresholds on the hedonic tone of odour from different animal production (pig, poultry and dairy operations) using a panel of 16 persons and following the EN 13725:2003 odour measurement standard. The panel found odours from dairy cows to be more pleasant than odour from fattening pigs and laying hens. Individual odour thresholds were immersed to be important for a rating of the hedonic tone (Nimmermark, 2011). Blazy *et al.* (2015) correlated the chemical composition with the odour concentration from pig sludge using GC–MS and olfactometry. Three main odorous compounds were found

in the 66 samples analysed (trimethylamine, H_2S and mercaptans (methanethiol)) and the odour concentration was 1000 $ou_E m^{-3}$ (Blazy *et al.*, 2015).

2.1.2.2 Volatile compounds found as AD process intermediates

Figure 2 identifies the primary intermediate products of the AD process i.e. monomers (sugars, amino acids), long-chain fatty acids (lauric, myristic and palmitic acid), alcohols, VFAs (propionate, butyrate & isobutyrate, valerate and isovalerate) nitrate, sulphate, and acetate. Page *et al.* (2015) studied the reduction of VFAs and odour offensiveness by AD digestion and solid separation of dairy manure during manure storage. The results showed that the dominant VFAs were acetic acid and AD reduced total VFAs by 86%-96% (Page *et al.*, 2015).

2.1.2.3 Volatile compounds found in digestates

Figure 2 illustrated the final products expected as part of the biogas stream (i.e. NH_3, nitrogen gas N_2, H_2S, CH_4, H_2, and CO_2). Besides these gases, AD also produces a digestate. Digestate typically contains a "readily available nitrogen" source of ammonia and may release other odours. It is therefore common to perform shallow land injection of the digestate instead of using a splash plate system when applying digestate to land (WRAP, 2016). When comparing digestate with slurry, digestate has been stated to be a better fertiliser with more trace elements and has a considerably lower odour signature. Therefore the spreading operations of the digestate will be considerably less odorous than the current operations which use slurry (WRAP, 2012). Ammonia is one typical odour present during AD and whilst it is an crucial nutrient for bacteria to grow up, if it is present in high concentrations it can inhibit the production of methane during the AD process (Yenigün and Demirel, 2013). To avoid ammonia to be present at a high concentration, Tao *et al.* (2017) studied the impact of ammonia when it was continuously being removed from the digestion of thermally hydrolysed sewage sludge using ion-exchange resin and zeolite. Removing ammonia allowed an increase in microbial density and a resulting increase in methane production and a pH reduction by 0.2-0.5 units. The authors found that by removing ammonia, the pH could decrease, resulting in a greater degradation efficiency of feedstocks based polymers as well as intermediate VFAs and increase the microbial density, therefore the reactors were performing more efficiently (Tao *et al.*, 2017).

2.1.4 Need for monitoring the AD process performance

Biological waste treatment processes like AD are extremely sensitive to process disturbances and it has the need to be continuously monitored with a reliable method (e.g. flow sensors, electrochemical sensors, auto-titrator, chromatography and spectroscopy) controlled using process control techniques (Nguyen *et al*., 2015). Real-time monitoring and automated control would promote a stable performance of the reactor. Offline analysis can lead to inefficiencies and errors because of the heterogeneity in physical characteristics and bio-chemical compositions of the feedstock or due to potential errors from inappropriate sampling and a delay in analysis which allows changes in the matrices to occur (e.g. release of CO_2, consumption of VFAs amongst others). Therefore, the lack of monitoring can lead to a deficiency of knowledge from the operator and process disturbances in the AD systems (Nguyen *et al.*, 2015).

An on-line monitoring measurement intends to be continuous and real-time, or with an adequate intermittency with automated results provided in seconds or minutes. An offline measurement is associated with sampling and performance of analysis off-line at the site or sent to eternal laboratories. Williams *et al.* (2013) showed that continuous monitoring on a full-scale reactor based on microbial profiling in combination with intermediates (e.g. VFAs, ammonia) and alkalinity monitoring could facilitate and improve the digester management from operators by giving them important perceptions about the status of the digestion process. So, they could take wise decisions with the objective to improve the digester stability and facilitate the digester optimization (Williams *et al.*, 2013).

Methodologies frequently applied for monitoring key parameters are based on offline measurement or olfactometric methods or lab-based technologies that can provide an accurate description of chemical compositions of gases (e.g. Gas chromatography–mass spectrometry, GC-MS) but they are time-consuming, labour intensive, expensive and provide only a snapshot of the process. For measuring odours, the idea of using chemical instrumentation instead olfactometry expert panels, has long been pursued to avoid health problems or reduce the subjectivity in the measurement or reduce costs (Eiceman *et al.*, 2016). To fill this need, fast running devices that combine high sensitivity with identification of compounds, easy to operate, with real-time monitoring capability and easy to carry are actively being developed nowadays. Using non-specific sensor arrays may offer an objective and online instrument for evaluating olfactive annoyance or other types of equipment, such as photoionization detector, GC-IMS, ultraviolet-visible spectroscopy, infrared spectroscopy, and fluorescence spectroscopy.

Matz *et al.* (2005) tried different methods for fast on-site measurement of odorous compounds, especially for aerosol-bound chemical compounds from waste gases from food industry. For sampling, it was used several methods such as aerosol sampling techniques, and enrichment on solid phase micro extraction (SPME). Aerosol sampling proved be a useful method for sampling polar organic compounds. For detection of waste gas compounds, it was used thermal desorption–gas chromatography–mass spectrometry (TD–GC–MS), gas sensor arrays and GC-IMS. The sensor measurements were compared with olfactometric results providing good results with a good correlation between sensor and olfactometric measurements (Matz *et al.*, 2005).

Important intermediates of the AD process essential to monitor are VFAs. The methods to measure VFAs can be classified as traditional methods (e.g. titration, distillation and column chromatography) or instrumental methods (e.g. visible spectroscopy and chromatographic techniques). Fernández *et al.* (2016) reviewed the analytical methods for the measurement and monitoring of shortest VFAs (acetic acid to valeric acid). There were based on sample pre-treatment procedures (filtration, centrifugation, extraction techniques, derivatization, different analytical methods (GC, high-performance liquid chromatography (HPLC), capillary electrophoresis), limits of detection and linear dynamic range for calibrations. VFAs have an important role in the bioprocess as indicators and for that reason, several techniques had been developed during recent years. The author advised the use of GC-MS or GC-FID for complex samples with some steps as pre-treatment (Fernández *et al.*, 2016).

In 2013, an interlaboratory comparative study was developed to assess the analytical performance of 25 laboratories to measure VFAs in aqueous samples and standards. It used GC and/or HPLC to estimate sources of error (e.g. sample preparation, equipment failure, human error, inadequate calibration, sample transport and storage) to monitoring VFAs and harmonize analytical quantification. The study concluded HS-GC (automatic injection with split system, and oven-temperature programming), with acid acidification by phosphoric acid (H_3PO_4), and including 4–6 concentration levels to make a calibration was an accurate methodology to detect VFAs (Raposo *et al.*, 2013).

A comparison study for the four different titration procedures for monitoring VFAs on biogas process was made by Lützhøft *et al.* (2014), where the authors concluded that the best option should be the two pH end-points because it is simple and provide a good accuracy (Lützhøft *et al.*, 2014). Boe *et al.* (2008) suggested propionic acid was the best VFA to monitor if a reactor was under stress due to an organic overload while the use of the biogas production should be used as the main control parameter (Boe *et al.*, 2008).

In another study from the same author, the author refers the combination of acetic and propionic acid and biogas production could be a better combination to monitor digesters more successfully (Boe *et al.*, 2010). Jin *et al.* (2017) suggested the use of a bio-electrolytic sensor with a microbial electrolysis cell could be a simple and cost-effective method for rapid monitoring of VFAs in AD process (Jin *et al.*, 2017).

Ward *et al.* (2011) suggested to measure the gas phase from a reactor with a micro gas chromatography calibrated to measure H_2, CH_4, CO_2, H_2S, N_2 and O_2, and a membrane-inlet mass spectrometry to measure VFAs, CH_4, CO_2, H_2S, reduced organic sulphur compounds, and p-cresol. While monitoring the liquid phase a pH probe to control the pH. The near-infrared spectroscopy was equipped with a diffuse reflectance probe to monitor VFA and the best technologies would be near-infrared spectroscopy, micro gas chromatography, pH probe could provide reliable results and had low maintenance (Ward *et al.*, 2011).

A company called Camlin developed an advanced, real-time online VOCs monitoring for raw biogas or clean biomethane for upgrading plants such as bio-waste treatment plants, agricultural plants with bio-waste or biogas upgrading at wastewater treatment plant to be managed more efficiently. The technique is based on optical absorption spectroscopy (ultraviolet light) to determine individual spectral fingerprint from each VOC (acetone, 2-butanone, 3-carene, α-pinene, β-pinene, limonene, p-cymene, hydrogen sulphide, ammonia, xylenes, dimethyl sulphide, carbon disulphide) and their concentration in the gas sample, in a single measurement at sub-mg/Lv level. It can get results in a few minutes and has the ability to do multi-point sampling (up to eight sampling points) (Camlin, 2020).

Near infrared spectroscopy (NIR) is a technology that could potentially improve and optimize (especially for the feeding recipe) the AD performance in order to improve the production of biogas and degradation of materials. Charnier *et al.* (2017) correlated NIR measurements with COD, nitrogen, carbohydrate, lipid contents measurements, using 295 solid wastes samples (e.g. fruits, vegetables, manure, cereals, oils, fats, meat and fish). The author created a model to predict the biochemical composition content from feedstocks based in a NIR dataset with PLS (Charnier *et al.*, 2017).

Reed *et al*. (2011) showed the importance to have a tool for online monitoring of anaerobic sewage sludge digesters performance, mainly for differentiation between different stages in the process and differentiate between feedstocks and digestates. The author used reflectance Fourier transform near infrared (FT-NIR) spectroscopy to predict

reactor performance based on FT-NIR measurement combined with principle components analysis (PCA), partial least squares regression (PLS-R) to build predictive models for sludge characteristics (solids content, alkalinity and VFAs) (Reed *et al*., 2011). In another study, the same author collected data from FT-NIR combined with PLS-R and PCA to predict values for VFA, BA and VS and independently validated for each digester. This technology, when applied online, could be used for monitoring instabilities in the digester (Reed *et al*., 2013).

FT-NIR can be used for continuously measure and quantify the amount of ammonia release during thermal batch drying from mechanically dewatered sewage sludge and potential for nitrogen recovery which could be facilitated by acid absorption or adsorption on activated carbon or biochar. During the dry process gas ammonia release was between 4900 and 6200 mg/kg TS, although the amount of total nitrogen contained (i.e. NH_4^+, NH_3, NO_x^-, organic N was 53,000 mg/kg TS) and it was not recovered because it was bound in cell structure and could not be released (Horttanainen *et al.*, 2017).

To improve AD performance, mathematical models based on biological and physicochemical characteristics, bacterial growth kinetics, substrate consumption, and product synthesis have been attempted. However, combining all of these characteristics is a difficult undertaking, and the process's complexity mandates exceedingly elaborate models (Ramachandran *et al*., 2019). Some approaches can be used to reduce data size, cluster data based on similarities, or visualize large datasets to identify potential clusters. SOM, for example, is a type of unsupervised artificial neural network that visualize high-dimensional data and reduces input data to a low-dimensional discretized pattern in order to represent it as a map (Kohonen, 1998). As a result, SOM is made up of neurons arranged in an array that generates a map with comparable samples clustered together. Ramachandran *et al.* (2019) successfully employed the SOM network to model the operation of anaerobic wastewater treatment plant even when data was unavailable. The authors were able to anticipate variations in methane and total gas output with high accuracy in response to changes in input parameters (Ramachandran et al., 2019).

2.2 ODOURS

2.2.1 Definition of odour

The European directive 2004/42/CE considers a VOCs any organic compound having an initial boiling point less than or equal to 250°C measured at a standard pressure of

101.3 kPa" (The European Parliament and the Council of the European Union, 2004). However, the United States Environment Protection Agency classify it in a different way according to their boiling point range the inorganic/organic pollutants. A VOC with boiling point range below 0°C to 50-100°C (e.g. propane, butane, methyl chloride) it is considered a "very VOC", while just considered as "VOC" had the boiling point between 50-100°C to 240-260°C (e.g. formaldehyde, d-limonene, toluene, acetone, ethanol, 2-propanol, hexanal) and "semi-VOC" had between 240-260°C to 380-400°C (e.g. pesticides (DDT, chlordane, plasticizers (phthalates), fire retardants (PCBs, PBB)) (EPA, 2019).

According to the Environment Agency in England and Wales, odours are a stimulus to the olfactory sensory system. A fragrance is generally considered to be a pleasant odour resulting from a composition of well-selected ingredients (raw materials) and a malodour is considered as an unpleasant odour, potentially generated by metabolites from chemical or biological processes (fermentation, degradation, combustion, spontaneous chemical reactions) (Churchill, 2006; Environment Agency, 2007).
Examples of odorous compounds and related monitoring techniques have been described in the following sections. Many of unpleasant odorous emissions to the atmosphere are consequence from municipal, industrial, and agricultural activities (e.g., composting plants, wastewater treatment, livestock farming, food processing, petroleum refining, paint finishing, or chemical production) (Ranau *et al.*, 2005).

2.2.1.1 Chemical family

Some compounds may be produced by microbiological processes from different microorganisms and they are mixtures of various compounds with different functional groups, including acids, alcohols, aldehydes, esters, ketones, lactones, pyrazines, amines, sulphur compounds, and terpenoids.

- Ketones

Ketones have a carbonyl group where an atom of carbon is bound to oxygen in a double bond (R-C=O-R'). For example, 2-butanone has the empirical formula of $CH_3COCH_2CH_3$ where R is CH_3 and R' is CH_2CH_3.

- Terpenes

Terpenes are hydrocarbons based on isoprene ($CH_2=C(CH_3)-CH=CH_2$) units that can be arranged to form rings with a strong odour. They can be found in essential oils (aromatic liquid substances) that can be extracted from flowers, leaves, roots, fruits, wood, resins and are commonly used for fragrances in food, cosmetics, and personal care products

(Rodríguez-Maecker *et al.*, 2017). Terpenes can be formed by all kingdoms of life including prokaryotes, where β-pinene is an antimicrobial (antifungal, antibacterial) (Schulz-Bohm *et al.*, 2017) and d-Limonene exist in the citrus oil, dill oil, oil of cumin, neroli, bergamot, and caraway (The Danish Environmental Protection Agency, 2013).

- Aromatic hydrocarbons

Aromatics are hydrocarbons that have an aromatic ring (benzene ring) with 6 carbon and 6 hydrogen atoms. The mixture of benzene, toluene, ethylbenzene, and xylenes is commonly referred to as BTEX and benzene can be found in crude oil with similar smell to petrol.

- Volatile fatty acids

Are short volatile organic acids with carbon numbers from 2 to 9 with an unpleasant smell especially between C_4-C_9 (Rappert and Müller, 2005).

2.2.2 Odour characteristics

The sensory properties depend on *Odour Concentration*, *Intensity, Quality,* and *Hedonic Tone* (Environment Agency, 2007). The combined effect of these properties is related to the degree of nuisance that an odour can cause. It is a logarithmic relationship between the perception of intensity with the odour concentration, and some odours can enhance or suppress other odours. The odour threshold value is the minimum concentration required to be present for detecting odours (Churchill, 2006; Environment Agency, 2007; Rappert and Müller, 2005).

2.2.2.1 *Odour Concentration*

EN 13725:2003 (European Standard for olfactometry) defines odour concentration as "the number of European odour units in a cubic metre of gas at standard conditions ($ou_E m^{-3}$)". This $ou_E m^{-3}$ is "defined as an odour concentration experienced equivalent to the response when exposed to a concentration of 40 µg/L n-butanol by volume (123 $\mu g/m^3$) and this concentration represents the odour threshold for a human individual with sensitivity comparable to the average in the human population" (Nimmermark, 2011). The odour unit is calculated from the number of times that a gas sample has to be diluted in order to be detected by a percentage of 50% of a group of people adequately trained for this purpose (a panel) (Environment Agency, 2007; Nicell, 2009).

2.2.2.2 *Odour Intensity*

According to the German Standard Olfactometry Determination of Odour Intensity (VDI 3882 Part 1, 1992), odour intensity is how a person perceives the magnitude of an odour and it is determined by an odour panel of trained people. It is related to the impact the odour (odour intensity) has on the overall smell (Table 1) (Rappert and Müller, 2005).

Table 1: Odour intensity

ODOUR INTENSITY	LEVEL	ODOUR INTENSITY	LEVEL
Very Strong	5	**Weak**	2
Strong	4	**Very Weak**	1
Medium	3	**Not perceptible**	0

2.2.2.3 Hedonic Tone

The hedonic tone is the degree to which an odour is perceived as pleasant or unpleasant (Table 2). Such perceptions differ widely from person to person and are strongly influenced by previous experience and emotions at the time of odour perception. Table 3 shows examples of odours description and their chemical constituents can be used by panel to describe different odours.

Table 2: Classification for hedonic tone according to VDI 3882 part 2

HEDONIC TONE	LEVEL	HEDONIC TONE	LEVEL	HEDONIC TONE	LEVEL
Extremely pleasant	+4	**Weakly Pleasant**	+1	**Unpleasant**	-2
Very pleasant	+3	**Neutral**	0	**Very Unpleasant**	-3
Pleasant	+2	**Weakly Unpleasant**	-1	**Extremely Unpleasant**	-4

Table 3: Examples of functional groups, odour description and volatile compounds produced (adapted from Rappert and Müller, 2005)

Compound	Odour description	Volatiles
Acids	Pungent, sour, rancid	Acetic acid, propionic acid, butyric acid
Alcohols	Alcohol, pungent	Propanol
	Sweet	Ethanol
Alcohols	Fruit, balsamic	Pentanol
	Butter, pungent	Pentenol
	Green	1-Hexanol

Table 3 continuation: Examples of functional groups, odour description and volatile compounds produced (adapted from Rappert and Müller, 2005)

Aldehydes	Fruity, cherry, sour, sharp, pungent, bitter almond	Aliphatic aldehydes
	Tallowy, fat, green, citrus	Nonanal
	Tallowy, floral, lime, orange peel	Decanal
	Almond, nutty, grass-like	Benzaldehyde
Amines	Fishy	Histamine, dimethylamine, trimethylamine
Esters	Fruity	C2–C4 alkyl esters, long-chain fatty acids, methyl salicylate
	Fruity, berrylike, flora, pineapple	Ethyl acetate
Furans	Sweet, bitter, almond-like	3-Methyl furan, 2-penthyl furan
Ketones	Dairy, blue cheese, cheese, mushroom, rose	Methyl ketones, 2-alkanones, diketones
	Herb, butter, resin	Octanone
	Mushroom	3-Octanone
Lactones	Fruity, coconut, very sweet	γ -Octanolactone
	Nut, fat, fruit	γ-heptalactone
Pyrazines	Nutty, roasted, green, damp forest, potato-like	Various pyrazines
	Earthy	3-Methoxy-2-isobutylpyrazine
	Nutty, bready, sweet	2,5-Dimethylpyrazine
	Roasty, potato-like, musty, malt-like	2,3,5-Trimethylpyrazine
	Burnt coffee-like, musty, chemical	Tetramethylpyrazine
	Earthy, roasty	3,6-Dimethyl-2-ethylpyrazine
Sulphur compounds	Sulfidic, rotten egg-like	Hydrogen sulphide
	Sharp, green radish, cabbage	Dimethyl sulphide
	Decayed cabbage	Dimethyl disulphide, dimethyl trisulfide
	Potato-like, sweet	Methyl mercaptan
	Roasty (coffee)	Furfurylthiol
Terpenes	Soil odour	2-Methylisoborneol, geosmin
Terpenoids	Citrus, mint, musty, earthy, woody	Various terpenoids

2.2.3 Example of odorous compounds

One of the first papers relating odours characteristics with microorganisms was made on 1922 by V. L. Omelianski. The author described different aroma-producing microorganisms and the odour produced maybe from a general group of microorganisms or from a specific specie. These microorganisms can be found in the soil, water, hay, plants, and in milk. The accumulation of organic acids and alcohols can formed complex

esters like esters of acetic. Butyric and valeric acids were the most often acids produced by microoganisms (Omelianski, 1922).

Some studies showed that odorous compounds can modify the biological activity by promoting or inhibiting growth of neighboring organisms in their habit, especially between bacteria, fungi and plants interactions. These responses to VOCs can affect bacteria by modulation of antibiotic resistence, growth inhibition, growth promotion, increased secondary metabolite production, biofilm production, motility, virulence, and antibacterial (Schulz-Bohm *et al.*, 2017). According to Gallego *et al.* (2012), numerous chemical substances are responsible for several olfactory nuisances. The majority of these chemicals substances were VOCs and most VOCs are odorous substances. Some odours can be arranged by compound family; alcohols, aldehydes, aliphatic and cyclic hydrocarbons, aromatic compounds, esters, ethers, ketones, nitrogen-containing compounds, organic acids, oxygen-containing compounds, terpenes, hetero groups (Table 4).

In landfill sites the main odour compounds are styrene, toluene, xylene, acetone, methanol, n-butanone, n-butylaldehyde, acetic acid, dimethyl sulphide, dimethyl disulphide and ammonia, while MSWs had more oxygenated compounds and sludges more ammonia (Fang *et al.*, 2012). Rappert and Müller (2005) reviewed the odour emissions for agricultural operations and food industries by providing insight about the odour problem (e.g. challenge for odour detection, quantification, and identification the sources, ways of reducing or controlling the odour problem). Without a clear understanding of what odour is, how to measure it, and where it originates, it will be difficult to control the odour and select the best-suited odour treatment (Rappert and Müller, 2005).

In agricultural operations malodours come from livestock's operations and the application of biosolids or manure in the soil. Compounds such as VFAs, aromatic compounds (e.g. indoles and phenols), nitrogen-containing compounds (i.e. ammonia and volatile amines), sulphur-containing compounds (i.e., hydrogen sulphide and mercaptans) can be present from the degradation of proteins or carbohydrates by bacteria. Phenol, p-cresol, 4-ethylphenol, and phenylpropionate are products from microbial degradation of tyrosine (protein), while phenyl acetate and phenyl propionate from degradation of phenylalanine (protein). Degradation of tryptophan (protein) makes indole and indoleacetate and these two compounds are subsequently converted into 3-methylindole (skatole). Ammonia can be produced from urea, nitrates or from the deamination of amino acids by anaerobic bacteria. While volatile amines are made via

decarboxylation of amino acids at pH 5 to 6. Compounds with sulphur (hydrogen sulphide and mercaptans) are produced via sulphate reduction and metabolism of sulphur-containing amino acids (Rappert and Müller, 2005). Emission rates of odour from pig slurries were measured by GC-MS and olfactometry from liquid wastes with the main compounds identified were hydrogen sulphide, ammonia, phenol, 4-methyl phenol, 4-ethyl phenol and indole respectively (Hobbs *et al.*, 1998).

A study was made from the cooling gases of coffee bean roasting industry. The bioscrubber performs well for aldehydes and ketones (typical fat oxidation products) but not for heterocyclic compounds (e.g. pyridine, pyrazines, acetophenone, guaiacol).The amount remained almost unchanged and for some compounds (dimethyl disulphide, 3-hydroxy-2-butanone, carboxylic acids), it had an increased after bioscrubber treatment. For exhaust air of fat and oil processing it was studied a combined option for treatment (a bioscrubber, a biofilter, and an activated carbon adsorber), only small amounts of aliphatic, unsaturated, methylated, and cyclic alkanes and aromatic remained in the waste gas (Ranau *et al.*, 2005).

2.2.4 Challenges in odour measurement

Two fundamental challenges in this field are (i) identifying specific odorous compounds, particularly within environmental settings where numerous compounds could be present, and (ii) performing an accurate quantification of compounds once identified. The human nose can detect odours at very low concentrations, around parts per billion (µg/L) level, and most field available equipment cannot detect odours at that level. For some substances (e.g. limonene, mercaptan, ammonia, VFAs) it is only necessary for a few aromatic molecules to be present to create a smell. The odours can be pleasant such a perfume, but if the concentration of that perfume is high the smell that before was pleasant can transform into an unpleasant odour (Environment Agency, 2007).

The human nose is a useful tool to qualitatively detect/measure/analyse odours and its effectiveness has assisted human evolution to this day. However, when using human nose, the measurement can be subjective as some people can detect one specific smell while others cannot. So, the variance between results of a sensory-based test will reflect this variation in detector performance and is open to individual subjectivity. In addition, with time and repeated exposure to odorous compounds, some people can develop an adaptive capacity for the smells that they are exposed to, providing further potential variations in perception of odours (Environment Agency, 2007).

Table 4: Characterization of odour compounds in the different environmental field

STUDY	FIELD	*ANALYSIS / DETECTION*	FAMILY COMPOUND
(Gallego *et al.*, 2012)	Mechanical-biological waste treatment plant with AD	**TD–GC/MS**	Alkanes, Aromatic Hydrocarbons, Alcohols, Ketones, Halocarbons, Aldehydes, Esters, Acids, Terpenes, Organosulfur, Ethers, Furans, and Others
(Blazy *et al.*, 2015)	Pig slaughterhouse sludge composting and storage	**GC-MS**	Ketones, N-Compounds, S-Compounds, Alcohols, Aromatic Hydrocarbons, Aliphatic Hydrocarbons, Terpenes, S and N Compounds, Acids, Aldehyde
(Takuwa *et al.*, 2009)	Landfill	**Gas portable detector, detector tubes, GC-MS**	Siloxanes, Halogenated VOCs, Alkanes, Aromatic Hydrocarbons
(Fang *et al.*, 2012)	Landfill	**GC-FID/PFPG, SPME-GC-FID, HPLC**	Ammonia, Aromatics, Sulphur-Compounds, Oxygenated compounds, Amines, Fatty acids
(Qamaruz *et al.*, 2012)	FW	**Sensory analysis**	Ammonia and VFA
(Zhang *et al.*, 2012)	Mechanical-biological waste treatment plant with AD	**GC × GC FID**	Esters, Alcohols, Aldehyde, Ketones, Chlorinated, Alkenes, Aromatics, Alkanes
(Kleeberg *et al.*, 2005)	Waste gas from the fat refinery	**SPME, GC-MS, GC-FID/O**	Alkenes, Aromatics, Ketones, Aldehyde, Furans, Terpenes, Acids
(Blanes-Vidal *et al.*, 2009a) (Blanes-Vidal *et al.*, 2009b)	Swine Slurry	**Sensory analysis, GC-MS, gas detection tubes**	Alcohols, Aldehydes, Acids, Ketone, S-Compounds, N-Compounds, Terpenes, Aromatic Hydrocarbons
(Talaiekhozani *et al.*, 2016)	Wastewater collection and treatment systems	**N/A**	Mercaptan, S-Compounds, N-Compounds, Aldehydes, Phenol Compounds, Acids, Aromatic Hydrocarbons,

2.2.5 Measuring odours

For the identification of drugs and explosives based on their odour, it is recurrent the use of trained dogs, especially in airports. While the food & fragrance industries fall back on sensory panels to do olfactometric investigations (Liedtke *et al.*, 2018). Bockreis *et al.* (2005) advised that it is important to have different sampling methods depending on the types of source of the odour and the local conditions (Bockreis and Steinberg, 2005). The analysis of odours can be defined in two types: human sensory analysis (related with perception analysis) or molecular analysis (related with chemical behaviour).

2.2.5.1 Human sensory analysis (perception analysis)

Throughout history, humans have used their senses to evaluate and judge the quality of products and food. The nose was a valuable tool for detecting the presence of harmful microorganisms. To be analytical, the sensory analysis of a trained panel can focus on the description of sensory characteristics (descriptive tests) and on discrimination of slight differences (discriminant analysis, for example, paired comparison – Table 1). An effective method is a hedonic tone where the panel classifies the odours as nuisance or annoyance (degree of pleasantness or unpleasantness) (Schiffman *et al.*, 2001). Aatamila *et al.* (2011) evaluated the correlation between odour perception & annoyance with self-reported physical symptoms (associations between waste odours and human health) in residents living nearby five waste treatment centres with composting plants. It was based on personal characteristics, odour exposure, and symptoms during the preceding 12 months, in a cold country as Finland. The results show the common symptoms reported related to odours were eye irritation, unusual shortness of breath or tiredness, hoarseness/dry throat, toothache, fever/shivering, joint pain or muscular pain (Aatamila *et al.*, 2011).

2.2.5.2 Molecular analysis (chemical behaviour)

For molecular analysis of odours, advanced instrumental techniques are necessary. Table 5 explains the operational principles of the different analytical instruments in the literature and their advantages and disadvantages. One of the golden and universal analytical standard techniques to identify chemicals is the GC-MS, while other techniques using sensors are often referred to as “electronic noses”.

Littaru (2007) compared the sensorial analysis with electronic noses and concluded that the combination of sensorial analysis and electronic noses are complementary to each other because electronic noses increase repeatability and reproducibility in the

measurement and sensorial analysis allows a descriptive analysis (Littarru, 2007). Sironi *et al.* (2007) believed that it is also possible to use electronic noses for environmental analysis (Sironi *et al.*, 2007).

Persaud (2017) reviewed the progress in electronic nose technologies, especially for hybrid systems combining biological odour-recognition elements with physical transducers for security, environmental and medical applications. Electronic noses present some limitations/problems such as calibration, data processing, sampling, problems of sensor drift (Persaud, 2017).

Rappert *et al.* (2005) said electronic sensor such as electronic noses still suffer from the influence of environmental fluctuations (e.g. humidity or temperature) on sensor base-lines or lack of sensitivity and need periodic calibrations (Rappert and Müller, 2005). Burlachenko *et al.* (2016) reviewed several approaches to sample handling for electronic nose technology based on headspace analysis, sample injection, system recovery, sample enrichment, dynamic separation and future trends in the field for complex mixtures (Burlachenko *et al.*, 2016). While Vásquez Quintero *et al.* (2016) developed an smart radio frequency identification label with inkjet-printed multisensing platform for environmental applications such as to measure ammonia concentration (Vásquez Quintero *et al.*, 2016). For measuring toxic gaseous compounds sensor arrays could be a reliable option (Matz *et al.*, 2005).

GC-MS needs a clean environment to work as a laboratory base, and for this reason, it is not suitable for monitoring *in situ* while electronic noses can present some issues with the reproducibility of results. For these reasons, a technique such as GC-IMS could be a suitable technique for the monitoring of AD processes, for which analytes can be measured. GC-IMS can be used to analyse complex matrices influence by multiple analytes. GC-IMS could be a superior technique in comparison with techniques such as NIR which are based on a correlation technique whose results can be influenced by an overload of signals from different molecules in the same spectral area. Another unavoidable obstacle is the complexity of NIR spectra, which necessitates the understanding of chemometric techniques in order to comprehend any correlative relationship between the generated spectra and the characteristics of the researched samples (Aouadi *et al.*, 2020). In this research, GC-IMS was used because it was thought to be a more robust fingerprinting approach in which molecules are separated based on retention time and drift time. GC-IMS can be calibrated using chemical standards to identify substances, without the need to use chemometrics tools at first instant. Aside from being a selective approach and allowing a direct analytic method.

Table 5: Comparison of different equipment for chemical analysis for volatile compounds

STUDY	EQUIP.	OPERATING PRINCIPLE	ADVANTAGES	DISADVANTAGES
(Baumbach, 2006; Blazy *et al.*, 2015; Kleeberg *et al.*, 2005; Márquez-Sillero *et al.*, 2011a; Tran *et al.*, 2015)	**Gas Chromatography-Mass Spectrometry (GC-MS)**	The GC column separates a complex sample into molecules when heated. Each molecule is separated based on the boiling point, column temperature, and affinity-solubility in the stationary phase. After the sample is separated, the equipment breaks each molecule into ionized fragments and detects these fragments using their mass-to-charge ratio.	GC/MS has high sensitivity, selectivity, reproducibility and is used for detecting trace elements. It can provide considerable information on the chemical compositions of samples and can be used for highly volatile compounds. Enables compound identification and quantification.	GC-MS is slow, expensive, with high maintenance and is not suitable for monitoring in situ. It needs a clean environment to run. Needs pure nitrogen or helium as carrier gas and vacuum. Requires a very "pure" sample and trained operatives.
(Baumbach, 2006; Denawaka et al., 2014; Garrido-Delgado et al., 2015, 2011; Vautz et al., 2006b)	**Gas Chromatograph-Ion Mobility Spectrometry (GC-IMS)**	The detection process is based on the drift of ions, at ambient pressure, under the influence of an external electric field. The compounds are separated by GC and detected in a Faraday plate. Thus, databases of ion mobility values allow the identification of gaseous analytes and run standards as well.	High sensitivity (µg/Lv/ pptv ranges) with low technical expenditure. High-speed data acquisition. Rapid on-site monitoring and compact and ambient air can be used as the carrier gas. Can measure complex sample matrixes (solids, liquids, gases) and does not need complicated sample preparation. An autosampler can be used for easy and precise injection. Tritium is less harmful than other ionization sources available.	Normally, is not used to identify unknown compounds. Cannot measure compounds with less proton affinities than water (for example, alkanes). The ability of IMS to operate under atmospheric pressure can also be a disadvantage if complex samples are analysed since they induce ion-molecule and ion-ion competitive reactions in the ionization chamber.
(Gallego *et al.*, 2012; Materić *et al.*, 2015; Rodríguez-Navas *et al.*, 2012)	**Thermal Desorption and Gas Chromatography-Mass Spectrometry (TD–GC/MS)**	TD–GC/MS has the same principle as GC-MS but first uses packed tubes to absorb and concentrate the sample. After this step, the tube is moved into a desorption oven and heated to promote thermal desorption of the mixture, into the headspace of the tube. Then, the headspace is sampled and used for GC-MS.	It allows a good chromatographic separation (sensitivity) and reliable identification of the target compounds (reproducibility). It can be used for quantification of a wide range of compounds at very low concentrations. The sample can be stored in tubes and analysed less than one month later. The method can separate very similar chemical compounds.	It is not suitable for real-time measurements or where fine time resolution is required. It can have difficulty in measure complex mixtures. It requires a sample preconcentration. High equipment costs and difficult to deploy in the field (i.e. is generally limited to laboratory analysis).
(Littarru, 2007; Sironi *et al.*, 2007; Tran *et al.*, 2015)	**Electronic noses**	Consists of a matrix of sensors and an informatics system of recognition, for classifications of odours and, mimics the human olfactory system.	Avoids the problem of synergic effects of mixed odorous substances. Other advantages such as simplicity, time-saving, economical aspect, and repeatability of the results, the sample can be analysed with a very low odour level and can measure hazardous chemicals when compared with the trained panel. It can be used for continuous odour monitoring.	It can be difficult to apply to complex samples, such as environmental samples. The equipment does not provide indications on the chemical composition of the sample. The equipment is sensitive to humidity or carbon dioxide, the instability of the sensor baseline that needs frequent calibration, sensor poisoning, and reproducibility.

2.2.6 Odour management and treatment technologies

According to Kleeberg *et al.* (2005), odorous emissions can include hundreds of chemicals, however only a small number of these compounds are responsible for the odour. They are frequently found at lower concentrations (such as ppb levels) and with lower thresholds (Kleeberg *et al*., 2005). The chosen odour treatment must take into account the physical, chemical, and biological properties of odours to treat. Odour management should be based on an odour assessment where it is recorded and characterised all actual and potential odour emission sources and by selecting the appropriated odour treatment technologies. A especial focus should be set on fugitive emissions, which may have an enormous impact on the overall odour problem. Most common treatment options are adsorption (e.g. with activated carbon, activated alumina, silica gels, zeolites), absorption (physical absorption; chemical absorption), biological waste gas treatment (e.g. bioscrubber; biotrickling filters; biofilter), waste gas incineration (e.g. thermal afterburners; catalytic incinerators; regenerative thermal oxidation), non-thermal oxidation processes (ozone, UV, non-thermal plasma) (Schlegelmilch *et al.*, 2005b).

2.3 GAS CHROMATOGRAPHY ION MOBILITY SPECTROMETRY

IMS alone will most likely not suffice for the identification of each analyte in a complex mixture because these complex mixtures can have similar mobilities. As a result, hyphenated approaches like GC, MCC, SPME, or MS can be employed to enhance the analysis of these complex real-world samples (Cumeras et al., 2015a).

2.3.1 Fundamental working principles of Gas Chromatography

Chromatography is an analytical method of separation and analysis of the elements present in a sample (which potentially contains a complex mixture of possible analytes) based on the boiling point of the molecules, the affinity of these molecules to the stationary phase that comprises a solid or a liquid bound to media packed within the column, and the differences in the speed which these elements travel through the stationary phase. The mobile phase refers to a liquid or gas that is used to carry the molecules of interest through the instrument (column) to the detector. If a liquid is used as a mobile phase then it is called High Performance Liquid Chromatography (HPLC), and if the mobile phase is gas then it is called GC (Bhardwaja *et al.*, 2016; Rouessac and Rouessac, 2007). GC is used for mixed samples where the elements can be vaporized or have high volatility (i.e. they can relatively easily be moved to the gas phase)

and the column must be matched to the chemicals of interest in order to ensure detection based on the interaction between the stationary phase and mobile phase, the dimension of the column, the separation efficiency, the temperature programming and flow of the carrier gas (Bhardwaja *et al.*, 2016; Rouessac and Rouessac, 2007).

2.3.2 Sample preparation for Gas Chromatography

The sample must have sufficient volatility (preferably at temperatures between 0°C to 260°C) to not contaminate the column or the instrument; be thermally stable because the temperature can influence the volatility of the analytes or deteriorate them. If the analytes cannot be vaporized, these molecules may have derivatization reactions that produce thermally stable products to be analysed with a reproducible method (Bhardwaja *et al.*, 2016). Ideally, from collecting a sample to its introduction to the detector, no sample preparation should be required in order to avoid altering the initial sample as this may lead to loss of volatile compounds or may at least introduce the potential for other human or analytical error. However, particularly when trying to identify or quantify low concentrations of substances in complex matrices, this is often not possible and some preparation steps are required. For example, some analytical methods rely on pre-concentrating the compound of interest (e.g. thermal desorption (TD, SPME)) or extract it from the matrix to remove the interference of other species. It is also a common requirement to have to dilute the sample in order to bring the analysis output into a range the equipment can detect without saturation. Sample preparation is one of the most important steps in developing a method because the main objective is to ensure that the sample that is introduced to the instrument is appropriate for analysis by the specified equipment (Rouessac and Rouessac, 2007; Tipler, 2013).

The SPME is a sampling and pre-concentration technique typically used prior to GC-MS analysis. The modified syringe is coated with fibres (extracting phase) to concentrate the sample within a predefined time range. Regardless of sample volume, the amount of analyte extracted is proportional to its concentration in the sample. The sampling procedure is considered complete when the concentration between the sample matrix and the fibre coating reaches an equilibrium (Pawliszyn, 2012). Following sample collection, the fibre is placed in the GC for thermal desorption and analysis. This method is a solvent-free sample preparation, is simple to use, economical and has good selectivity and sensitivity. However, characteristics such as calibrations, temperature, relative humidity, and flow velocity must be carefully evaluated when sampling (Cruwys *et al*., 2002; Kleeberg *et al*., 2005). This technique has already been applied to measure odourous gases from a landfill (Davoli *et al*., 2003), to characterize odours from an

industrial fermentation (Yang *et al*., 2019), to measure odours before and after treatment in a fat refinery (Kleeberg *et al*., 2005), to detect the influence of anthocyanins on VOCs metabolites in faeces and urine (Tian *et al*., 2021), to measure VOCs metabolites from Listeria bacteria (Taylor *et al*., 2017), and to detect gram-positive and gram-negative bacteria (Ramírez-Guízar *et al*., 2017).

The materials required to be analysed in this thesis are, in the most part, complex mixtures of organic materials at varying stages of anaerobic degradation. They can therefore potentially contain a broad range of substances at a wide range of concentrations. In order to separate the target compounds (predominantly volatile and semi-volatile compounds) from this complex matrix, a headspace technique was used to extract the substance of interest from the unwanted substances in the sample. Solvents could be used to extract these volatiles, however, they are expensive, toxic and after use, they create chemical waste, and their use places limitations on the applicability of the final method in terms of health and safety. Once the sample has been prepared such that it is physically and chemically compatible with the analytical technique, the sample analysed by the instrument is subject to the next phase of analysis i.e. the separation of compounds of interest from the sample matrix.

2.3.2.1 Headspace (incubation conditions)

Headspace sampling is a thermo-physical technique that separates volatile or semi-volatile compounds from a solid or liquid matrix to headspace. It can be used to ensure that only target, or at the very least compatible chemicals are introduced to the instrument column and detectors to avoid damage (Tipler, 2013). Burlachenko *et al.* (2016) defined headspace as “the gaseous/vapour medium formed because of evaporation from surface of the object (placed in a hermetic container) that is in equilibrium with it” (Burlachenko *et al*., 2016). Some chemical and physicochemical proprieties of compounds influence the analysis, such as boiling point, vapour pressure, polarity, solubility, water partition coefficient, Henry’s law constant, and acidity (Agapiou *et al*., 2013). Compound transfer between the liquid phase and a gaseous phase is defined as the concentration of that compound in each phase relative to the equilibrium concentration between the phases by Henry's Law. The concentration of a gas dissolved in a liquid is directly proportional to the partial pressure of that gas above the liquid's surface at constant temperature. Factors such as temperature or pressure have the greatest influence on the adsorption-desorption equilibrium of compounds in the headspace (Burlachenko *et al*., 2016). Heating and stirring the sample allows the rapid transfer of volatiles and semi-volatiles to the headspace where they are available for

introduction to the instrument (Tipler, 2013). The evaporation process is affected by temperature because Henry's constants have distinct temperature dependencies, therefore their ratio in the gas phase will change at different temperatures. As a result, the same compound measured at different temperatures could be measured as a different compound (Burlachenko *et al*., 2016).

The hydrophobicity and hydrophilicity profile describes an analyte's proclivity to "prefer" a non-aqueous environment over an aqueous environment or vice-versa. The majority of chemicals that dissolve in nonpolar solvents are nonpolar and may have high vapour pressures. As a result, while water molecules are polar, hydrophobic substances tend to be nonpolar and hence prefer other neutral molecules and nonpolar solvents (Eiceman et al., 2016). Chemical reactions in an anaerobic reactor's liquid phase yield a wide spectrum of weak acids, bicarbonate, and ammonia. The solution involves a two-way reaction where the chemical species dissociate into the conjugate base and the H^+ion or H_3O^+. The system is considered to be in dynamic equilibrium when the concentrations of its components do not change over time due to the fact that both forward and backward reactions occur at the same rate. The H^+ concentration is determined by the overall functioning of the system. At pH 7 the water (H_2O) molecules are in equilibrium with the acid (H^+) and the base (OH^-). When the pH rises over 7, the ammonium $(NH_4^+$ dissociates, releasing gaseous ammonia. When the pH falls below 7, the acid (R-COOH) dissociates into R-COO$^-$ and (H^+) (Mata-Alvarez, 2003). Lowering the pH and adding acidifying salts can increase the concentration of acid compounds in the headspace (Cruwys *et al*., 2002), whilst raising the pH can increase the concentration of basic compounds in the headspace.

Figure 3 is a representation of the headspace sampling for a sample (liquid), where in Figure 3A is the initial movement of molecules and Figure 3B after to achieve the equilibrium between the two phases. The most volatile chemicals (in the picture represented in red) tend to leave the liquid phase in the sample and enter the gas phase (headspace). Less volatile molecules will stay in the liquid phase (in the picture is representing in yellow). Raising the temperature and agitation will reduce the time that the molecules require to enter the gas phase, and will result in a broader range of volatiles and semi-volatiles being present in the headspace (depending on characteristics such as boiling point and partial pressure). If high concentrations of compounds are present, an equilibrium between liquid and gas-phase concentrations can be reached.

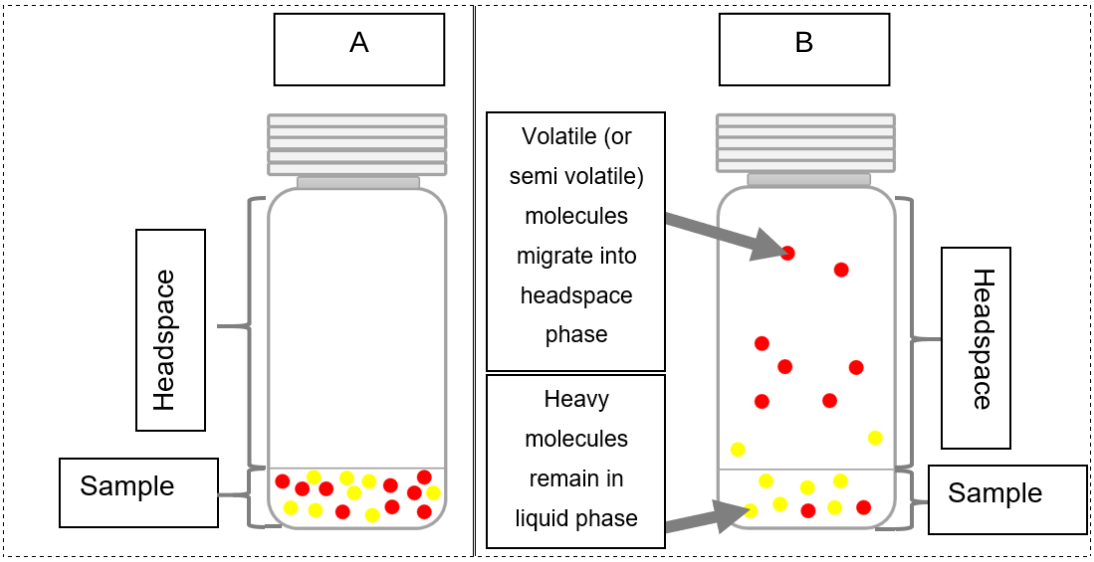

Figure 3: Depiction of separation of volatiles and semi volatiles to headspace prior to analysis, (A) prior to heating and agitation, (B) with heating, agitation and introduction the sample in a sealed vial

To summarise, the target of using different sample preparation processes is to improve VOC detection and reproducibility by altering sample ionic strength, polarity, or solubility, resulting in a higher concentration of VOCs in the gaseous phase. Adding salts, bases, acids, freeze-drying techniques, altering the phase ratio (the ratio of sample volume to gas volume in a vial), and using SPME fibres all contribute to influence the performance of sample analysis using GC-IMS (Aggarwal *et al*., 2020).

2.3.3 Sample injection, column and carrier gas for Gas Chromatography

The sample introduction can be done by a manual syringe injection or using an autosampler. The manual syringe injection uses a gastight syringe, where it is possible to manually introduce the sample directly to the GC column. The syringe used has a plunger and a high performance Teflon tip. Using this method, the sample is not diluted with a carrier gas. However, the manual injection does present some challenges. The manual injection would require a manual collection of the gas sample from the headspace of the sample vial containing the solid / liquid source material, followed by manual transfer and injection of the collected gas to the column injection port. This process has the potential to introduce errors associated with human error and a result of the potential lack of homogeneity of the introduced samples between duplicates, for example. In the automated gas syringe injection, the autosampler ensures the homogeneity of the introduced samples, reduces errors associated with manual

injection, therefore, improving reproducibility, and can operate automatically providing time savings for the operator.

The most frequent type of column used on GC is a capillary column (stationary phase coats the inside of the column) or a packed column (stationary phase coats packing material within the column). Compound separation is based on interactions between the mobile phase and the stationary phase. The separation and detection process is influenced by physical (internal diameter, length, film thickness, and stationary phase) and parametric (temperature and flow velocity) column variables. Columns with a small internal diameter but with long column length offer better separation and resolution, but require longer runtimes due to their lower possible maximum flow rate, when compared to larger internal diameter columns. This is due to the ability of these columns to accommodate higher flow rates and a greater sample loading capacity (Rahman *et al*., 2015). Columns can be classified from non-polar, intermediate polar, polar, highly polar to extremely polar (Rahman *et al*., 2015). In this study, the polarity of the column stationary phase ranges from low polarity (e.g. SE-54 column) to high polarity (Nukol™ fused silica column). When the stationary phase and analyte polarities are similar, then the attractive forces are strong, allowing for good separation of compounds. For example, a polar column will provide high performance when used to separate polar compounds, whereas a non-polar column will separate non-polar molecules. Therefore, a Nukol column (polyethylene glycol) will work effectively polar compounds such as alcohols, acids, ethers, esters, amines, and thiols. The carrier gas is an inert gas under the conditions encountered within the column and detector, and typically either nitrogen, hydrogen, or helium are used. The gas can be supplied using bottles with gas regulators or using a nitrogen generator.

2.3.4 Identification of volatile organic compounds on GC using the Kovats' retention index

Zellner *et al* (2008) explained it is important to create a standardized system to determine the retention data for the identification of chemicals in GC, and the retention index (RI) values are a valuable parameter/tool (Zellner *et al.*, 2008). The RI is used to convert the retention times into constants which are independent to the operating conditions (like applied linear velocity, temperatures, phase ratio, and column length) with the exception of the stationary phase polarity (Rodríguez-Maecker *et al.*, 2017; Zellner *et al.*, 2008). To calculate the RI, a series of chemical standards that behave like the compound of interest in terms of retention time are used to create a uniform scale on which the compound of interest can be positioned (Zellner *et al.*, 2008). The comparison of RI from

unknown chemicals with available retention data databases is a common tactic in the confirmation of compound identification because they are easy to use and interpret. Babushok *et al.* (2011) said using a small and reliable RI database, would enhance significantly the identification for essential oil constituents (Babushok *et al.*, 2011).

2.3.5 Fundamental working principles of IMS

Ion mobility spectrometry is the "characterization of substances from the speed of swarms (defined as ensembles of gaseous ions) derived from a substance, in an electric field and through a supporting gas atmosphere" (Eiceman *et al.*, 2016). The carrier gas (nitrogen) brings the compounds extracted from the sample to be ionized in a chamber (reaction region or ionization region) (Fig. 4A). The ionization process is based on a soft chemical-ionization originated by a low-radiation source such as tritium (Fig. 4B). Inside the drift tube and after the formation of ions, in the reaction region, they are exposed to a shuttered slit that opens and closes for a few milliseconds to allow the passage for a drift region, creating a barrier that makes the chemicals leave at the same time from the reaction region to the detector (faraday plate).

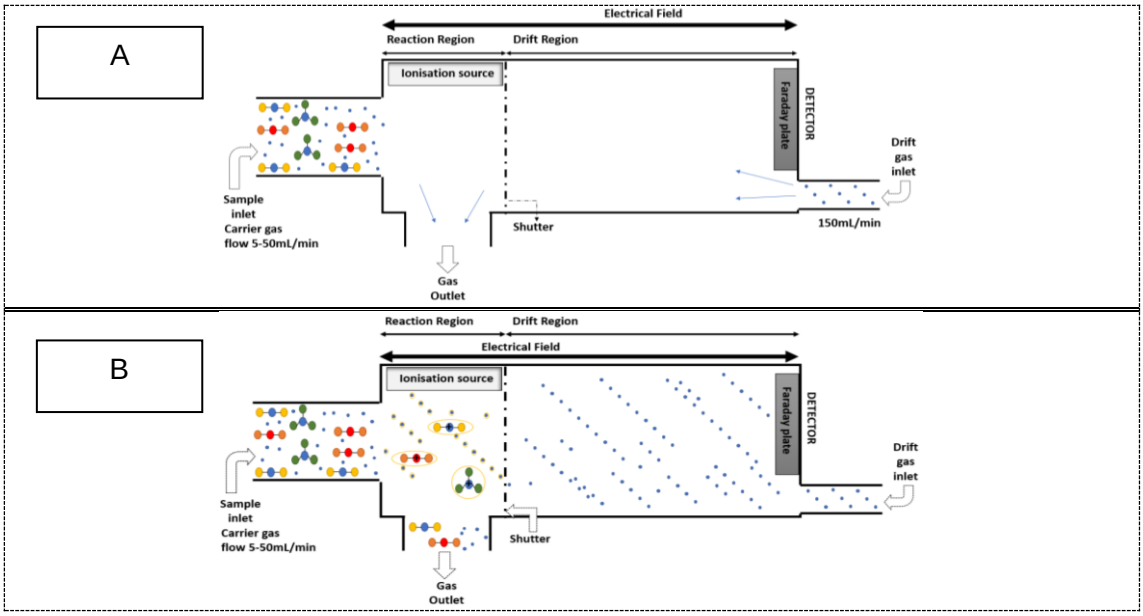

Figure 4: Schematic of drift tube for ion mobility spectrometry with a reaction region and a drift region both under an electrical field, the ion shutter, the faraday plate and the inlet for the sample and drift gas (flowing in the opposite direction from the detector) and gas outlet (A) three types of the neutral sample coming from the column are introduced into the ionization region, (B) the soft ionization process that occurs in the drift tube

When the ions are at a low concentration, they will have similar behaviour as the drift gas itself but when they become exposed to an electrical field, they will be accelerated

by this electrical field and pass through the gas into the direction of the field. While the ions are moving in the direction of the field, they will suffer collisions with the drift gas, these collisions will slow them down, and these ions will, therefore, have a lower drift velocity. Larger ions endure more collisions because they are physically bigger than small ions, so their drift velocity and mobility are generally slower when compared with small ions. The mobility itself is related to the size and shape of the ion in the gas phase and so is dependent on the structure, as well as the mass, of the ions (Fig. 5).

The ions were differentiated based on the study of their movement in an electric field, using a drift tube detector as a function of time

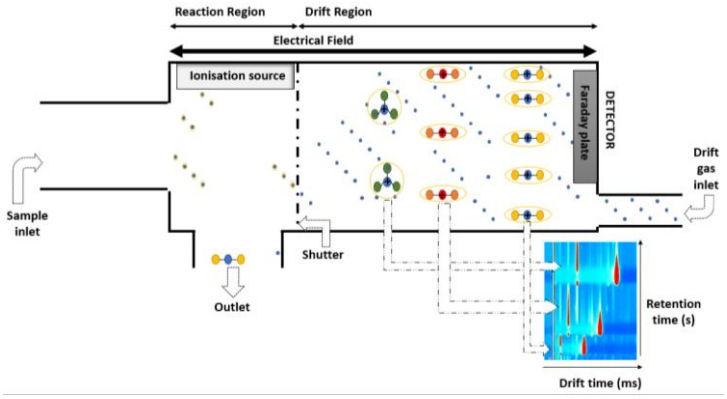

Figure 5: Schematic of the drift tube where sample molecules were ionized. Ions are injected using a shutter into the drift region and there are separated according to their mobility

Because this mobility is related to the structure of the ions, it is possible to differentiate between particles that have the same mass/charge but different shapes, like isomers. However, Borsdorf *et al.* (2011) said "the differences in ion mobility spectra of isomers can arise from the formation of different ions and not from differences in shape or size" (Borsdorf *et al.*, 2011), and even Puton *et al.* (2008) said the velocity of ions was proportional to the mobility coefficient (Puton *et al.*, 2008). The charge plays an important role in mobility because if the ion has more change than others, it will be deflected more in the electric field within the drift tube (Fig. 4) (Baumbach, 2006; Denawaka et al., 2014; Garrido-Delgado et al., 2015, 2011; Vautz et al., 2006b).

The signal is expressed in terms of voltage units and as a function of time. It is measured by an electrometer, a Faraday plate, where the ion swarm is neutralized and generates a current in a scale of picoamperes (Fig. 4) (Arroyo-Manzanares *et al.*, 2018). In summary, the ions are subjected to an electrical field and fronting a drift gas (nitrogen), the ion swarm moves at different speeds depending on his size/shape/charge/weight (m/z) mass/geometric structure from colliding with the drift gas molecules until arriving at the detector allowing the detection of volatile and semi-volatile compounds.

2.3.6 Ion formation on IMS

The ion formation can be made from several ways, such as by beta radiation (nickel or tritium), photoionization & laser ionization, corona/partial discharge ionization, surface ionization and electrospray ionization (Borsdorf *et al.*, 2011). The ionization process can be gained using a soft chemical-ionization initiated by a low-radiation source as tritium (H^3) or nickel (^{63}Ni), or by using a 10.6eV UV-lamp. In the low-radiation source, the mechanisms of ionization go through several stages, including primary ionization, and the chemical ionization of the sample components through a series of a cascade of reactions ion-molecule (Waraksa *et al.*, 2016). Denawaka *et al.* (2014) believed that the hydroxonium ion ($H^+(H_2O)_n$) is the key to the understanding of the chemistry involved in the generation of monomers (analyte molecule+proton), dimers, and trimers (Denawaka *et al.*, 2014) and for Borsdorf *et al.* (2011) beta sources can produce several reactant ions from in hydrated forms, such as NH_4^+, NO^+, and H_3O^+; that is, $NH_4^+(H_2O)_n$, $NO^+(H_2O)_n$, and $H_3O^+(H_2O)_n$ (Borsdorf *et al.*, 2011). The ionization process within the GC-IMS happens when nitrogen (N_2), is ionized by beta radiation from the ionization source (tritium) known as primary ionization (Equation 1). The ionization is based on the emission of primary electrons, which collide with nitrogen. Then, the ion will react with the water molecules to form reactant ions described as $H^+(H_2O)_n$ (Equation 2), through a series of ion–molecule reactions. The Reactant Ion Peak (RIP) representing the total of all ions available to react with the sample, in other words, it is the reservoir of electric charge, which can be transferred for ionization of analyte molecules, and normalized the areas. The water arises from the carrier gas (which is not fully dry) and the drift gas. “The quantity of water molecules (n) is determined by the gas temperature and the level of moisture in the gas atmosphere within the analyser's region with the ion source” (Cumeras et al., 2015a).

$$N_2 \rightarrow \beta \rightarrow N_2^+ + \beta' + e^-$$

Equation 1: Nitrogen ionization by beta radiation

$$N_2^+ + H_2O \rightarrow H^+(H_2O)_n$$

Equation 2: Formation of reactant ion through beta emitters in the air at ambient pressure and in absence of a reagent gas

In equation 3, M is the sample or analyte molecules, $H^+(H_2O)_n$ is a positive reactant ion, $MH^+(H_2O)_n$ is a cluster ion and $MH^+(H_2O)_{n-x}$ is a product ion (the protonated monomer), which is made by the shift of adducted water, making a product ion. The reaction from equation 3 determines transformation efficiency of molecules of a given compound into

ionic products. The protonated monomers or proton bound dimmers or trimers depend on the concentration of the sample to be formed.

$$M + H^+(H_2O)_n \rightarrow MH^+(H_2O)_n \rightarrow MH^+(H_2O)_{n-x} + (H_2O)_x$$

Neutral sample — Reactant ion — Cluster ion — Product ion (protonated monomer) — Water

Equation 3: The reactant ions collide with analyte molecules (M), which leads to the proton transfer reactions

When the concentration of the analyte M increases, a second product ion can be made because of another neutral sample connected to the protonated monomer, moving a water molecule and making a proton-bound dimer $M_2H^+(H_2O)_{n-x}$ (Equation 4). Dimers were made by a dimerization reaction that is an addition reaction in which two molecules of the same compound react with each other to give the adduct, otherwise the final product was specified as proton bound cluster (Puton *et al.*, 2008). Trimers (or even higher ions) are possible to be made, notwithstanding, in some cases, their decomposition is too rapid to allow measure their mobility in the drift tube. The positive reactant ion will react, by chemical ionization, with the sample and generates protonated species, which are separated on the basis of their mass, shape, size, and charge by the electric field in the drift tube.

$$M + MH^+(H_2O)_n \rightarrow M_2H^+(H_2O)_{n-x} + (H_2O)_x$$

Neutral sample — Product ion (protonated monomer) — Proton bound dimer — Water

Equation 4: The formation of dimers

It is also possible to produce negative ions (Equation 5). A sample (M) reacts with a negative reactant ion and $MO_2^-(H_2O)_{n-x}$ is a product ion. The equation 3 explain how the machine works in positive mode and the equation 5 how the machine works in negative mode (Denawaka *et al.*, 2014; Eiceman *et al.*, 2016; Garrido-Delgado *et al.*, 2011; Waraksa *et al.*, 2016).

$$M + O_2^-(H_2O)_n \rightarrow MO_2^-(H_2O)_n \rightarrow MO_2^-(H_2O)_n + (H_2O)_x$$

Neutral sample — Negative reactant ion — Cluster ion — Product ion — Water

Equation 5: The product ions were formed in negative polarity by association of a molecule (M) and an oxygen anion

The formation of the product ions depends on several parameters like, for example, the physical and chemical properties of each analyte, their concentration and the equipment performance and design (Criado-García *et al.*, 2015). The reactions happening on GC-

IMS are led by kinetic and thermodynamic mechanisms. The yield of the reaction is described by so-called collision rate constant and the reaction equilibrium constant describes the concentration of ionic reaction products and processes of ion production were thermodynamically controlled (Puton *et al.*, 2008). Most of the ions formed by IMS was through a multistep reaction chain with several chemical reactions by proton transfer (involves to transfer a proton from a hydronium ion $H^+(H_2O)_n$ to the molecule of the analyte), or charge transfer or nucleophilic attachment (Márquez-Sillero *et al.*, 2011a). However, the dominant process of product ion generation is through proton transfer (if the sample have a greater proton affinity (PA) than that of the RIP) (Creaser *et al.*, 2004) and the other mechanisms of ionization (e.g. processes of adduct formation or charge transfer) to ionize compounds with low PA values (Waraksa *et al.*, 2016).

Creation of positive analyte ions

- **Proton transfer**

  $(H_2O)_xH^+ + M \rightarrow MH^+ + {}_xH_2O$

- **Charge transfer**

  $(H_2O)^+ + M \rightarrow M^+ + H_2O$

- **Nucleophilic attachment**

  $(H_2O)_yNO^+ + M \rightarrow MNO^+ + {}_yH_2O$

The PA is a significant parameter for the efficiency of chemical ionization, when the RIP collide with the analyte molecule. PA is a parameter, which defines the probability of reaction and it is related to energetic effect of proton transfer reaction (Puton *et al.*, 2008). For compounds with lower PA, such as ketones or alcohols, the efficiency of chemical ionization is based on the PA, and the process of creation of their ions is controlled thermodynamically. However, for compounds with a high value of PA, (for example, higher than 840 kJ/mol), such as ammonia, amines, or organophosphates. For these chemicals, the ionization efficiency is already high so it is not based on the PA value (Waraksa *et al.*, 2016).

In the case of benzene and phenol, Criado-García *et al.* (2015) explained the process for the creation of these ions. It all started when it appears a compound with a higher proton affinity than water (697 kJ/mol), for example benzene (750.4 kJ/mol) or phenol (817.3 kJ/mol) in the ionization chamber to be ionized. The RIP signal intensity will decrease in the spectrum because the benzene ion or phenol ion had a higher ion mobility than the cluster ion $H^+(H_2O)_n$. The amount of $H^+(H_2O)_n$ depend the constant equilibrium (for clustering and declustering reactions), water concentration and drift gas temperature. When the concentration of H_2O is low, the main proton present is $H^+(H_2O)_n$, however if the concentration increase, then it is possible to have $H^+(H_2O)_2$. This ion has a proton affinity of 808 kJ/mol and can be a problem for the ionization of benzene. The authors believed benzene ions can react with NO^+, from a charge transfer reaction. In

the case of phenol, the authors believed the molecule had an easier ionization reaction occurred due to its higher proton affinity where the MH^+ ion was formed by a proton transfer reaction (Criado-García *et al.*, 2015).

2.3.7 Dopant effect on IMS

For the purpose of improving the detection quality, some substances (e.g. admixtures or dopants or shift reagents or gas modifiers) are added to the gases passing through the detectors, especially introduced into drift gas or in the carrier gas or in drift tube's atmosphere, to interact with the analyte. This action can interfere with the formation of ions or to control mobility coefficients or avoid the ionization of interfering chemicals. These substances can improve the ionization of analytes with low proton affinities, and consequently, to promote the photoionization. The term "gas modifiers" refers to substances that can change the mobility of ions without altering the chemistry of the ionization and a "dopant" a substance that changes the course of the ion-molecule reaction occurring in the detector (Gaik *et al.*, 2017; Waraksa *et al.*, 2016).

When just the carrier gas flowed through the system without any sample, the so-called reactant ions (RIP) are generated (because the primary ionization and some ion–molecule reactions), nevertheless, when exist a presence of a dopant substance, the reactant ions are so-called **alternative reactant ions (ARI).** They are built from dopant molecules or their fragments, and they are different from RIP ions and they react and interact with the sample in a different way than the RIP by changing the course of the ion-molecule reaction. Equations 6 (a proton transfer reaction) and 7 represent the production of ARI for monomer and dimer. D is the dopant, $H^+(H_2O)_n$ the reactant ion, $DH^+(H_2O)_{n-1}$ the ARI monomer, H_2O the water molecule, $D_2H^+(H_2O)_{n-1}$ the ARI dimer (Waraksa *et al.*, 2016).

$$D + H^+(H_2O)_n \leftrightarrow DH^+(H_2O)_{n-1} + (H_2O)$$

Dopant Reactant ion ARI Monomer Water

Equation 6: The formation of monomer for the dopant

$$D + DH^+(H_2O)_{n-1} \leftrightarrow D_2H^+(H_2O)_{m-1} + (H_2O)$$

Dopant ARI Monomer ARI Dimer Water

Equation 7: The formation of dimer for the dopant

While equation 8 and 9 show the interaction between the ARI and the analyte sample and the process of forming the analytes ions. M the neutral sample, $DMH^+(H_2O)_{n-1}$ the

asymmetric dopant dimers, $M_2H^+(H_2O)_{n-1}$ the dimer analyte ion (Hill *et al.*, 2004; Waraksa *et al.*, 2016). For the purpose to improve the selectivity of the detection of certain compounds, it is common to use compounds, such as ammonium, or acetone and higher ketones, or chloride as AIR (Waraksa *et al.*, 2016).

$$\underset{\text{ARI Dimer}}{D_2H^+(H_2O)_k} + \underset{\text{Neutral sample}}{M} \leftrightarrow \underset{\text{Asymmetric dopant dimers}}{DMH^+(H_2O)_k} + \underset{\text{Dopant}}{D}$$

Equation 8: Process of forming the analyte ions

$$\underset{\text{Asymmetric dopant dimers}}{DMH^+(H_2O)_k} + \underset{\text{Neutral sample}}{M} \leftrightarrow \underset{\text{Dimer analyte ions}}{M_2H^+(H_2O)_k} + \underset{\text{Dopant}}{D}$$

Equation 9: Process of forming the analyte ions

Hill *et al.* (2004) summarised the reason why to use these chemicals. Mainly, the ion products produced with the dopants are more stable than without them; it shifts the peaks in the drift-time spectra to be easy to detect the analyte of interest and to avoid the overlap of peaks; and, the dopant can interact with analytes but not with the interfering chemicals by creating extra peaks in the spectrum (Hill *et al.*, 2004).

2.3.7.1 Ammonia

When ammonia is used as a dopant, it can make clusters based on the NH_4^+ ion. This hydrated ammonium ion ($NH_4^+(H_2O)_{n-x}$), which is the ARI, normally transfers the proton only to the compounds who had a bigger PA than it. Equation 10 shows the formation of hydrated ammonium ion ($NH_4^+(H_2O)_{n-x}$), were created in the process of proton transfer from hydronium ($H^+(H_2O)_n$) to ammonia molecule (NH_3). If the concentration of ammonia continues to grow, then it is possible to have a dimerization reaction where it is created a hydrated dimer ammonium ion $[(NH_3)(NH_4)(H_2O)_{n-x}]^+$ (see a representation of this on equation 11). This has been applied for detection of drugs or chemical weapons or explosives (Waraksa *et al.*, 2016).

$$\underset{\text{Dopant}}{NH_3} + \underset{\text{Reactant ion}}{H^+(H_2O)_n} \leftrightarrow \underset{\text{ARI Monomer}}{NH_4^+(H_2O)_{n-x}} + \underset{\text{Water}}{(H_2O)_x}$$

Equation 10: The formation of monomer for the dopant (ammonia)

$$\underset{\text{Dopant}}{NH_3} + \underset{\text{ARI Monomer}}{NH_4^+(H_2O)_{n-x}} \leftrightarrow \underset{\text{ARI dimer}}{[(NH_3)(NH_4)(H_2O)_{n-x}]^+} + \underset{\text{Water}}{(H_2O)_x}$$

Equation 11: The formation of dimer for the dopant (ammonia)

2.3.7.2 Application of the dopant

Recently, research has been improving the detection limits and creating an effective and optimal method on GC-IMS (Eiceman *et al*., 2016). Some studied the application of dopant substances. Cheng *et al.* (2017) used 2-butanone as dopant-assisted positive photoionization to improve the detection of biogenic amines, especially for trimethylamine (TMA), getting LODs of 1µg/L in standards. This technique was applied on real food, such as oyster or shrimp because TMA is a good indicator of food spoilage due to its volatility and fishy odour. The biogenic amines, as TMA result from enzymatic and microbial degradation of amino-acids (Cheng *et al*., 2017). Another application of dopants is in the CWA field (Satoh *et al*., 2015). In the food and quality control field, Li *et al* (2019) used a dopant-assisted in positive mode based on fingerprinting analysis with chemometrics to identify and classify green tea aromas and compare it with sensory evaluation by a human panel. Acetone was used as dopant in this research and the results obtained could help in the process monitoring during tea manufacture (J. Li *et al*., 2019).

Jiang *et al.* (2018) performed a trial experience with six patients, where it was monitored online the anesthesia depth, using propofol (an analgesic) as analyte and toluene as dopant gas to remove the interference of sevoflurane, from breathing out of patients. To eliminate the moisture from exhaled breath, a time-resolved purge introduction was used as sample preparation and a dopant-assisted photoionization positive ion mobility spectrometry (DAPI-PIMS) as detection technique. The study was improved to get a selective and sensitive method with detection range for propofol from 0.2 µg/L to 45 µg/L (Jiang *et al.*, 2018).

Shahraki *et al.* (2018) tried to improve the detection of explosives by having a new negative ionization source with a thermal ionization and assisted by doping chlorinated hydrocarbon molecules. To produce the AIR, it is adding a dopant-assisted chlorinated compound (e.g. CCl_4) and in contact with the heating element, it can produce Cl^- reactant ions. The technology works with air samples so it can improve the development of a portable IMS-based detector of explosives in the air, such as TNT (Shahraki *et al.*, 2018).

To improve the recognition and the limits of detection for aromatic compounds with lower PA, Gaik *et al*. (2017) tried a dopant (NO_x) because the LODs were strictly depend on the ionization of the analyte. In this study, three aromatic compounds were used with lower PA (benzene, toluene, and toluene diisocyanate) and two compounds with high PA (dimethyl methylphosphonate and triethyl phosphate). In conclusion, by adding the

NO_x dopant the LODs decrease for the lower PA but did not affect the detection of others compounds with high PA (Gaik *et al*., 2017).

The ammoniacal nitrogen residue represent the sum of ammonia and ammonium compounds and it is one of the big challenge for environmental field because it can kill many aquatic organisms. It appears from several sources (e.g. as cattle excrement, waste incineration, sewage treatment, and car exhausts, fertilizers, industrial emissions, and volcanic activity) and it is relevant to have a quick method to measure it. Jafari *et al.* (2008) determinate ammonia using corona discharge ion mobility spectrometry with an alternate reagent gas (pyridine), in water samples, getting good results (LOD 9.2×10^{-3} µg/mL, with linear dynamic range from 0.03 to 2.00 µg/mL and 11% for standard deviation) (Jafari and Khayamian, 2008).

2.3.8 Identification of volatile organic compounds on IMS

Combining pre-separation techniques (GC) with IMS improves IMS's ability to detect individual compounds in complex combinations. As a result, each analyte is associated with two parameters: a specific ion mobility value and the time necessary to elute from the column (or retention time). At a given temperature, pressure, column length, polarity, and flow rate, this value is very unique to the analyte. Compounds in an unknown sample can be identified by incorporating these two values (Cumeras et al., 2015a). The identification of a compound using GC is based on the retention time compared with a reference compound database using the same experimental conditions (Rouessac and Rouessac, 2007) whilst for IMS, the separation is based on the specific drifts times that ionized compounds need to pass a fixed distance in the drift tube at ambient pressure, under the influence of a constant and external electric field, and be detected in a Faraday plate. To improve the resolution of the spectrum (due to peak overlapping subsequent from ion-ion or ion-molecule reactions in the ionization region) and the selectivity (especially for the detection of individual substances in complex mixtures), the compounds are previously separated by GC. Thus, databases of ion mobility values allow the identification of gaseous analytes based on the drift time of the ions because the drift time is specific from each ion. The peak height and the area correlated to the analyte concentration so it is likely to quantify it.

In the literature, it is possible to see data related to GC-IMS expressed as retention index, ion velocity as an arrival time (Rt retention time in seconds) or a drift time (Dt in ms) or drift time (normalized to RIP drift time) or it is normalized to standard temperature and

pressure as reduced ion mobility (K_0) or an inverse reduced ion mobility ($1/K_0$) (Garrido-Delgado *et al.*, 2015; Jünger *et al.*, 2012; Rodríguez-Maecker *et al.*, 2017).

The retention time and drift time are dependent on the analytical method, so to compare results between several studies the best option is using the K_0 or the $1/K_0$ because these results are not affected by operating conditions. Garrido-Delgado *et al.* (2015) and Jünger *et al.* (2012) presented their data using the Rt and K_0 while Rodríguez-Maecker *et al.* (2017) used the RI, Rt, Dt (normalized to RIP drift time). According to Babushok *et al.* (2011), the goal of creating The National Institute of Standards and Technology (NIST) database was to have a comprehensive and evaluated database of RI where exist nowadays more than 346757 data records for more than 70839 compounds (Babushok *et al.*, 2011). The software provides the compound name, the CAS number, the chemical formula, the molecular weight (MW), the retention index (RI), the retention time (Rt in seconds), the drift time (Dt in RIP relative; ms) of compounds already analysed and entered into the library. Using all this information is it possible to characterize the compound of interest more precisely without running chemical standards or using techniques such as GC-MS although it is recommended to do this to confirm the accuracy of the result (Rouessac and Rouessac, 2007).

2.3.8.1 Ion mobility

For ion mobility measurements, the time that an ion swarm takes to pass through the inert gas-filled drift region (ion cluster formation) from the ion shutter to the detector under the influence of an electric field is related to the mobility (K) of the ion (equation 12) (Kanu and Hill, 2008; Ruzsanyi *et al*., 2012; Vautz *et al*., 2009, 2006b).

$$K = \frac{\vartheta_d}{E} = \frac{\frac{d}{t_d}}{E}$$

Equation 12: Formula for mobility (K)

Where:

K is the ion mobility ($cm^2V^{-1}s^{-1}$);

d is the length of the drift region (cm);

t_d is the drift time (s);

ϑ_d is the velocity of the drifting ion;

E is the electric field (V/cm);

The reproducibility of the ion mobility measurement depends on the accuracy of the measurement for drift velocity and retention time. These two parameters are affected by

environmental conditions such as temperature and pressure and as such this can impact the identification of the analytes (Vautz *et al.*, 2009). For this reason, K is commonly normalized to the absolute temperature in Kelvin and pressure in Torr or Pascal, producing the reduced mobility coefficient (K_0) (Eiceman *et al.*, 2016). The reduced ion mobility (K_0) is calculated based on the drift time of each chemical, the machine parameters (electric field strength, length of drift tube), the pressure and the temperature as showing in equation 13. It is important to report the data as K_0 so as to be independent on instrument design, experimental setup or ambient conditions and to enable comparison with other IMS data (Cumeras et al., 2015b; Vautz et al., 2009, 2006b). In the literature, if the uncertainties were lower than 2% (~0.02 cm2V-1s-1) than it was accepted a published K_0 value to match one with another (Criado-García *et al.*, 2015).

$$\boldsymbol{K_0} = \frac{l}{tE}\left(\frac{T_0}{T}\right)\left(\frac{P}{P_0}\right); \text{ and } \frac{\mathbf{1}}{\boldsymbol{K_0}} = \frac{1}{\frac{l}{tE}(\frac{T_0}{T})(\frac{P}{P_0})}$$

Equation 13: Formula for reduced ion mobility (K0) and inverse reduced ion mobility (1/K0)

Where:

K_0 is the reduce ion mobility;

$\frac{1}{K_0}$ is the inverse reduce ion mobility;

l is the length of the drift region in cm;

t is the drift time in seconds and varies for each chemical being detected;

E is the electrical field strength (V/cm);

T_0 is the standard temperature;

T is the drift tube temperature (K);

P is a combination of drift tube and operational pressure (kPa).

P_0 is the atmospheric pressure;

2.3.9 Data-processing and chemometrics for IMS data

The output the equipment is export as a comma-separated values (CSV) file or a figure and using chemometrics such as Principal Component Analysis (PCA) help to understand better complex information related to the sample and extract the essential information from a large amount of data and clusters them according to their similar proprieties or to discover patterns or help to see where the data changes or to reduce data size ad help to process it. According to Szymańska *et al.* (2016), the disparity in IMS measurements associated with the use of different equipment from distinct manufactures is limiting advances in the field. However, this has led to the development and application of chemometrics for data analysis including data pre-processing and

pattern recognition (Szymańska *et al.*, 2016). When the signal intensity of the analyte is normalised to the intensity of the RIP, this helps to attenuate variations in the temperature and pressure that exist and that could lead to variations of the drift time of the analyte, and helps the reproducibility between different samples and conditions so it enables an inter-comparison between different measurements even from different devices with slightly different performance (Liedtke *et al.*, 2018).

2.3.10 IMS general development in time (1895 until the present)

2.3.10.1 The discovery and innovation period (1895 to 1960)

Since 1895 with the discovery of x-rays, it was possible to study the ionization in ambient air using radioactive ion source and, with this achievement, began the science behind the mobility of ions in different gases after electrical discharges in ambient air. By 1903, J. J. Thompson reviewed the principles and practices for all the ion sources used in IMS nowadays, and by 1938, was showing the ions were affected by temperature, pressure, moisture and gas purity. Later on, Langevin studied the influence on mobility from ion-neutral interactions that were affected by an electric field, while van de Graaff produced the first mobility spectrum with x-axis as drift time (ms) and y-axis as detector response (au). As well, Van de Graaff started the creation of ions shutters for the injection of ion pulses inside the drift tube and, later on, Bradbury improved it, known today as Bradbury-Nielson shutters. Lovelock findings were possible to correlate the presence of organic vapour in the air with the response in ionizing detectors and Mason, Albritton and McDaniel constructed and upgraded the drift tubes (Armenta et al., 2020; Cumeras et al., 2015a; Eiceman et al., 2016; Sorribes-Soriano et al., 2018a).

2.3.10.2 IMS as an analytical technique for the measurement of chemicals weapons, explosives, and illegal drugs (1960 to 1990)

Early 1960 started the study to apply this technology for the measurements of chemical weapons (CWA) and later, in the 70th by changing large laboratory instruments into more portable military-grade analysers was possible to commercialize this equipment for security purpose. Karasek developed a huge number of applications of the technique for abroad range of chemical families with a lower range of detection. In the 90th this technology was operating on-site for the detection of explosives and illegal drugs after two planes being destroyed and several lives were lost (Eiceman *et al.*, 2016; Vautz *et al.*, 2018a).

2.3.10.1 IMS as an analytical technique for abroad range of application (1990 until to the present)

Sorribes-Soriano *et al.* (2018) presented the evolution in publications from 1967 to 2017 related to the words “ion mobility spectrometry” and “plasma chromatography”, using data from Elsevier B.V. database. From 1967 to 1987 the main focus was on plasma chromatography with almost 100 papers published and it was kept constant until 2017. Ion mobility spectrometry started with very low publications achieved from 1967 to 1987 (average of 11 papers per year from 1967 to 1999) and had a slow increase from 1987 to 2007 but the situation changed in the last past 10 years with an exponential increase (Sorribes-Soriano *et al*., 2018a).

While Baumbach (2008) presented the same idea, where between 1985 to 1996 on average was accessible 12 papers per year and 26 average of papers per year between 1996-2000 and then it increased for 48 between 2001-2005 and 68 just between 2006-2007. The most common topics from 1983 to 2007 were IMS was applied and it is possible to see the main applications were explosives, chemical weapons, coupling IMS with MS but new topics were starting appearing, such as detection of SF_6 or breath analysis (Baumbach, 2008).

Related to the names of the journals, both authors agree that mostly the papers were published in the “Analytical Chemistry” and then followed by the “International Journal for Ion Mobility Spectrometry” (Baumbach, 2008; Sorribes-Soriano *et al*., 2018a). The data used to build Figure 6 was collected from the database “Web of Science” (WOS, BCI, BIOSIS, CCC, DRCI, DIIDW, KJD, MEDLINE, RSCI, SCIELO, ZOOREC) using the topic “ion mobility spectrometry”, consulted on 07/02/2020 to get the number of publication from 1975 to 2020. Between 1975 and 1999, on average 17 papers were published, between 2000 and 2009, 73 papers and between 2010 and 2019, 303 papers were published on average. Just during the two months of 2020 62 papers were published showing an increased interest in this technology (Clarivate, 2020).

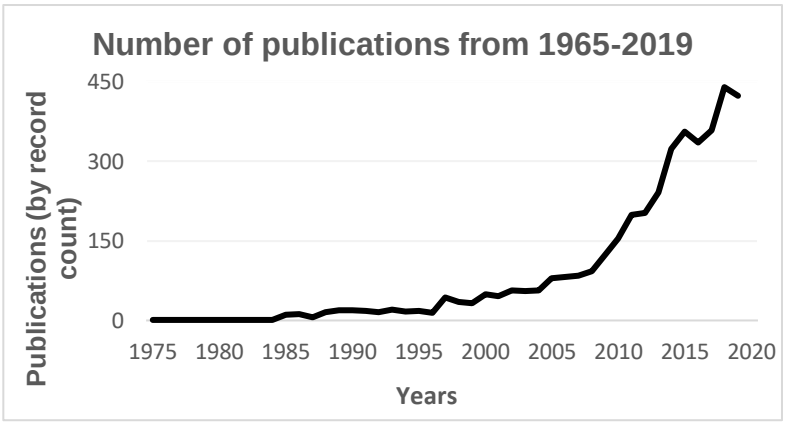

1975	1	**2001**	46
1983	1	**2002**	57
1984	1	**2003**	56
1985	11	**2004**	57
1986	12	**2005**	79
1987	6	**2006**	82
1988	16	**2007**	85
1989	19	**2008**	93
1990	19	**2009**	124
1991	18	**2011**	199
1992	16	**2012**	203
1993	21	**2013**	241
1994	17	**2014**	323
1995	18	**2015**	356
1997	43	**2016**	335
1998	35	**2017**	358
1999	33	**2018**	440
2000	49	**2019**	424

Figure 6: Summary of the evolution in research related to the topic "ion mobility spectrometry" from Web of Science

The equipment could be considered a versatile and universal analytical instrument for qualitative and quantitative applications in large and complex samples (e.g. chemical weapons, air, water, biological fluids and tissues, industrial solvents on superficies). This variety of samples need different sample introduction methods depending on the type of sample analysed. For example, vapour or gas samples from chemical weapons can be introduced from semipermeable membranes or by discrete sampling with a six-port valve. Thermal desorption or GC could be used for semi-volatiles compounds while electrospray nebulization for aqueous samples and direct analysis in real-time or desorption electrospray ionization for solid samples (Eiceman *et al.*, 2016). Section 2.1.4 includes further detail of the several applications for IMS, especially for GC-IMS.

2.3.11 IMS applications

The trend for the applications for IMS mainly started from military use (chemical weapons) and security purposes (detection of explosives, illegal drugs) after the early years of discovery. Notwithstanding, with the biological revolution by applying IMS in different fields as a modern analytical method (e.g. medical, food industry applications), the ability to make gas-phase ions directly from a liquid or solid samples and coupling a pre-separation technology as GC to IMS or coupling it to MS (IMS-MS), new fields began to appear and expanded his practicality application (Eiceman *et al*., 2016). Armenta *et al.* (2011) reviewed how IMS was applied for the pharmaceutical, food, medical, environment field, until 2011 (Armenta *et al*., 2011). In 2020, the authors conducted another review covering other topics such as illegal drugs, pesticides, explosives, chemical warfare agents and others (Armenta *et al*., 2020). While Wang *et al.* (2020) reviewed the most recent progress in food flavour analysis using GC-IMS (Wang *et al*., 2020).

2.3.11.1 Detection of explosives, chemical weapons

By 2006, more than 10 thousand IMS analysers were present at control posts in airports (all over the world), to detect trace-level explosives (e.g. NTO, HMX, TNT, RDX, and PETN in the air) due to their strong responses to IMS (Zolotov, 2006). This technology is being applied in routine luggage checks and for post-explosion settings because of the low detection range (µg/L level) that it could achieve, the reproducibility of the measurement and commercial instruments have been sophisticated to provide a high-speed response and a reliable measurement on-site (Ewing, 2001).

An improvement in this fields was made by Shahraki *et al.* (2018), where they developed a non-radioactive source that was suited to portable devices simple, long-lived, low-cost, and do not have the limitations of use as the radioactive sources, such as ^{63}Ni (Shahraki *et al.*, 2018). Matz *et al.* (2001) evaluated the interference of seventeen compounds that may compromise the accurate detection for TNT by IMS due to the false-positive results from the presence of a contaminant or a false negative response because a contaminant would decrease the IMS sensitivity and the explosive residue would go undetected. All compounds could be found in air pollution (alkyl-nitrated phenols), tobacco by-products, perfumes (musk compounds), and pesticides. Only seven of the seventeen compounds were detected by IMS but only one compound (4,6-dinitro-o-cresol) had similar mobility as TNT, but when the peaks overlapped, the drift time for TNT could be discriminated (Matz *et al.*, 2001).

One of the biggest challenges for these technologies is still increasing the detection reliability, reduce the frequency of false responses and limited detection capability. IMS was the most common technology used for chemical monitoring by the military besides other applications such as detection of chemical warfare agents (CWAs) and toxic industrial chemicals (TICs), illicit drugs and explosives (Sferopoulos, 2009). According to Eiceman *et al.* (2016) IMS offer one of the best responses for the detection of nerve agents based on organophosphorus compounds (Eiceman *et al.*, 2016)

2.3.11.2 Illegal drugs

To get an updated summary of the evolution in the combat drug trafficking, the Armenta *et al.* (2020) paper should be considered. The analytes were mainly cocaine and metabolites, heroin, cannabinoids and cannabinoids synthetic, fentanyl and his analogues, opioids derivatives, amphetamines, new psychoactive substance (NPS). Most of the studies used thermal desorption to pre-concentrated the VOCs for GC and

^{63}Ni as the ionization source. The injection temperature was most of the time above 200°C and the drift temperature between 25°C – 288°C, with LOD around µg to pg (Armenta *et al.*, 2020).

- New psychoactive substance

Until December 2017, more than 800 new psychoactive substance (e.g. amphetamine and cathinone derivatives, and synthetic cannabinoids) was introduce in the black market by the United Nations Office on drugs and crime (UNODC). This situation forced governments and competent authorities to find solutions to quickly detect trace amounts in the mail, imported articles, suspects clothing, luggage (e.g. airports). Furthermore, the UNODC recommended IMS as an analytical tool to detect illegal drugs in seized materials. The combined use of IMS and high-resolution mass spectrometry (HRMS) could be used for simple and rapid separation and identification of NPS in few milliseconds, getting LOD around 50-160 pg (Yanini *et al.*, 2018).

- Cannabis

Contreras *et al.* (2018) used thermal desorption-ion mobility spectrometry (TD-IMS) with chemometrics (principal component analysis with linear discriminant analysis, PCA-LDA) to distinguish several cannabis varieties plant from non-cannabis plants using their spectral fingerprint for the screening of cannabinoids after hexane extraction. The objective to use non-cannabis plants was to assess for false-positive responses and using chemometrics, PCA-LDA to cluster them in a different group to those of cannabis types. This method could be used as data reduction and pattern recognition in-field measurements because the equipment had rapid analysis time, simplicity, sensitivity, and portability. The author referred that hexane (672.5 kJ/mol) has a lower PA than water (691.0 kJ/mol), several signals from hexane that may interfere with the compounds of interest were detected, creating a loss of sensitivity and contamination of the detector. For this reason, nicotinamide (918.3 kJ/mol) was used as internal standard to increase the selectivity of the analysis but it reduced the number of the markers detected (Contreras *et al.*, 2018).

- Cocaine, amphetamine, and others

Other research has been done for detection of illegal drugs such as cocaine, amphetamine-type substances (Sorribes-Soriano *et al.*, 2019), in oral fluid (e.g. saliva) (Armenta and Blanco, 2011) has been widely studied besides in hand for THC (Sonnberg

et al., 2015) and contaminated air with cocaine (Armenta *et al.*, 2014) using different sample preparation (e.g. magnetic molecularly imprinted polymers (Sorribes-Soriano *et al.*, 2018b), molecular imprinting (Sorribes-Soriano *et al.*, 2017)) but mainly IMS with ^{63}Ni as the ionization source.

2.3.11.3 Biological and medical applications

Eiceman *et al.* (2016) and Chouinard *et al.* (2016) reviewed the IMS application for a clinical setting, like rapid disease screening (breath analysis, diagnosis of vaginal injection); the analysis of complex biological matrix; detection of metabolomics profiling for target compounds in human, bacteria, fungi; and characterization of biological macromolecules such as proteins (Chouinard *et al.*, 2016; Eiceman *et al.*, 2016).

- Breath analysis

During the last years, breath analysis had especially attention from the scientific community. The technique had the potential to be rapid, noninvasive sampling and investigated biomarkers for characterization of breath patterns for various disease states without the need of pre-concentration the sample or off-line collection (Chouinard *et al.*, 2016). Ruzsanyi *et al.* (2005) detected human metabolites using two polar columns (MCC-IMS OV-5 and a capillary column VOCOL), with ^{63}Ni as ionization source from breath analysis and compared it with a healthy person and a patient ill with a lung infection. The study reported reduced mobilities and detection limits for different analytes (Ruzsanyi *et al.*, 2005).

Baumbach *et al.* (2009) summarized an analytical method for metabolic profiling in humid air with the possibility to be used for breath analysis, improving the separation by using a multi capillary column where separated humidity from the analytes and ^{63}Ni as ionization source and this indicated that humidity can affect the ionization process for alpha-pinene (Baumbach, 2009). IMS was used to check the status of patients when they were doing real-time hemodialysis, using breath ammonia, as a biomarker for medical diagnosis of renal pathologies. Notwithstanding, breath ammonia could be used as evidence of renal impairment or for screening and diagnostic tools or real-time continuous monitoring hemodialysis efficacy and it could guarantee the adequacy of treatment for these patients (Neri *et al.*, 2012).

Szymańska *et al.* (2015) suggested using chemometrics (wavelet transform, mask construction, and sparse-PLS-DA) to do data size reduction for the classification of

breath and air samples using MCC-IMS (Szymańska *et al.*, 2015). Perl *et al.* (2010) applied a simple linear regression as an alignment procedure for retention time and ion mobility from MCC-IMS for measuring VOCs for breath analysis and the goal of the study was to create a universal correction procedure to increase the accuracy in the identification of peaks because small deviations in column temperature and carrier gas flow rate can affect the retention time (Perl *et al.*, 2010). While Bödeker *et al.* (2008) suggested using eucalyptol as a biomarker in breath analysis to reduce the data points to be detected in the different measurements, and with that, had a fast search in large databases (Bödeker *et al.*, 2008). Jünger *et al.* (2010) started creating a reference database to improve the identification of 16 compounds (e.g. ketones, terpenes, alcohols, aldehydes), using MCC-IMS and confirmed by TD-GC-MS, in breath analysis. This database reported $1/K_0$ for monomer and dimer (Jünger *et al.*, 2010).

- Breath and skin analysis

Mochalski *et al.* (2018) identify 17 VOCs, with LOD between 0.05–7.2 µg/L, emitted from the skin and breath under conditions that mimic entrapment. The author advises the creation of a library of retention and drift times, to help the identification and monitoring of VOCs released by the human body (Mochalski *et al.*, 2018). Other medical applications were the detection of volatiles metabolites from the skin at µg/L level. Compounds such as aldehydes come from fatty acids (e.g. oleic acid from skin sebum) by activity of UV radiation or bacterial lipid peroxidation. These compounds are part of body odour but other factors, such as consumed food, lifestyle, gender, environmental exposure, genetics and medication could affect the body odour. The author suggested octanal, nonanal, and decanal, were produce by the skin as volatile metabolites because their concentration increased for almost every person during the sampling period (1 hour) (Ruzsanyi *et al.*, 2012).

- Oral fluids analysis

Criado-García *et al.* (2016) improved the sampling for oral fluids by using a micro-solid-phase extraction (µSPE) with a mixture of sorbents of different polarities to extract toxic compounds (e.g. benzene, toluene, butyraldehyde, benzaldehyde, and tolualdehyde) present in saliva. Before running the samples, a desorption step was carried out in the headspace vials positioned in the device and it was possible to get LOD 0.38-0.49 mg/L (Criado-García and Arce, 2016).

- Urine analysis

Instead of using skin and breath VOCs, Rudnicka *et al.* (2010) suggested using human urine as an indication of human presence during rescue operations after earthquakes or other disasters. The author identified seven VOCs as fingerprint compounds (Rudnicka *et al.*, 2010). Jafari *et al.* (2011) proposed three-phase HF-LPME as sample treatment and ESI-IMS as an analytical tool to detect two tricyclic antidepressants (trimipramine and desipramine), in biological fluids (e.g. urine and plasma), getting LOD of 5 µg/L and a methodology that was novel, cheap, rapid, simple, with low detection limits and requiring small sample volume (Jafari *et al.*, 2011). Rister *et al.* (2020) reviewed the application of IMS with liquid chromatography for the detection of steroids and steroid isomers in human urine and serum samples but more research should be done on this field because these biomolecules can be used as biomarkers for detection of diseases or abuse in sports (medical and sports performance settings) and they are derivatives of cholesterol (it is a type of lipid) (Rister and Dodds, 2020).

- Pathogenic bacteria

Jünger *et al.* (2012) studied MCC-IMS as an advanced diagnostic method to rapidly detect pathogen bacteria, by their emitted VOC patterns which allowed progress for appropriate medical treatment, as soon as possible. The microorganisms were incubated during 24 hours on Columbia blood agar plates, at 37°C, after that the headspace of these cultures was analyzed by the MCC-IMS and results were validated by TD-GC-MS. The results showed a differentiation between different infecting pathogen at and their VOCs patterns. The study reported the identification using $1/K_0$ for monomer and dimer (Jünger *et al.*, 2012).

Thompson *et al.* (2018) used the headspace of suspension medium for detecting hydrogen sulphide (H_2S) as fingerprint signal from 61 pathogenic bacteria. In the study, the LOD obtained was 1.6 ng/mL, LOQ was 5.5 ng/mL, K_0 was 1.837 $cm^2V^{-1}s^{-1}$, using a static headspace multi capillary column gas chromatography ion mobility spectrometry (SHS-MCC-GC-IMS), in negative mode. The odour from hydrogen sulphide resembles a rotten egg even at low concentrations. In the anaerobic respiration, hydrogen sulphide is a by-product mainly from degradation of amino acids (e.g. cystine and cysteine derivative from proteins degradation), and thiosulfate and bacteria use sulphate as a terminal electron acceptor, instead of oxygen. Other by-products from cysteine degradation are pyruvic acid and ammonia and from thiosulfate is the sulphite (Thompson *et al.*, 2018).

For an immune-compromised people and pregnant woman, the presence of *Listeria monocytogenesis,* could be a high risk due to the potential of acquiring an infection, especially from food poison, because this bacteria is an opportunistic food-borne pathogen. Taylor *et al.* (2017) tried to differentiate between *Listeria monocytogenes* and *Listeria ivanovii*, from their VOC response to α-mannosidase activity (it is an hydrolytic enzyme), using GC-IMS and obtained good results (Taylor *et al.*, 2017).

2.3.11.4 Food production & industrial process

Nowadays, consumers are more aware of the quality (aroma, taste, appearance) and origin of the food products that they consume and, despite economic interests such as cost reduction and short duration of the production process, the quality of the final product should be guaranteed for the customer (Vautz *et al.*, 2006a). Currently, industries and universities are looking to apply advance instrumental analytical technologies to improve the quality and storage of food products, evaluation of freshness and spoilage, monitoring the production process, and detection of frauds and adulterations (Wang *et al.*, 2020).

- Olive oil

Garrido *et al.* (2011) investigated the performance of two types of IMS: a UV-IMS light (UV as ionization source) and a GC-IMS (tritium as ionization source) with chemometrics to classify 49 Spanish olive oils as one of three different grades (extra virgin olive oil (EVOO), olive oil (OO) and pomace olive oil (POO)), as a pattern or fingerprint. The GC-IMS got better results than the UV-IMS. The price of commercial olive oil can vary according to their quality, being the EVOO the most expensive one and GC-IMS can be used to get a global chemical volatile profile of the sample and confirm they have the correct label. Using the chemical structure of the molecules, some compounds may show a type of preferred response in one polarity over the other. According to the author, the GC–IMS could be used to classify olive oils according to commercial grade and detect situations of fraud (Garrido-Delgado *et al.*, 2011).

In another study, Garrido *et al.* (2012) used 98 olive samples to classify their origin based on chemical profile and sensorial analysis and 97% were classified successfully. It was identified by 8 chemicals successfully based on K_0. This technology could be applied as a reliable analytical screening technique to access the correct label of final product according to their quality (Garrido-Delgado *et al.*, 2012). Furthermore, continuing the research, Garrido *et al.* (2015) compare a capillary column (CC) and a multi capillary

column (MCC) performance to understand which provides better results for olive oil samples. The CC provided better results (92%) then MCC (87%), although the MCC had lower runtimes. A database for identification of olive oils was made by identifying 18 volatile compounds such as aldehydes, alcohols, ketones, and esters (Garrido-Delgado *et al.*, 2015).

Gerhardt *et al.* (2017) used GC-IMS with a temperature-programmed for the differentiate the geographical origin (Italy and Spain) of extra virgin olive oil samples, using VOCs as fingerprint and chemometrics such as PCA with linear discriminant analysis (LDA) and k-nearest neighbour. The results obtained provided a successful between the distinction between the oils from two different countries (Gerhardt *et al.*, 2017). While Contreras *et al.* (2019) used two different chemometric models for olive oil classification based on spectral fingerprint for non-targeted compounds and a targeted approach based on peak-region features (markers) from 701 samples. The spectral fingerprint chemometric approach provides better classification and validation for results but generates large-size data files with a laborious and time-consuming analysis and for this reason, the use of markers would be more advantageous for the oil industry (Contreras *et al.*, 2019).

Liedtke *et al.* (2018) improved the GC-IMS by adding to it a laser desorption (LD) to apply for semi and non-volatile compounds, besides the volatile compounds, from a liquid sample (e.g. olive oil). The runtime was 10 min with a possibility to be optimized for less than 2 min, with a detection range between 0-50 ng/g for decanal, limonene, 2-ethyl-1-hexanol, E-2-hexenal and using only 100 µL of olive oil. However, experimental setup should be optimised, in spite of LD-GC-IMS was lower run times than HS-GC-IMS because sample preparation is one most timing-consumable step in the analysis and for that reason the author suggested the use of LD. The composition of volatile of a sample is determined by compounds released from its surface which dependents on experimental conditions and the identification of these chemical signatures were made by TD-GC-MS, using standards. When the author compared the traditional HS-GC-IMS with the LD-GC-IMS, the last provided detection of more chemical signatures with better resolution.The author advises the creation of a database could be applied with the purpose of quality control in the food industry or oil authentication for fraud identification for food products or for other fields (Liedtke *et al.*, 2018).

- Other edible oils

Others studies were made for sesame oil by Zhang *et al.* (2016) where the author used IMS with chemometrics to detect adulterated and counterfeit sesame oils based on

fingerprints. The study distinguishes between pure sesame oil from adulterated sesame oil (cottonseed and soybean) (Zhang *et al.*, 2016). Chen *et al.* (2018) used GC-IMS with pattern recognition methods (histogram of oriented gradient and multiway principal component analysis) to detect adulteration of 147 samples of canola oil with other low price vegetable oils (e.g. sunflower, soybean, and peanut) and build a model for predicting the adulterated oil in canola oil. Aggregate the two pattern recognition methods, prove to be the best method for extraction of data and partial least square to predict more precisely a scenario of fraud in canola oil (Chen *et al.*, 2018).

In another research, GC-IMS was used for a rapid screening analysis by characteristic volatile fingerprints analysis to detect adulteration of crude palm oil by spiking it with residual oils (palm fibre oil and sludge palm oil). The author could detect the presence of seven VOCs from palm fibre and twenty-one VOCs from sludge in the crude sample. One reason for this procedure, in the industry, is to increase oil volume and consequently to increase the profit for the companies. However, adding the sludge palm oil to the crude palm oil, this product is not suitable for human consumption because of acids proprieties (Othman *et al.*, 2019).

- Cheese

Gallegos *et al.* (2017) used GC-IMS to identify four volatile metabolites from lactic acid bacteria to allow their differentiation during their growth, using their GC-IMS fingerprint with PCA. It can affect the aroma profile of many foods or help to detect rotten food. Lactic acid bacteria are commonly used in cheese making and influence in the flavour in dairy products because of their acidifying and proteolytic activities (for example, hydrolyse caseins in peptides or amino acids). Lipolysis is the breakdown of lipids (e.g. fats, oils, waxes, vitamins such as A, D, E, and K), by hydrolysis to make free fatty acids (VFAs), then these VFAs are oxidized to β-ketoacids and decarboxylated to ketones with one less carbon atom, thereby producing ketones compounds. Alcohols can be made by catabolism of amino acids, degradation of linoleic and linolenic acids, aldehyde reduction of lactose or lactate metabolism and the degradation of leucine (hydrophobic amino acid) producing 3-methyl-1-butanol that had the smell of fresh cheese. During the experience was measured the pH and the values decreased from 6.00 to 4.70 or 3.57 depending on the bacteria. This evinced the rapid consumption of carbohydrates and an accumulation of acids such as lactic or acetic acid. This technology can screen volatiles to control bioprocess on-line so it can be applied for process control in diverse industries during the fermentation or the maturation process (Gallegos *et al.*, 2017).

- Milk with different flavours and linseed oil with omega-3

Márquez-Sillero *et al.* (2014) studied the application of HS-GC-IMS to track back the production of undesirable fishy odours related to lipid degradation (e.g. from the oxidation of polyunsaturated omega-3 acids) that make the food putrid. The degradation of food products (e.g. fish oil) produce ketones, alcohols, and aldehydes that are derivatives from the decomposition of peroxides. The researched used milk with different flavours (cacao, fruits, cereals, and nuts), linseed oil (enriched with omega-3 acids), using hexanal, 2-butanone, acetone, and dimethyl sulphide as fingerprint profile for quality control. The authors concluded the storage conditions that affected more the milk samples was the light and the temperature for the linseed oil and the concentration of these fingerprints increased, during the 36 days, being the profile dependant on the presence of polyunsaturated omega-3 acids because when was not add anything to the milk, the IMS signal was kept constant during the 36 days while others milk with omega-3 increased the IMS signal (Márquez-Sillero *et al.*, 2014).

- Beer

Vautz *et al.* (2006) suggested using GC-UV-IMS to detect 2,3-pentanedione and diacetyl (diketone with an intense “butter-aroma” that occurs naturally in alcoholic beverages from enzymatic production of the amino acid valine or microbiological contamination or non-enzymatic oxidation of the beer) as key parameters for assessing the quality and deliver process control in the brewing of beer. This study could increase the productivity of the companies because by detecting fast the degradation of these chemicals, the fermentation process could finish early and saving time in the food production process (Vautz *et al.*, 2006a).

- Iberian ham

Currently, here is no technology to assess the authenticity of dry-cured Iberian ham products by detecting possible frauds in their labelling, and with this to detect agricultural food adulteration. The data gained comparing the two columns (a polar or non-polar) show the non-polar column had lower runtime than the polar column, which could be a good option for future research but no significant difference was found in terms of classification rate. GC-IMS can produce several data points, and for that reason, at the beginning, it was applied data processing such as MATLAB with the PLS Toolbox using the whole spectrum. After, a smoothing procedure (second-order Savitzky-Golay filtering), baseline correction and a reduction of the amount of data. The second strategy,

Arroyo-Manzanares *et al.* (2018) selected individual markers that appeared throughout the spectrum and processed it with PCA-LDA, OPLS-DA and S-plot. The second approach delivered better results with a classification rate of 100% but both approaches could be used to classify between acorn-fed ham and feed-fed ham samples (Arroyo-Manzanares *et al*., 2018).

Continuing the work done by (Arroyo-Manzanares *et al*., 2018), Martín-Gómez *et al*. (2019) focus on a non-destructive sampling method that involves using a needle (in the rump as the traditional method for olfactory system) to absorbs the fat (volatile compounds) from the ham to analysed by GC-IMS and chemometrics to not damage the physical integrity of the ham (Martín-Gómez *et al*., 2019) to differentiate pigs breed.

- Wines

Márquez-Sillero *et al.* (2011) used GC-IMS with single-drop microextraction (IL-SDME) as a pre-concentration step for detected 2,4,6-tricholoroanisole (2,4,6-TCA) in several red and white wines getting LOD 0.01 ng/L. When the 2,4,6-TCA concentration is between 10 to 40 ng/L it can affect the wine quality and consumer acceptance and it was found more in samples with cork stoppers then rubber or thread stoppers (Márquez-Sillero *et al.*, 2011b). However using HS-MCC-GC-IMS provided better results and getting concentration of 2,4,6-TCA 0.012 ng/L for wine (liquid sample) and 0.28 ng/g for the cork stopper (solid sample) (Márquez-Sillero *et al.*, 2012).

Li *et al.* (2020) studied the effect of alcoholic fermentation by doing a sensory evaluation, fermentation behaviour, basic composition, volatile profile and biogenic amine levels for raspberry wine. In the study, GC-IMS was used to understand the variation of aromas during the manufacture of wines. This technology can improve the quality of final products, getting the desirable organoleptic characteristics (aroma and taste) as process control. *Saccharomyces cerevisiae* yeast guarantees a rapid and reliable fermentation process, with a consistent product (uniformly plain taste and flavour) but *Torulaspora delbrueckii* yeast can improve the organoleptic characteristics for the final product. Most of the chemicals detected by GC-IMS were esters, VFAs, alcohols, aldehydes, ketones, terpenes (Li *et al.*, 2020).

- Fish

Biogenic amines (e.g. histamine, putrescine, cadaverine, tyramine, β-pheny ethylamine, spermine and spermidine) are byproducts with nitrogen compounds made from

decarboxylation of free amino acids during degradation of proteins that could be found in canned fish samples. To improve the detection of these compounds, without overlap of peaks and derivatization steps, Parchami *et al.* (2017) used headspace solid-phase microextraction with nanostructured polypyrrole fiber coupled to modified ionization region (18-crown-6 as complexation reagent into carrier gas) ion mobility spectrometry (HS-SPME-MIR-IMS). The extraction parameters were optimized for pH, salt effect, extraction time and temperature. Higher pH (at 12) presented better recovery than at lower pH (at 6) because at higher pH had less dissociation and were at non-ionic form. The temperature of the fibre to extract the compounds is one of key parameters so it was studied between 30-80°C and the optimum was at 60°C during 30 minutes. While the optimum concentration of the salt (NaCl) was at 3.5 mol/L. Using this methodology, the LOD was between 0.6 to 1 ng/g (Parchami *et al.*, 2017).

- White bread

Pu *et al.* (2019) used GC-IMS with chemometric and dynamic sensory analysis (temporal dominance of sensations – TDS) to characterize the aroma and the perception liberated from the chewing process of white bread and the key odorants. The most abundant chemicals presented were alcohols, VFAs and ester in the mouth. Ethanol detected concentration above 3300 µg/L and it was derivate from the fermentation of starch by yeast while others alcohols were generated by degradation of lysine or from lipid oxidation. The esters were produced during the fermentation as by-products of acetyltransferase reactions. The VFAs were derivated from fermentation and lipids oxidation and aldehydes produced as a byproduct from protein breakdown (leucine) while hexanal and heptanal were derivated from oxidation of unsaturated lipids. During the fermentation 2,3-butanedione was a byproduct produced through glycolysis of pyruvic acid and had buttery and creamy properties (Pu *et al.*, 2019).

- Other areas in the food industry and process control

In 2019, a few papers were published using GC-IMS to assess the quality of food products in the matrix, such as eggs (Cavanna *et al*., 2019), honey (Arroyo-Manzanares *et al*., 2019), pickled ginger (X. Li *et al*., 2019), and kumquats (Hu *et al*., 2019), for frauds and adulterations along the production chain. Cavanna *et al.* published a paper where the goal the study was to assess the possibility to use GC-IMS with chemometrics to be a fast, reliable, sensitive, cost-effective, simple method to inspect the freshness and age in eggs products based on markers identification (volatile fingerprint such as butyl acetate, 1-butanol, heptanal, dimethyl disulphide and dimethyl trisulfide). With this

procedure, it was possible to avoid that not fresh egg batches end up in the production lines for other food products.

Arroyo-Manzanares *et al.* (2019) used GC-IMS with chemometrics (orthogonal partial least squares discriminant analysis OPLS-DA models) to differentiate adulterations in honey due to the addition of corn syrup and sugar cane. In this study, pure broom honey was mixed corn or sugar syrup by different percentage (25%, 50%, and 75% adulterated) and compare it with pure broom honey, pure sugar syrup and pure corn syrup to trace fingerprint. It was possible to use two markers as fingerprint from honey and marker 22 as fingerprint of corn and sugar syrup. This fingerprint method can prove the presence of adulteration of the honey and when this method was applied for commercial honey, seven of nine commercial honey proved being adulterated (Arroyo-Manzanares *et al.*, 2019). Li *et al.* (2019) used GC-IMS with PCA and fingerprint chart method to determine the VOCs during the production of pickled ginger to improve the quality of the product and keep it longer storage. Sixty and four signal peaks were detected mainly alcohols, aldehydes, ketones, terpenes and esters and PCA distinguish between pickled ginger, fresh ginger and soy sauce. The amount of heptanal and heptanone reduce during the experience, while butanal, butanone and methional increased (X. Li *et al.*, 2019).

Hu *et al.* (2019) used GC-IMS with PCA and heat map to check the flavour in preserved fruit processing (candied dried kumquats) by atmospheric hot air drying and vacuum sugar osmosis, to compare it with fresh kumquats. The findings belong to terpenes, esters, aldehydes, ketones, and alcohol could be used as target key analytes. From previous studies, the essentials oils presented in the fruit were monoterpenoids and sesquiterpenoids. Therefore, terpenes were the major compounds, being limonene the larger chemical in this fruit. However, the findings showed 3-pentanone as the major component in fresh kumquats after 1-hexanol and Z-3-hexen-1-ol. In the vacuum process 2-hexen-1-ol, ethyl acetate and for atmospheric drying benzaldehyde and furfurol (Hu *et al.*, 2019).

2.3.11.5 Environmental applications

Przybylko *et al.* (1995) studied the viability of online monitoring aqueous ammonia by IMS by detecting the ammonia LOD (1.2 mg/L) and the range of linear was between 0-10 mg/L for calibration. The response of aqueous ammonia is dependent on the pH and ammonium ion concentration. The equipment technique could be used on laboratories or for continuous process monitoring applications (Przybylko *et al.*, 1995).

Li *et al.* (2002) the environmental application for IMS were detection of benzene, toluene, xylenes, and alkenes in environment, detection MTBE in ambient air or water, detection of alcohols using UV-IMS and for on-site and industrial application (Li *et al.*, 2002). In Hill *et al.* (2004) book, the application on the environmental field for IMS, was principally to monitoring different compounds (e.g. nitrate, nitrite, perfluorocarbons, organic compounds) present in environmental field samples (e.g. air, water and soil), besides the detection of proteins (Hill *et al.*, 2004).

Márquez-Sillero *et al.* (2011) revised IMS applications in the environmental field and some limitations such as the complexity of environmental samples or the challenge to measure target compounds (e.g. MTBE) due getting lower LOD could influence the equipment performance and the analysis. Moreover the machine limitations for selectivity and sensitivity (e.g. difficult to apply in complex matrices, the need to form gaseous ions, the humidity's influence, and the low limits of detection), the author presented some guidance to solve these issues with existing methods to improve future developments like techniques for extraction or pre-concentration of analytes, or coupling the equipment with others technologies (Márquez-Sillero *et al.*, 2011a).

Borsdorf *et al.* (2011) summarised for the industrial and environmental applications. They are: explosives (PETN, RDX, TNT, NTO, HMX), MTBE from water, ammonia in water, microbial VOCs from moulds (2-Methyl-3-buten-2-ol, alcohols, dimethyl disulfide, acetone, 2-methylfurane, ketones), toxic industrial (acetone, benzene, cyanogen chloride, DIMP, DPM, hydrogen cyanide, sulfur dioxide, TDI), sulfur-free odorant (methylacrylate, ethylacrylate), explosives in the hair (TNT, NG, EGDN, TATP), over-the-counter drugs and beverages (acetaminophen, aspartame, bisacodyl, caffeine, and further compounds) (Borsdorf *et al.*, 2011).

Armenta *et al.* (2011) reviewed the scientific literature for environmental applications of IMS focus on air quality, water & liquid samples, solids & aerosols for monitoring the quality of outdoor and indoor air, measure contaminants in water and discharge effluents, determine VOCs and semi-VOCs from potentially contaminated soil samples. In air quality was detected for VOCs, BTEX (mixture of benzene, toluene, ethylbenzene, and xylene) and inorganic compound (ammonia). While for water & liquid samples were analysed for VOCs (methyl tert butyl ether - MTBE), halogenated substances (tetrachloroethylene, trichloroethylene, trihalomethanes, chloroethenes, chlorobenzenes & aromatics, chlorophenols), pesticides (malathion, ethion, dichlorovos sevin, amitraz, metalaxyl, ethyl parathion, toluene, 2,4-diisocyanate, atrazine and ametryn) and inorganic compounds (nitrite, nitrate and ammoniacal nitrogen). For solids and aerosols

was observed for halogenated substances (chlorocarbons, gaseous VOCs), pesticides (malathion, atrazine and ametryn), VOCs (α-pinene) (Armenta *et al.*, 2011).

As Eiceman *et al.* (2016) said in his book, "Ion Mobility Spectrometry", environmental applications (environmental monitoring and testing) are still missing, although the analytical properties of IMS, could be an outstanding tool for this field, especially in-field measurements (e.g. brownfields, estuaries, or water-processing plants). The aim of this technology, for on-site measurements, could be a fast and viable alternative against the laboratory-based technique, although is not the reality nowadays. This could be related to the rigorously limits legal for portability or transportability of the radioactive ion source. However, there are some alternatives to deal with the ion source problem (e.g. electrospray ionization), but the scientific community is showing disinterest in this technology and no known ongoing applications have been evaluated (Eiceman *et al*., 2016).

For characterization of plant's metabolites pattern and their interactions with the environment and correlated it with the effect of climate change on ecosystem function & biodiversity and to discriminate plant taxa and their phenology, GC-IMS was used as analytical tool. The taxon-specific patterns were able to discriminate the nine plants in this study and chemicals such as terpenes (e.g. 3- carene, limonene, γ- terpinene) and aldehydes were presented but it was necessary to do further research (Vautz *et al.*, 2018b).

Chen *et al.* (2019) reviewed the fundamentals and applications (from 2000-2018) for ultraviolet radiation photoionization ion mobility spectrometry (UV-IMS) and further improvements, especially for, environmental contaminants, national defence (for trace explosives and chemical warfare agents detection), food safety & quality, and clinical diagnosis. For environmental contaminants, UV-IMS was applied for detecting the following chemicals acetone and BTEX (LODs 60 µg/Lv), in air; naphthalene and its derivatives MTBE in gas and solids samples (LODs between 50-100 µg/Lv to 0.49-1.21 mg/L); terpenes (LODs 1 µg/Lv) in humid air; hydrogen sulphide (LODs 23.7 ng/L) in sewage; polycyclic aromatic compounds (PCAs) in solid surfaces in air, glass surfaces in air and soils (LODs between mg/Lv to ≤ ng); chlorobenzene in water; chlorinated ethenes and chlorinated benzenes (LODs ≥ µg/L) in water (Chen *et al.*, 2019).

In terms of implementing the GC-IMS in real-time (on-line), the manufacturing company (G.A.S.) created an equipment called "GC-IMS-ODOR" for a reliable, automated, at-site, continuous on-line monitoring of methyl acrylate, ethyl acrylate, tert-butyl-mercaptan in

natural gas samples. And a “GC-IMS-SILOX” to measure linear and cyclic siloxanes (L2, L3, L4, L5, D3, D4, D5 and D6) from biogas present on landfills or other environmental plants like sewage plants.

2.3.12 Summary of GC-IMS parameters and methodology

Although GC-IMS is being applied successfully for different fields discussed previously, it has not been applied for a real environmental process, especially focused on the performance monitoring of AD processes including monitoring and controlling odours. A summary of applications of GC-IMS is presented in Table 6 for food, VOCs and environmental studies focusing on the type of matrix / sample, the analyte measured, the sample treatment, the analytical method, the identification of analytes, and the LOD and LOQ.

Table 7 presents LODs for difference substances from G.A.S. website, the manufacturer of the equipment (G.A.S, n.d.). This information could be a guideline to create a methodology for such complex samples as AD matrices related samples. Whilst IMS has also been known to have limited resolution; the standalone IMS analysis suffers from lack of specificity, so there is a need for some pre-separation technique such as GC; and it can only detect volatile compounds that are ionisable, some interfering compounds can take part in the proton transfer reaction, making the detection of the sample difficult (Jünger *et al*., 2012; Vautz *et al*., 2018a; Waraksa *et al*., 2016).

GC-IMS seems to have has also numerous analytical advantages. These include speed in data collection and with total separation times of several minutes and individual peaks several seconds wide (rapid detection). It can be coupled with preparation and gas-phase detection methods (e.g., chromatography), and various detection methods (e.g. mass spectrometry). It can be applied to online measurements, it can be used to analyse complex samples, seems to have high sensitivity, low cost, analytical flexibility, and real time monitoring capability, no vacuum was required, durability, reliability, inexpensive devices, power consumption, and potential for miniaturization and portability (Chouinard *et al*., 2016; Gallegos *et al*., 2017; Gao *et al*., 2014; Li *et al*., 2002; Liedtke *et al*., 2018; Márquez-Sillero *et al*., 2014; Rudnicka *et al*., 2010; Ruzsanyi *et al*., 2005; Vautz *et al*., 2018a).

Table 6: Application of IMS for food and environmental applications

Food production & industrial process						
Matrix / sample	**Analyte**	**Sample treatment**	**Method**	**Identification**	**LOD and LOQ**	**Ref.**
Beer	Diacetyl; 2,3-pentanedione	100 mL sample was heated at 60°C during 20 min and the carrier gas took the analytes into a 10 mL sampling loop to be introduced into the GC-column	**GC:** column Restek MXT-OV1 (size× I.D. 30m × 0.53mm, df 0.3µm film thickness), nonpolar at 30°C; carrier gas 100 mL/min; **IMS:** UV ionisation source; drift gas 300 mL/min; runtime 10 min	K value for ethanol diacetyl and 2,3-pentanedione	50 µg/L	(Vautz *et al.*, 2006a)
Milk with different flavours, linseed oil	Hexanal ($C_6H_{12}O$); 2-butanone; acetone; dimethyl sulphide [$(CH_3)_2S$]	5 mL sample was placed into a vial with 20 mL volume. After 15 min of incubation at 40°C, a syringe (80°C) injected 100 µL headspace sample into injector (80°C). Nine blank milk and linseed oil samples were spiked with the target compounds at concentrations between 0.3 to 200 µg/L.	**GC:** MCC column OV-1701MCC (length of 20 cm, ca. 1200 capillaries with an inner diameter of 40 µm, a film thickness of 0.2 µm, and 3 mm diameter) at 40°C, carrier gas 30 mL/min; **IMS:** tritium as ionization source, at 60°C; drift gas 500 mL/min; runtime 10 min	Spectrum (with Rt and Dt); graphic with IMS signature vs days of storage; concentration of analyte	**LOD** 0.3 µg/L ($C_6H_{12}O$ in milk) to 3.0 µg/L [$(CH_3)_2S$ in linseed oil) **LOQ** 1.1 µg/L ($C_6H_{12}O$ in milk) and 9.6 µg/L (for $(CH_3)_2S$ in linseed oil)	(Márquez-Sillero *et al.*, 2014)
Olive oil	(E,Z)-2,4-dodecadiene; 1-dodecene; (E)-2-hexanal; phenol; β-pinene; benzaldehyde; acetic acid; limonene; 1-hexanol; nonanal; 1-heptanol; octanal	**Laser:** at 22°C ± 2°C; laser light wavelength at 2940 nm; laser energy 0.4 J; repetition frequency 3 Hz; laser pulses 6; distance focal length-sample surface 60 mm; transfer line temperature 70°C; sample flow 100 mL/min at ambient temperature for 2 min, then re-activated for 6 s to fill the sample loop and sample volume 100 µL. **HS-GC-IMS:** 1 mL sample was placed into a 20 mL vial and flushed continuously with 100 mL synthetic air. Prior to analysis, the vial with the sample was heated to 40°C for 10 min.	**GC:** sample loop volume 1.1 mL at 60°C; 6-port valve temperature 60°C; Column MCC-OV5 (min polar) (length 200 mm), at 40°C; carrier gas 150 mL/min; for 10 min; **IMS:** ^{63}Ni, 550 MBq as ionisation source; drift tube length 120mm; drift gas 100 mL/min at ambient temperature and pressure;	Spectrum (with Rt and $1/K_0$); graphic with identification from GC-MS and normalised signal intensity in a.u. for 5 different types of olive oil	**LOQ** limonene (dimer), decanal, 2-Ethyl-1-hexanol (dimer) E-2-Hexenal (dimer) between 0 to 50 ng/g	(Liedtke *et al.*, 2018)
Iberian ham	Nona-2-one; octan-2-one; heptan-2-one; hexan-2-one; trans-2-octenal; nonanal; octanal	1 g of sample was placed into 20 mL vial and incubated at 70 °C for 20 min, then an automated autosampler collected 100 µL of headspace to inject in the injector port (80 °C) using a syringe (80°C)	**GC:** non-polar column SE-54-CB (size× I.D. 30m × 0.32mm, df 0.25µm film thickness), at 50°C; polar column DB-WAX of Agilent (size× I.D. 30m×0.25mm, df 0.50µm film thickness); at 80°C; carrier gas 5 mL/min; **IMS:** tritium as ionisation source heated splitless injector with 2mm ID, 6.5 mm OD×78.5mm fused quartz glass; at 65°C; drift gas 150 mL/min; drift tube length of 5 cm	Identification using GC×IMS Library Search; Rt, Dt, K_0, intensity	N/A	(Arroyo-Manzanares *et al.*, 2018)

Food production & industrial process						
Matrix / sample	**Analyte**	**Sample treatment**	**Method**	**Identification**	**LOD and LOQ**	**Ref.**
Iberian ham	28 chemicals from aldehydes, ketones, alcohols, esters and monoterpenes	Storage time was 5–7 days at −18 °C until analysis. 1 g of sample was placed into 20 mL vial and incubated at 80 °C for 20 min, then an automated autosampler collected 100 µL of headspace to inject in the injector port (80 °C) using a syringe (80°C)	**GC:** non-polar column SE-54-CB (size× I.D. 30m × 0.32mm, df 0.25µm film thickness), at 50°C; carrier gas 9 mL/min; **IMS:** tritium as ionisation source; at 50°C; drift gas 150 mL/min; drift tube length of 5 cm	Identification using GC×IMS Library Search; Rt, Dt, K_0, intensity	N/A	(Martín-Gómez *et al.*, 2019)
Environmental applications						
Matrix / sample	**Analyte**	**Sample treatment**	**Method**	**Identification**	**LOD µg/L**	**Ref.**
Heat transfer fluid (HTF) samples	Benzene, phenol	100µL of sample was placed into 20 mL vial and incubated at 35 °C for 5 min, then an automated autosampler collected 200 µL of headspace to inject in the injector port (80 °C)	**GC:** column (size× I.D. 30m × 0.25mm, df 0.5µm film thickness), at 40°C, carrier gas 10 mL/min; **IMS:** tritium as ionisation source; at 65°C; drift gas 250 mL/min;	Spectra, K_0	Benzene: LOD 0.011 g/L LOQ 0.038 g/L Phenol: LOD 0.004 g/L LOD 0.014 g/L	(Criado-García *et al.*, 2015)
Air samples and liquid from fermentation exhaust gas of erythromycin	VOCs 2-methylisoborneol (2-MIB), geosmin, hexanal, octanal, decanal, and benzaldehyde	Gas samples: 1 mL sample was injected into the injector port Liquid samples: sample was placed into 20 mL vial and incubated at 65 °C for 15 min, then an automated autosampler collected 500 µL of headspace to inject in the injector port (80 °C)	**GC:** FS-SE-54-CB column (size× I.D. 15m × 0.53mm, df 1µm film thickness), heated split less injector operated at 150°C, and the column at 40°C (carrier gas ramped 5-100 mL/min) for gas and condensation water samples and 60°C (carrier gas ramped 2-130 mL/min) for fermentation broth samples; **IMS:** tritium as ionisation source; at 45°C; drift gas 150 mL/min;	Identification using GC×IMS Library Search	Concentration: 2-MIB 30-150 µg/L Geosmin 25 to 55 µg/L	(Yang *et al.*, 2019)
Leaves from nine common herbaceous plant species	Plant volatile organic compounds (pVOCs)	3 g of the leaves plant was placed into 20 mL vial (at 60 °C), then the vial was flushed with a nitrogen as carrier gas of 100 ml/ min for 5 min, and introduced into the sample loop for 10 s	**GC:** OV-5 column at 40°C, carrier gas 100 mL/min; **IMS:** 500 MBq Ni^{63} as ionisation source; at 40°C	Fingerprint and pattern recognition of metabolites x	N/A	(Vautz *et al.*, 2018b)

Detection of VOCs especially for odours						
Matrix / sample	**Analyte**	**Sample treatment**	**Method**	**Identification**	**LOD µg/L**	**Ref.**
Essential oils (EO)	Terpenes	100µL of standard or 1000 µL EO or 5g for food, cosmetic, and personal care products was placed into 20 mL vial and incubated at 35 °C, for 5 minutes, then an automated autosampler collected 100 µL of headspace to inject in the injector port (80 °C)	**GC:** non-polar column SE-54-CB (size× I.D. 15m × 0.25mm, df 0.5µm film thickness), at 50°C; carrier gas 25 mL/min; **IMS:** tritium as ionisation source; at 50°C; drift gas 100 mL/min;	RI Rt Dt	N/A	(Rodríguez-Maecker *et al.*, 2017)
Sock	Foot malodour	Sample was placed into 20 mL vial and incubated at 95 °C, for 5 minutes or 10 minutes for ammonia, then an automated autosampler collected between 1.5-2.2 mL of headspace to inject in the injector port (80 °C) and 95°C syringe temperature	**GC:** OV-5 and Carbowax 20M between 30-70°C; carrier gas between 10-150 mL/min; **IMS:** tritium as ionisation source; between 45-60°C; drift gas 500 mL/min;	Rt Dt K_0	Between LOD 0.1-472 ng LOQ 0.4-1573 ng	(Denawaka *et al.*, 2014)
Air samples from wastewater treatment plants	VOCs	N/A	GC-IMS and dynamic olfactometry according to EN 13725	Fingerprint	N/A	(Vera *et al.*, 2016)
Standards	VOCs (α-pinene, limonene and acetone)	SPME (the desorption of the NTD at 255 °C for 2 min, using 0.2 mL of nitrogen during 20 minutes).	**GC:** size× I.D. 10m × 0.25mm, df 0.25µm film thickness); **IMS:** ^{63}Ni as ionisation source; between 111°C; drift gas 200 mL/min;	Rt Dt K_0	LODs < 0.7 ng	(Reyes-Garcés *et al.*, 2013)

Table 7: LODs from several substances adapted from G.A.S. website

Substance	LOD (µg/L)	Matrix	Mode	Substance	Detection limit (µg/L)	Matrix	Mode
1,2,3-Trichlorpropane	1	N_2	Negative	2-butanone	1	Tap water	Positive
Geraniol	100	Tap water	Positive	2-decanone	5	Tap water	Positive
2,3-diethyl-5-methylpyrazine	50	Tap water	Positive	2-dodecanone	5	Tap water	Positive
2,6 Dichlorphenol	10	Tap water	Positive/ Negative	2-ethyl-3,5-dimethylpyrazine	50	Tap water	Positive
2-heptanone	1	Tap water	Positive	2-hexanone	1	Tap water	Positive
2-methylbutanol	5	Tap water	Positive	2-nonanone	5	Tap water	Positive

Substance	LOD (µg/L)	Matrix	Mode	Substance	LOD (µg/L)	Matrix	Mode
2-octanone	5	Tap water	Positive	2-pentanone	1	Tap water	Positive
3-methylbutanol	5	Tap water	Positive	3-octen-1-one	5	Tap water	Positive
4-Ethoxy-1,1,1-trifluor-3-buten-2-on	0.5	N_2	Negative	Acetaldehyde	1	Tap water	Positive
Acetic acid	20	Tap water	Positive	Acetone	1	Tap water	Positive
Acrolein, Propenal	5	N_2	Positive	alpha-Pinene	100	Tap water	Positive
Benzaldehyde	10	Tap water	Positive	Benzene	50	N_2	Positive
Butanal	1	Tap water	Positive	Butylacetate	1	Tap water	Positive
Butyric acid	50	Tap water	Positive	Carbon disulfide	200	Methane	Negative
Carbonyl sulphide	5	N_2	Negative	Cymene	50	N_2	Positive
Decamethylcyclopentasiloxane	2	N_2	Positive	Decamethyltetrasiloxane	2	N_2	Positive
Decanal	5	Tap water	Positive	Diacetyl	< 20	Tap water	Negative
Diethylether	1	Tap water	Positive	Dimethylbenzene	50	Ambient air	Negative
Dimethylsulfate	0.5	Tap water	Negative	Dimethylsulfide	50	N_2	Positive
Dodecamethylpentasiloxane	3	N_2	Positive	Ethanol	5	Tap water	Positive
Ethyl mercaptane	5	N_2	Positive	Ethyl-3-methylbutanoate	1	Tap water	Positive
Ethylacetate	1	Tap water	Positive	Ethylacrylate	1	Tap water	Positive
Ethylbenzene	50	N_2	Positive	Ethylene glycol	20	Tap water	Positive
Ethylhexanoate	5	Tap water	Positive	Fluorbenzene	10	N_2	Negative
Geraniol	100	Tap water	Positive	Guaiacol	100	Tap water	Positive
Heptanal	5	Tap water	Positive	Hexamethylcyclotrisiloxane	3	N_2	Positive

Substance	LOD (µg/L)	Matrix	Mode	Substance	LOD (µg/L)	Matrix	Mode
Hexamethyldisiloxane	3	N_2	Positive	Hexanal	1	Tap water	Positive
Hydrogen sulfide	5	N_2	Negative	i-Propanol	5	Tap water	Positive
Isoamylacetate	3	Tap water	Positive	Isobutylacetate	1	Tap water	Positive
Isoprene	100	Tap water	Positive	Iso-Propyl mercaptan	200	Methane	Negative
Isovaleric acid	50	Tap water	Positive	Limonene	100	Tap water	Positive
Linalool	100	Tap water	Positive	Methanol	0.2	N_2	Positive
Methyl mercaptane	5	N_2	Positive	Methylacrylate	1	Tap water	Positive
m-Xylene	20	N_2	Positive	Myrcene	100	Tap water	Positive
n-butanol	5	Tap water	Positive	n-decanol	5	Tap water	Positive
Nitrogen dioxide	5	N_2	Negative	n-octanol	5	Tap water	Positive
Nonanal	5	Tap water	Positive	n-pentanol	5	Tap water	Positive
n-Propanol	5	Tap water	Positive	Octamethylcyclotetrasiloxane	5	N_2	Positive
Octamethyltrisiloxane	3	N_2	Positive	Octanal	5	Tap water	Positive
o-Xylene	20	N_2	Positive	Pentanal	1	Tap water	Positive
Phenol	50	N_2	Positive	Propanal	1	Tap water	Positive
Propionic acid	20	Tap water	Positive	Propylene glycol	20	Tap water	Positive
p-Xylene	20	N_2	Positive	Styrene	10	N_2	Positive
Sulfur dioxide	10	Ethylene	Negative	tert.-Butylmethylether	0.5	Tap water	Positive
tert-Butyl mercaptan	5	Natural Gas	Positive	Tetrahydrothiophen	5	Natural Gas	Positive
Toluene	25	N_2	Positive	Trimethylpyrazine	50	Tap water	Positive

3. METHODOLOGY DEVELOPMENT FOR GC-IMS

3.1 INTRODUCTION

This chapter describes the logical and systematic development of a method to measure the samples of interest using GC-IMS. To achieve the objective of creating a methodology, some questions that define what the methodology should achieve should be considered first (Table 8). In order to develop an analytical method, in particular for gas chromatography, it is important to consider several aspects: the sample (sample preparation, dilutions); the method of injection of the sample into the equipment (using an autosampler, manual injection), the type of column (using the right GC column for the application, and control the physical parameters such as the temperature or the flow gas), and the carrier It is important to acknowledge that parameter such as environmental temperature, storage conditions, the time between sampling and/or analysis, and matrix effects have an important role in the analysis.

Table 8: Initial definition of the method

Question	Consideration	In the thesis
Should the method focus on qualitative or/and quantitative analysis	GC-IMS allows a qualitative analysis using the peak position in the spectrum and quantitative analysis from the peak intensity;	Figure 14
Is it possible to identify unknown chemicals	Running standards or looking in databases (e.g. NIST) is possible to identify unknown chemicals based on retention index, retention time, drift time, reduced ion mobility and/or inversed ion mobility;	See chapter 4 for more details
Can the samples/analytes be analysed by the equipment	This is the main objectives of this research	Figs. 12 and 17
How will the analytes (compounds of interest) be prepared and extracted from the sample matrix (and how will other components not of interest be dealt with)	The analytes measured on GC-IMS are semi-volatile and/or volatile compounds and they will be extracted from the matrix using the headspace for analysis;	See 2.1.1 section
Is there any chemical in the matrix that can interfere with the detection of analytes of interest or damage the instrument	During the research was shown that ammonia had an important role of interfering with the measurement	See chapter 5
How will the sample be introduced into the column	The sample can be introduced by autosampler or by manual injection	See section 3.2
Which column provides the best separation and resolution	This criteria depend on which are the compounds of interest and their polarity as polarity influence column selectivity and separation factor	See section 3.2.6.5
Which experimental parameters/ conditions should be optimised	The GC-IMS allows optimisation of the temperature in the headspace, the flow in the carrier gas and drift gas and the temperature in the column and in the drift tube	Chapter 3

The focus of this research was to analyse samples from AD sector using GC-IMS with an emphasis on odoriferous compounds. The sample types were mostly related to feedstocks, intermediates products, and final products. These samples could be considered a very complex type of matrix with the possibility of interference from some intermediates or products such as ammonia or VFAs. The remainder of this chapter describes the development of a robust and derivatization-free method that allows evaluating the mixture of analytes of interest, without the interference of the matrix.

3.2 MATERIAL AND METHODS

3.2.1 Sample

3.2.1.1 Sample acquisition

The initial samples used for creating the methodology were recovered from a full-scale AD plant. The samples used FWs which included Animal by Product (ABP) and final output from the digestion process (second digestate). These samples were chosen because they covered most of the typical samples from the AD sector from feedstocks to final products and provided a good range to work with. The samples were analysed as soon as possible, ideally on the day of collection or the following day. In the cases where there was a need to characterise them over a longer period of time, samples were kept in a fridge at 5°C or were frozen at -18°C in order to limit any degradation of the sample or loss of volatile compounds.

3.2.1.1 Samples

The AD plant started to be built in October 2015 and the first engine started producing energy in January 2016 and the second in February 2016. Figure 7 illustrates the general process flow of the AD plant process and, in red, where the samples were sourced. Figure 8 is a schematic representation of the layout of the plant and the location of the sample points. Feedstock preparation consisted of the reception of the FW in the reception area, where size reduction using a hammer mill takes place. The company receives FWs which include municipal wastes from the local authority, industrial waste, and restaurant waste. After the hammer mill step, the FW is blended with cattle slurry to make a pumpable liquid feedstock mix. The ABP is then stored in the buffer tank (point 2, figure 8A and 8B) until it is pumped to the primary digester (point 5, figure 8A and 8B). The cow slurry is stored in another tank (point 4, figure 8A and 8B). Maize is represented

in (point 3). The digestion process consisted of a primary digester heated at 38°C, (3,000 m^3 and runs between 93-98% capacity) and a secondary digester (3,000 m^3), however, the second digester was not heated. The primary digester loading was performed through SP1. Loading comprised of approximately 88 ton/day of FW/cow slurry, 4 ton/day of maize (if available), and recirculation of digestate (typically 100m^3/day). The digester was based on a semi-plugged flow design aided by gas mixing, which aimed to retain the solid fraction of the feedstocks for a longer digestion period avoiding short-circuiting and maintaining the denser materials in the digester for a longer period of time so as to maximise digestion (Namsree *et al.*, 2012; Sans *et al.*, 1995).

The process was continuous with approximately 33 days of hydraulic retention time (HRT) for the primary digester, 1 day HRT for the pasteurization tank and 33 days HRT for the storage tank. The material in the primary digester moved as a semi-plug flow from SP1 to SP8 and passed two bottom baffle systems placed between SP1 and SP3 which were intended to restrict the flow of solid material. In this primary digester, the sample points utilised by this study were SP1, SP2, SP3, SP4 and SP8 (Figure 8A and 8B). After the primary digester, the effluent or digestate was passed through a batch pasteurization process (heated to 71°C for 70 min) (point 6, figure 8A and 8B) and samples were also collected after the pasterisation process (Pasteur). After pasteurisation, the primary digestate was sent to the second digester, which really worked as a store for the digestate as the digester is stirred but is maintained only at ambient temperature. The last sample collected was then from the second digester (point 7, figure 8A and 8B).

As stated previously, the various organic feedstocks, hydrolysates, and digestate samples were sourced from a full-scale AD plant and they were labelled as follows: animal by-products (ABP – which comprise of municipal, commercial and industrial FW), cow slurry, samples points from the primary reactor which are sample point 1 (SP1), sample point 2 (SP2), sample point 3 (SP3), sample point 4 (SP4), sample point 8 (SP8), digestate pasteurised (Pasteur – digestate after pasteurization process) and second digestate (digestate from the storage tank). The following items sub-processes constitute the plant:

1. Combined Heat & Power (CHP)
2. ABP buffer tank
3. Energy crop (maize store) and Solid Feeder (for supply maize)
4. Non-ABP buffer thank (store tank for cow slurry)
5. Primary Digester
6. Pasteurisation Tank
7. Secondary Digester
8. Input feedstocks
9. Recirculation digestate

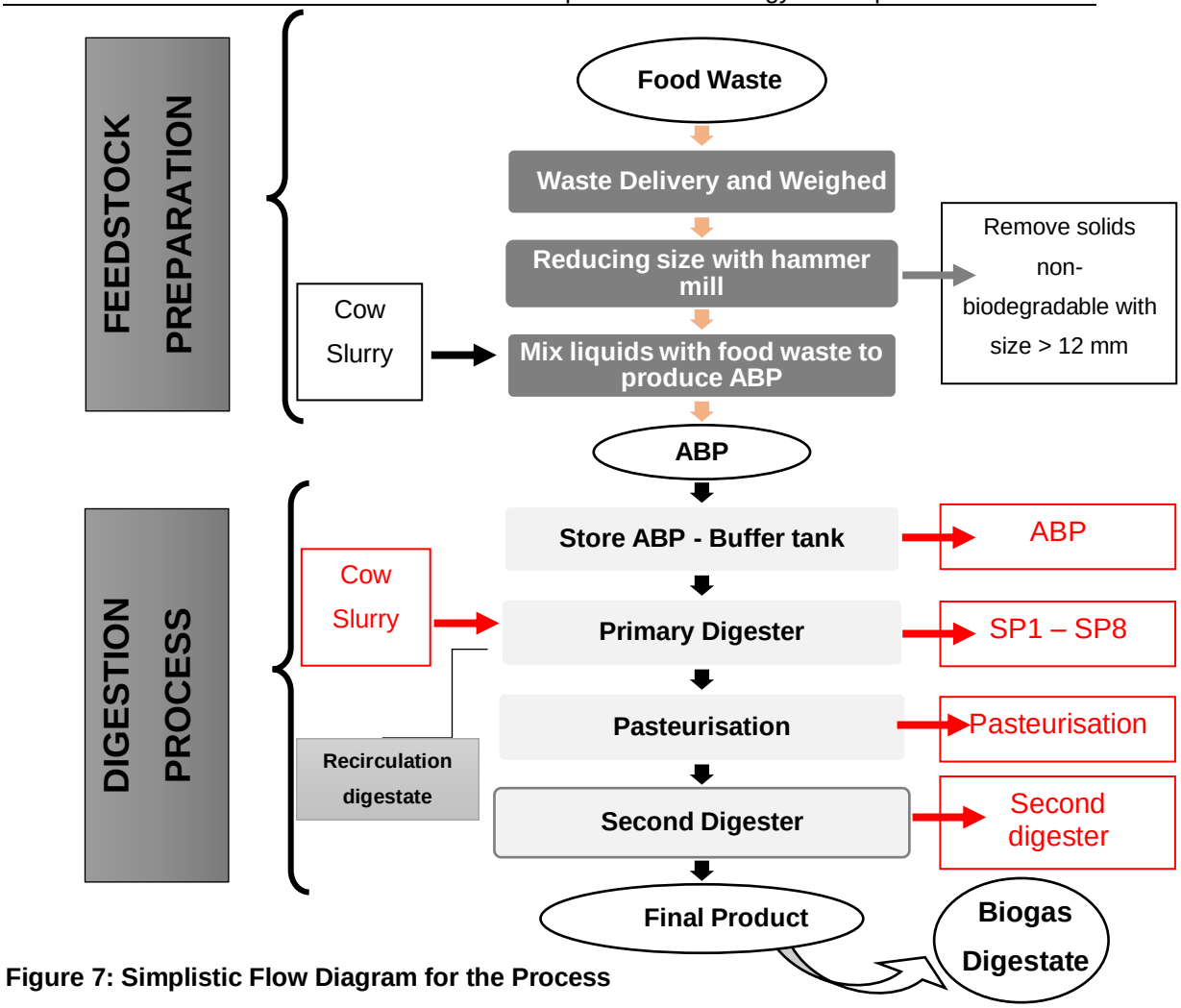

Figure 7: Simplistic Flow Diagram for the Process

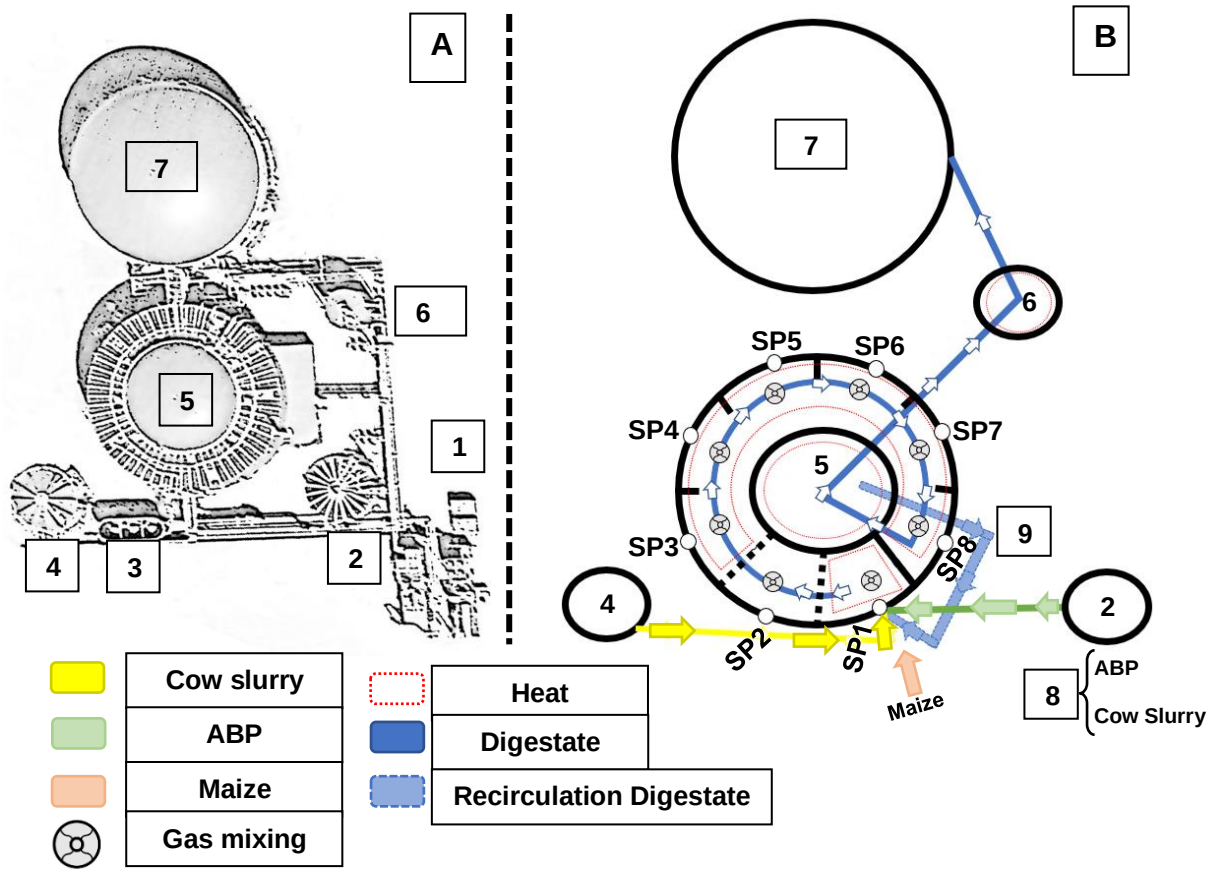

Figure 8: Google maps screenshot from plant (A), simplistic schematic design of plant (B).

3.2.1.2 Sample preparation and analysis

The principle for extracting the compound of interest from the matrix was based on headspace sampling as explained above. Using the autosampler was the first choice method for introducing the sample into the column, but when this was not possible due to the physical nature of the sample a manual injection could be used. A 1 mL sample was placed in a vial and the vials were sealed with magnetic screw caps with blue PTFE/white Silicone septa (diameter × thickness 17.5 mm × 0.060") from Restek. The vials were then placed onto the FlavourSpec® for automated processing and analysed. The syringe (a CTC Headspace HD-Type) sampled 100 µL of the headspace gas sample and injected it into the injection port. All samples were analysed in duplicate in order to give an indication of the reproducibility of results. Between samples, a vial of deionised water was introduced to enable cleaning of the system and so that spectra could be verified and contamination avoided.

3.2.2 Reagents

A number of chemical reagents were used to establish an initial calibration of the GC-IMS unit. The chemicals used were sourced from Sigma-Aldrich (UK). Table 9 presents the data for initial calibration related to the assay of each chemical, the empirical formula, the molecular weight, the CAS number and the density at 25°C.

Table 9: Data for reagents used for initial calibration

Product name	Reagent grade	Assay	Empirical formula	Molecular Weight	CAS Number	Density 25 °C
2-Butanone	ACS reagent	0.99	$C_2H_5COCH_3$	72.11	78-93-3	0.805
2-Pentanone	FCC. FG	0.98	$CH_3CO(CH_2)_2CH_3$	86.13	107-87-9	0.809
2-Hexanone	Reagent grade	0.98	$CH_3(CH_2)_3COCH_3$	100.16	591-78-6	0.812
2-Heptanone	Analytical standard	0.99	$CH_3(CH_2)_4COCH_3$	114.19	110-43-0	0.820
2-Octanone	Reagent grade	0.98	$CH_3(CH_2)_5COCH_3$	128.21	111-13-7	0.819
2-Nonanone	Reagent grade	0.98	$CH_3(CH_2)_6COCH_3$	142.24	821-55-6	0.820
Ammonia	28% in water	0.9999	NH_4OH	35.05	1336-21-6	0.90

3.2.3 Column Specification

At the beginning of the project the column installed was a Supelco Analytical Nukol™ Fused Silica Capillary GC Column (size × I.D. 30 m × 0.32 mm. df 0.25 µm film thickness), catalogue number 24131 Supelco from Sigma. It was a capillary polar column suitable for GC and the matrix active group was bonded, acid-modified poly(ethylene glycol) phase. This column can be applied to quantify free carboxylic acids (C_2-C_8) by GC (Sigma, 2019). During the method development and before applying the method on real samples a new column was installed i.e. a generic capillary GC column SE-54-CB1 (length 15 m by 0.53 mm ID. with 1 µm df). It was a classic non-bonded stationary phase based on a (5 %-Phenyl)(1 %-Vinyl)-(94 %) Methylpolysiloxane with lower polarity (Sciex. 2012). The second column was a more generic column than the first column (mainly for VFAs), that can measure a broad range of chemicals (e.g. esters, alcohols, aldehyde, and ketones) (Sigma Aldrich, 2019). In addition, column parameters were changed (it is shorter in 15 m, with a high inner diameter and thinner film) which allowed a reduction in runtimes from 59 minutes to 10 minutes without losing the resolution in the chromatogram (sharp and well resolved peaks) and getting a faster gas chromatographic separation. With the decrease of running times, this allowed a decrease in the final run time for analysis and it was possible to measure more samples compared with the same period of time before. The column used in each of the studies described in this thesis is specified in the relevant chapter. The unit used in this research only allowed an isothermal program, this means the temperature program stays constant in the column during all the run time.

3.2.4 Carrier and drift gas

The machine allowed three different setups after performing a run: “no action” (do not change any parameters); “cleaning” (turn the temperatures [>100°C] to clean the column and the IMS) or “standby” mode where the flow of mobile phase carrier gas can be reduced to save on gas usage. At the beginning of the lab work, the carrier, and drift gas were supplied using nitrogen gas bottles and the equipment was most on “standby” mode. During the lab work, it was realised that it was important to leave the nitrogen gas always on to flush the system even between runs and during the night to clean the system between runs from the previous injections. This would avoid cross-contamination between runs, carry-over of peaks, remove ghost peaks, and improve the equipment’s performance. A nitrogen generator (NITROSTATION 50L/LC from Leman Instruments) was therefore utilised in order to allow for consistency of carrier gas flow both during analysis and cleaning modes. Both drift and carrier gas were supplied by an electronic

pressure control unit (EPC). The EPC1 was the gas flow in the drift tube within the IMS (i.e. the drift gas) and it could be adjusted between 0-500 mL/min. The EPC2 was the gas flow in the column (i.e. the carrier gas) and it could be adjusted between 0-20 mL/min for the Nukol™ column and 0-150 mL/min for the SE-54 column. Both flows (carrier and drift gas) were determined by pressure.

3.2.5 Equipment (GC-IMS)

All measurements were conducted with the FlavourSpec® from Gesellschaft Für Analytische Sensorsysteme (G.A.S.) equipped with an autosampler (CTC-PAL. CTC Analytics AG. Zwingen. Switzerland) and with a radioactive source (Tritium). The equipment was setup in positive mode. Positive mode was described in chapter 2.1.2.1 Ion formation. The first task was to create a methodology for analysing the samples of interest. The key experimental parameters were related to establishing the settings of the temperature, gas flow, time, pressure, drift voltage (positive or negative) and any sample dilution requirements of the sample.

3.2.5.1 Data analysis

The equipment had the LAV software installed (IMS Software Suite version 2.2.1 from G.A.S. GmbH Dortmund Germany 2007-2013). It was used for processing of all the data and the creation of all the graphical plots. The software package allowed the creation of two and three-dimensional data visualisations, creation of a gallery plot, calibration of compounds and had the mathematical function of integrated Dynamic Principal Components Analysis (PCA) function. For the PCA the data required manual identification of peak height by the user and PCA extracted the essential information from a large amount of data and clustered them according to their similar proprieties. On the plots, the x co-ordinate is the drift time (milliseconds) and the y co-ordinate is the measurement run or retention time (seconds and it is the time that each compound takes to travel from the injection port to the detector). The software also had a Library Search version 1.0.3 with column normalisation to NIST 2014 that allowed the identification of the chemicals of interest, providing that they had already been included in the library. In this thesis, will be used the Rt, drift time (normalized to RIP drift time), K_0 and $1/K_0$ calculated and K_0 and $1/K_0$ reported by the software. To determine the reduced ion mobility (K_0), the system used is 9.8 cm as the length of the drift region; the system used as electrical field strength is 510V/cm, the standard temperature is 273.15 K and the drift tube temperature used was 45°C (273.15+45= 318.15 K) and the atmospheric pressure was 101.325 kPa. P is a combination of the drift gas (EPC1) and operational pressure

(kPa) because the ambient pressure can vary between measurements according to environmental conditions. In this thesis, chemometrics was used for pre-processing the alignment data (correction by the mobility of RIP or by K_0) (Chapters 4) and for pattern recognition (Self-Organization Maps, SOM) in Chapter 7.

3.2.6 Initial Methodology Development

Some parameters were not changed in any of the experimental work, either to allow comparison of results or because they were fixed within the instrument itself (Table 10). These fixed parameters included the amount of the liquid in the vial (it was always 1 mL of liquid (or ± 1gr solid) with 19 mL of headspace gas), the autosampler agitation speed (500 rpm), agitation time (7-second turn on and 3-second turn off) with an injection speed of 500 µL/s. The injection of the gas sample in the injection port was made by a gas-tight syringe. Each spectrum had an average of 6 scans, obtained using a repetition rate of 30 ms. In the GC-IMS manual, the averaging value is defined as how many raw spectra are averaged into one single resulting spectrum in the stored measurement file. Signal averaging increases the signal to noise ratio. A value of 0 (Off) disables averaging. A value n will result in an averaging of n+1 spectra. Modifying the averaging parameter affects the number of recorded spectra per time period. The shutter grid opening time of the IMS sensor was a typical trigger duration value of 100 µs. Table 10 summarises the parameters that were not modified during the research related to the equipment. The injection speed should be as high as possible in order to produce spectra peaks with as narrow base as possible which allows for identification of individual compounds present.

Table 10: Unchanged parameters throughout the research

Machine type & serial	FlavourSpec® & 1H1-00045
Flow record interval	6000 ms
Drift potential difference	5100 V
Drift tube length	98000 µm
IMS length	50 mm
Pressure Drift tube	101 kPa (ambient pressure)
Polarity (Voltage)	Positive mode
Spectra length/sample interval	30 ms
Averaging of scans	6

Continuation Table10: Unchanged parameters throughout the research

Trigger duration	100 µs
Amount of sample in the vial	1 mL of liquid (or ± 1gr solid) with 19 mL of headspace gas
Autosampler agitation speed	500 rpm
Agitation time	7-second turn on and 3-second turn off
Injection speed	500 µL/s

3.2.6.1 Experimental setup A1 (headspace equilibrium time)

The objective of Experiment A1 was to determine the required incubation time to create an equilibrium in the headspace. Initial GC-IMS conditions were according to Denawaka *et al* (2014) study for measuring malodours such as butyric acid on socks using GC-IMS, with the exception that the sample volume was reduced (to 100µL so as not to overload the instrument) and the run time that was high (one hour to see if the equipment could detect all peaks during that period of time). Denawaka *et al*. (2014) detected butyric acid, isobutyric acid, isovaleric acid, propionic acid, valeric acid with an OV-5 column having incubation conditions of 5 minutes at 95°C and the syringe at 85°C (Denawaka *et al.*, 2014). The column used was a Nukol™ for analyses of volatile acid compounds such as free fatty acids. This column was found to produce an excellent peak shape, defined as being high with a narrow base area.

The incubation time was the time necessary to achieve the equilibrium between the liquid and the gas phase inside the vial to create a headspace where the volatile compounds from the samples can be measured. For more information please see chapter 2.1.1.1 Sample preparation. Using the information that was gathered, incubation times tested were 5 min, such as Denawaka study, and 20 min. Table 11 presents the experimental conditions using ABP without any dilution (ND) as a reference sample.

A 1 mL of the concentrated sample was loaded into a 20 mL vial and closed with magnetic caps. After 5 minutes or 20 minutes of incubation at 95°C, in accordance with the goal of the study, 100 µL of gas sample was injected by a heated syringe (85°C) into the injector port (80°C). The GC column (80°C) separated the compounds and IMS (45°C) detected them. EPC1 (150 mL/min) was the flow of the drift gas in the IMS and EPC2 (15 mL/min) was the flow of carrier gas for the GC column. The runtime was approximately one hour.

Table 11: Experimental setup A1

Setup for autosampler

Column	Sample type	Sample Volume [µL]	T Incubation [°C]	Incubation Time [min]	T Syringe [°C]	GC-Runtime [min]
Nukol™	Headspace	100 µL	95 °C	5 and 20 min	85 °C	1:00:30

Setup for GC-IMS

T1 IMS [°C]	T 2 Column [°C]	T 3 Injection Port [°C]	Measurement Runtime [min]	EPC1 [mL/min]	EPC2 [mL/min]
45 °C	80 °C	80 °C	59 min	150	15

3.2.6.2 Experimental setup A2 (investigate reproducibility of results)

The objective of Experiment A2 was to establish the robustness and the system performance so whether the equipment could provide a reproducible result. To assess this, ABP samples in duplicate was used (with and without dilution) were placed in the autosampler using the same method as in A1, but with only 5 mins incubation time.

3.2.6.3 Experimental setup A3 (investigate dilution effect, change temperature in the column and carrier gas flow)

The objective of Experiment A3 was to evaluate the influence of dilution on the limits of detection and limits of quantification for the ABP sample (i.e. a real-world sample), and also to assess the effect of changing column temperature, carrier gas flow (EPC2), and total run time. During the experimental design one variable was changed each time (i.e. temperature, run time) and also the various variables were also change at the same time. The LOD was the minimum detectable level, even without being exact quantified and it can be express as 3.3×standard derivation of the regression line response and the slope from the calibration curves. The blank signal was the background noise and the LOQ (the lowest quantity of analyte which can be calculated with appropriate precision and accuracy) was calculated as 10×standard derivation of the regression line response and the slope from the calibration curves (Cumeras *et al*., 2015c). The sensitivity of the method was based on the slope of the calibration curve and reproducibility. The sample was diluted using serial dilutions with deionised water for the following range: dilutions of 10, 100, and 1000 times. For 10 times dilution (or 1:10 dilution), 1 mL of the sample was added to 9 mL of deionised water and the contents were mixed (using a vortex mixer equipment). In the cases of the preparation of 100 times dilution, 1 mL of 10 times diluted sample was added to 9 mL of deionised water. Figure 9 is a schematic for the serial dilution.

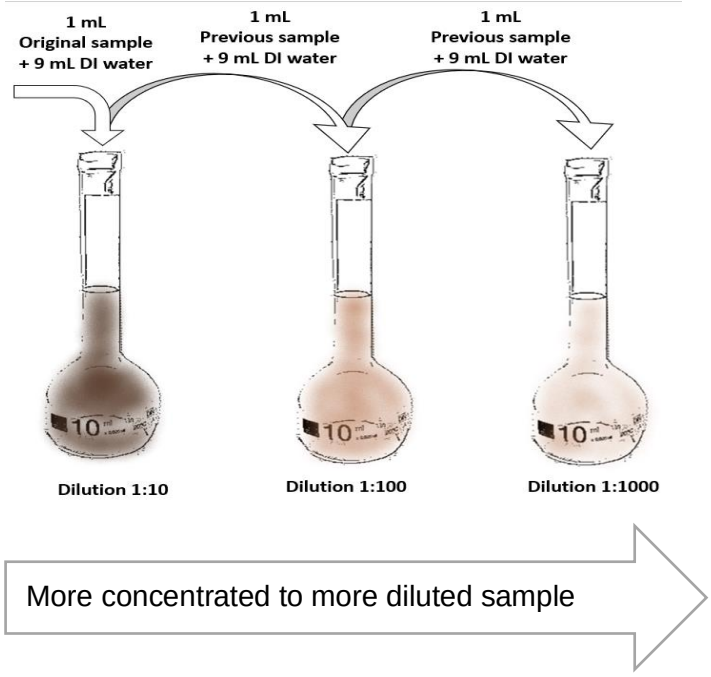

Figure 9: Schematic of the serial dilution

To compare the effect of changing the temperature in the column and the flow in the carrier gas (EPC2), column temperature was decreased from 80 to 45°C, carrier gas flow was increased from 15 to 20 mL/min and run time was reduced from one hour to 15 minutes. Table 12 presents the setup for experiment A3 with the red squares highlighting the differences from experimental setup A1.

Table 12: Experimental setup A3

Setup for autosampler and GC-IMS						
Column	**Sample type**	**Sample Volume [µL]**	**T Incubation [°C]**	**Incubation Time [min]**	**T Syringe [°C]**	**GC-Runtime [min]**
Nukol™	Headspace	100 µL	95 °C	5 min	85 °C	15:30

T1 IMS [°C]	**T 2 Column [°C]**	**T 3 Injection Port [°C]**	**Measurement Runtime [min]**	**EPC1 [mL/min]**	**EPC2 [mL/min]**
45 °C	45 °C	80 °C	15:00:020	150	20

3.2.6.4 Experimental setup A4 (dilution effect for digestate samples)

Used the same method (experimental setup A3) for the second digestate sample from a full AD plant, to see it was possible to measure it on the GC-IMS. The sample was diluted 1:10, 1:100, 1:1000 as previously explained.

3.2.6.5 Experimental setup B1 (establish the method for a SE-54 column)

In all Experiment B's the column was changed to a capillary GC SE-54 column (whereas Experiment A's the Nukol™ column was used). The column was changed in order to assess whether it would separate and therefore allow the detection of a wide range of compounds, specifically the heavier compounds, within a lower run time from the one hour required in Experiment A1, even when using a high flow. The reason why the runtimes were so high in Experiment A's was because the Nukol™ column had a small internal diameter resulting in excessive compound carry over and peaks with tailing. Consequently, it was necessary to shorten column length and increased the internal diameter. Experiment B1 was specifically undertaken to ascertain a calibration curve using standard chemicals. The method was developed using a ketones mix as the standard, according to the instrument manufacturer (G.A.S.). Ketones were found to be easy to use, reliable, helped the comparison between different samples, and to normalize the library and were compounds that could be found in the AD related samples. Table 13 shows the concentration for each standard solution.

Figures 10 (A, B and C) present how the standard solutions were prepared and Table 13 presents the concentrations of the ketones mixes. Table 14 explains the initial GC-IMS conditions using the capillary GC SE-54 column with the red squares to emphasize the differences between experimental setup A3 and Experiment B1. Comparing with the previous method, the incubation temperature was decreased from 95 to 60°C to avoid cooling of the sample because the maximum temperature in the injector was 80°C. Having a gas sample at a higher temperature than the injector port could result in condensation leading to damage of the column and the detector as well as introducing liquid contaminants into the instrument.

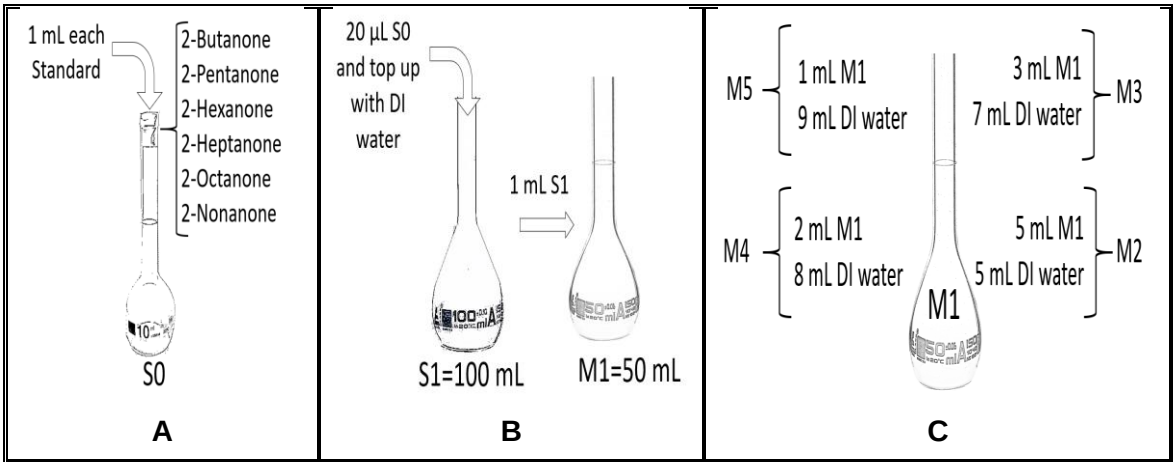

Figure 10: Preparation stock solution (A), preparation the standard solution S1 and M1 and preparation the standard solution M2, M3, M4 and M5 (C)

Table 13: Concentration for ketones mix

Concentration							
Chemical	g/mL	mg/L	µg/L	µg/L	µg/L	µg/L	µg/L
	S0	S1	M1	M2	M3	M4	M5
2-Butanone	0.114	22.770	455.400	227.700	136.620	91.080	45.540
2-Pentanone	0.113	22.652	453.040	226.520	135.912	90.608	45.304
2-Hexanone	0.114	22.736	454.720	227.360	136.416	90.944	45.472
2-Heptanone	0.116	23.194	463.886	231.943	139.166	92.777	46.389
2-Octanone	0.115	22.932	458.640	229.320	137.592	91.728	45.864
2-Nonanone	0.115	22.960	459.200	229.600	137.760	91.840	45.920
mg/L is equal to ppm			µg/L is equal to ppb				

Table 14: Experimental setup B1

Setup for autosampler and GC-IMS						
Column	Sample type	Sample Volume [µL]	T Incubation [°C]	Incubation Time [min]	T Syringe [°C]	GC-Runtime [min]
SE-54-CB1	Headspace	100 µL	60 °C	2 min	150 °C	15 min 30 sec

T1 IMS [°C]	T 2 Column [°C]	T 3 Injection Port [°C]	Measurement Runtime [min]	EPC1 [mL/min]	EPC2 [mL/min]
45 °C	45 °C	80 °C	15 min	150	50

3.2.6.6 Experimental setup B2 (investigate improvement of ketones separation)

The objective of Experiment B2 was to improve the separation between the ketones in the ketone mix, and specifically to determine the effect of decreasing the temperature in the syringe from 150 to 80°C to avoid condensation, and decreasing the carrier gas (EPC2) flow from 50 mL/min to 5 mL/min. The red squares highlight the differences from B1 (Table 15). Decreasing the pressure inside the column (achieved by the proposed decrease in the EPC2 flow rate) should improve the interaction between the stationary phase and the mobile phase (the sample and the carrier gas).

Table 15: Experimental setup B2

Setup for autosampler						
Column	Sample type	Sample Volume [µL]	T Incubation [°C]	Incubation Time [min]	T Syringe [°C]	GC-Runtime [min]
SE-54-CB1	Headspace	100 µL	60 °C	2 min	80 °C	15 min 30 sec

Table 15: Continuation of experimental setup B2

Setup for GC-IMS					
T1 IMS [°C]	**T 2 Column [°C]**	**T 3 Injection Port [°C]**	**Measurement Runtime [min]**	**EPC1 [mL/min]**	**EPC2 [mL/min]**
45 °C	45 °C	80 °C	15 min	150	5

3.2.6.7 Experimental setup B3 (investigate the improvement of ketones separation with extended run time)

In order to further investigate the potential to separate all of the peaks of the ketone mix, Experiment B3 used the same setup on B2, with the exception of increasing the run time from 15 minutes to 30 minutes (in order to improve separation). All 5 ranges of concentrations from M1 to M5 using all ketones were analysed.

3.2.6.8 Experimental setup B4 (investigate the improvement of ketones separation by reducing incubation temperature)

As the main objective of the research was to measure odours that were already in the gas phase at room temperature, Experiment B4 investigated the potential to reduce the incubation temperature from 60 to 45°C. In order to allow an equilibrium between the liquid and the gas phase, the incubation time was increased from 2 minutes to 14 minutes. G.A.S. advised that the column would perform better at 40 than 45°C for ketone separation and for this reason, the temperature for the column was also decreased accordingly. Flow in the carrier gas (EPC2) was increased in a stepwise manner (ramped) with the objective of decreasing the run time from 30 minutes to 16 minutes and half without losing any ketone peak. Table 16 shows all experimental parameters. All ketones were used in 5 different concentrations and the analysis undertaken in triplicate.

Table 16: Experimental setup B4

Setup for autosampler and GC-IMS						
Column	**Sample type**	**Sample Volume [µL]**	**T Incubation [°C]**	**Incubation Time [min]**	**T Syringe [°C]**	**GC-Runtime [min]**
SE-54	Headspace	100 µL	45 °C	14 min	80 °C	16 min 30 s

T1 IMS [°C]	**T 2 Column [°C]**	**T 3 Injection Port [°C]**	**Measurement Runtime [min]**
45 °C	40 °C	80 °C	16 min

Table 16: Continuation experimental setup B4

Program for flow on drift gas and carrier gas			
Time	**EPC1 [mL/min]**	**EPC2 [mL/min]**	**Recording**
00:00.000	150	2	Starting recording
10:00.000	150	50	Recording
15:00.000	150	150	Recording
16:00.000	150	150	Recording
16:00.020	150	150	Stop recording

3.2.6.9 Experimental setup B5 (investigate the improvement of ketones separation by varying the flow of the carrier gas)

In Experiment B5 a new program for the carrier gas (EPC2) was created in order to optimise the separation between all ketones, in particular for 2-butanone, 2-pentanone, 2-hexanone, and 2-heptanone. For the first two minutes the flow was 5 mL/min and then ramped to 50 mL/min until 10 minutes. The flow was further increased to 150 mL/min for 5 minutes with that flow held for one more minute at 150mL/min. Table 17 shows the new program for the time, flow on drift and carrier gas. The conditions for autosampler and GC-IMS were kept the same as experimental setup B4. After injection, the chemicals take ± around 40 seconds to pass the column and be detected in the Faraday plate. So, holding for two minutes the flow at 5mL/min has the objective to take into account this fact. Increasing the flow in the column (carrier gas – EPC2) to 150mL/min for the last 6 minutes is primarily intended to flush the column and remove possible contaminants between analyses rather than specifically for detection purposes. To study this, a fresh M1 solution from the ketones mix was prepared.

Table 17: Experimental setup B5

Program for flow on drift gas and carrier gas			
Time	**EPC1 [mL/min]**	**EPC2 [mL/min]**	**Recording**
00:00.000	150	5	Starting recording
02:00.000	150	5	Recording
10:00.000	150	50	Recording
15:00.000	150	150	Recording
16:00.000	150	Hold to 150	Recording
16:00.020	150	150	Stop recording

3.2.6.10 Experimental setup B6 (investigate method optimization)

Experiment B6 was intended to investigate the final methodology to be employed. This was a modified version of B5, however, in order to reduce run time and allow 32 samples (one autosampler tray) to be analysed within one day, the final 6 minutes of carrier gas flushing was removed. This would reduce the time for running 32 samples from over eight and a half hours to 5 hours and 20 minutes (Table 18). In addition to the final 6 minutes of the B5 runs not being useful for detecting any chemicals, it was decided it would be better to do a thorough clean after running all samples at the end of the day, instead of flush the system in between runs. Flushing with gas could not ensure the removal of all contaminants. For this, using the "clean mode" and raising the temperature in the column was required.

Table 18: Experimental setup B6

Program for flow on drift gas and carrier gas			
Time	**EPC1 [mL/min]**	**EPC2 [mL/min]**	**Recording**
00:00.000	150	5	Starting recording
02:00.000	150	5	Recording
10:00.000	150	50	Recording
10:00.020	150	50	Stop recording

3.2.6.1 Experimental setup B7 (establishing a method for measuring VFAs)

A different method to measure VFAs was created from the previous one to make it easier to detect VFAs by increasing the volatility of compounds, to avoid excessive peak tailing, and to increase the peak resolution. The sample volume was increased, the temperature and the incubation time in the autosampler and the time for all analysis. Besides the changes in the conditions in the autosampler being changed, the program for flows (EPC1 and EPC2) was adapted to specific measure VFAs. Table 19 shows the conditions for the equipment.

Table 19: Experimental setup B7, for measuring VFAs

Setup for autosampler						
Column	**Sample type**	**Sample Volume [µL]**	**T Incubation [°C]**	**Incubation Time [min]**	**T Syringe [°C]**	**GC-Runtime [min]**
SE-54	Headspace	500 µL	60 °C	20 min	80 °C	20 min 30 sec

Table 19: Continuation experimental setup B7, for measuring VFAs

Setup for GC-IMS

T1 IMS [°C]	T 2 Column [°C]	T 3 Injection Port [°C]	Measurement Runtime [min]
45 °C	40 °C	80 °C	20 min

Program for flow on drift gas and carrier gas

Time	EPC1 [mL/min]	EPC2 [mL/min]	Recording
00:00.000	150	2	Starting recording
5:00.000	150	2	Recording
15:00.000	150	50	Recording
20:00.000	150	50	Recording
20:00.020	150	50	Recording
20:00.040	150	50	Stop recording

3.3 RESULTS AND DISCUSSION

The results of the experiments undertaken to develop the final analytical methodology are described below. The aim of the methodology was to get the best separation of the analytes of interest, to lose the least amount of information from the spectrum and to collect the most information as possible. Where numerous compounds are present in one sample, the method should be capable of separating those of interest with each peak having a distinct retention time without overlapping with other compounds and allow comparison with the standards to confirm the accuracy of the result.

3.3.1 Experimental setup A1

From the results obtained (Figure 11) the equilibrium between the liquid and gas phase was already achieved at 5 minutes (Figure 11A). This is demonstrated as there was no observable difference between the results where a 20 minute incubation (Figure 11B) was used compared with a 5 minute incubation. As such, a 5 minute incubation time was used for the final methodology. In the x-axis was represented the IMS drift time in milliseconds, in the y-axis was represented the GC retention time in seconds and the z-axis represents peak intensity base on colour grade (where the light blue is the least intense peak while the more intense peak was represented in red).

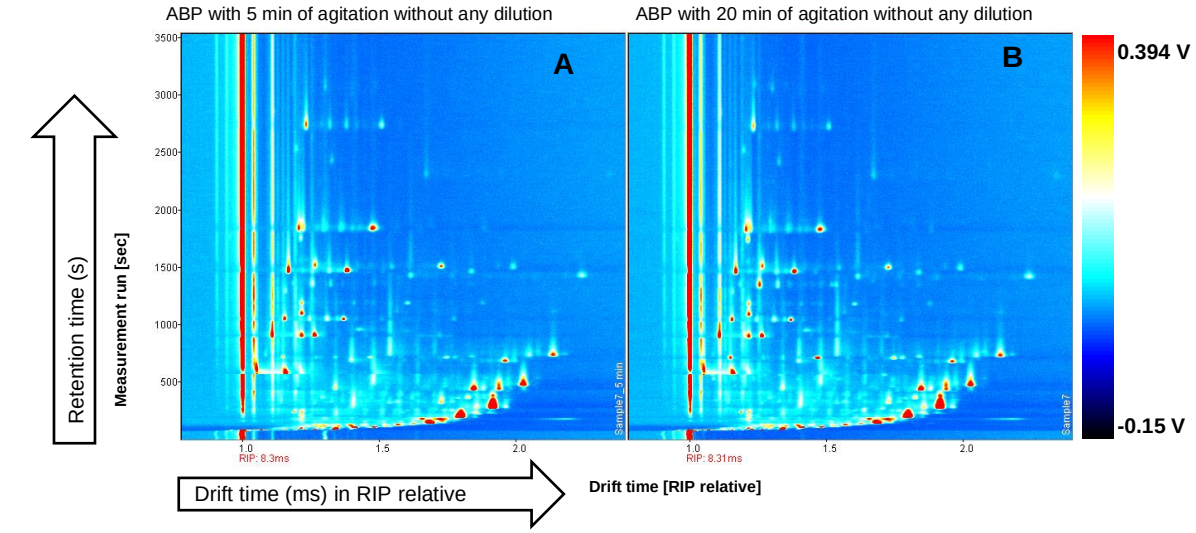

RT between 13s to 3500s; DT(RIP relative) between 0.8ms to 2.4ms

Figure 11: Comparison of GC-IMS spectra generated for ABP with 5min (fig. 11A) and 20 min (fig 11B) of agitation for creating an equilibrium on headspace.

3.3.2 Experimental setup A2

Figure 12 shows the GC-IMS performance when the same sample was analysed in two different runs. There were no clear differences between both spectra (Figure 12A and Figure 12B) indicating a reproducible result.

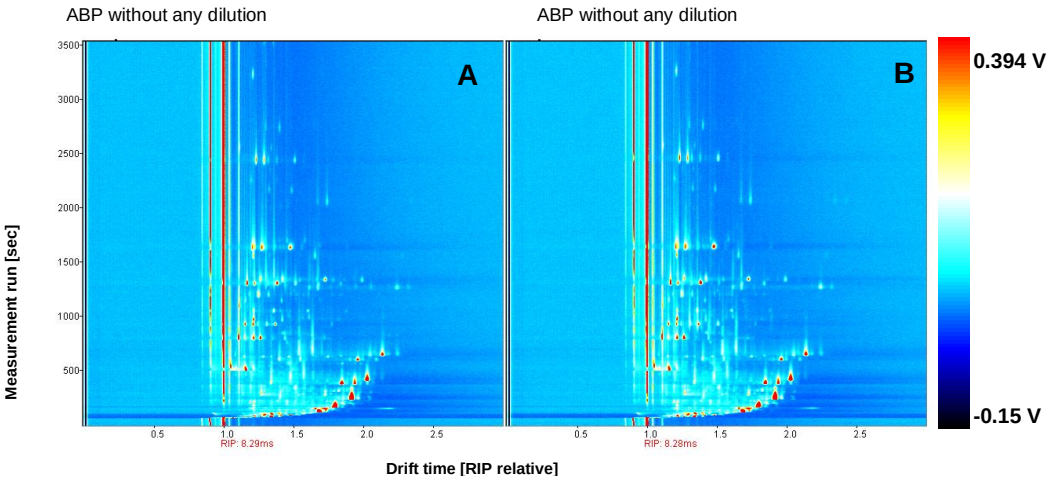

RT between 13s to 3500s; DT(RIP relative) between 0.02ms to 3.0ms

Figure 12: Spectra of ABP to assess equipment reproducibility

3.3.3 Experimental setup A3

Comparing results from column temperatures of 45 °C and 80 °C (Fig. 13), it is evident that a temperature of 45 °C (A3) provides a clearer spectrum with a better resolution than at 80°C (A1). It is also possible to see the effect of dilution on the spectra generated. With a run time of 15 minutes, it was evident that some compounds were taking longer

than this to be separated (and were, therefore, missing from the spectrum). Given that one objective of using GC-IMS is to be a fast analytical method run times of 59 minutes were also considered too long. For this reason, the column was changed from 15 to 20 mL/min to reduce the run times because the latter allowed big carrier flows.

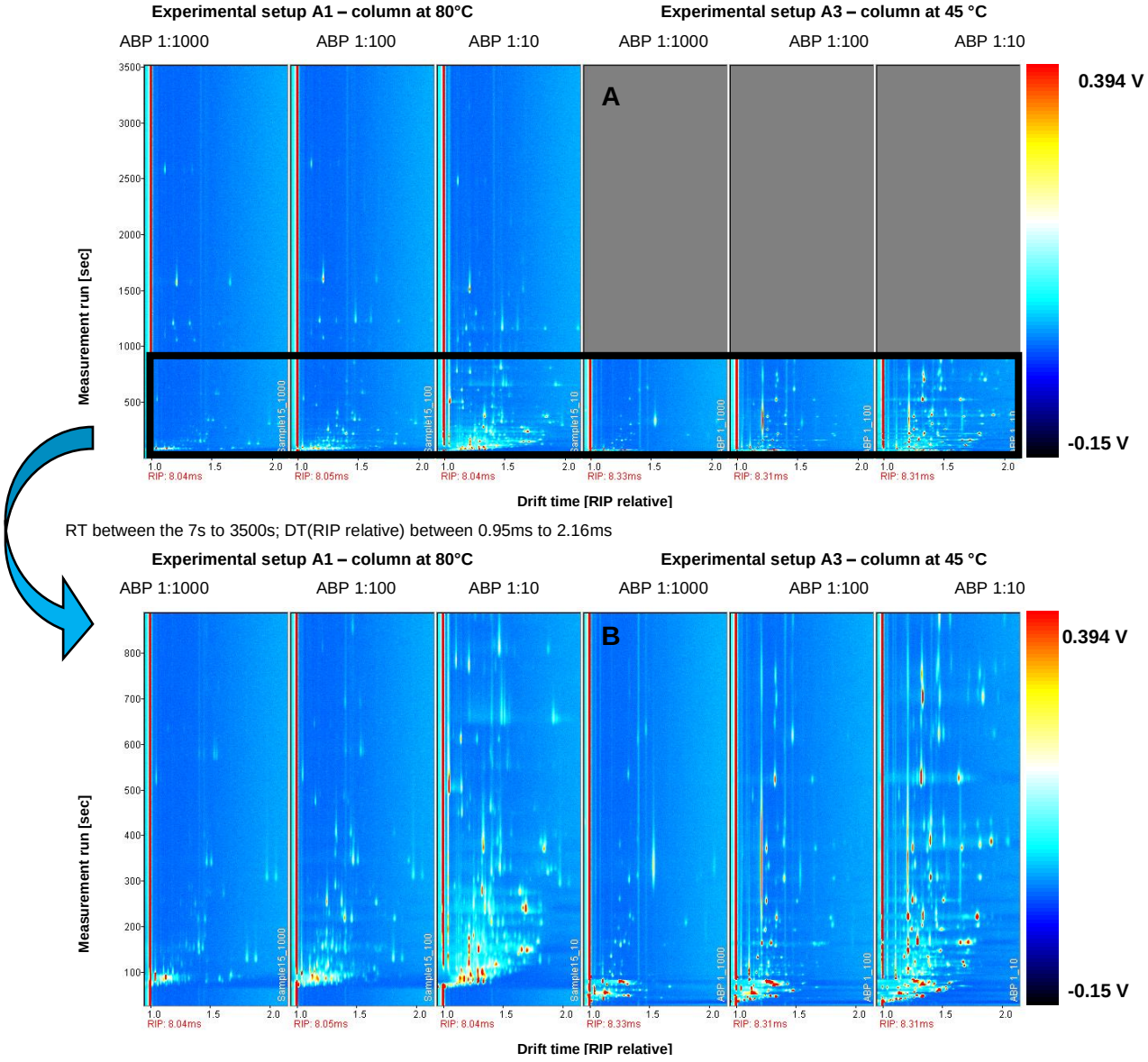

Figure 13: Assess the best temperature for the column

The concentration of the sample is one of the most important aspects to analyse when a method is developed. If the sample is saturating the column, then the analyte should be diluted or a lower mass of sample utilised in order to decrease the concentration of the analytes present in the headspace sample. The following experimental setup had the objective to detect the target compounds without overloading the instrument. Figure 14 (A) shows the results when a compound increased in concentration. At dilution 1:1000 a signal had started appearing as light blue (i.e. a small peak with low intensity). At the increased concentration of 1:100 the peak had become white and yellow and at 1:10

dilution the peak had a larger area and a strong signal with intensity starting to be red. Figure 14 (B) is the chromatogram from figure 14 (A).

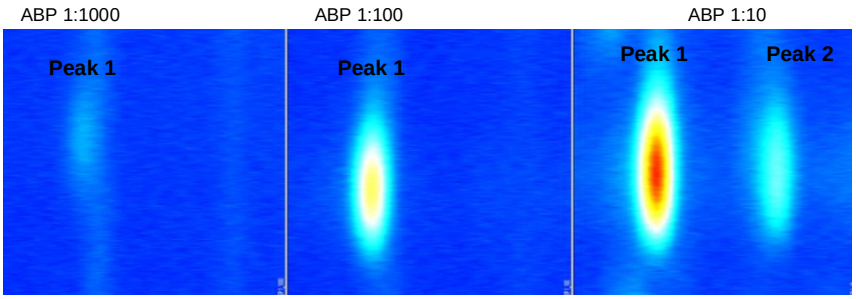

RT 311s; DT(RIP relative) peak 1=1.405ms peak 2=1.461ms

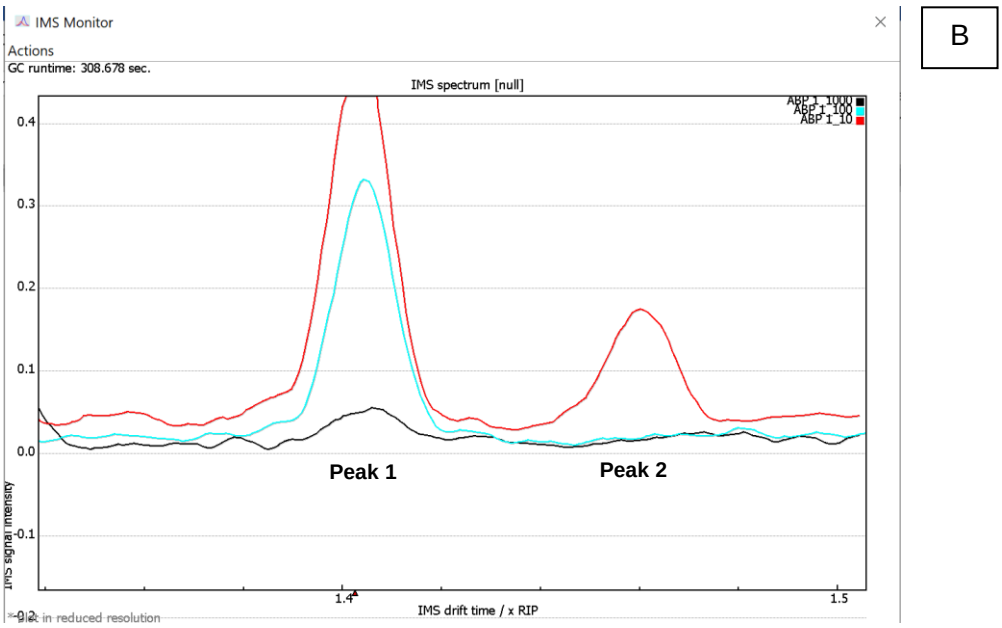

Figure 14: Assess the impact of diluting a sample

Figure 15 (A) shows that the peak also changes in shape depending on concentration. At dilution 1:1000 the peak was a circle whereas at dilution 1:100 and 1:10 the peak has become a less well-defined shape. A similar result can be seen in figure 15 (B). As dilution was reduced, the presence of other chemicals reduced the ability of the target compounds to be ionised and clearly defined in the spectrum. There is a balance between having a sample that is so dilute that the signal intensity is too weak and the spectra not well defined. On the other side, if the sample is too concentrated where ionisation of competing molecules makes the spectra uncertain.

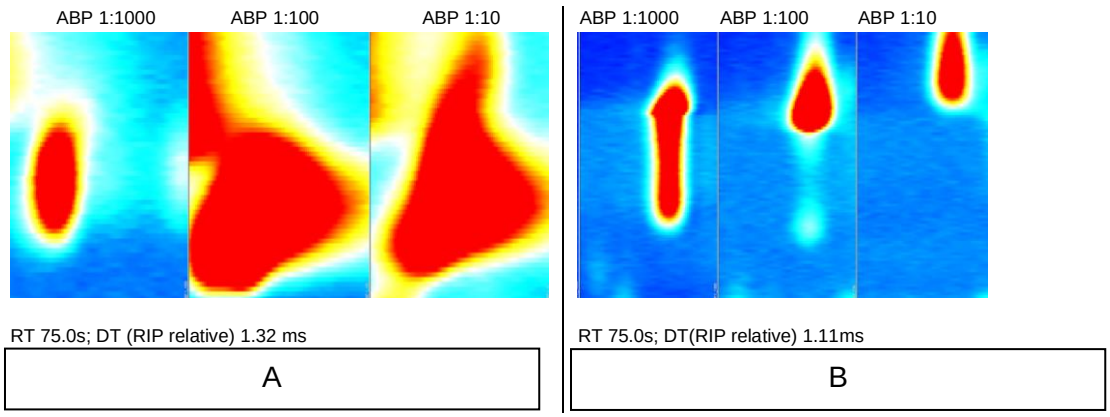

Figure 15: Peak evolution when the concentration increase (A) and losing the ability to be ionized (B)

Figure 16 (A) shows the output when the RIP is lost. This occurs when the introduced sample contains more molecules than can be ionised by the finite ionisation source, i.e. when concentrations are too high. As such the loss of RIP is more evident in the 1:100 and 1:10 dilutions. In Figure 16 (B) the peaks are clear and distinct in dilutions 1:1000 and 1:100, while in dilution 1:10 the first peak decreased its intensity because the second peak overtakes it. This demonstrated the interaction between the presence of competing chemicals in high concentration samples and the finite ionisation capacity of the instrument.

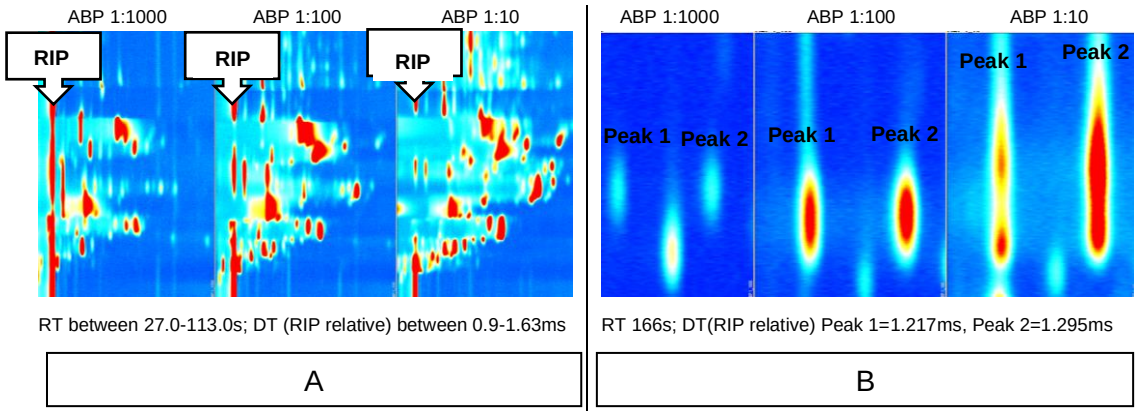

Figure 16: Losing the RIP (A) and the effect of increasing the concentration (B)

3.3.4 Experimental setup A4

Figure 17 shows the output when analysing the second digestate sample from an AD plant. When the dilution factor decreased and the concentration increased, it was possible to see a carrier over that is likely to be from ammonia (Fig. 17A). The peak starts before the injection, which indicated it was from the previous run. It was also possible to observe the loss of the RIP at 1:10 dilution indicating that concentrations were too high for the instrument. The observation that ammonia can be readily carried over between samples represents a considerable challenge when the aim of the research was to use

the instrument to analyse samples from AD plants that regularly contained ammonia concentration of between 200 and 5,000 mg/l (or higher). **In Chapter 5 this problem is explored in more detail and several solutions are presented to solve this problem.**

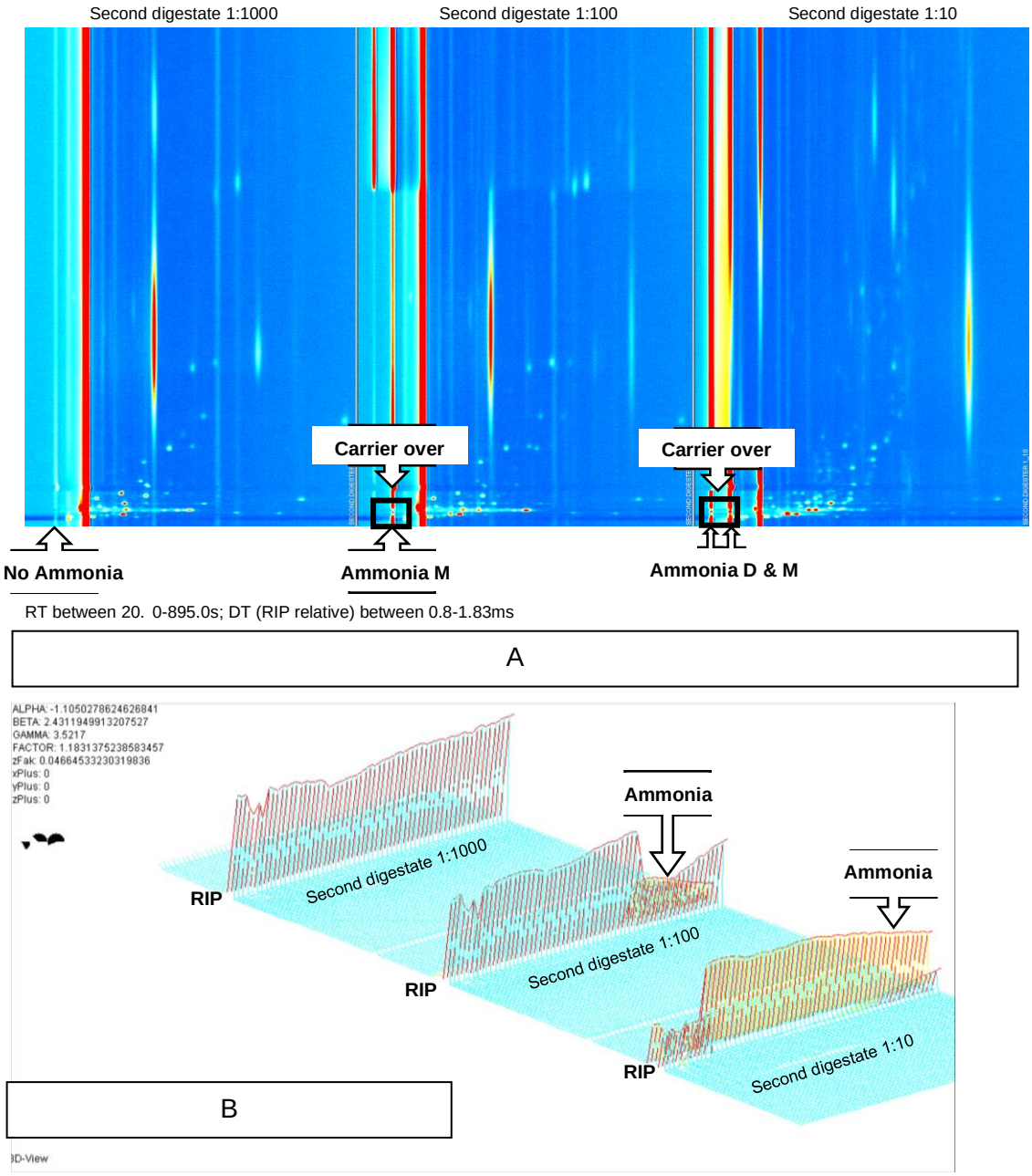

Figure 17: Spectral differences according to dilution Plots: Second digestate sample on GC-IMS at dilution 1:1000, 1:100 and 1:10 (A) and a 3D-view plot at default view corner where in yellow is the suspect ammonia peak and in red the RIP for second digestate sample on GC-IMS (B)

To assess if the samples were regularly allowing any carrier over to the following run, blank samples were introduced between samples. This blank initially comprised of deionised water, with 1 mL of DI water placed between samples using the same method that was being applied to the samples. Figure 18 is a 3D-view for a blank before and

after running several samples where Fig. 18A is the spectrum, 18B a front 3D-view and 18C a corner 3D-view. Blank samples were then changed to a vial containing ambient air and then to a vial containing nitrogen. Vials were filled with nitrogen within a nitrogen filled plastic bag to limit the presence of contaminants to as low as practicable. The reason of using air, and subsequently nitrogen, was to evaluate whether contamination could be brought to the system by the syringe (i.e. physical contamination of the syringe) as well as due to carry over from high concentration samples. In the event that carries over was identified within a spectrum (i.e. it contained peaks contaminating the system), the equipment was placed on clean mode to heat the column and remove these compounds. As such, the quality of the RIP provided a quick indication as to how well the equipment was performing, whether samples were providing too high concentration of molecules to the ionisation stage, and whether the instrument required cleaning.

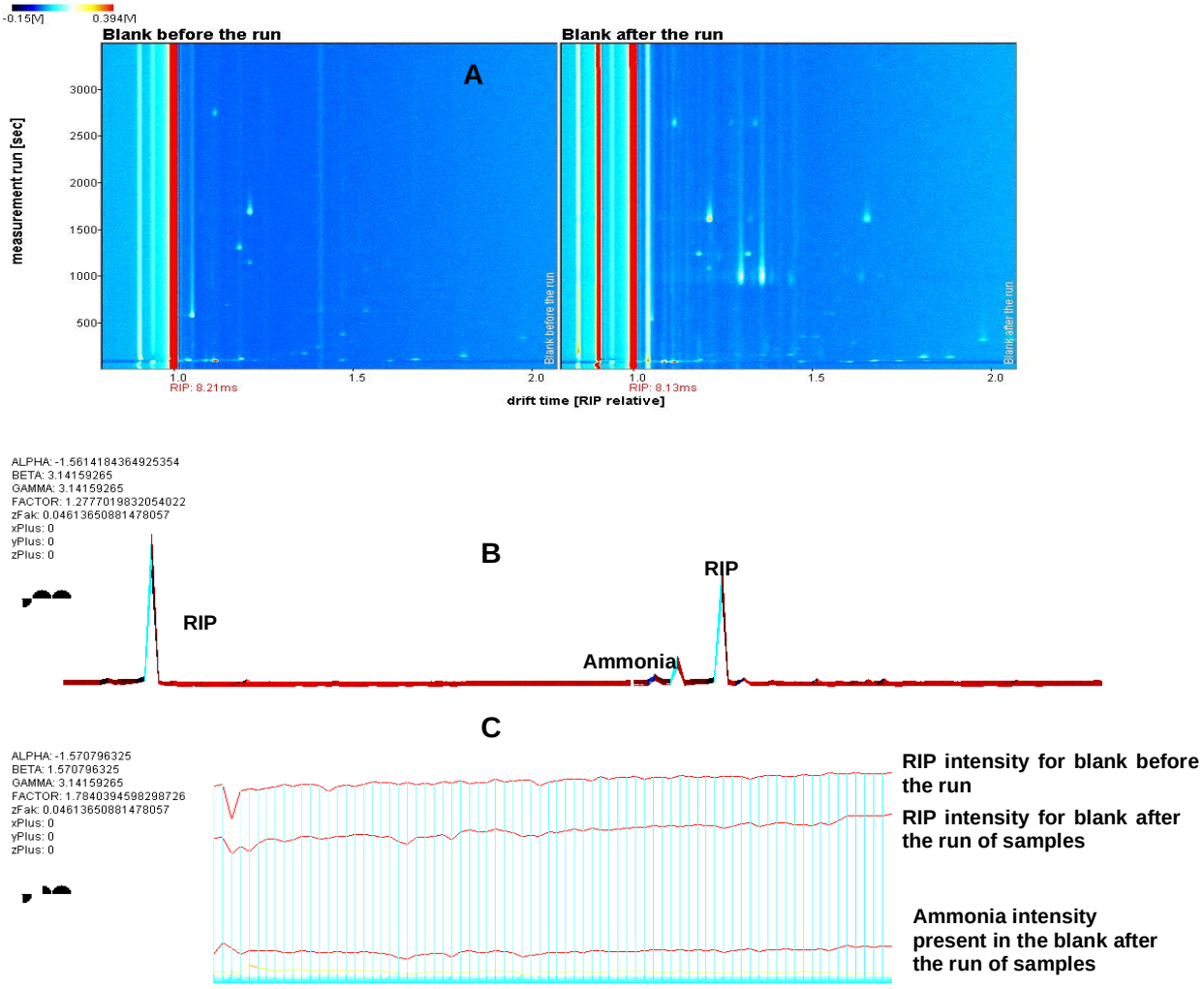

Figure 18: Blank made by deionised water before and after running samples where (A) represents the plot spectrum, (B) a 3D-view plot the chromatogram front view (B) and (C) a side view

3.3.5 Experimental setup B1 and B2

With the increase of the flow in the carrier gas, the pressure inside the column should increase accordingly, and the retention time should decrease. In Figure 19 (A) the ketones mix was analysed with a high flow of the carrier gas and it was observed that peaks at the bottom of the spectrum were suppressed, without a good resolution. With lower flow peaks for 2-butanone, 2-pentanone and 2-hexanone were seen to be more observable (Fig. 19B).

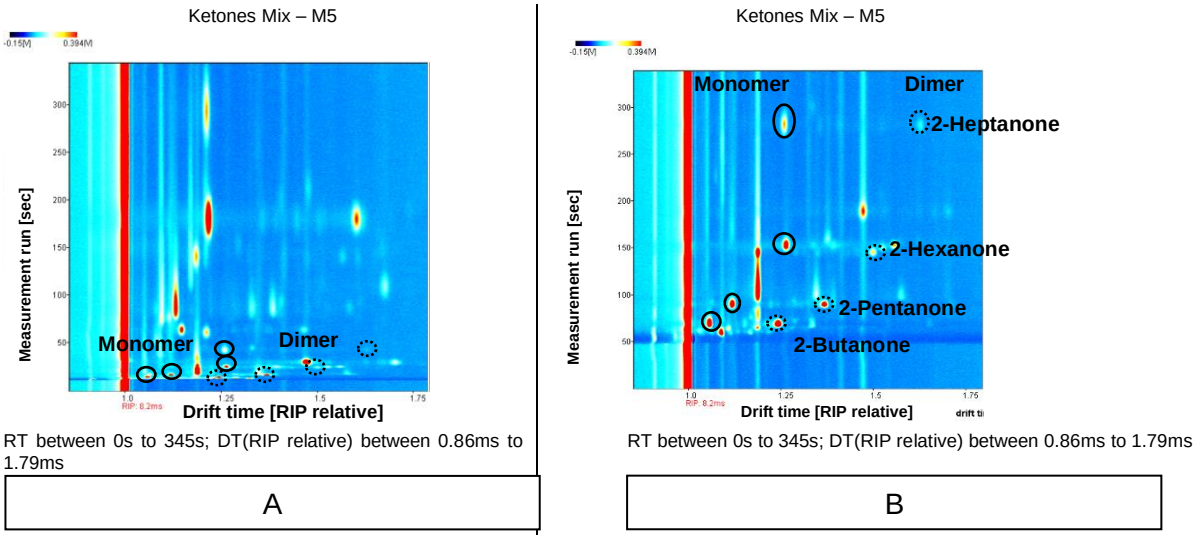

Figure 19: Experimental setup B1 (A) and experimental setup B2 (B)

3.3.6 Experimental setup B3

Figure 20 (A) shows the spectra from the ketones mix from concentrations M5 to M1. The result shows a good separation between all compounds (2-nonanone, 2-octanone, 2-heptanone, 2-hexanone, 2-pentanone, and 2-butanone) suggesting that the general methodology applied is effective and in figure 20 (B) zoom in 2-hexanone, 2-pentanone, and 2-butanone from Figure 20 (A).

To improve the separation and peak quality in the lighter compounds (2-hexanone, 2-pentanone, and 2-butanone) lower carrier gas flow (and therefore higher retention time) was required, most likely between 2-5 mL/min. For the heavy compounds (2-nonanone, 2-octanone, 2-heptanone) a higher flow rate (and lower retention time) is required to allow good peak definition within the run time. In this experiment, the heaviest ketone, 2-nonanone, is detected at around 24 minutes and for this reason, the variable ramped flow rate was proposed.

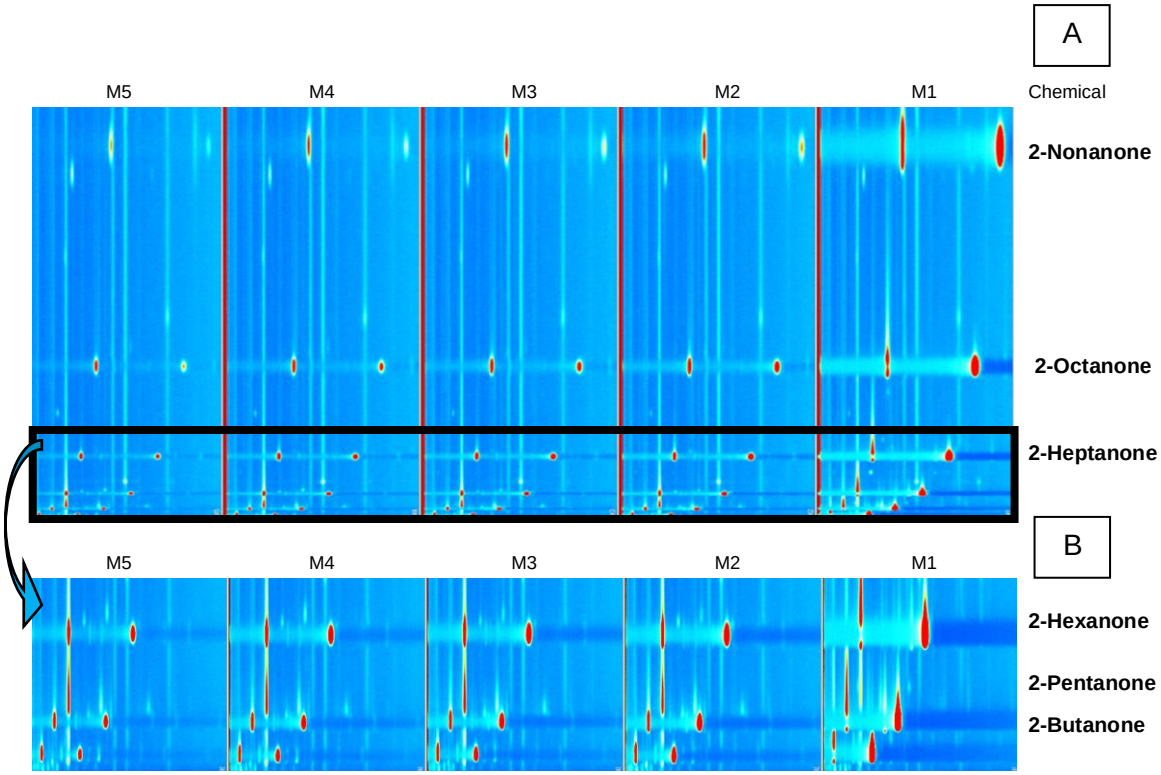

RT between 62s to 170s; DT(RIP relative) between 1.0ms to 1.95ms

Figure 20: Experimental setup B3 using ketones mix (A) and figure 20 (B) is an amplification from figure 20 (A)

3.3.7 Experimental setup B4

Table 20 shows that the retention index, the retention time (in seconds) and the drift time relative to the RIP (in milliseconds) for the dimer of ketones were all increased with the molecular weight of the molecule. All groups increased their numbers in all categories. This is because as the molecular weight of the compound increases it will take a longer time to move through the stationary phase and arrive at the detector. Figure 21 (A) shows the locations of the markers for ketones in the spectrum, and Figure 21 (B) shows a gallery plot for all ketones in triplicate. It is possible to see that the dimer for 2-nonanone only appeared with a strong peak for M1 and the intensity for the peaks between triplicates were constant, showing a good reproducibility for the method using GC-IMS. Due to the ramping of the flow for the carrier gas, it was possible to decrease the retention time for 2-nonanone from approximately 24 minutes (Experiment B3) to 496 seconds (8 minutes and 26 seconds) in experimental setup B4. Whilst the lower mass of ketones showed a good separation, it was considered that further improvements would be desirable because in real-world samples the overloading of peaks would be unlikely to happen because the carrier gas flow would be too fast to separate them, resulting in poor peak definition.

During the experiment, it was observed that the spectrum had become less well defined than in previous experiments. The only significant change made prior to the experiment was the changing of the septa in the injection port before the run. It was important to monitor the number of injections made to injector port septa because after approximately 100 injections the system began to lose pressure in the column and the RT of the peaks could change. Thus, the optimised methodology included regularly changing the septa followed by running the instrument on clean mode to remove any contamination introduced to the instrument from changing the septa.

As a further check for contamination in the system, and to normalize the library (the retention index), a ketone mix solution was analysed as a check solution at the beginning of every day. Fresh S1 solution and solutions from M5 to M1 were prepared each day to ensure that volatiles were present at consistent concentrations. If the result from ketones mix was satisfactory then more samples could be run. If the ketone mix results were not satisfactory then the equipment was switched to clean mode or any other necessary remedial procedures could be undertaken. This simple step delivered a significant improvement in the overall efficiency of the method as it drastically reduced the number of occasions on which samples were analysed when the instrument was not fully clean.

Figure 21 (C) presents peaks that were found to be present in all spectrums generated in this experiment. The peak on the left side was identified as contamination from within the instrument and, after the injection of nitrogen, the peak on the right side was identified as originating from the syringe. Contamination present within the instrument could only be addressed by putting the system within clean mode for several days. Any contamination remaining after this step could no longer be removed and, if producing a peak that interfered with those of the target chemicals, a new column would need to be replaced. The syringe related contamination peaks were most likely associated with solvents such as 2-propanol or methanol used to clean the syringe that was not fully removed prior to using the instrument. Using this information, it was possible to consider these peaks as background noise and ignore them.

Table 20: Identification of dimers for ketones

Markers	Compound	Retention Index ± 15	Rt GC [s]	Dt [RIPrel]ms ± 0.01
1	2-Nonanone	1095.6	496.939	1.8876
2	2-Octanone	996.5	303.796	1.7619
3	2-Heptanone	892.2	191.684	1.6352
4	2-Hexanone	784.2	127.429	1.5066
5	2-Pentanone	688.6	91.656	1.3741
6	2-Butanone	589.4	76.541	1.2485

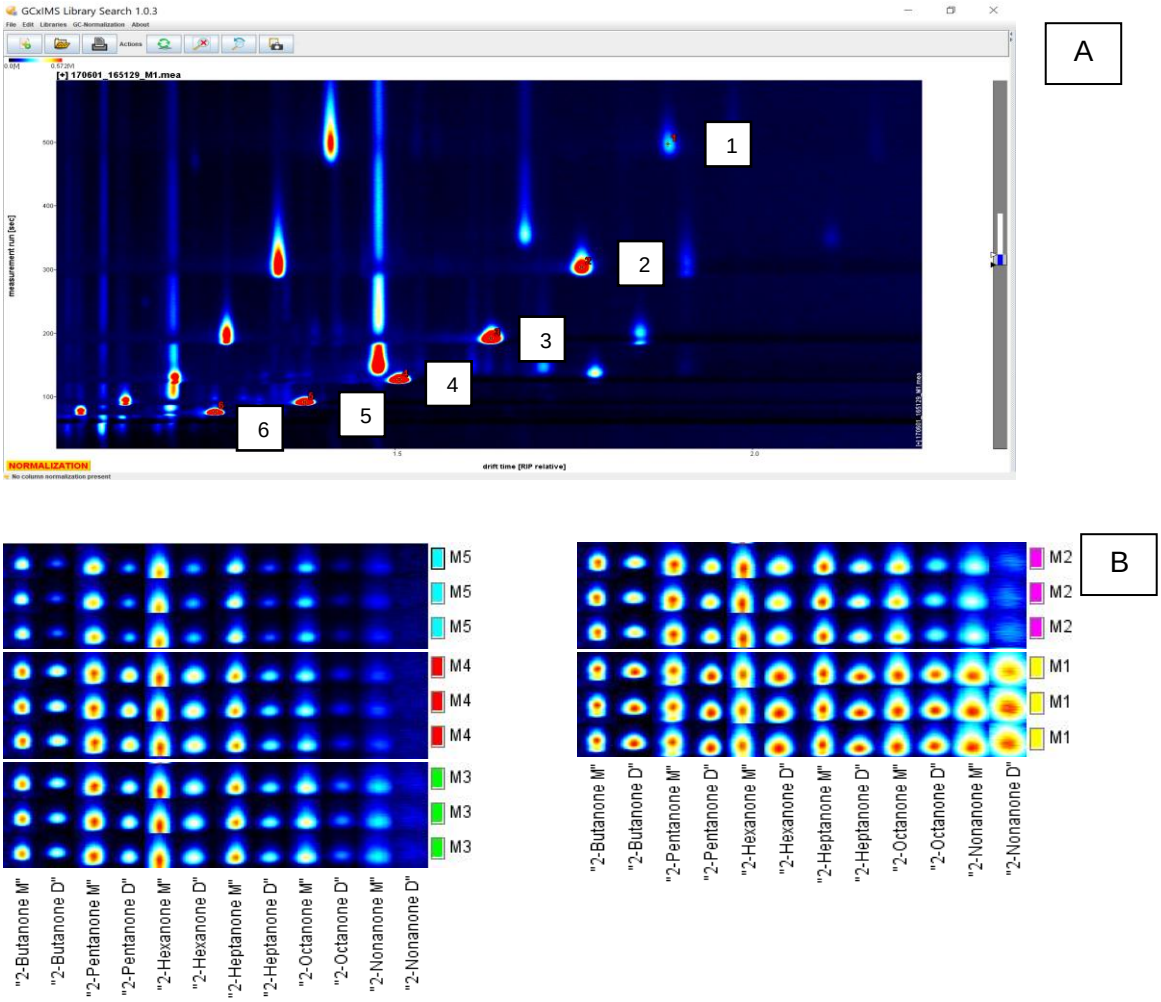

RT between 34s to 596s; DT(RIP relative) between 0.97ms to 1.70ms

Figure 21: Identification of the markers in the ketones' spectrum (A); Gallery plot for all ketones mix in triplicate (B) On the left side the contamination from the equipment and on the right side the contamination from the syringe (C).

3.3.8 Experimental setup B5

Table 21 presents the retention index, the retention time and the drift time for experimental setup B4 and B5. In both experiments, the retention index had exactly the same number and the drift times were the same to 2 decimal places. Retention time differed as desired. At the beginning of Experiment B4, 2-butanone was located at 77 seconds whereas in Experiment B5 was located at 69 seconds, an 8 second decrease in retention time. This reduction in retention time was as a result of increasing the carrier gas flow rate to 5 mL/min (in B5) from 2 mL/min (in B4). For 2-pentanone, the difference in retention time between Experiments B4 and B5 was not significant - it was located at 92 seconds (B4) 93 seconds (B5). However, the relative difference between the retention times for 2-butanone and 2-pentanone it is significant. In Experiment B4, 15 seconds separated these two chemicals and in B5 was 25 seconds. The additional 10 seconds retention time difference will allow for better separation between them and clearer identification on the spectra. The retention time difference between 2-pentanone and 2-hexanone was similarly improved from 36 to 60 seconds of difference, and for 2-heptanone to 2-nonanone an increased retention time difference of approximately 36-43 seconds was achieved. Improving the separation of all ketones was achieved at the cost of increasing the run times. The heaviest ketone 2-nonanone was located at 497 seconds (B4) and in B5 was located at 533 seconds. This demonstrated the compromise between achieving a good separation of the peaks through increasing carrier gas flow rate and achieving as low a runtime as possible. Figure 22 shows the row data between B4 and B5 program.

Table 21: Comparison between B4 and B5 to identify the dimers for ketones

	Experimental setup B4			Experimental setup B5		
Compound	**RI ± 15**	**Rt GC [s]**	**Dt [RIPrel] ms ± 0.01**	**RI ± 15**	**Rt GC [s]**	**Dt [RIPrel] ms ± 0.01**
2-Nonanone	1095.6	496.939	1.8876	1095.6	533.217	1.8814
2-Octanone	996.5	303.796	1.7619	996.5	347.235	1.7602
2-Heptanone	892.2	191.684	1.6352	892.2	229.993	1.6350
2-Hexanone	784.2	127.429	1.5066	784.2	153.159	1.5042
2-Pentanone	688.6	91.656	1.3741	688.6	93.264	1.3711
2-Butanone	589.4	76.541	1.2485	589.4	68.694	1.2469

Compound	**B4 Rt [s]**	**B5 Rt [s]**	**B4 difference [s]**	**B5 difference[s]**	**B5-B4 [s]**
2-Nonanone	**497**	**533**	193	186	36
2-Octanone	**304**	**347**	112	117	43
2-Heptanone	**192**	**230**	64	77	37
2-Hexanone	**127**	**153**	36	60	26
2-Pentanone	**92**	**93**	15	25	1
2-Butanone	**77**	**69**	0	0	-8

RI Retention Index; Rt Retention time, Dt Drift time

Example: B4 difference: (2-pentanone)-(2-butanone)=92-77=15 sec

B4 difference: (2-hexanone)-(2-pentanone)=127-92=36 sec

B5-B4: (2-butanone B5)-(2-butanone B4)=69-77=-8sec

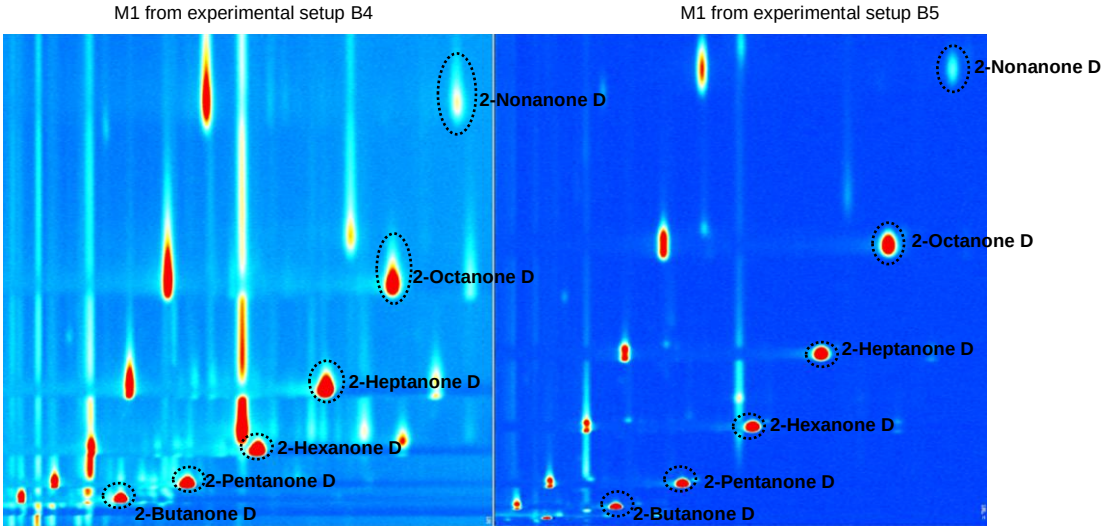

RT between the 50s to 570s; DT(RIP relative) between 1.02ms to 1.95ms

Figure 22: Comparing different programs (B4 and B5)

3.3.9 Experimental setup B7

Figure 23 represents the program to measure VOC for AD samples (experimental setup B6) and a program to measure VFAs (experimental setup B7). It was used the ketone mix to compare both programs. The experimental setup B7 injected more volume than B6 and for that reason the peak was strong and had a long run time.

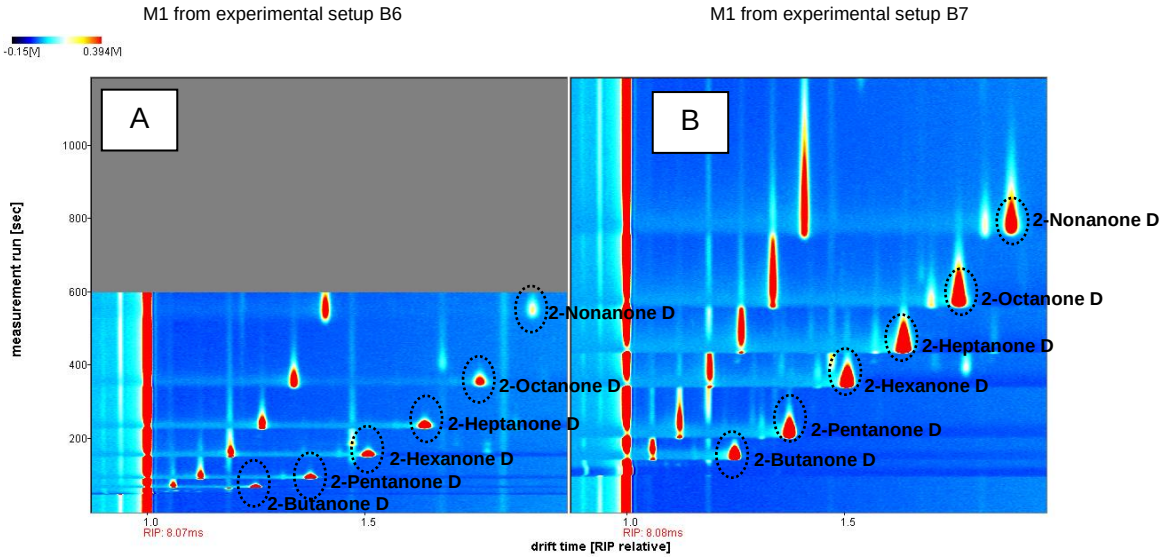

RT between the 50s to 1200s; DT(RIP relative) between 0.8ms to 1.95ms

Figure 23: Final method for general VOCs on AD samples (24A) and VFAs (24B)

3.3.10 Assessment of the precision of the GC-IMS method

To validate an analytical method and to see if the system is performing well, some parameters can be used such as the precision, the linearity or the robustness (Bhardwaja *et al.*, 2016). As Bhardwaja *et al.* (2016) said "the robustness is defined as the measure of the ability of an analytical method to remain unaffected by small but deliberate variations in method parameters (e.g. pH, mobile phase composition, temperature and instrumental settings) and provides an indication of its reliability during normal usage". The linearity of an analytical technique is its capability (within a specified range) to get an analytical response that is directly proportional to the quantity of interest (e.g. concentration of analyte in the sample). For calibrations at least five different concentrations are used, and ideally having three range of magnitude (e.g. 10 mg/L, 100 mg/L and 1000 mg/L). The precision can be verified by the method precision (the repeatability that is the intraday variation) and by intermediate precision (the reproducibility that is the interday variation). In this case, to investigate the repeatability a solution containing a ketone mix was used (2-butanone, 2-pentanone, 2-hexanone, 2-heptanone, 2-octanone and 2-nonanone) at 500 µg/L. The same sample was run 6 times using different vials, during the same day with the same program for flows and temperatures. The reason why these compounds were selected to perform this trial was because they appear in the same region for Rt and dt as the target VOCs for AD samples and they have different fingerprint signatures, therefore it is easier to differentiate each compound.

For the intermediate precision (B) was evaluated by running in total 18 samples contained 2-butanone and 2-pentanone at beginning of each day and for the intermediate precision (C) was included as well runs done between AD samples or running at end of the day to perform a total of 28 analysis. 2-Butanone and 2-pentanone had the same concentration as the repeatability trial encompassing a time period approximately of 3 months. The reason why only two compounds were selected to do this investigation was because they can be present in AD samples, especially in digestate samples.

Table 22 presents the results for the precision (repeatability and intermediate precision B and C) where they were expressed as standard derivation (SD), the average (avg.) for the peak intensity, and relative standard derivation in percentage (RSD %) of normalized peak intensity. This means, after data acquisition, each peak was aligned in retention and drift time scales using the position of the RIP as reference in LAV software to normalize the peak intensity. The LAV software collected the intensity of each peak and

calculated the SD, avg., RSD. The RSD was calculated by dividing the SD for the avg. and multiplied for 100 to get the percentage.

Table 22: Repeatability and intermediate precision study

Compound	Repeatability (A)			Intermediate precision (B)			Intermediate precision (C)		
	SD	Avg.	RSD (%)	SD	Avg.	RSD (%)	SD	Avg.	RSD (%)
2-Butanone M	0.02	1.10	1.53	0.03	1.09	2.69	0.07	1.06	6.19
2-Butanone D	0.04	2.93	1.39	0.08	2.92	2.79	0.14	2.90	4.70
2-Pentanone M	0.01	1.08	1.20	0.03	1.07	3.13	0.06	1.04	6.04
2-Pentanone D	0.04	2.63	1.45	0.11	2.59	4.38	0.18	2.57	6.88
2-Hexanone M	0.01	0.94	1.32						
2-Hexanone D	0.03	2.45	1.19						
2-Heptanone M	0.02	0.93	2.39						
2-Heptanone D	0.03	1.87	1.72						
2-Octanone M	0.02	0.93	1.77						
2-Octanone D	0.03	0.87	3.87						
2-Nonanone M	0.02	0.75	2.30						
2-Nonanone D	0.03	0.31	9.09						

The repeatability results were very satisfactory because in general the RSD was lower than 5%, except for 2-nonanone dimer that was 9.09%. As Contreras *et al.* (2019) explained the reason why 2-nonanone had this higher RSD could be related to the lower solubility of 2-nonanone in water, especially for the dimer of this analyte (Contreras *et al.*, 2019). In general, the peak intensity is higher for dimer than monomer for ketones excepted to 2-octanone and 2-nonanone that is the opposite. Comparing the intensity of all peaks, the intensity decreased when the molecular weight increased in the compound, so 2-butanone had the biggest value for the intensity and 2-nonanone the lowest value, except for 2-heptanone monomer and 2-octanone monomer that had similar values.

The intermediate precision (B) had better results than the intermediate precision (C) where all results were lower than 5%, while for intermediate precision (C) was lower than 7%. This could be explained because for the intermediate precision (C) data it was included as well data from runs done at end of the day or between real samples and the machine had a small influence (e.g. for example some carry over of ammonia). The repeatability trial performed better than the intermediate precision, for 2-butanone and 2-pentanone because there were lower values for RSD, however it is possible to conclude that these results demonstrated that the analytical method was highly robust and the system performed well.

Contreras *et al.* (2019) measured the precision of their GC-IMS method by using 2-butanone, 2-pentanone, 2-hexanone, 2-octanone, and 2-nonanone as reference standards. The repeatability study, consisted of 5 standard solutions analysed on the same day and used 58 standard solutions across a time period of 3 months, for the intermediate precision. The repeatability values were lower than 8.2% and lower than 10% for the intermediate precision. Jafari *et al.* (2018) used GC-IMS as an analytical tool with SPME nanofibers to detect organophosphorus pesticides (e.g. tetraethoxysilane polyacrylonitrile, chlorpyrifos, malathion) in liquid environmental samples (e.g. farm wastewater, and river water) or products for human consumption (e.g. fruit juice and milk). His method obtained a RSD between 4-6% for the intra-day precision (3 samples) and 13-15% for the inter-day precision (Jafari *et al*., 2018). Criado-Garcia *et al*. (2015) detected benzene and phenol in heat transfer fluid samples by GC-IMS. To evaluate the repeatability of the method, the authors measured the same sample 6 times, during the same day using the same experimental conditions. The reproducibility study measured the sample for three consecutive days (9 samples in total). Results showed 9.2% for the repeatability study and 13.3% for the reproducibility study (Criado-García *et al*., 2015). GC-IMS was used by Márquez-Sillero *et al*. (2014) to monitor the degradation of milk products with flavours and linseed oil samples enriched with omega-3 acids. The intraday precision varied between 2.4 to 6.7% (n = 5), and the interday precision between 2.7 to 7.0% (n = 15) (Márquez-Sillero et al., 2014). Baumbach *et al.* (2003) detected gasoline additives (methyl tert-butyl ether), nitrogen, monoaromatics compounds (benzene, toluene, and m-xylene) by GC-IMS (with a radioactive and UV ionization source) in water samples. They achieved a good reproducibility with RSD between 2.9 to 9% (Baumbach *et al*., 2003). Comparing the results from this research with available literature, the repeatability varied 2.9-9.2% and for most between 4-8.2%. It has therefore been found that the results are in accordance with published work. The reproducibility in this work was lower than 6% and in the case of Contreras *et al.* (2019) who used the same standards as in this study, they achieved a value lower than 10%.

3.4 OUTCOME FROM THIS CHAPTER

Chapter 3 evidenced an analytical method which was acceptable to measure a specific compound such VFAs or ammonia, with simplified procedures that delivered a reliable measurement. As a result, the final approach achieved the goal of allowing the analysis of samples derived from the AD sector using the following conditions. 1mL of the sample (even diluted samples if was that the case like in ratio of 1:10 or 1:100) was loaded into a 20 mL vial and closed with magnetic caps. After 9 minutes of incubation at 45°C, 100 µL of headspace gas sample was injected by a heated syringe (80°C) into the injector

port (80°C). The column (SE-54 at 40°C) separated the compounds and IMS (45°C) detected them. The flow rate for IMS was constant (EPC1 150 mL/min) and for the column (EPC 2) varied between 5-50 mL/min and has a run time of 10 minutes. Samples were analysed in duplicate as a minimum in order to assess reproducibility of the method. Table 23 summaries the final conditions for the analytical method. In summary, the analytical method development confirmed that an accurate and reliable measurement could be performed.

Table 23: Final method for generic VOCs

Setup for autosampler

Column	Sample type	Sample Volume [µL]	T Incubation [°C]	Incubation Time [min]	T Syringe [°C]	GC-Runtime [min]
SE-54-CB1	Headspace	100 µL	45 °C	9 min	80 °C	10 min 30 sec

Setup for GC-IMS

T1 IMS [°C]	T 2 Column [°C]	T 3 Injection Port [°C]	RIP Voltage	Av	Trigger-D [µs]	Measurement Runtime [min]
45 °C	40 °C	80 °C	+	6	100	10 min

Program for flow on drift gas and carrier gas

Time	EPC1 [mL/min]	EPC2 [mL/min]	Recording
00:00.000	150	5	Starting recording
02:00.000	150	5	|
10:00.000	150	50	|
10:00.020	150	50	Stop recording

3.5 CONCLUSIONS

The aim of the project was to devise a rapid and inexpensive methodology, with the minimum sample preparation as possible and with the potential to be automated for online to be apply in the AD sector. GC-IMS has the advantages of allowing the separation of complex mixtures into their constituents, uses small sample volumes (100µL), has good precision, sensitivity, reproducibility for qualitative, and quantitative analysis. However, the technique does require that the target analytes be volatile enough to be moved into the gas phase and not be thermally unstable to the temperatures used. The research presented in this Chapter describes a methodology that provided good reproducibility for a sample that was run in triplicate (figure 22B):

- The best column for the target compounds (experimental setup B1);
- The ideal time for headspace equilibrium (experimental setup B2);

- Method optimization using the least run time as possible without losing sensitivity (experimental setup B6); and the other physical parameters conditions for the analysis, like flow or column temperature (experimental setup B1 and B2);
- Identified important parameters related to samples such as dilutions (experimental setup A1, A3) to avoid overload of the equipment without losing the ability to measure the compounds;
- Identified possible interfering compounds that should be studied more in detail such as ammonia (this topic will be developed more in detail in Chapter 5);
- Identified compounds in various matrices (this point will be more developed on Chapter 4) based on their retention time, drift time and Kovats indices;
- studied the importance of using blanks between samples and the value of good maintenance and cleaning of the equipment;
- The methodology developed is likely to work for VFA measurements.

4. IDENTIFICATION AND QUANTIFICATION OF VOLATILE CHEMICALS USING GC-IMS

4.1 INTRODUCTION

AD processes treat a multitude of organic feedstocks with a wide range of physical and chemical compositions that produce a range of intermediate and final products. These intermediates and products can include chemical groups such as alkanes, alcohols and VFAs. Understanding the concentration of these materials within various stages of the process can provide information relating to the effectiveness of the treatment process and the potential for producing odours, and can, therefore, influence the way in which the plant is operated to improve overall efficiency, or reduce nuisance associated with odours. Whilst Chapter 3 focused mainly on the establishment of a general methodology for GC-IMS which was found appropriate to analyse AD related samples, this chapter describes the methodology used and the results obtained when identifying these chemical signatures in standard solutions and in samples from an AD plant.

4.2 MATERIAL AND METHODS

4.2.1 Samples

The samples used for this chapter were the same used for Chapter 3. They comprised commercial and industrial FW (ABP) and digested material (second digestate) and were recovered from an AD plant. The only sample preparation undertaken was a 10 times dilution (1mL of sample in 9 mL deionised water) to ensure that results were within detectable limits.

4.2.1.1 Preparation of standard solutions for GC-IMS analysis

Table 24 present the reagent grade, assay, empirical formula, molecular weight, CAS number, density (at 25°C) and boiling point for each chemical standard. Working solutions for aromatics and terpenes were prepared by placing 20µL of the standard solution into 100 mL (S1), then remove 1mL of S1 and put into a 50 mL volumetric flask (M1). For ketones, the solution was based on data present in experimental setup B1 for M1 (Chapter 3). For VFAs (acetic acid, propionic acid and butyric acid) a stock solution of 1000 mg/L was prepared and the several dilutions were performed using deionised water. Table 25 presents the concentration of each standard.

4.2.2 GC-IMS

4.2.2.1 GC-IMS instrumentation and operational conditions

For the identification of chemicals using standard solutions and for AD samples, the analytical method used was the final method described in Chapter 3 for generic VOCs (experimental setup B6) and a specific method for VFAs (experimental setup B7). One of the parameters that the GC-IMS Library Search software version 1.0.3 offered was the Kovats' Retention Index, which was referenced to the NIST GC retention index database and the GC-IMS library. To normalize the library, a ketone mix measurement with the range of concentration 0 – 450 µg/L (the preparation was explained in the experimental setup B1) was undertaken with results loaded onto the GC-IMS Library Search (figure 25). This allowed the normalization of the retention time using a known chemical and allowed correlation with other specific retention indices included in the database. Once this was complete a compound list related to ketones mix was imported from the default files containing the following information: compound name, CAS number, the chemical formula, MW, RI, Rt, Dt in RIP relative (figure 25). Choosing the dimer of each ketone, the position of the selected item in the compound list item (e.g. 2-butanone) was adjusted to normalize the retention time and drift time based on the actual position of each dimer in the spectrum (Figure 26). For example, Figure 27 shows the right position for 2-butanone dimer in the spectrum. The correct place to choose the retention time in the spectrum of a known compound was in the middle of the peak because it is where the peak had the maximum area (intensity). Figure 28 presented the changes in the retention time for all ketones and the graphic for the retention index normalization using a logarithmic function. The y-axis showed retention index ranging from 600 to 1100 and the x-axis showed the logarithmic retention time in seconds from 1.9 to 2.7. As an example of the adjustments required, the database defaulted for 2-butanone were RI = 589.4, Rt = 5.984 sec, and drift (in RIP relative) = 1.2497 ms. After normalization these became RI = 589.4, Rt = 71.586 sec, and Dt (in RIP relative) = 1.2463 ms. Pre and post normalisation the RI remained the same, the drift time had a difference of 0.0034ms and the retention time had a difference of 65.602 seconds. Figure 29 shows an attempt to identify unknown chemicals after being normalized by the RI. A standard solution was prepared containing benzene, toluene and ethylbenzene for this demonstration. In this example, the software indicated the unknown chemical was toluene as expected. The left side shows the red histograms where the green lines show the drift time for toluene and on the right side the chemical that matches for that retention index (761.6), retention time (141.993 sec) and drift time in RIP relative (1.0178 ms) for the column SE-54 according to NIST2014 library. It is possible to find out by using the

compound CAS number or by name or by RI, in GC×IMS Library Search. The retention index had an error ±15 and the drift time (in RIP relative) an error of ±0.01. To normalize the library, it was always necessary to run the ketones mix with the same program, and it was only possible to identify chemicals with an RI between 600 to 1100. If a chemical had a RI out of this range then it was not possible to identify it. It is important to do the normalization to account for changes in retention time due to operational conditions, the type of column and the performance of the equipment. The reduce ion mobility and inverse reduce ion mobility present in the results was calculated based on the equation 7 and it was compared using the software VOCal 0.0.1.

4.2.3 GC-MS

4.2.3.1 Sample preparation

To support identification of the AD samples using GC-IMS, initial analyses using GC-MS were performed. The GC-MS analyses were performed by an external company using the methodology for measuring VOCs and at the same tried to mimic the program already setup for GC-IMS for general compounds (experimental setup B6). For sample the GC-MS analysis followed the same preparation i.e. 300mg NaCl was added to 1 mL of each sample and the adsorption with the fibre occurred for 1 hr at 45°C and extracted for 20 minutes using DVB/CAR/PDMS fibre in the GC-MS inject port. The objective for using the fibre was to concentrate the sample while this was stirred. Samples used were ABP, cow slurry, SP1, SP2, SP3, SP4, SP8, digestate after pasteurization and digestate from the storage tank as illustrated on Figure 8.

4.2.3.2 Instrumentation and operation conditions

The analysis of VOC and SVOC was performed by GC-MS using an Agilent 6890 gas chromatograph coupled to an Agilent 5972 mass selective detector. The instrument was equipped with a split/splitless injector, fitted with a low volume 0.75 mm ID Ultra Inert straight liner (Agilent, Santa Clara, US), a Merlin Microseal and an HP–5ms (30 m × 0.25 mm × 0.25 µm, Agilent J&W, Santa Clara, US) analytical column. The injection port was operated in splitless mode and held at a constant 250°C. The carrier gas was helium (99.9995%) at a constant flow rate of 1 ml/min. The following oven temperature program was employed: 35°C for 5 min; a temperature ramp of 3°C/min to 300°C; and then 300°C held for 15 min. The transfer line temperature was set to 280°C. The quadrupole mass spectrometer was operated in scan mode, with a mass range from 38–500 amu, and was tuned on PFTBA.

Table 24: Standard used for identification of peaks

Product name	Reagent grade	Assay	Empirical formula	Molecular Weight	CAS №	Density g/mL at 25 °C	B. P. (°C)
Functional group: Ketones							
2-Butanone	ACS reagent	0.99	$C_2H_5COCH_3$	72.11	78-93-3	0.805 g/mL	80°C
2-Pentanone	FCC. FG	0.98	$CH_3CO(CH_2)_2CH_3$	86.13	107-87-9	0.809 g/mL	101-105°C
2-Hexanone	Reagent grade	0.98	$CH_3(CH_2)_3COCH_3$	100.16	591-78-6	0.812 g/mL	127°C
2-Heptanone	Analytical standard	0.99	$CH_3(CH_2)_4COCH_3$	114.19	110-43-0	0.820 g/mL	149-150°C
2-Octanone	Reagent grade	0.98	$CH_3(CH_2)_5COCH_3$	128.21	111-13-7	0.819 g/mL	173°C
2-Nonanone	Reagent grade	0.98	$CH_3(CH_2)_6COCH_3$	142.24	821-55-6	0.820 g/mL	192°C
Functional group: Aromatics							
Benzene	Analytical standard	0.999	C_6H_6	78.11	71-43-2	0.874 g/mL	80°C
Toluene	Anhydrous	0.998	$C_6H_5CH_3$	92.14	108-88-3	0.865 g/mL	110-111°C
Ethylbenzene	Analytical standard	0.995	$C_6H_5C_2H_5$	106.17	100-41-4	0.867 g/mL	136°C
Functional group: Terpenes							
α-pinene	Analytical standard	0.985	$C_{10}H_{16}$	136.23	7785-70-8	0.858 g/mL	155-156°C
γ-terpinene	Analytical standard	0.95	$C_{10}H_{16}$	136.23	99-85-4	0.850 g/mL	182°C
3-carene	Analytical standard	0.985	$C_{10}H_{16}$	136.23	13466-78-9	0.857 g/mL	168-169°C
Limonene	Analytical standard	0.99	$C_{10}H_{16}$	136.23	5989-27-5	0.842 g/mL	176-177°C
p-Cymene	Analytical standard	0.995	$CH_3C_6H_4CH(CH_3)_2$	134.22	99-87-6	0.860 g/mL	176-178°C
Functional group: Ammonia							
Ammonium hydroxide	(28% NH_3 in H_2O)	0.9999	NH_4OH	35.05	1336-21-6	0.90 g/mL	38°C
Functional group: Acid							
Acetic acid	Analytical standard	0.998	CH_3COOH	60.05	64-19-7	1.049 g/mL	117-118°C
Propionic acid	Analytical standard	0.995	CH_3CH_2COOH	74.08	79-09-4	0.993 g/mL	141°C
Butyric acid	Analytical standard	0.995	$CH_3(CH_2)_2COOH$	88.11	107-92-6	0.964 g/mL	162°C

Table 25: Concentration of each Standard used for identification of peaks

Product name	Assay	Density at 25 °C	S0 (g/mL)	S1 (mg/L)	M1 (µg/L)
Functional group: Ketones					
2-Butanone	0.99	0.805	0.11	22.77	455.40
2-Pentanone	0.98	0.809	0.11	22.65	453.04
2-Hexanone	0.98	0.812	0.11	22.74	454.72
2-Heptanone	0.99	0.820	0.12	23.19	463.89
2-Octanone	0.98	0.819	0.12	22.93	458.64
2-Nonanone	0.98	0.820	0.12	22.96	459.20
Functional group: Aromatics					
Benzene	0.999	0.874	N/A	174.63	3492.50
Toluene	0.998	0.865	N/A	172.65	3453.08
Ethylbenzene	0.995	0.867	N/A	172.53	3450.66
Functional group: Terpenes					
(+/-)-Alpha-pinene	0.985	0.858	N/A	169.03	3380.52
Gamma-terpinene	0.950	0.850	N/A	161.50	3230.00
3-carene	0.985	0.857	N/A	168.83	3376.58
Limonene	0.990	0.842	N/A	166.72	3334.32
p-Cymene	0.995	0.860	N/A	171.14	3422.80
Functional group: Acid					
Acetic acid, propionic acid, butyric acid (mg/L)			0.00; 5.00; 25.00; 50.00; 100.00; 200.00; 250.00; 300.00;400.00; 500.00;		

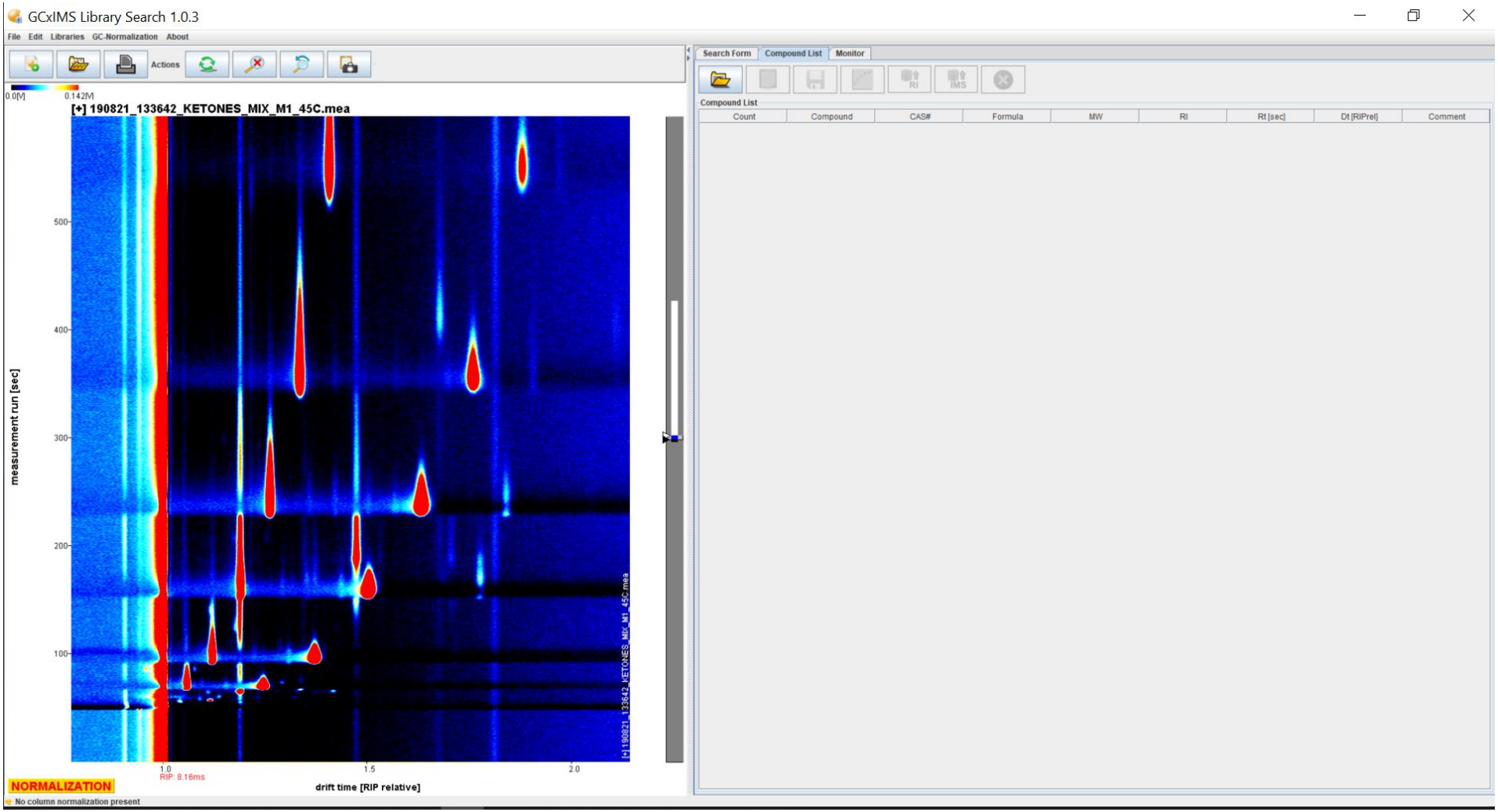

Figure 24: Ketones measurement file upload on GC×IMS Library Search 1.0.3 software

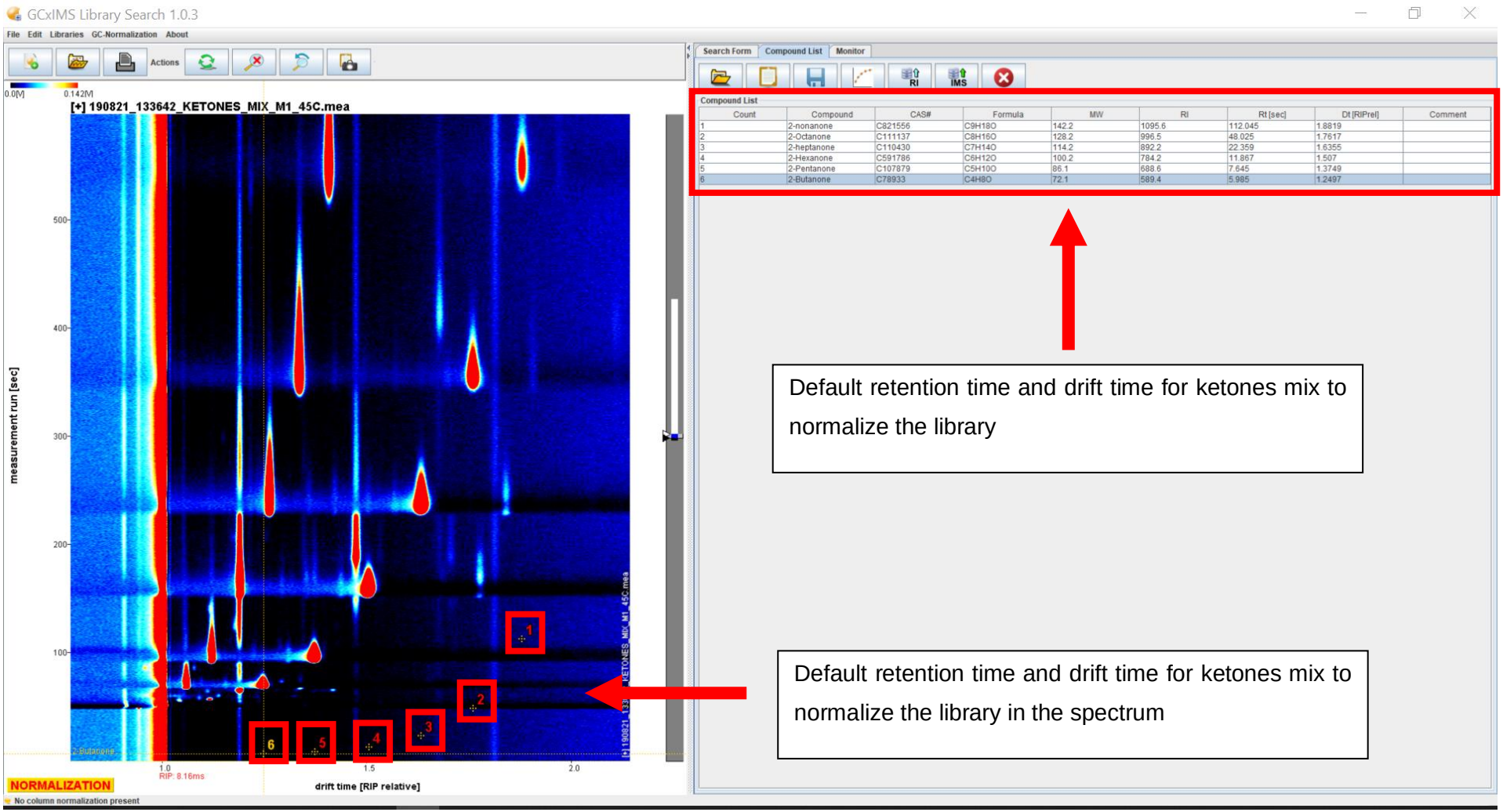

Figure 25: Upload the compound list for ketones

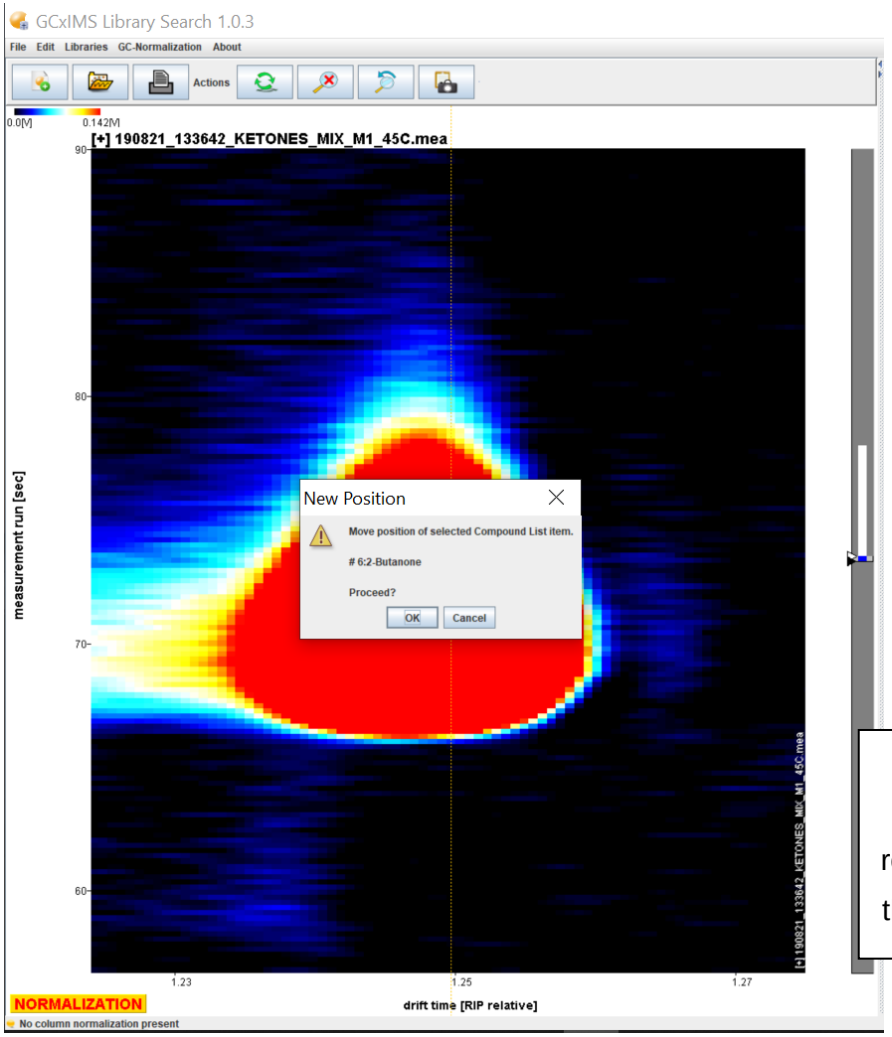

Figure 26: Normalization the retention time and drift time for 2-butanone dimer

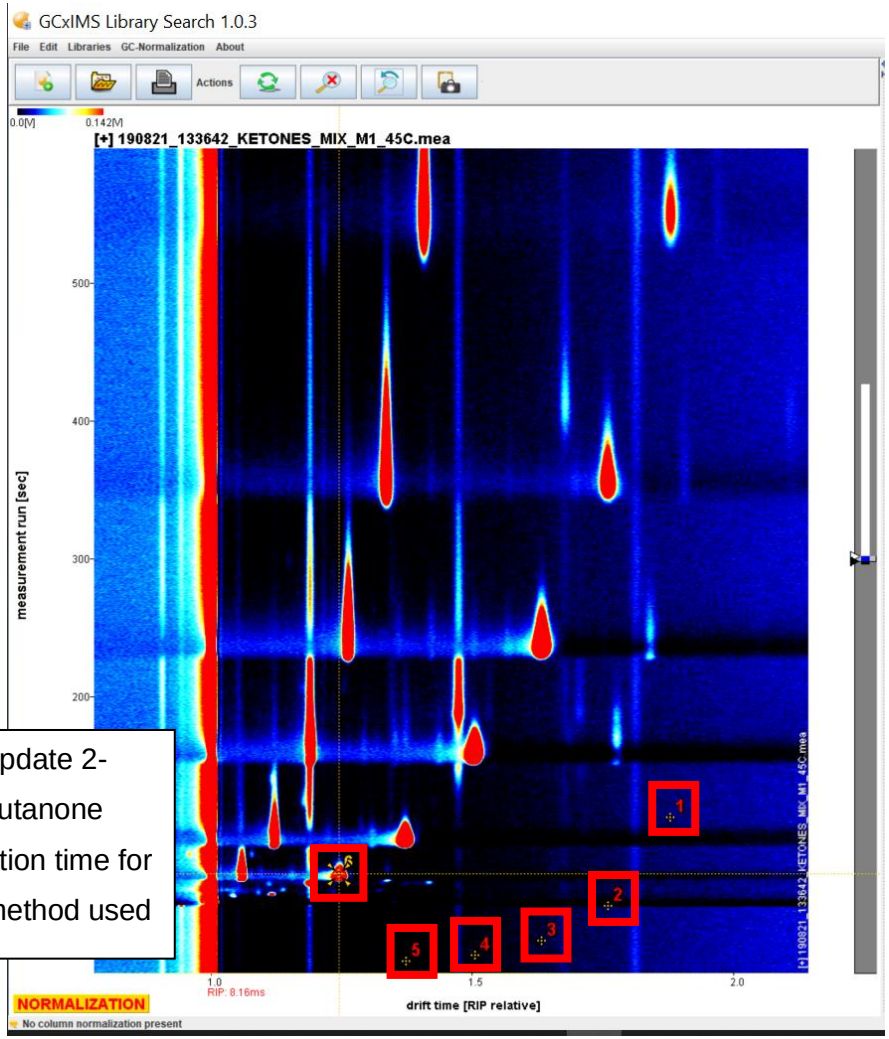

Update 2-butanone retention time for the method used

Figure 27: New retention time and drift time for 2-butanone dimer

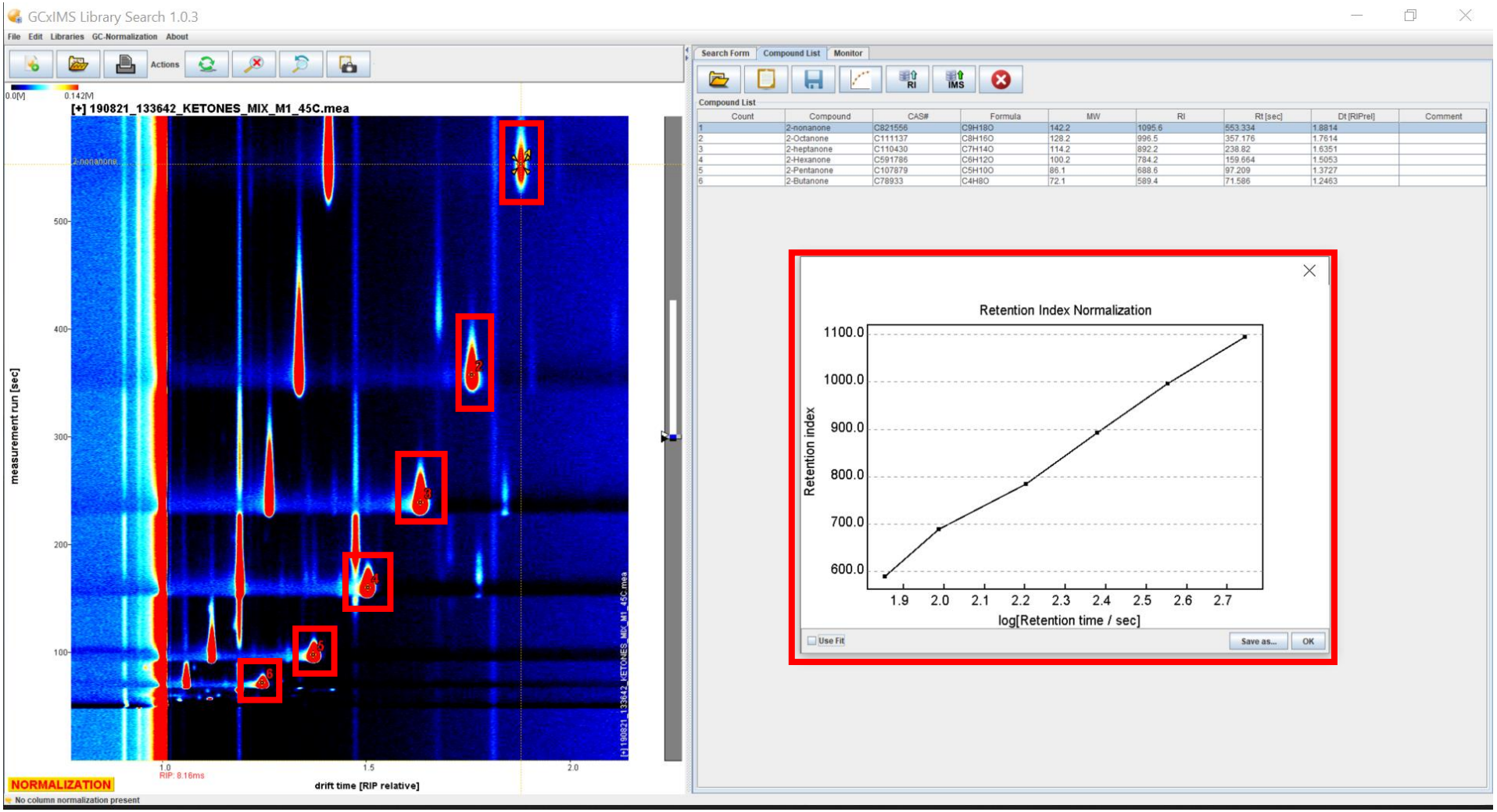

Figure 28: Normalization the retention time and drift time for all ketones and the graphic for the retention index normalization

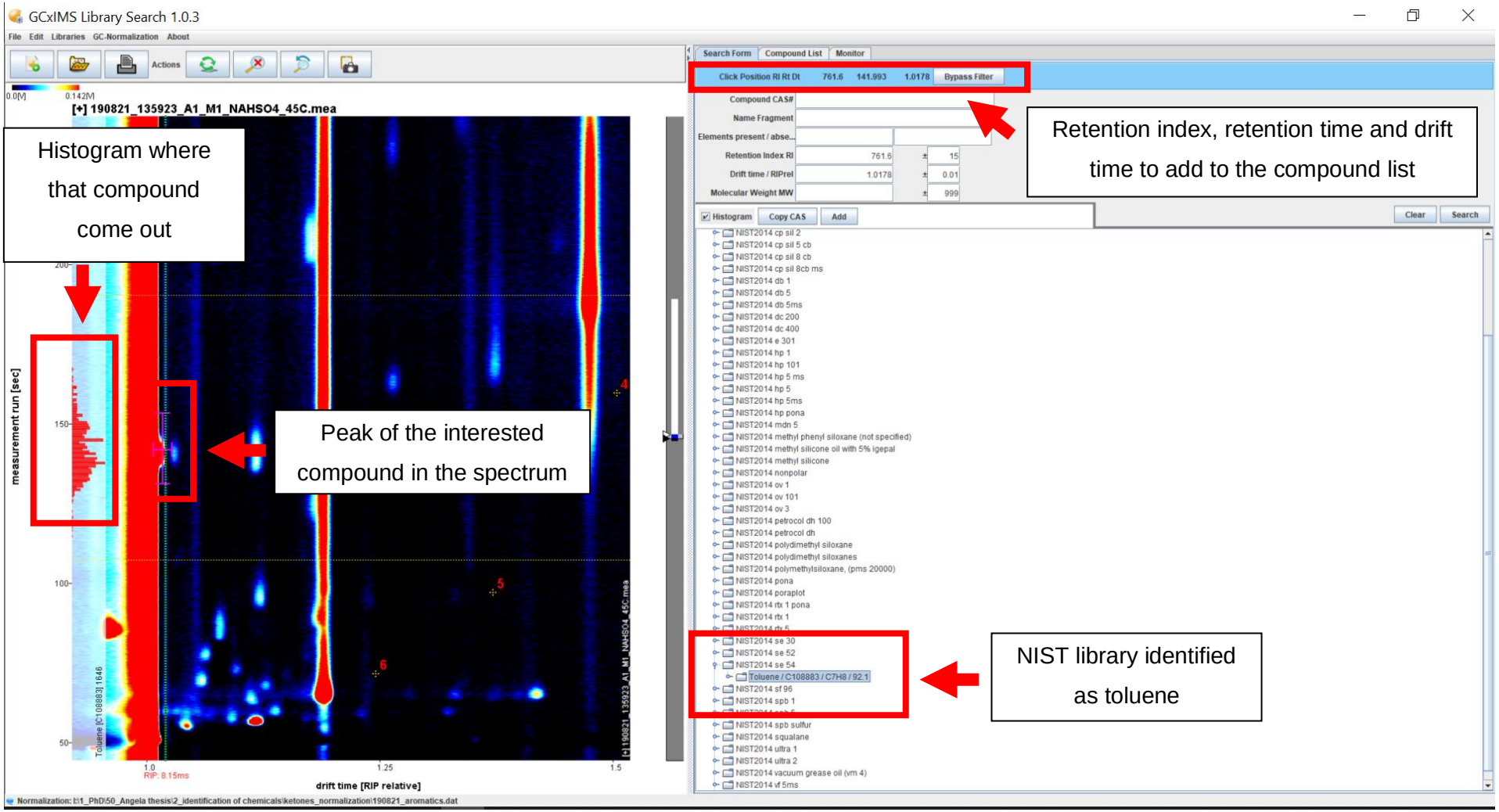

Figure 29: Identification of unknown peak

4.3 RESULTS AND DISCUSSION

Until now, GC-IMS had not been applied on AD samples before. For this reason, a database for identifying these volatile chemicals was extremely limited. The identification of compounds allowed an improved understanding of the process performance and the monitoring of process indicators such as VFAs or ammonia. Reporting data in the way that it was possible to compare with other research studies, it was fundamental and for that reason the K_0 and $1/K_0$ were relevant parameters to present data from GC-IMS. GC-IMS besides being a screening tool able to identify differences in the processes and non-targeted compounds, it could also be a tool to identify VOC in different matrices. The main objective of this chapter was to compare GC-IMS data, especially related to RI, K_0, $1/K_0$ with the results already published in the literature to be able to identify VOCs present in AD samples. To achieve this, targeted analytical standards were used with results compared with the NIST library database. As an additional mechanism to confirm results, samples were analysed using GC-MS in addition to GC-IMS for comparison of results. GC-MS is one of the most common techniques to identity and quantify compounds, and it is considered an universal technique to identify unknown compounds. GC-MS analysis would support a calibration of the GC-IMS. The GC×IMS library search did not include ammonia and for that reason this was only possible to identify using an analytical standard.

4.3.1 Identification using standard solutions:

4.3.1.1 Identification of VFAs

Figure 30 shows the spectrum for all VFAs at concentration 25, 250 and 500 mg/L whilst Figure 31 presents an amplification of Figure 30. The VFAs were identify using the GC×IMS library search. It was possible to see the increase of intensity for the dimer when the concentration increased. The spectrum of VFAs was imported into the GCxIMS Library Search (v.1.0.3) and normalised using a M1 ketones mix to allow for their identification. The peaks were identified as reported in section 4.2.2 taking into consideration that the peak intensity increased according to the concentration increase. A challenge posed was that there were also other analytes which showed peaks by the GC-IMS spectrum as they were present in the standards and their intensity increased when the standard concentration increased as well. For example, it was detected by GC GCxIMS Library Search (v.1.0.3) one of the peaks, which was ethyl propanoate (Rt

246.0s; Dt 1.454ms and RI 715.5). One option to confirm this would be to analyse the analytical standard using GC-MS.

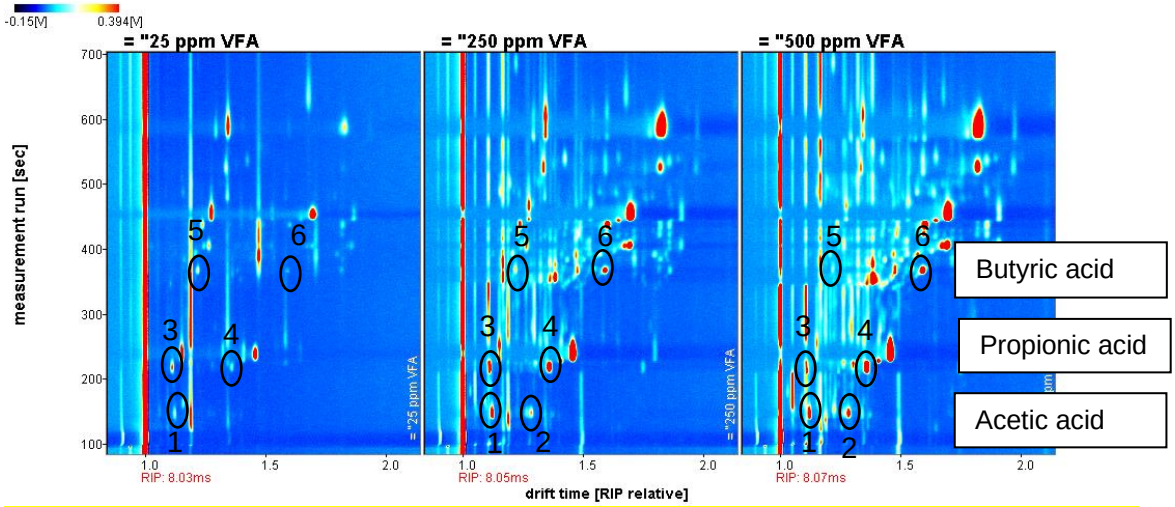

Figure 30: Identification VFAs (acetic acid, propionic acid and butyric acid) in the GC-IMS spectrum (1 acetic acid monomer, 2 acetic acid dimer, 3 propionic acid monomer, 4 propionic acid dimer, 5 butyric acid monomer, 6 butyric acid dimer) at concentration 25, 250 and 500 mg/L.

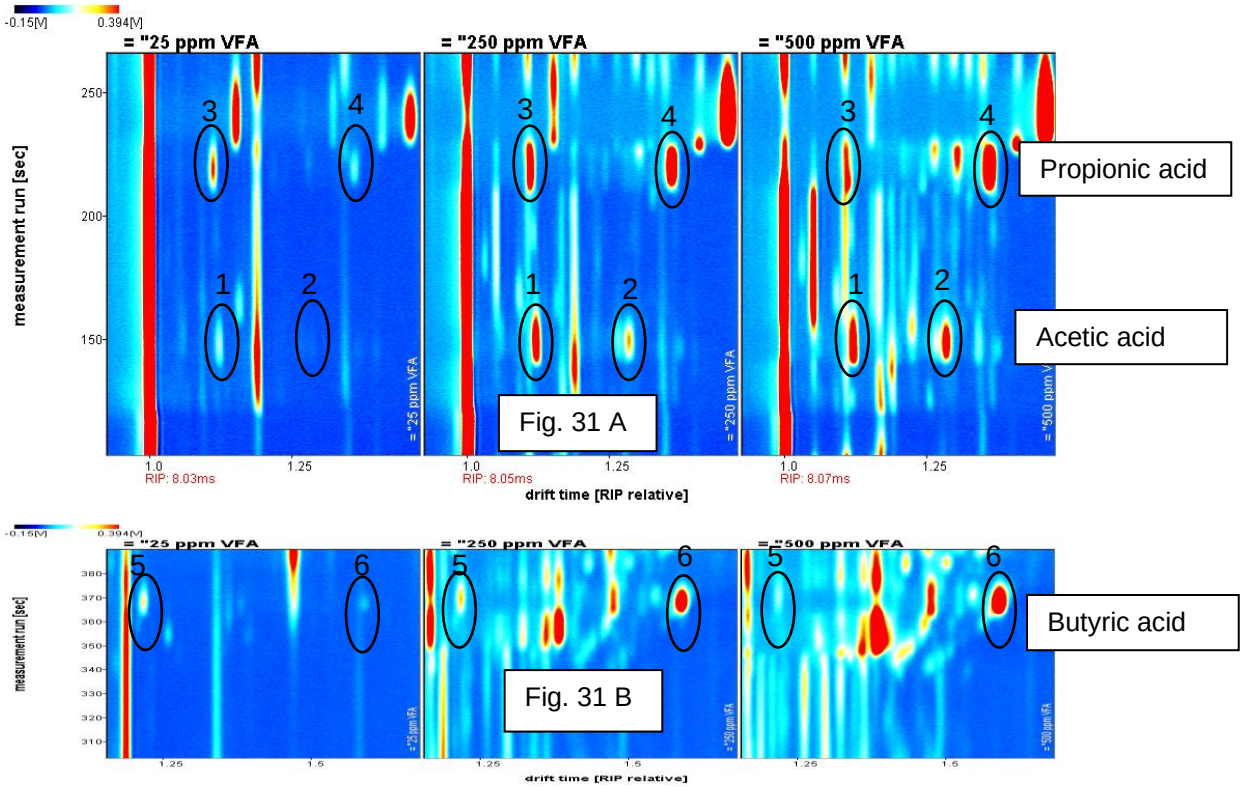

Figure 31: Amplification of the spectrum from Figure 30

4.3.1.2 Aromatics, terpenes and ketones

Table 26 presents the results obtained for retention index, retention time, drift time (normalized to RIP drift time), K0 calculated, K0 report by VOCal 0.0.1, 1/K0 calculated, 1/K0 report by VOCal 0.0.1 when standards for ketones, aromatics and terpenes were analysed using GC-IMS. The monomer and dimer for each compound are shown when present. The only compound that reported a trimer was p-cymene. Measured RI's ranged from 600.5 (2-Butanone) to 1,098.4 (2-Nonanone). Comparing the RI data obtained from instrument / software and what was published in the literature, all values were within ±15 error, with Limonene and 2-octanone presenting the largest deviations from literature of 13.5 and 10.33, respectively. 2-Hexanone presents the smallest RI difference of just 0.47. Thus, it is possible to conclude all results are in accordance with published literature. Figure 32 summarises all the spectra from the identification of the standard solutions. The identification of toluene presents some challenges because the peak is very close to the RIP.

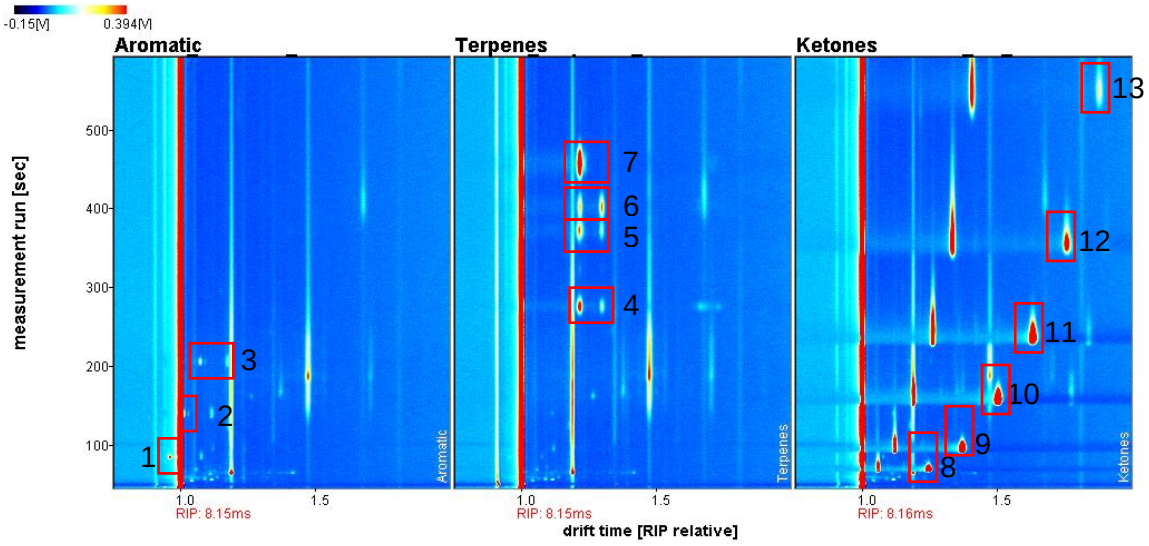

Number	Compound	Number	Compound	Number	Compound
1	Benzene	6	Limonene	10	2-hexanone
2	Toluene	7	γ-terpinene	11	2-heptanone
3	Ethylbenzene	8	2-butanone	12	2-octanone
4	α-pinene	9	2-pentanone	13	2-nonanone
5	3-carene				

Figure 32: Identification aromatics, terpenes and ketones in the spectrum

4.3.2 GC-MS analyses in AD samples

Samples from a full-scale AD plant were analysed by GC-MS to establish the VOCs present and to help with the identification using GC-IMS. Table 27 indicates the labels applied in Table 28.

Table 26: Parameters for the identification of standards using GC×IMS Library Search and VOCal

		Monomer							Dimer							
Result from	**Product name**	**RI ±15**	**Rt(s)**	**Dt*[1] ±0.01**	**K_0 calculated**	**K_0 report software**	**$1/K_0$ calculated**	**$1/K_0$ reported by software**	**RI ±15**	**Rt(s)**	**Dt*[1] ±0.01**	**K_0 calculated**	**K_0 report software**	**$1/K_0$ calculated**	**$1/K_0$ reported by software**	**Ref**
Functional group: Ketones																
GC-IMS	2-Butanone	600.50	73.170	1.058	1.915	1.923	0.522	0.520	595.70	72.094	1.246	1.626	1.633	0.615	0.612	
GC-IMS	2-Pentanone	691.60	97.889	1.121	1.807	1.816	0.554	0.551	691.30	97.742	1.372	1.476	1.484	0.677	0.674	
Literature	**2-Pentanone**	**687.79**														**A**
GC-IMS	2-Hexanone	790.50	162.106	1.189	1.704	1.711	0.587	0.585	792.80	163.544	1.505	1.346	1.354	0.743	0.739	
Literature	**2-Hexanone**	**790.03**				**1.716**		**0.581**					**1.555**		**0.640**	**B**
GC-IMS	2-Heptanone	898.50	244.623	1.262	1.605	1.613	0.623	0.620	893.00	239.456	1.632	1.241	1.247	0.806	0.802	
Literature	**2-Heptanone**	**891.70**				**1.618**		**0.617**					**1.256**		**0.793**	**C**
GC-IMS	2-Octanone	1001.60	364.892	1.337	1.516	1.524	0.660	0.656	998.90	360.575	1.762	1.150	1.157	0.870	0.865	
Literature	**2-Octanone**	**991.27**														**A**
GC-IMS	2-Nonanone	1098.40	558.840	1.408	1.439	1.446	0.695	0.691	1096.60	554.525	1.881	1.077	1.083	0.928	0.924	
Literature	**2-Nonanone**	**1092.50**				**1.452**		**0.688**					**1.093**		**0.904**	**B**
Functional group: Aromatics																
GC-IMS	Benzene	653.10	86.241	0.959	2.114	2.116	0.473	0.473								
Literature	**Benzene**					**1.940**										**E**
GC-IMS	Toluene	762.40	141.339	1.017	1.993	2.010	0.502	0.498								
GC-IMS	Ethylbenzene	855.20	207.418	1.074	1.887	1.894	0.530	0.528	856.60	208.491	1.178	1.722	1.732	0.581	0.577	

Continuation of Table 26 related to the parameters for the identification of standards using GC×IMS Library Search and VOCal

		Monomer							Dimer							
Result from	Product name	RI	Rt(s)	Dt*1	K_0 calculated	K_0 report software	$1/K_0$ calculated	$1/K_0$ reported by software	RI	Rt(s)	Dt*1	K_0 calculated	K_0 report software	$1/K_0$ calculated	$1/K_0$ reported by software	Ref
Functional group: Terpenes																
GC-IMS	α-pinene	932.20	277.152	1.216	1.667	1.670	0.600	0.599	932.50	277.450	1.300	1.559	1.556	0.641	0.639	
Literature	**α-pinene**	**936.10**														**D**
GC-IMS	3-carene	1008.20	375.143	1.216	1.668	1.674	0.600	0.597	1007.20	373.449	1.301	1.559	1.567	0.641	0.638	
Literature	**3-carene**	**1011.30**														**D**
GC-IMS	Limonene	1026.00	405.661	1.219	1.664	1.671	0.601	0.598	1025.40	404.529	1.301	1.558	1.567	0.642	0.638	
Literature	**Limonene**	**1039.50**				**1.680**		**0.593**					**1.556**		**0.643**	**C**
GC-IMS	γ-terpinene	1056.30	463.223	1.218	1.665	1.674	0.600	0.597								
Literature	**γ-terpinene**	**1059.70**														**D**
GC-IMS	p-Cymene	1020.50	395.998	1.190	1.704	1.714	0.587	0.583	1018.80	393.001	1.215	1.669	1.679	0.599	0.596	

Trimer

Result from	Product name	RI	Rt(s)	Dt*1	K_0 calculated	K_0 report software	$1/K_0$ calculated	$1/K_0$ reported by software	Ref
GC-IMS	p-Cymene Trimer	1018.80	393.001	1.280	1.584	1.591	0.631	0.629	
Literature	**p-cymene**	**1024.30**							**D**

Dt*1 Drift time in RIP relative (ms)

Continuation of Table 26 related to the parameters for the identification of standards using GC×IMS Library Search and VOCal

		Monomer							Dimer							
Result from	**Product name**	**RI**	**Rt(s)**	**Dt*[1]**	**K_0 calculated**	**K_0 report software**	**$1/K_0$ calculated**	**$1/K_0$ reported by software**	**RI**	**Rt(s)**	**Dt*[1]**	**K_0 calculated**	**K_0 report software**	**$1/K_0$ calculated**	**$1/K_0$ reported by software**	**Ref**
Functional group: Acid																
GC-IMS	Acetic acid	596.5	158.754	1.1212	1.8119	1.82	0.552	0.549	586.0	153.189	1.2845	1.5815	1.591	0.632	0.629	
Literature	**Acetic acid**					**1.913**										**F**
Literature	**Acetic acid**					**2.18**										**G**
GC-IMS	Propionic acid	693.0	221.656	1.1123	1.8264	1.839	0.548	0.544	693.0	221.656	1.3594	1.4944	1.503	0.669	0.665	
Literature	**Propionic acid**					**1.86**										**G**
Literature	**Propionic acid**		**87.0**	**1.22**		**1.92**					**1.60**		**1.46**			**H**
GC-IMS	Butyric acid	806.7	370.255	1.2171	1.6691	1.676	0.599	0.597	804.9	368.691	1.592	1.2760	1.283	0.784	0.779	
Literature	**Butyric acid**					**1.75**										**G**
Literature	**Butyric acid**		**174**	**1.27**		**1.87**					**1.42**		**1.67**			**H**

Dt*[1] Drift time in RIP relative (ms)

References

A - (Fatemi, 2002)
B - (Fatemi, 2002; Jünger *et al.*, 2010; Vautz *et al.*, 2009)
C - (Babushok *et al.*, 2011; Jünger *et al.*, 2010; Vautz *et al.*, 2009)**.**
D - (Babushok *et al.*, 2011)
E - (Criado-García *et al.*, 2015)
F - (Mochalski *et al.*, 2018)
G - (Masár *et al.*, 2020)
H - (Denawaka *et al.*, 2014)

In Table 28 if the square is white the compound was not detected by GC-MS but if the square was shaded, then the compound was present. The data is organized by feedstocks (ABP - number 1; cow slurry - number 2), then the primary reactor (from SP1 to SP8, digestion start SP1 with number 3, SP2 number 4, SP3 number 5, SP4 number 6 and SP8 number 7). Number 8 refers to the digestate sample after being pasteurized and number 9 it was a sample from the storage tank (second digester). The compounds present in all samples were toluene, p-xylene, β-pinene, limonene, and (-)-camphor. Limonene was the compound with highest area in the ABP sample, and for cow slurry, it was 4-methyl-phenol and for all digestate samples were p-cymene. Besides limonene, the FW sample presented other compounds principally from the acid group, and it was very different from the cow slurry and digestate samples in terms of the volatile profile. Cow slurry presented a number of aromatic organic compounds such as indole, phenol, 3-ethylphenol; 4-ethylphenol; benzene, 2-methylindole, and p-xyene.

The results from GC-MS seemed to be in accordance with the results from Arrhenius *et al.* (2016). In this study, the authors reported terpenes, especially monoterpenes, were up to 90% of all VOCs in the biogas from a FW plant. P-cymene was the main VOCs in digestate and biogas samples, while D-limonene was more present for feedstock. Other terpenes identified were γ-terpinene, eucalyptol, α-terpinene, 3-carene, β-pinene, β-myrcene, camphene and α-pinene. Terpenes can bring problems to AD plants related to odour problems, indoor air quality issues at workplaces and operational problems (damage to plastic pipelines, damage to components in the gas grid, dissolve electrical cables) (Arrhenius *et al.*, 2016). Terpenes are also limited in terms of gas injection into the UK network.

Table 27: Labels for table 28

	Number	Sample label		Number	Sample label
Primary digester	**3**	SP1	**Feedstocks**	**1**	ABP
	4	SP2		**2**	Cow slurry (CS)
	5	SP3			
	6	SP4	**P**	**8**	Digestate after pasteurization
	7	SP8	**2Dig**	**9**	Digestate from second digestate tank

Table 28: Identification of compounds from feedstocks, primary reactor, digestate after pasteurization tank and digestate from storage tank

		Feedstocks		Primary Reactor					P	2Dig
CAS	Name	1	2	3	4	5	6	7	8	9
75-15-0	Carbon disulphide									
78-93-3	2-Butanone									
78-92-2	2-Butanol									
107-87-9	2-Pentanone									
96-22-0	3-Pentanone									
110-86-1	Pyridine									
108-88-3	Toluene									
120-92-3	Cyclopentanone									
1757-42-2	3-Methylcyclopentanone									
100-41-4	Ethylbenzene									
106-42-3	p-Xylene									
108-38-3	m-Xylene									
95-47-6	o-Xylene									
108-94-1	Cyclohexanone									
110-43-0	2-Heptanone									
96-48-0	Butyrolactone									
105-66-8	Propyl butyrate									
539-82-2	Ethyl valerate									
80-56-8	α-Pinene									
79-92-5	Camphene									
100-52-7	Benzaldehyde									
928-68-7	6-Methylheptan-2-one									
95-49-8	2-Chlorotoluene									
106-43-4	4-Chlorotoluene									
2436-90-0	Dihydromyrcene									
127-91-3	β-Pinene									
142-62-1	Hexanoic acid									
62-53-3	Aniline									
500-00-5	3-p-Menthene									
3777-69-3	2-Pentylfuran									
106-68-3	3-Octanone									
108-95-2	Phenol									
13466-78-9	3-Carene									
29050-33-7	(+)-4-Carene									
99-86-5	alpha-Terpinene									
123-66-0	Hexanoic acid, ethyl ester									
535-77-3	M-Cymene									
527-84-4	O-Cymene									
99-87-6	**P-Cymene**									
138-86-3	**Limonene**									
470-82-6	Eucalyptol									
104-76-7	2-Ethylhexan-1-ol									
1074-17-5	1-Methyl-2-propylbenzene									
6781-98-2	2-Chloro-1,3-dimethylbenzene									
556-97-8	5-Chloro-m-xylene									
99-85-4	γ-Terpinene									
95-48-7	o-Cresol									
98-86-2	Acetophenone									
106-49-0	p-Toluidine									
15537-55-0	cis-(+/-)-4-Thujanol									
108-39-4	m-Cresol									
106-44-5	**4-methyl-Phenol or P-Cresol**									
586-63-0	Isoterpinolene									
1195-79-5	Fenchone									
821-55-6	2-Nonanone									

		Feedstocks		Primary Reactor					P	2Dig
CAS	Name	1	2	3	4	5	6	7	8	9
124-19-6	Nonanal									
586-62-9	Terpinolene									
576-26-1	2,6-Dimethylphenol									
471-15-8	beta-Thujone									
93-58-3	Methyl benzoate									
626-77-7	Propyl hexanoate									
60-12-8	2-Phenylethanol									
111-11-5	Methyl octanoate									
3289-28-9	Ethyl cyclohexanecarboxylate									
464-48-2	(-)-Camphor									
138-87-4	beta-Terpineol									
123-07-9	4-Ethylphenol									
620-17-7	3-Ethylphenol									
106-32-1	Ethyl octanoate									
65-85-0	Benzoic acid									
103-82-2	Benzeneacetic acid									
7786-67-6	Isopulegol									
10458-14-7	p-Menthan-3-one									
2216-51-5	l-Menthol									
10458-14-7	p-Menthan-3-one									
562-74-3	Terpinen-4-ol									
98-55-5	α-Terpineol									
619-01-2	Dihydrocarveol									
7764-50-3	Dihydrocarvone									
645-56-7	4-Propylphenol									
89-83-8	Thymol									
499-75-2	Carvacrol									
629-50-5	Tridecane									
80-26-2	α-Terpinyl acetate									
621-27-2	3-Propylphenol									
17699-14-8	α-Cubebene									
80-26-2	α-Terpinyl acetate									
3856-25-5	Copaene									
95-20-5	2-Methylindole									
120-72-9	Indole									
624-13-5	Propyl octanoate									
110-42-9	Methyl decanoate									
2021-28-5	Ethyl 3-phenylpropionate									
83-34-1	3-Methylindole									
118-65-0	Isocaryophyllene									
629-59-4	Tetradecane									
1604-34-8	6,10-Dimethylundecan-2-one									
87-44-5	β-Caryophyllen									
17699-05-7	α-Bergamotene									
110-38-3	Ethyl decanoate									
6753-98-6	Humulene									
17066-67-0	beta-Selinene									
644-30-4	α-Curcumene									
4630-07-3	Valencene									
495-60-3	α-Zingiberene									
629-62-9	Pentadecane									
495-61-4	β-Bisabolene									
128-37-0	Butylated Hydroxytoluene									
483-76-1	(+)-delta-Cadinene									
53585-13-0	(E)-γ-Bisabolene									
544-76-3	Hexadecane									
495-61-4	β-Bisabolene									

4.3.3 Comparison between GC-MS and GC-IMS for real samples

The standards used to calibrate the GC-IMS were based on the results obtained previously from the GC-MS, which suggested the presence of these chemicals in either ABP or second digestate samples. Figure 33 presents the identification from GC-IMS for ABP samples using the information collected from the GC-MS report. The red histogram represents where toluene supposed to separate out. Comparing the results from GC-IMS and GC-MS is possible to see that heavy chemicals (with a longer retention time, ± 20 min retention time) that could be detected by GC-MS were not able to be detected using GC-IMS.

One reason to explain this different is that GC-MS can reach higher temperatures compared to GC-IMS, so compounds such as indole or β-Caryophyllen where identified on the GC-MS but not on the GC-IMS. Figure 34 is a GC-MS spectrum where toluene and limonene peaks are shown. Figure 35 is a possible identification for the second digestate sample from GC-IMS library search and Figure 36 a GC-MS chromatogram for the same sample. A couple of compounds were not possible to see on GC-IMS but still possible to see on GC-MS and this could be considered one of limitation of method / equipment.

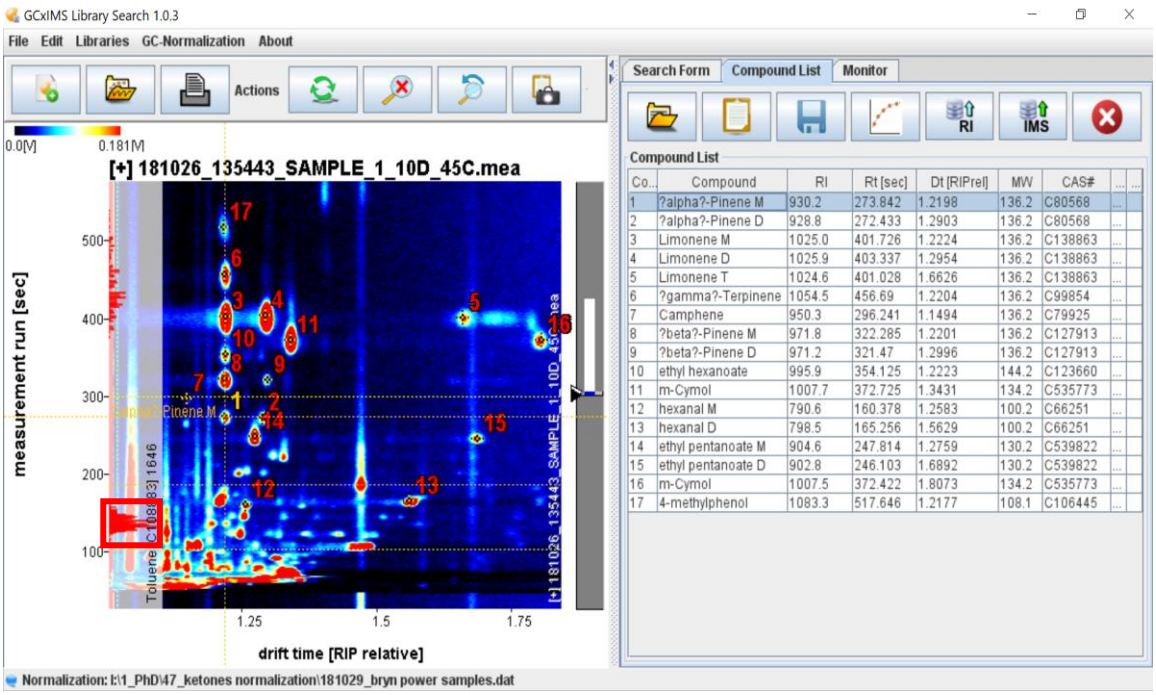

Co...	Compound	RI	Rt [sec]	Dt [RIPrel]	MW	CAS#
1	?alpha?-Pinene M	930.2	273.842	1.2198	136.2	C80568
2	?alpha?-Pinene D	928.8	272.433	1.2903	136.2	C80568
3	Limonene M	1025.0	401.726	1.2224	136.2	C138863
4	Limonene D	1025.9	403.337	1.2954	136.2	C138863
5	Limonene T	1024.6	401.028	1.6626	136.2	C138863
6	?gamma?-Terpinene	1054.5	456.69	1.2204	136.2	C99854
7	Camphene	950.3	296.241	1.1494	136.2	C79925
8	?beta?-Pinene M	971.8	322.285	1.2201	136.2	C127913
9	?beta?-Pinene D	971.2	321.47	1.2996	136.2	C127913
10	ethyl hexanoate	995.9	354.125	1.2223	144.2	C123660
11	m-Cymol	1007.7	372.725	1.3431	134.2	C535773
12	hexanal M	790.6	160.378	1.2583	100.2	C66251
13	hexanal D	798.5	165.256	1.5629	100.2	C66251
14	ethyl pentanoate M	904.6	247.814	1.2759	130.2	C539822
15	ethyl pentanoate D	902.8	246.103	1.6892	130.2	C539822
16	m-Cymol	1007.5	372.422	1.8073	134.2	C535773
17	4-methylphenol	1083.3	517.646	1.2177	108.1	C106445

Figure 33: Possible identification for ABP sample

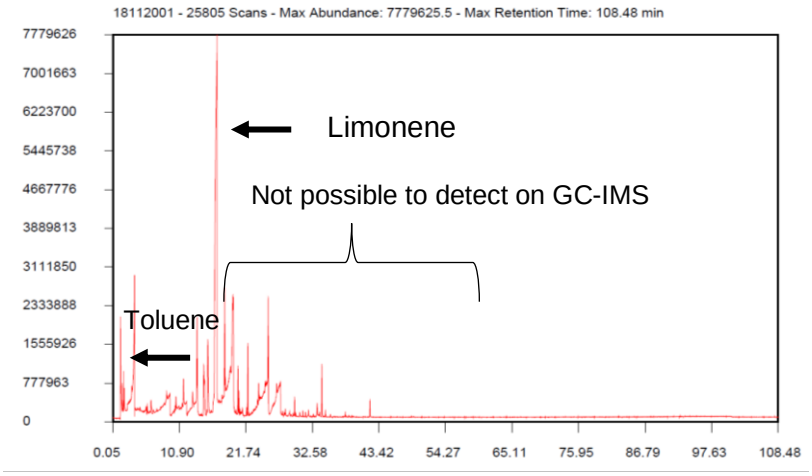

Min Abundance: 54211.148; Max Abundance 7779625.5; min retention time 0.05 min; max retention time 108.48 min; nr scans; 25805; ions:999040; scan delay: 0.05 min; scan interval:0.00 min (251 milliseconds)

Figure 34: GC-MS chromatogram for the ABP sample

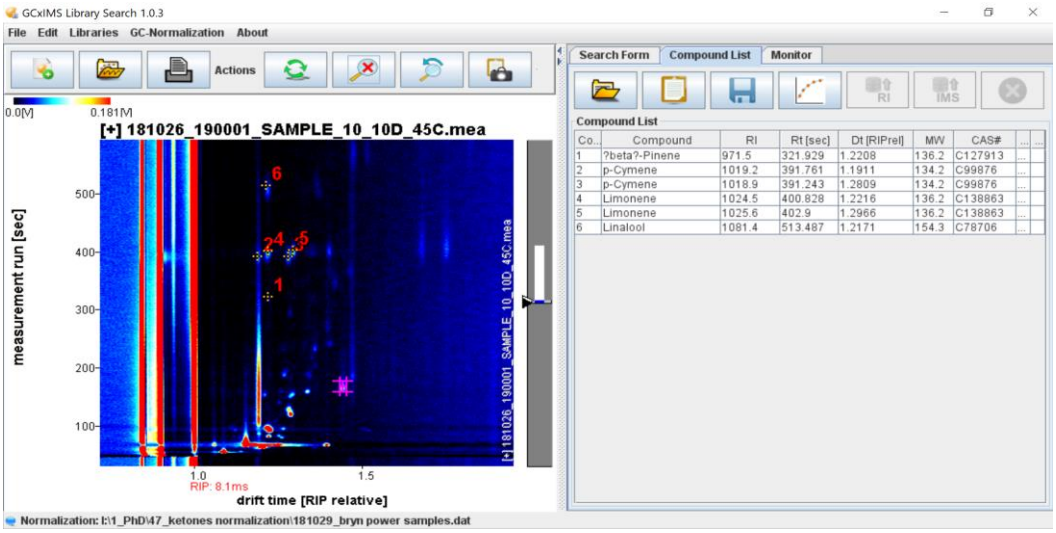

Figure 35: Possible identification for the second digestate sample

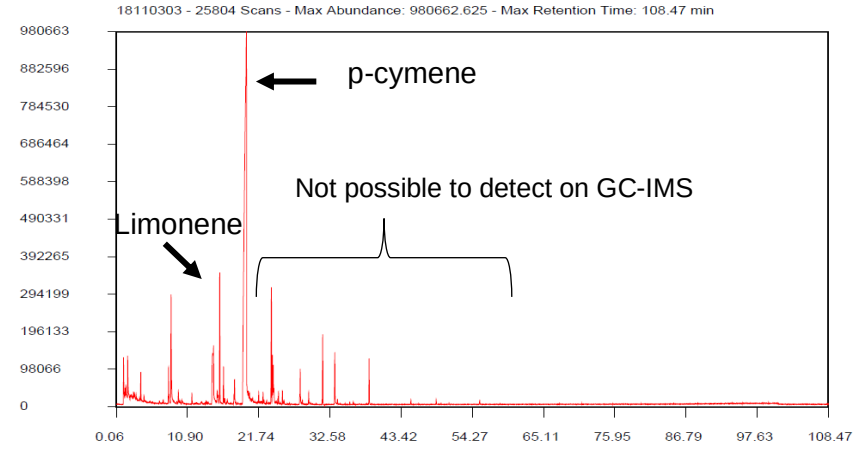

Min Abundance: 5278.8095; Max Abundance 980662.625; min retention time 0.06 min; max retention time 108.47 min; nr scans; 25804; ions:154356; scan delay: 0.06 min; scan interval:0.00 min (251 milliseconds)

Figure 36: GC-MS chromatogram for the second digestate sample

4.3.4 Initial compounds quantification

The quantification by GC-IMS of real samples with a complex matrix can be a very challenging mission, mostly due to the influence of other components (for example, for digestate samples the presence of ammonia) or lower volatility of compounds (such as VFAs) or low proton affinity (that influence the ionization of the chemicals) (Criado-García *et al.*, 2015). For a digester which operates with a good efficiency, VFA concentrations at typically below 500 mg/L, with digesters with VFAs concentrations higher than 1500 mg/L creating problems in the organics conversion and a reduced biogas production (Lee *et al*., 2017; Tao *et al*., 2017; Williams *et al*., 2013) and for this reason it is important to quantify these compounds.

Quantitative analysis are also known as calibration processes where the quantification of compounds can be made by using calibration curves. A calibration curve is a mathematical function that compares the relationship between the response signal (e.g. intensity, peak height, or peak area) with the known analyte concentration from analytical standards. This procedure was the advantage to calibrate the instrument and to determine the concentration of unknown samples. As Cumeras *et al.* (2015a) said “a calibration curve is prepared by plotting the data or by fitting them to a suitable mathematical equation” (Cumeras et al., 2015a).

It this study ,calibration curves were prepared for ammonium hydroxide, limonene, 2-butanone, 2-pentanone, 2-hexanone, 2-heptanone, 2-octanone, 2-nonanone, acetic acid, propionic acid and butyric acid. The final concentration ranges chosen were 51-1223 mg/L for ammonium hydroxide, 84.2-589.4 µg/L for limonene, ±45-463 µg/L for ketones, and 0-500 mg/L for all VFAs. The pH of VFAs stock solution was around 62.9. Initially, the analyses were performed on LAV software by visual inspection of the spectrum where each compound (monomer, dimer, or trimer) was detected in RIP relative using the information collected previously relates to the identification of compounds in terms of Rt and dt. After this step, the data collected was reported in terms of intensity of each peak for maximum height range in the area and copied to excel to further process the data.

Criado-García *et al.* (2015) used a second order polynomial equation and a linear equation to analyse his samples (Criado-García *et al.*, 2015). Following this idea, a calibration curve was created for each compound using a second order polynomial equation ($y = \boldsymbol{ax^2} + \boldsymbol{bx} + \boldsymbol{c}$), with their corresponding correlation coefficient (R^2) (Appendix

2). It was only possible to get a good regression coefficient (R^2 superior than 0.99) for dimers of 2-pentanone, 2-hexanone, 2-heptanone, 2-octanone, 2-nonanone, acetic acid, propionic acid, and butyric acid and for 2-nonanone monomer.

From this data it was possible to conclude the dimers were the best fitting for the quantification, which had also been the recommendations from the manufacturer. For VFAs dimers, it was observed a linear tendency ($y = ax + b$), where y was the peak intensity, a the slope of calibration curve, x the concentration and b the intercept, with a good regression (R^2 superior than 0.99) at lower concentration levels (Fig. 37 A to C), with approximately 2 orders of magnitude. The concentration range used to create the linear equation was between 0-400 mg/L for acetic acid, 0-250 mg/L for propionic acid and 0-300 mg/L for butyric acid.

LOD and LOQ values were based on the standard deviation of the response and the slope of linear equations, where this was used to calculate the LOD and LOQ values (Fig. 37 D). As Cumeras *et al.* (2015b) suggested the LOD was calculated as 3.3 times the standard error of y-intercept divided by the slope of the calibration equation and LOQ was calculated as 10 times the standard error of y-intercept divided by the slope of the calibration equation (Cumeras et al., 2015b). Butyric acid had the lower values for LOD and LOQ and acetic acid the higher concentration range (Fig. 37 D). The lower end of the calibration curves should be further studied in terms of detection limits and best fit equation.

The VFAs analysis was performed using a stock solution that contained all three VFAs (acetic acid, propionic acid, and butyric acid). Further advancements in methodology and calibration should focus on using each VFA in separate solutions. In addition to evaluating the sample size; the temperature effect in vaporisation to the headspace; the addition of acidifying salts such as $NaHSO_4$ to adjust the pH. Beyond the use of blanks between samples to assess carry over effects such as the effect of accumulation compounds in the column and the testing of different columns with a more polar behaviour. Finally, there is a need to test this method on real samples.

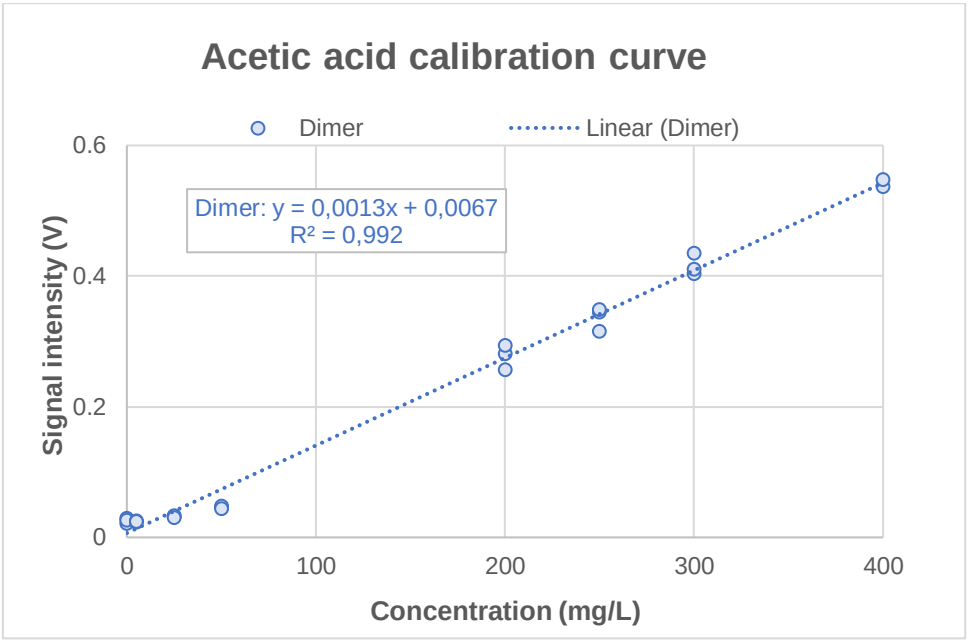
Acetic acid calibration curve
Dimer
Linear (Dimer)
Dimer: y = 0,0013x + 0,0067
R² = 0,992
Signal intensity (V)
Concentration (mg/L)
0
0.2
0.4
0.6
0
100
200
300
400

A

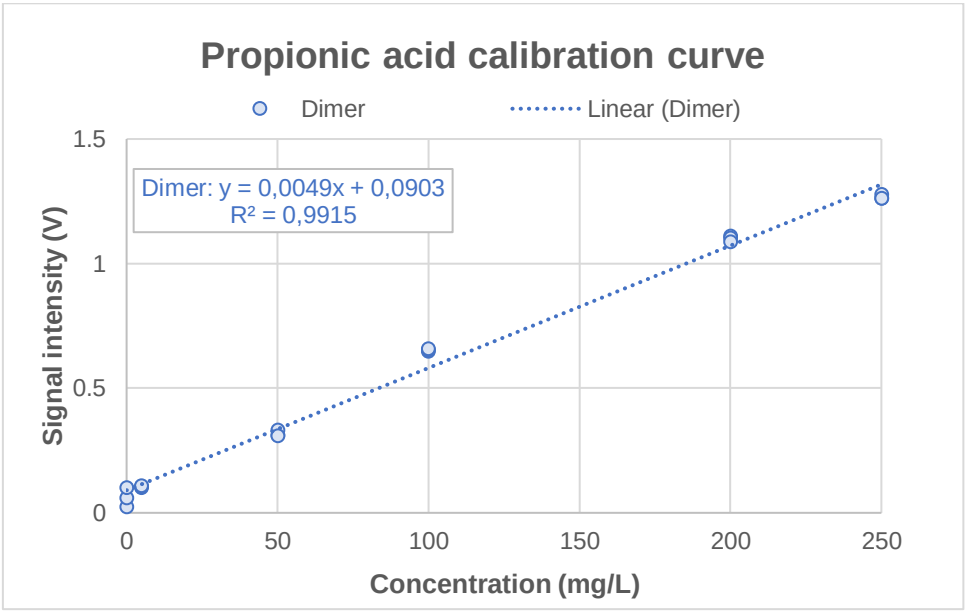
Propionic acid calibration curve
Dimer
Linear (Dimer)
Dimer: y = 0,0049x + 0,0903
R² = 0,9915
Signal intensity (V)
Concentration (mg/L)
0
0.5
1
1.5
0
50
100
150
200
250

B

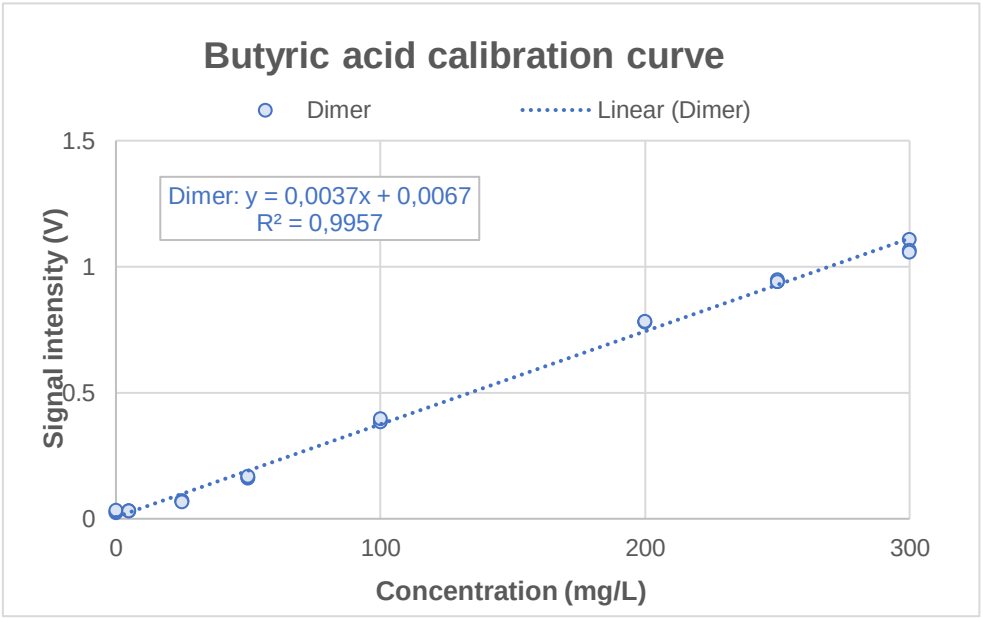
Butyric acid calibration curve
Dimer
Linear (Dimer)
Dimer: y = 0,0037x + 0,0067
R² = 0,9957
Signal intensity (V)
Concentration (mg/L)
0
0.5
1
1.5
0
100
200
300

C

Compound	Concentration range (mg/L)	Calibration equation	R^2	LOD * (mg/L)	LOQ * (mg/L)
		$y = ax + b$			
Acetic acid D	0-400 mg/L	$y = 0.0013x + 0.0067$	0.9920	7.4124	22.4618
Propionic acid D	0-250 mg/L	$y = 0.0049x + 0.0903$	0.9915	10.6122	32.1 583
Butyric acid D	0-300 mg/L	$y = 0.0037x + 0.0067$	0.9957	13.2299	40.0906

D

Figure 37:Linear calibration curves for acid acetic (A), propionic acid (B) and butyric acid (C) and calibration equations, concentration range, regression coefficients, LOD & LOQ (D).

The software from the manufacturer included a plug for performance quantifications and this was used to improve the quantification for limonene and for ketones. The calibration function chosen was a Boltzmann function based on the intensity (height) above the baseline and the concentration of standards. A Boltzmann function followed the following equation **Function: p1+(p0-p1)/(1+exp((log(x)-p2)/p3)),** where AIP intensity = f(concentration). Figure 38 A shows the p1, p2, p3 for each chemical to fill the equation, while the graphs for ketones are presented in Figure 38 B (monomer) and 38 C (dimer) and Figure 38 D for limonene.

A

Name	p0	p1	p2	p3
Ketones				
2-butanone M	0.381909	1.37088	42.97	-44.8513
2-butanone D	3.02567	1.23368	4.8462	-0.43901
2-pentanone M	-7655.72	1.03258	7.41454	$-8.90741e^{-002}$
2-pentanone D	2.9278	0.693976	4.73144	-0.721501
2-hexanone M	0.808124	1.02233	5.67737	-0.823695
2-hexanone D	2.85065	0.703889	4.75054	-0.811521
2-heptanone M	0.902917	$-9.27996e^{-003}$	3.71897	$-3.64601e^{-002}$
2-heptanone D	2.42063	0.238068	5.1894	-0.714471
2-octanone M	1.25414	-36.7415	-5.33919	-2.4383
2-octanone D	1.63806	$-9.59799e^{-003}$	5.94946	-0.577253
2-nonanone M	1.01013	$7.28918e^{-002}$	5.4272	-0.676129
2-nonanone D	1.80149	$-1.58128e^{-002}$	6.89627	-0.557244
Terpenes				
Limonene M	0.697512	-0.641799	4.18241	-0.392112
Limonene D	-0.392112	-194.289	-8.46077	-2.9296

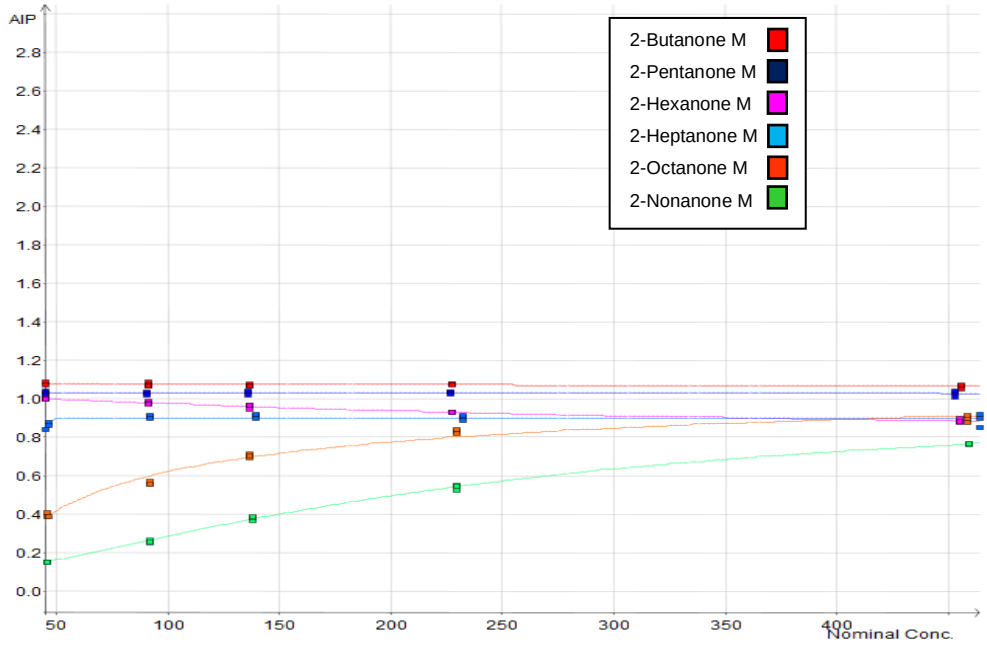
B
AIP
2-Butanone M
2-Pentanone M
2-Hexanone M
2-Heptanone M
2-Octanone M
2-Nonanone M
Nominal Conc.

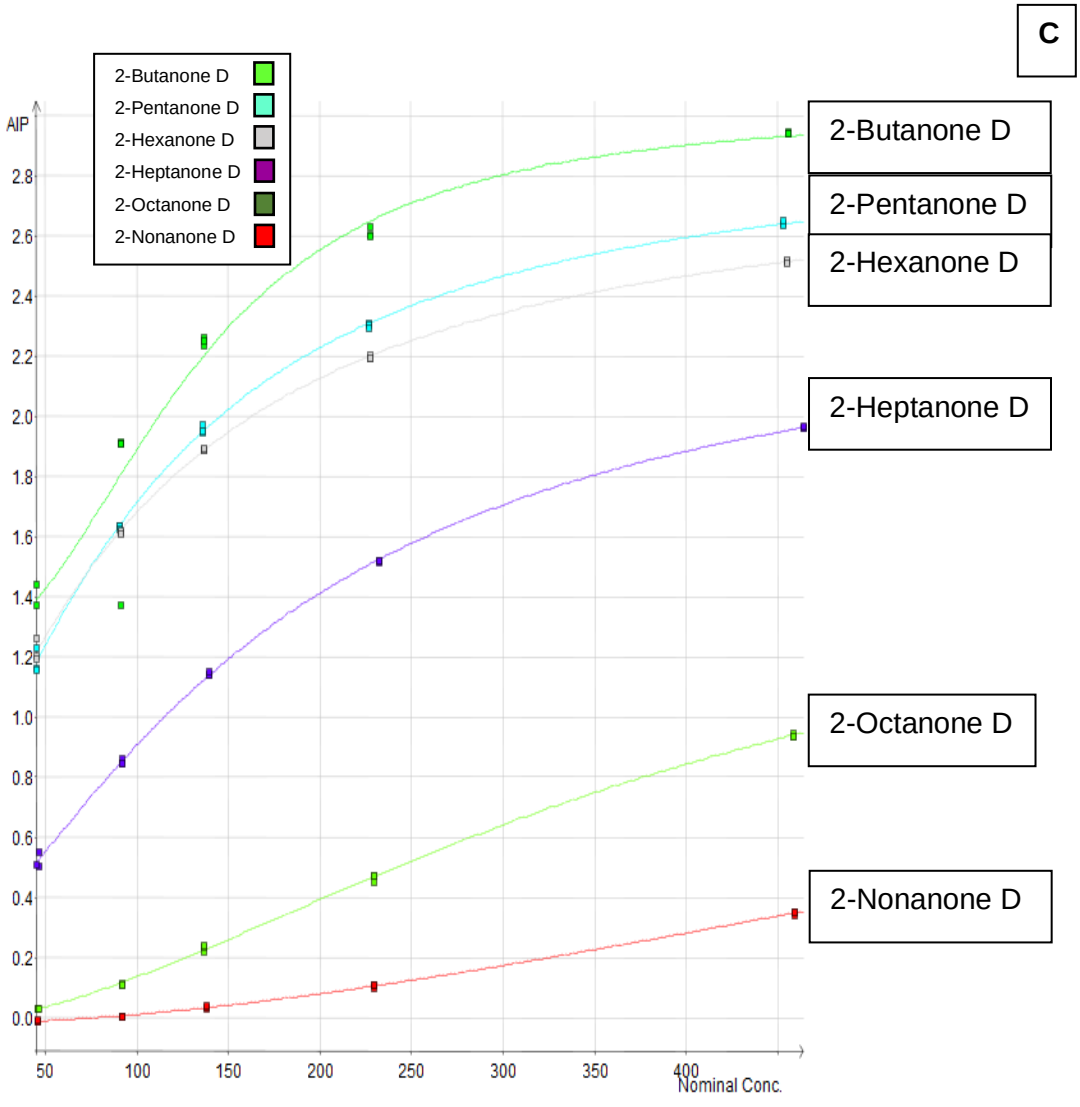
C
AIP
2-Butanone D
2-Pentanone D
2-Hexanone D
2-Heptanone D
2-Octanone D
2-Nonanone D
Nominal Conc.

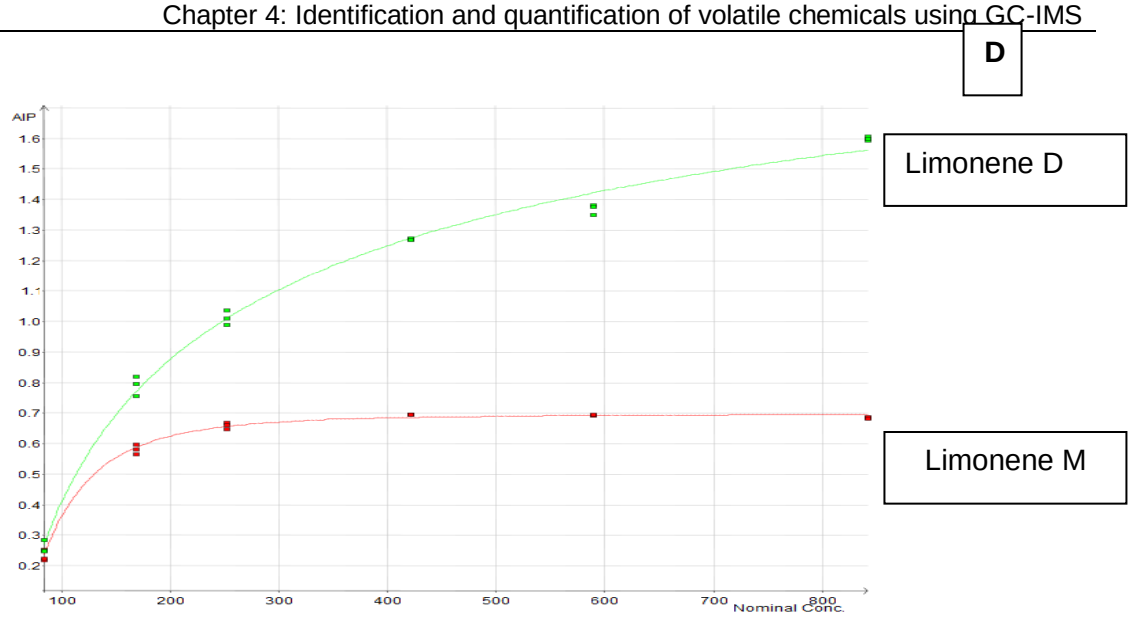

Figure 38: The coefficients p0, p1, p2, and p3 for the Boltzmann function (A), calibration curve for ketones monomer (B), dimers (C), and limonene (D).

Table 29 presented the nominal concentrations (A) and the concentrations calculated by using the Boltzmann function (B) where results were very similar, showing this function could be an option to quantify compounds, however more investigations should be carried out to establish the most adequate statistical function to use for calibrations. One of the GC-IMS challenges for quantification of analytes is due to the IMS response as it is non-linear, especially at ppmv (µg/L or µg/kg) and pptv level (Wang *et al*., 2020). Therefore, there have been a significant range of methodologies used in order to perform calibrations. For example, Márquez-Sillero *et al.* (2014) averaged the value of three replicates and created a linear equation. LOD and LOQ values were calculated as 3 and 10 times the SD of the blank signal divided by the slope of the calibration curve (Márquez-Sillero *et al.*, 2014). Criado-García and Arce (2016) quantified toxic compounds (e.g. benzene, toluene, butyraldehyde, benzaldehyde, and tolualdehyde) from human saliva by SPME-GC-IMS. The calibration curves were performed as Márquez-Sillero *et al.* (2014) to determine the LOD, the LOQ, and to quantify the concentration of the compound of interest. The authors used linear regression in water and saliva samples (Criado-García and Arce, 2016). Orellana-Silla *et al.* (2018) used the same approach as (Márquez-Sillero *et al.*, 2014) to detect and quantify forchlorfenuron in fruit juices in terms of LOD and LOQ by using a linear calibration curve (with an R^2 of 0.997) in the range of calibration from 50 – 300 µg/L prepared in 2-propanol (Orellana-Silla *et al*., 2018). Masár *et al*. (2020) used microchip electrophoresis with IMS to measure VFAs and the similar approach as Márquez-Sillero *et al*., (2014) to quantify the compounds except instead of being 3 times for the LOD, the author used 3.3 times the SD of the blank. LOD ranges varied from 0.07 to 2.61 mg/L and LOQ between 0.20–7.92 mg/ L. The linearity in the

calibrations curves were observed between 1.5 to 25 mg/L with a $R^2 < 0.993$ (Masár *et al*., 2020). Contreras *et al.* (2019) created a chemometric model to calibrate and classify olive oil samples based on specifique spectral fingerprints (targeted and non-targeted markers) (Contreras et al., 2019). Some of these metholodgies may be worth investigating further for the calibration of GC-IMS when applied in AD and biorefining systems.

4.4 OUTCOME FROM THIS CHAPTER

The information collected in this chapter helped to develop a tool that is more suitable for monitoring biotech processes and organic waste matrices. It identified compounds in various matrices based on their retention time, drift time and Kovats indices. It was possible to use the Kovats Indices to identify unknown compounds, therefore using the GCxIMS Library Search & Editor software and the normalisation of known compounds and it was possible to identify compounds by their retention index.

4.5 CONCLUSIONS

It seems possible to use GC-IMS as an analytical tool for the identification of unknown chemicals related to AD matrices. Combining the retention time from gas chromatography and drift time from the IMS should increase the amount of available information for this identification, in addition to increasing the separation between several compounds. Taking into consideration the NIST database for retention index with the IMS drift times should allow high certainty for the identification of chemicals. Likewise, to take into account varying operational conditions, the data should be presented as reduced ion mobility or inverse ion mobility. Seventeen standards were used from different chemical groups (VFAs, ketones, aromatics and terpenes) and created a database of results including specific retention index, reduced ion mobility, inverse reduced ion mobility, drift time and retention time. This database could be used for fingerprint identification of these odour generating compounds in environmental samples, including those from the waste management and AD sector. The major odorous compound present in AD feedstock and digestate were identified by GC-IMS as being the terpenes, limonene and p-cymene, with results confirmed with GC-MS. The demonstrated methodology enabled the analysis of samples without any pre-treatment except for sample dilution and it was simple to use and provided results within a few minutes with excellent repeatability. However, the problem related to carrying over of ammonia should be solved to improve the methodology.

Table 29: Compounds nominal concentration (A) and calculated concentration (B)

2-Butanone D (µg/L)		2-Pentanone D (µg/L)		2-Hexanone D (µg/L)		2-Heptanone D (µg/L)		2-Octanone D (µg/L)		2-Nonanone D (µg/L)		Limonene D (µg/L)	
A	B	A	B	A	B	A	B	A	B	A	B	A	B
45.54	51.61	45.30	49.38	45.47	49.68	46.39	50.01	45.86	47.86	45.92	40.31	84.20	82.19
45.54	42.82	45.30	43.70	45.47	43.60	46.39	43.87	45.86	47.21	45.92	44.06	84.20	85.85
91.08	42.23	45.54	43.36	45.30	43.23	45.47	44.94	46.39	47.21	45.86	62.76	84.20	81.79
91.08	103.01	90.61	90.34	90.94	90.73	92.78	91.02	91.73	87.67	91.84	86.82	168.40	165.20
91.08	102.26	90.61	90.46	90.94	91.01	92.78	93.40	91.73	90.41	91.84	84.65	168.40	182.81
91.08	102.47	90.61	89.04	90.94	89.90	92.78	91.02	91.73	88.59	91.84	84.65	168.40	175.92
136.62	145.30	135.91	135.75	136.42	136.81	139.17	140.00	137.59	135.65	137.76	135.29	252.60	265.12
136.62	141.72	135.91	136.82	136.42	136.81	139.17	140.38	137.59	141.09	137.76	139.91	252.60	243.63
136.62	143.57	135.91	139.92	136.42	138.28	139.17	141.90	137.59	142.64	137.76	148.84	252.60	252.93
227.70	221.36	226.52	226.69	227.36	224.88	231.94	228.96	229.32	222.45	229.60	220.00	421.00	420.30
227.70	214.66	226.52	224.52	227.36	228.93	231.94	232.07	229.32	232.17	229.60	234.55	421.00	422.10
227.70	212.63	226.52	222.37	227.36	225.28	231.94	230.82	229.32	231.38	229.60	232.35	421.00	416.74
455.40	492.14	453.04	451.84	454.72	455.48	463.89	463.77	458.64	456.14	459.20	460.39	589.40	537.73
455.40	486.50	453.04	449.24	454.72	460.77	463.89	461.95	458.64	462.07	459.20	454.26	589.40	530.33
455.40	486.50	453.04	463.89	454.72	450.30	463.89	468.40	458.64	458.10	459.20	463.01	589.40	499.80
												842.00	919.36
												842.00	953.31
												842.00	921.91

A – Nominal concentrations; B – concentrations calculated by using the Boltzmann function

5. INFLUENCE OF AMMONIA ON GC-IMS BASED MONITORING

5.1 INTRODUCTION

Previous chapters demonstrated that GC-IMS was able to detect and identify a wide range of organic compounds from the headspace from complex samples. Ammonia was found to create issues such as carry over, and therefore a more in-depth investigation was established as to the impact of ammonia and possible ways to minimise its effect. From the literature review, it was found that was possible to improve the detection by adding admixtures such as dopant or 'gas modifiers' such as ammonia to prevent the ionization of interfering chemicals or by shifting the peaks in the drift-time spectra, or by enabling ionization of analytes with low proton affinities (Waraksa *et al.*, 2016). In this research, however ammonia was observed to be acting as a chemical which was interfering with the analysis of others chemicals. An evaluation was defined to establish the impact of ammonia on the concentration of ketones, aromatics and terpenes and also define possible solutions to avoid its impact.

5.2 MATERIAL AND METHODS

5.2.1 Study the impact of ammonia on other chemicals (ketones, aromatics and terpenes)

To assess the impact of ammonia in three different functional groups (ketones, aromatics, terpenes) several solutions were prepared. Table 30 presents the concentration of each chemical in the final solution, whilst Figures 39, 40, and 41 explain how these solutions were prepared.

Table 30: Final concentration for each chemical when add to ammonia solution and the ammonia concentration for each solution

Ketones (M1)	Conc. (µg/L)	Aromatics (M2)	Conc. (µg/L)	Terpenes (M3)	Conc. (µg/L)	Ammonia (A1 to A5)	Conc. (mg/L)
2-Butanone	409.86	**Benzene**	3143.25	**α-pinene**	3042.47	**A1**	50.94
2-Pentanone	407.74	**Toluene**	3107.77	**γ-terpinene**	2907.00	**A2**	254.70
2-Hexanone	409.25	**Ethylbenzene**	3105.59	**3-carene**	3038.92	**A3**	509.40
2-Heptanone	417.50			**Limonene**	3000.89	**A4**	1528.20
2-Octanone	412.78					**A5**	2547.00
2-Nonanone	413.28						

Preparation the ketones solution (M1)	
One mL of each standard (2-butanone, 2-pentanone, 2-hexanone, 2-heptanone, 2-octanone, 2-nonanone) was add to a flask to make up 7 mL final volume and this was considered solution (S0). Then 20 µL was removed from S0 and put in a volumetric flask with 100 mL and top up with deionised water to make the solution S1. The following step was to sample 1 mL from S1 and add 49 mL deionised water to make the **solution (M1)**.	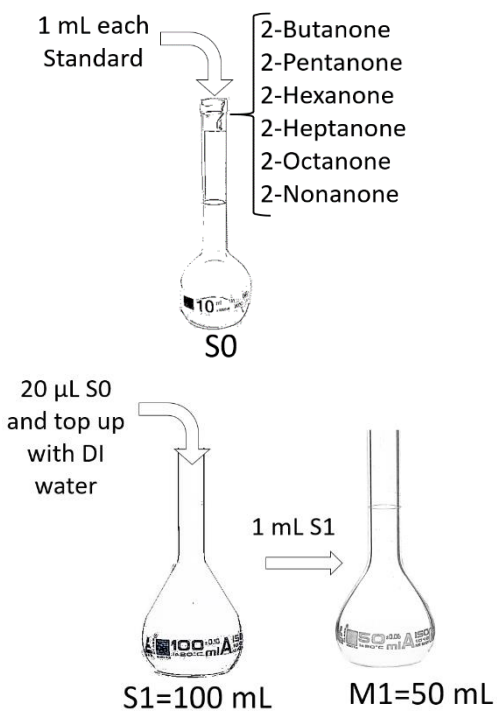
Preparation of the aromatics solution (M2)	
Solution S1 (S1) was prepared by adding 20 µL each standard (benzene, toluene, ethylbenzene) and top up with DI water. **Solution (M2)** was prepared by adding 1mL from solution S1 with 49 mL DI water. M2 was the solution used in the experiment.	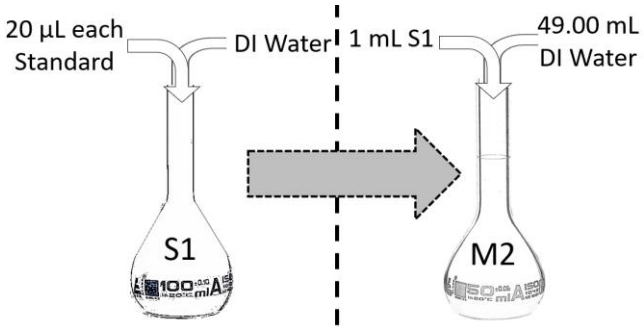
Preparation of the terpenes solution (M3)	
Solution S1 (S1) was prepared by adding 20 µL from each standard (α-pinene, γ-terpinene, 3-carene, limonene) and top up with DI water. **Solution (M3)** was prepared by adding 1mL from solution S1 with 49 mL DI water. M3 was the solution used in the experiment.	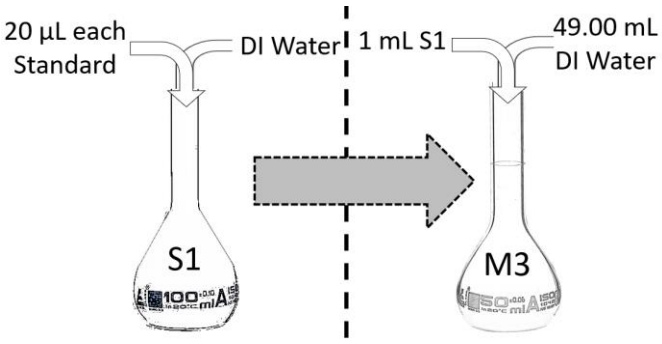

Figure 39: Schematic for the preparation of ketones, aromatics, and terpenes solutions

Preparation of several ammonia solutions

Solution (A1) was prepared by adding 0.1 mL from the standard Ammonia to 99.9 mL DI water. **Solution (A2)** was prepared by adding 0.5 mL from the standard Ammonia to 99.5 mL DI water. **Solution (A3)** was prepared by adding 1.0 mL from the standard Ammonia to 99.0 mL DI water. **Solution (A4)** was prepared by adding 3.0 mL from the standard Ammonia to 97.0 mL DI water. **Solution (A5)** was prepared by adding 5.0 mL from the standard Ammonia to 95.0 mL DI water

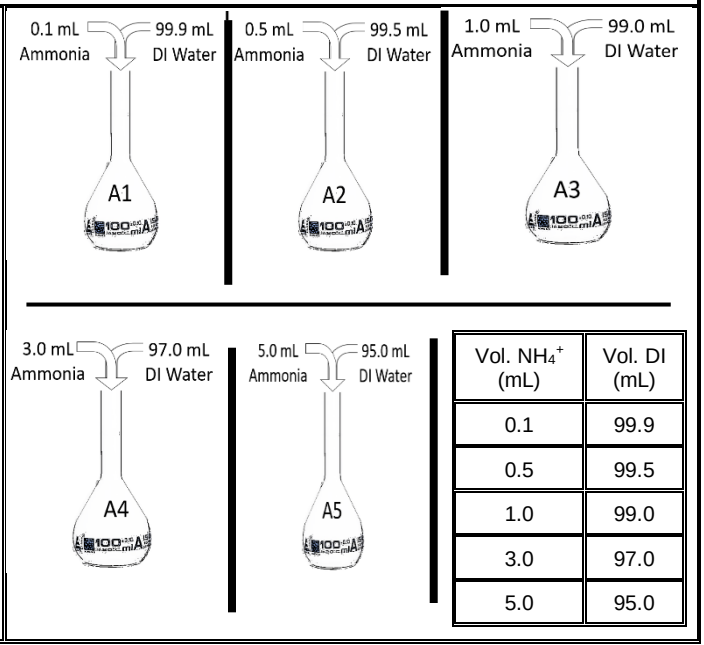

Vol. NH_4^+ (mL)	Vol. DI (mL)
0.1	99.9
0.5	99.5
1.0	99.0
3.0	97.0
5.0	95.0

Figure 40: Schematic for the preparation of ammonia solutions

5.2.1.1 Final solutions of ammonia added to ketones, aromatics, and terpenes (A1, A2, A3, A4, A5 to M1, M2, M3)

Preparation of the solutions for the experiment (ammonia + ketones)

To prepare the final solution (A1 + M1) to run on the GC-IMS, 1 mL A1 solution (ammonia) was added to 9 mL of solution M1 (ketones mix) to make 10 mL final volume. To prepare the final solution (A2 + M1) to run on the GC-IMS, 1 mL A2 solution (ammonia) was added to 9 mL of solution M1 (ketones mix) to make 10 mL final volume. To prepare the final solution (A3 + M1) to run on the GC-IMS, 1 mL A3 solution (ammonia) was added to 9 mL of solution M1 (ketones mix) to make 10 mL final volume. To prepare the final solution (A4 + M1) to run on GC-IMS 1 mL A4 solution (ammonia) was added to 9 mL of solution M1 (ketones mix) to make 10 mL final volume. To prepare the final solution (A5 + M1) to run on the GC-IMS, 1 mL A5 solution (ammonia) was added to 9 mL of solution M1 (ketones mix) to make 10 mL final volume. The others solutions followed this procedure.

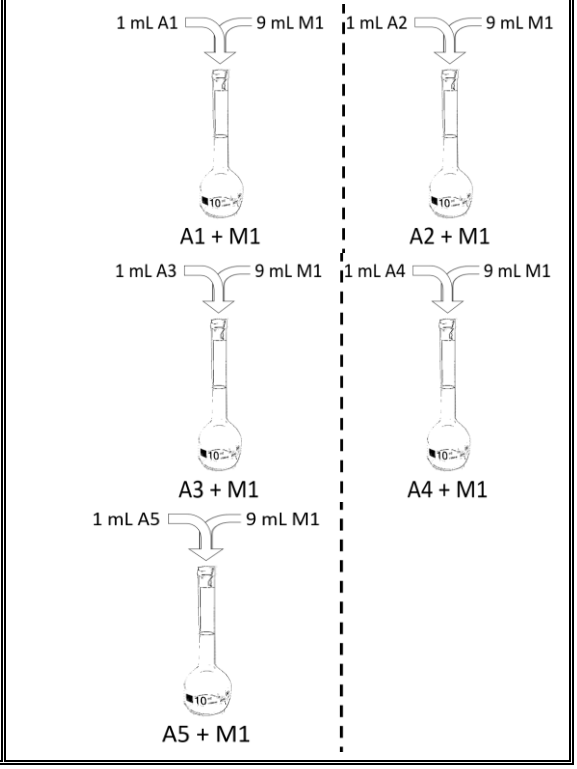

Figure 41: Preparation of the final solution of ammonia with ketones

5.2.2 Study the effectiveness in using salt ($NaHSO_4$)

Cruwys *et al.* (2002) used a saturated solution of $NaHSO_4$ (at 62% w/v, ≈ 620 g/L) to acidify VFAs samples in wastewater matrices, using GC-FID (Cruwys *et al.*, 2002) and Raposo *et al.* (2013) recommended the acidification process to making the VFAs more non-polar and volatile and to precipitate other contaminants (Raposo *et al.*, 2013). A similar approach was used here with the objective of adding salt to decrease the pH of the solution and avoid the vaporization of ammonia to the headspace and stop this chemical interfering with others chemicals. The solutions used were prepare as explained in Section 5.2.1.1 and Table 31 summaries the experiment.

Table 31: Evaluation of the impact of ammonia on ketones, aromatics and terpenes analyses using GC-IMS and the effect of salt addition

Ketones (M1)		Aromatics (M2)		Terpenes (M3)	
Experiment without the salt	**Experiment with the salt**	**Experiment without the salt**	**Experiment with the salt**	**Experiment without the salt**	**Experiment with the salt**
1 mL solution (A1 + M1)	1 mL solution (A1 + M1) + 1 mL $NaHSO_4$ 62%	1 mL solution (A1 + M2)	1 mL solution (A1 + M2) + 1 mL $NaHSO_4$ 62%	1 mL solution (A1 + M3)	1 mL solution (A1 + M3) + 1 mL $NaHSO_4$ 62%
1 mL solution (A2 + M1)	1 mL solution (A2 + M1) + 1 mL NaHSO4 62%	1 mL solution (A2 + M2)	1 mL solution (A2 + M2) + 1 mL NaHSO4 62%	1 mL solution (A2 + M3)	1 mL solution (A2 + M3) + 1 mL NaHSO4 62%
1 mL solution (A3 + M1)	1 mL solution (A3 + M1) + 1 mL NaHSO4 62%	1 mL solution (A3 + M2)	1 mL solution (A3 + M2) + 1 mL NaHSO4 62%	1 mL solution (A3 + M3)	1 mL solution (A3 + M3) + 1 mL NaHSO4 62%
1 mL solution (A4 + M1)	1 mL solution (A4 + M1) + 1 mL NaHSO4 62%	1 mL solution (A4 + M2)	1 mL solution (A4 + M2) + 1 mL NaHSO4 62%	1 mL solution (A4 + M3)	1 mL solution (A4 + M3) + 1 mL NaHSO4 62%
1 mL solution (A5 + M1)	1 mL solution (A5 + M1) + 1 mL NaHSO4 62%	1 mL solution (A5 + M2)	1 mL solution (A5 + M2) + 1 mL NaHSO4 62%	1 mL solution (A5 + M3)	1 mL solution (A5 + M3) + 1 mL NaHSO4 62%

5.2.3 Salt limitation to cancel ammonia concentration

Nine digestate samples from a full scale AD-plant were analysed by GC-IMS and compared with an ion chromatography analyser (model Eco IC from Metrohm) to determine NH_4^+ concentration. The ion analyses were carried out by another researcher. The objective was to establish NH_4^+ concentration, which was available in the soluble form and establish the amount to salt required.

5.2.4 GC-IMS instrumentation and operational conditions

The analytical method used was described in Chapter 3 for generic VOCs (experimental setup B6) and each sample was run in duplicate and a blank (a vial full with nitrogen) was placed in between the samples to guarantee no cross-contamination.

5.3 RESULTS AND DISCUSSION

In Chapter 3, it was observed that digestate samples contained ammonia, and this ammonia was impacting on measurements of the ketone mix used to normalize the GC×IMS library search, as it seemed to be creating interfering ions. The ketone mix was used to benchmark the performance-related to favourable ionization chemistry (higher proton affinity when compared with water). Figure 42 elucidates the changes in the spectrum from the presence of ammonia in the equipment after running a digestate sample. The impact of this ammonia carry over between sample runs is significant and requires the system to be cleaned to avoid cross contamination or influence between analysis. The carryover was not the only issue that ammonia created when ketones were being measured. Ammonia influenced the ionization process on the ketones mix. Figure 43 is an amplification from Figure 42 where it shows the monomer and dimer for 2-Pentanone with extra peaks (adduct products).

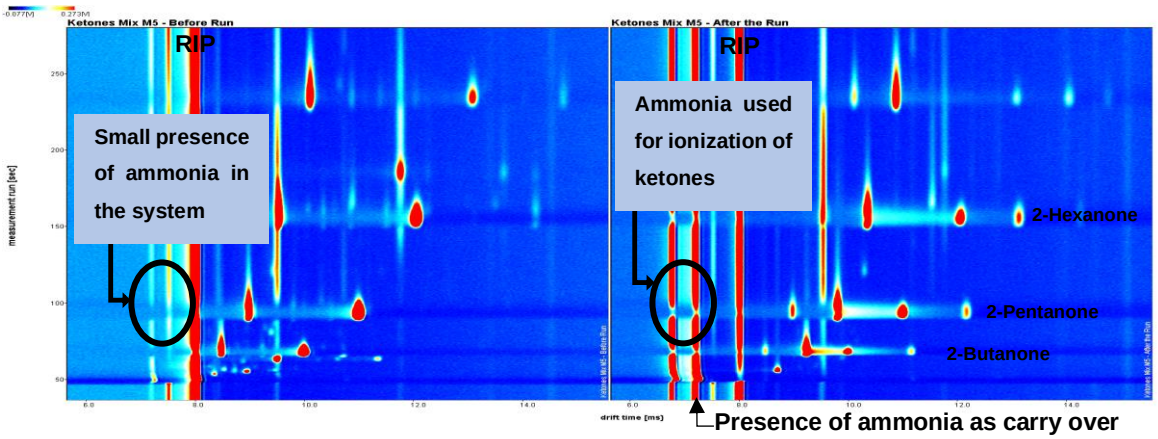

Figure 42: Ketones mix (M5) before and after running samples with ammonia content

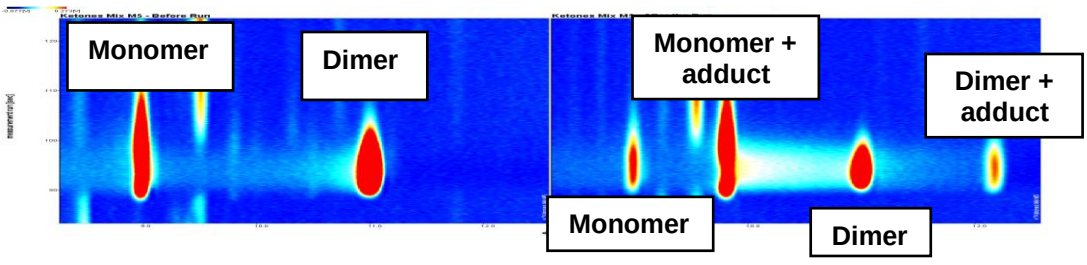

Figure 43: Amplification from Figure 42 for 2-pentanone where it is possible to see the monomer, dimer and the adduct products

5.3.1 Study the impact of ammonia in other chemicals (ketones, aromatics and terpenes)

Figure 44 shows the impact when the ammonia concentration increased from 50.94 mg/L (solution A1) to 2547.00 mg/L (solution A5) on the ketones (Fig. 44 A), aromatics (Fig. 44 B), and terpenes (Fig. 44 C). When the amount of ammonia increased, dimerization happened, which meant that there was a creation of dimers, across the drift-time spectrum (equation 10 and 11).

For ketones when the ammonia concentration was 254.70 mg/L (solution A2), extra peaks started appearing from the ammonia adduct, so instead of having just a monomer and a dimer, there were a monomer (M), monomer+adduct ($M.NH_4^+$), dimer, and a dimer+adduct ($D.NH_4^+$). When the ammonia concentration was 509.40 mg/L (solution A3), the monomer intensity decreased and monomer+adduct intensity increased. When ammonia concentration was 2547 mg/L (solution A5), the monomer and dimer was almost not present, there were mainly only monomer+adduct and dimer+adduct.

With the aromatics, the impact of ammonia was different. It was observed that for this functional group, ammonia did not create any extra peaks. However, the intensity of the aromatic compound decreased when the concentration of ammonia increased (Fig. 44 B). Ammonia impact on terpenes showed similar reaction as for ketones where it was observed a presence of extra peaks and a decrease of the intensity of the ketone (monomer and dimer). This can be seen in Figure 44C when the concentration of ammonia increased (the red colour represent the high intensity and blue the lower). Figures 45, 46, and 47 amplify the ammonia effect on these compounds (for just one type of concentration).

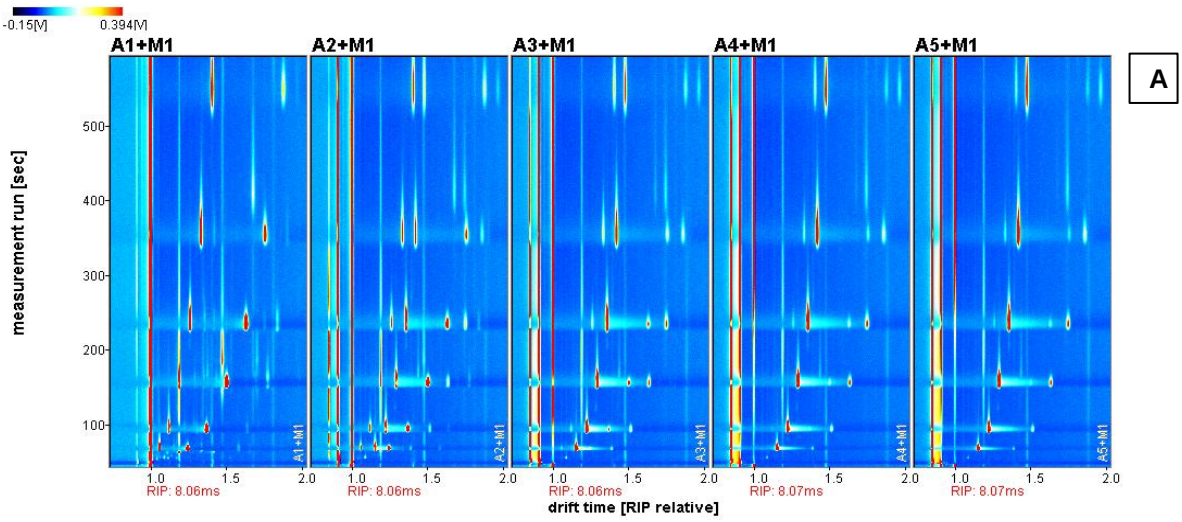

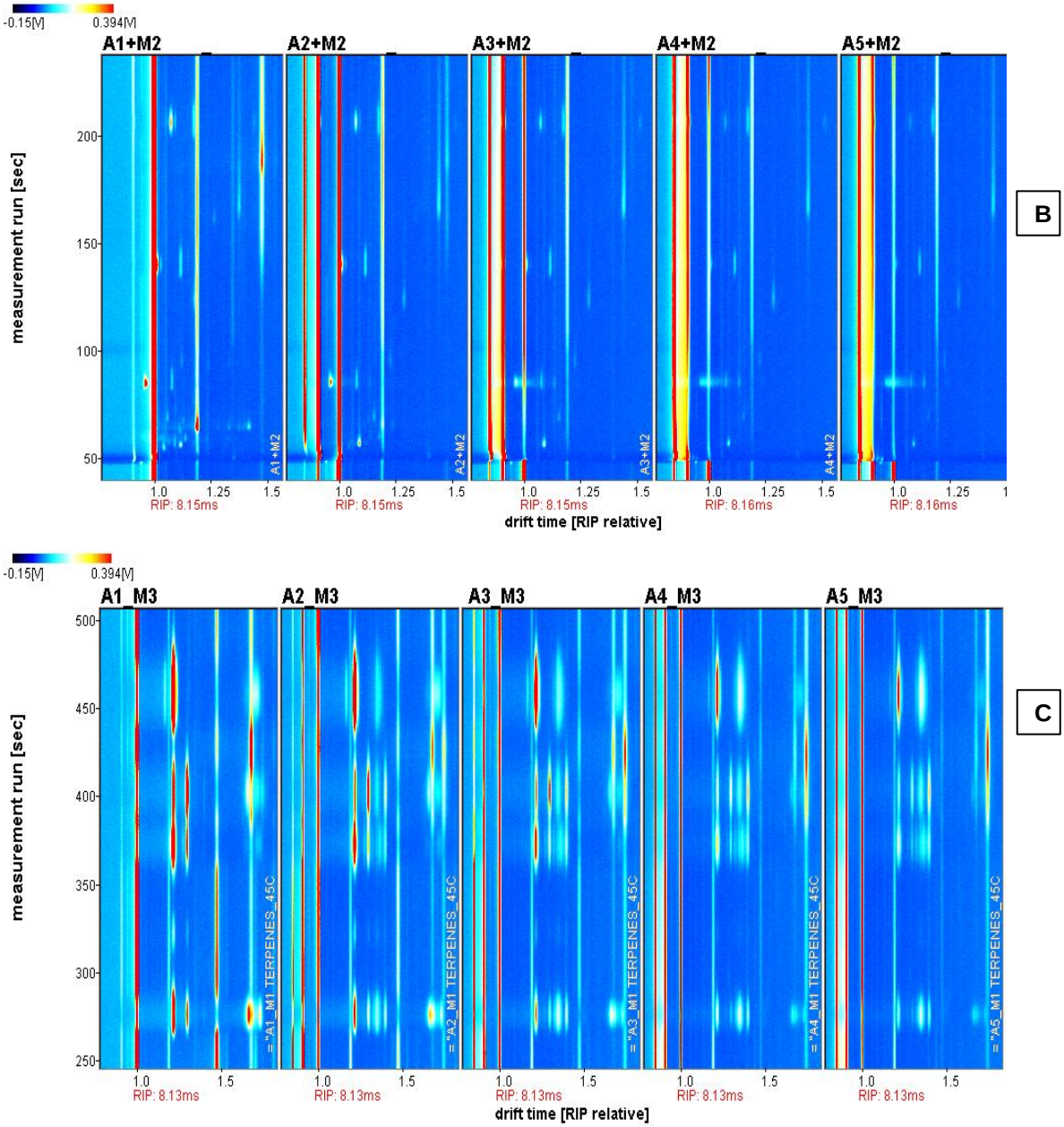

Figure 44: Ammonia effect on ketones (M1) (A), aromatics (M2) (B), and terpenes (M3) (C)

When ammonia concentration is high, ammonia is going to compete with other chemicals to be ionized. Ammonia has high a PA (853.6 kJ/mol) and for example benzene has a lower PA (750.4 kJ/mol), followed by toluene (784.0 kJ/mol), ethylbenzene (788.0 kJ/mol), 2-butanone (827.3 kJ/mol), 2-pentanone (832.7 kJ/mol) (NIST Chemistry WebBook, 2018), 2-butanone (820 kJ/mol), 2-hexanone (826 kJ/mol), 2-nonanone (837 kJ/mol) (Safaei *et al.*, 2019). Therefore, ammonia will be ionized first then only the other compounds will be ionised.

As Eiceman stated in his book when a mixture of compounds was injected in the ionization region on a drift tube (on positive mode), a charge competition between these

several analytes can take place, and the compound with superior PA will be preferentiality charged. Therefore, the compound with higher PA might be totally ionized before other compounds have an opportunity to obtain the charge and be protonated. However, in the spectrum, others compounds might be possible to be seen but a true quantification and calibration can be a challenge due to the lack of information on the ion suppression process (Eiceman *et al.*, 2016).

Besides this, ammonia had high proton affinity and high efficiency of ionization and it can block the ionisation of most organic compounds. This meant that the ammonia ionization reaction went practically only in forward direction where the reactant was converted to stable produced ions because all the analyte (NH_3) which have possibility for interaction with reactant ions ($H^+(H_2O)_n$), could be transformed into ionic form ($NH_4^+(H_2O)_{n-x}$) (equation 10). However, for analytes with lower proton affinity, such as ketones or alcohols, the reversal of the reaction of proton attachment was an important parameter for these chemicals be ionized (Puton *et al.*, 2008).

The difference why aromatics did not create extra peaks as terpenes and ketones, could be related to the fact that the ionization of the aromatics could be performed by charge transfer (Criado-García *et al.*, 2015), while for ketones and terpenes it has frequently been presumed that the ionization is carried out based on the proton or hydronium transfer from ($NH_4^+(H_2O)_{n-x}$) to the analyte (Valadbeigi *et al.*, 2019).

Puton *et al.* (2008) said the mechanism of dopant's interaction for ammonia with the narcotics, pyridine, formaldehyde, dinitroalkanes was by control of proton transfer, clusterisation and ammonia was recognised to change the ion–molecule chemistry in the sample on the ionisation region or the conditions for the drift of ions (Puton *et al.*, 2008). Arce and Valcarel (2013) suggested that for the $[(H_2O)_zNH_4]^+$, it was arise as a result of proton transfer from the $[(H_2O)_xH]^+$ (Arce and Valcarcel, 2013). Eiceman *et al.* (2016) also stated that the principal reactant ions in positive mode will be made by hydrated protons and the product ions made by proton transfer, except for alkanes, alkenes, aromatic hydrocarbons, and some alcohols that will be by charge exchange reactions.

In the proton transfer ionization, a $(H_2O)_xH^+$ molecule can react with the sample (M) to transfer a positive hydrogen to make the ion (MH^+) and a water molecule ($_xH_2O$), while for charge transfer the $(H_2O)_xH^+$ molecule will transfer a positive charge to the sample (M) to make the ion (M^+) and a water molecule ($_xH_2O$). This could explain the changes happening for ketones and terpenes. Another explanation for what was happening with aromatics compounds may be because at atomic level, the benzene is composed by six

carbon atoms covalently bonded to six hydrogens and with the one unpaired electron from each carbon becomes conjugated into the ring and having free movements around all six carbons. This property to create a ring makes benzene a very stable molecule and this extra stability is referred to as aromatic stability. Subsequently, a lot of energy is necessary to conduct an addition reaction on benzene because it will destroy the ring and normally benzene do substation reactions.

To explain the presence of extra peaks on ketones, Valadbeigi *et al.* (2019) explained in detail what happened related to the chemical ionization mechanism in corona discharge (CD) as the ionization source, on positive mode of operation, with and without the dopant (ammonia), for a series of organic molecules (2-nonanone, cyclopentanone, acetophenone, pyridine, and di-tert-butylpyridine – DTBP) using an ion mobility spectrometry with time-of-flight mass spectrometry (IMS-TOFMS). The equipment allowed analysing the molecules' structure and understanding the ionization mechanism. The reactant ions studied were $H_3O^+(H_2O)_n$ (RIP without the dopant) and $NH_4^+(H_2O)_n$ (ARI as dopant). Without the dopant the sample suffered ionization, when the $H^+(H_2O)_n$, attach to the organic molecules followed by partial dehydration and formation of product ions $MH^+(H_2O)_x$ or $M_2H^+(H_2O)_x$. With the dopant, two type of product ions were produced $MH^+(H_2O)_x$ and $MNH_4^+(H_2O)_x$. To explain this chemical ionization, the $NH_4^+(H_2O)_x$ is attached to the sample (M) and an intermediate as $MNH_4^+(H_2O)_x$ is formed. Afterwards this intermediate can lose H_2O to produce $MNH_4^+(H_2O)_{x-1}$ as product ions or lose H_2O and NH_3 to produce $MH^+(H_2O)_{x-1}$ as product ions. For products with lower basicity it was produced $MNH_4^+(H_2O)_x$ because of strong $MH^+{-}NH_3$ interaction and for molecules with high basicity the $M{-}H^+$ interaction is stronger leading to the formation of $MH^+(H_2O)_{x-1}$ as product ions (Valadbeigi *et al.*, 2019)

5.3.2 Study the effectiveness of using salt ($NaHSO_4$)

Figure 45 shows the effect of salt for ketones + ammonia (solution A3) + salt in comparison with ketones + ammonia (solution A3). Figure 46 shows the effect of salt for (aromatics + ammonia (solution A3) + salt) vs (aromatics + ammonia (solution A3)). Figure 47 shows the effect of salt for (terpenes + ammonia (solution A3) + salt) in contrast with (terpenes + ammonia (solution A3)). When salt was added to the sample, the ammonia peak was not present and it did not interfere with other chemicals. The amount of salt ($NaHSO_4$) used in this experiment was sufficient to cancel the presence of ammonia from solution A1 to A5 and kept the other chemicals.

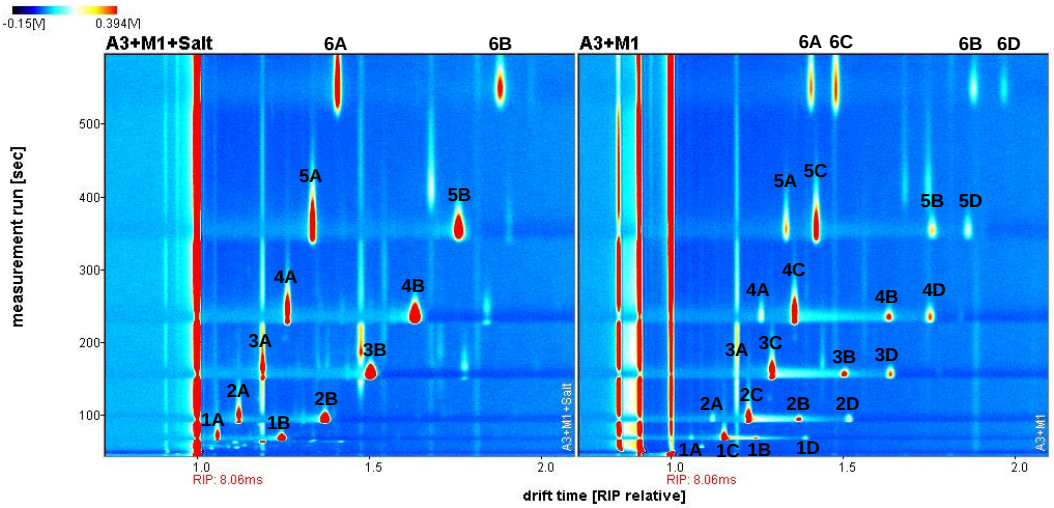

Label	Compound	Label	Compound	Label	Compound
1A	2-Butanone monomer	**2A**	2-Pentanone monomer	**3A**	2-Hexanone monomer
1B	2-Butanone monomer	**2B**	2-Pentanone monomer	**3B**	2-Hexanone monomer
1C	2-Butanone monomer + **adduct**	**2C**	2-Pentanone monomer + **adduct**	**3C**	2-Hexanone monomer + **adduct**
1D	2-Butanone dimer + **adduct**	**2D**	2-Pentanone dimer + **adduct**	**3D**	2-Hexanone dimer + **adduct**
4A	2-Heptanone monomer	**5A**	2-Octanone monomer	**6A**	2-Nonanone monomer
4B	2-Heptanone monomer	**5B**	2-Octanone monomer	**6B**	2-Nonanone monomer
4C	2-Heptanone monomer + **adduct**	**5C**	2-Octanone monomer + **adduct**	**6C**	2-Nonanone monomer + **adduct**
4D	2-Heptanone dimer + **adduct**	**5D**	2-Octanone dimer + **adduct**	**6D**	2-Nonanone dimer + **adduct**

Figure 45: Ketones with ammonia and salt vs ketones with just ammonia (concentration 509.40 mg/L)

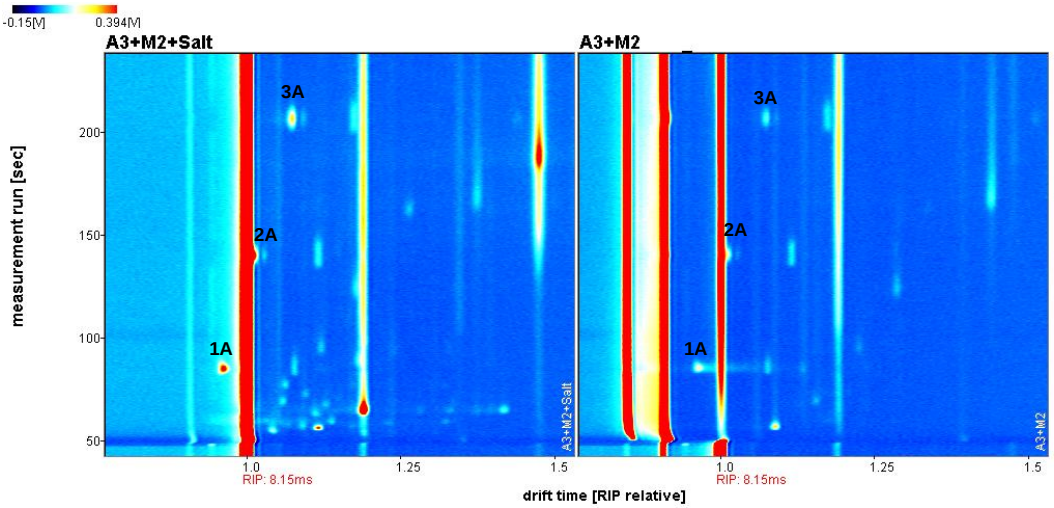

Label	Compound	Label	Compound	Label	Compound
1A	Benzene	**2A**	Toluene	**3A**	Ethylbenzene

Figure 46 Aromatics with ammonia and salt vs aromatics with just ammonia (concentration 509.40 mg/L)

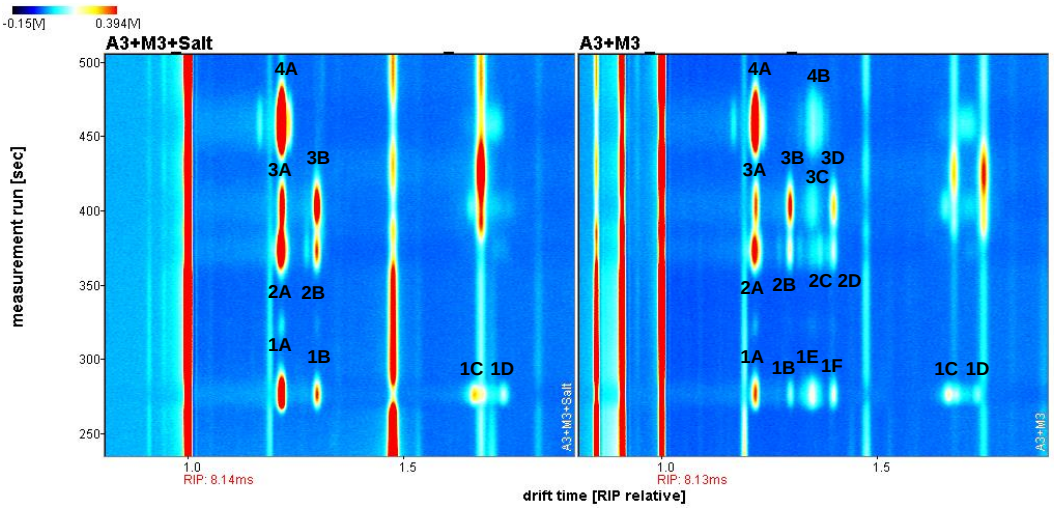

Label	Compound	Label	Compound	Label	Compound
1A	α-pinene	**2A**	3-carene	**3A**	Limonene
1B	α-pinene	**2B**	3-carene	**3B**	Limonene
1C	α-pinene	**2C**	3-carene + **adduct**	**3C**	Limonene + **adduct**
1D	α-pinene	**2D**	3-carene + **adduct**	**3D**	Limonene + **adduct**
1E	α-pinene + **adduct**			**4A**	γ-terpinene
1F	α-pinene + **adduct**			**4B**	γ-terpinene + **adduct**

Figure 47: Terpenes with ammonia and salt vs terpenes with just ammonia (concentration 509.40 mg/L)

5.3.3 Investigate the salt concentration required to cancel ammonia impact on GC-IMS analysis

One of the experiments performed with nine digestate samples was to evaluate the salt concentration required to avoid ammonia ionisation effects. Duplicate samples were run on the GC-IMS and samples were analysed using ion chromatography. The results for GC-IMS (Fig. 48A) were compared with the results from ion chromatography (Fig. 48B). The result for GC-IMS was based on the ammonia peak intensity whilst for ion chromatography it was ammonia concentration (Fig. 48). From the GC-IMS results, sample 1 and 2 have an intensity of around 0.1, then from sample 3 the ammonia peak intensity started to build up until it reached the maximum for sample 4B (1.299), after that the intensity started to decrease. Comparing with the result from ion chromatography the concentration for sample number 3 was 7.63 g/L and for sample 4 was 8.09 g/L. It is possible to conclude that samples with ammonia concentration below 4.0 g/L, the salt concentration would be more effective to cancel the impact of ammonia and between ammonia concentrations of 4.0 g/L to 7.0 g/L the cancellation would still be performed reasonably but any higher ammonia concentration, it would result in reaching saturation

point and would not be effective any longer. A carry over effect was also observed in Figure 48 with the intensity after the sample 5 being so high, because the column was contaminated with ammonia from sample 4 and was transferred to the following sample analyses.

(A) Intensity ammonia peak measure by GC-IMS

Sample	Ident	Intensity	Graph
Sample 1A_ND_45C	???	0.093	
Sample 1B_ND_45C	???	0.098	
Sample 2A_ND_45C	???	0.121	
Sample 2B_ND_45C	???	0.134	
Sample 3A_ND_45C	???	0.204	
Sample 3B_ND_45C	???	0.308	
Sample 4A_ND_45C	???	0.848	
Sample 4B_ND_45C	???	1.299	
Sample 5A_ND_45C	???	1.255	
Sample 5B_ND_45C	???	1.227	
Sample 6A_ND_45C	???	1.076	
Sample 6B_ND_45C	???	1.159	
Sample 7A_ND_45C	???	1.115	
Sample 7B_ND_45C	???	1.076	
Sample 8A_ND_45C	???	0.982	
Sample 8B_ND_45C	???	0.930	
Sample 9A_ND_45C	???	0.902	
Sample 9B_ND_45C	???	0.892	

(B) Concentration of NH_4^+ measured by ion chromatography

Sample	Concentration NH_4^+ (g/L)
Sample 1	4.0009
Sample 2	5.4134
Sample 3	7.6253
Sample 4	8.0938
Sample 5	4.7354
Sample 6	5.6251
Sample 7	3.0943
Sample 8	2.4281
Sample 9	5.4978

Figure 48: Comparing ammonia intensity peak using GC-IMS (A) and concentration from ion chromatography (B), for all nine digestate samples

Cruwys *et al.* (2002) had previously showed that by adding the acidic salt ($NaHSO_4$) to fermentates and digestates that contained VFAs, it improved the analyte response by increasing the peak area when measured by GC-HS. The analyte headspace concentration increased due to pH reduction in the sample, and the ionic strength of salt, besides reducing the sample preparation time (Cruwys *et al.*, 2002).

The free ammonia is a combination of free unionized ammonia (NH_3) with the ionized ammonium nitrogen (NH_4^+). Rajagopal *et al.* (2013) showed that the percentage of free ammonia, in a solution (from 0 to 100%), by varying the pH (from 6.0 to 11.0), at different temperatures (20°C, 35°C, and 55°C). When the pH was lower than 6 the percentage of ammonia was almost zero and started to increase around 10% at 55°C, when the pH was 7.5. The 50% free ammonia was reached when the pH was around 8.5 (at 55°C), 9.0 (at 35°C), and 9.5 (at 20°C). At pH 11 almost all the ammonia was 100% as free ammonia (Rajagopal *et al.*, 2013). Another important aspect to have in consideration is due to the ammonia partitions (between gas and aqueous phase) exist in reversable equilibrium with the aqueous ammonium ions according to equation 14 and it depends on the pH and temperature. Increasing the concentration of OH^- in solution, will increase

the pH, therefore will facilitate the volatilization of ammonia (Jafari and Khayamian, 2008; Rajagopal *et al*., 2013).

$$NH_3 + H_2O \rightleftharpoons NH_4^+ + OH^-$$

Equation 14: Equation between ammonia and ammonium

In addition, the ammonia will also likely to react with the acid and to form the ammonium salt:

$$2NaHSO_4 + 2NH_3 \rightarrow Na_2SO_4 + (NH_4)_2SO_4$$

Equation 15: Reaction between the acid and ammonia to form ammonium salts

As there are multiple reactions taking place, the exact concentration required for acid addition for the purpose of reducting ammonia ionisation, will need to be further evaluated.

5.4 OUTCOME FROM THIS CHAPTER

The data collected in this chapter helped to understand better the ionization process for some functional groups and the impact of interferences such as ammonia in the measurement. A possible solution was implemented and the results collected from using a salt to minimise the effect on ammonia on the ionisation of other compounds were valuable.

5.5 CONCLUSIONS

The ionization for ketones and terpenes show similar results when it was produced an ammonia adduct, however the aromatic did not show this effect and could be related to the fact that terpenes and ketones were ionised by proton transfer and aromatics by charge transfer. When the salt was added ammonia adduct products in the spectrum stopped appearing.

In this chapter, a procedure was proposed to solve the issue of ammonia carry over in the system and as an interference in the ionization of other compounds. To achieve that was suggested to add 1.0 mL of $NaHSO_4$ (62%, w/v, ≈ 620 g/L) with 1.0 mL the sample into standard 20 mL vials. This salt concentration proved to be very effective at avoiding the impact of ammonia concentrations of 2.5 g/l and was acceptable for ammonia concentrations up to 7.6 g/L. When the concentration of ammonia increased further, the salt was no longer effective. To minimise this problem, it would be recommended that a

sample dilution would take place before analysis with a follow on addition of the salt. One limitation of using the salt for sample preparation, would be that compounds that have nitrogen could potentially not be detected such as like amines. A further evaluation of the type and concentration of the salt and the impact of a wider spectrum of analytes would be required.

6. ONE-STAGE AND MULTI-STAGE REACTORS PERFORMANCE

6.1 INTRODUCTION

The investigations conducted in this chapter were designed to a) understand the performance differences between a one-stage reactor (a continuous stirred-tank reactor – CSTR reactor) and a multi-stage reactor (a plug flow reactor - PF reactor) and explore how these relate to b) the "fate" of VOCs from feedstocks to final products by monitoring degradation that occurs in the reactors during staged treatment as compared to a single-stage process.

6.2 MATERIAL AND METHODS

6.2.1 Inoculum

The inoculum used for this experiment was provided from the same full scale AD plant as in previous chapters. Digestate was collected from the primary digester from the last section of the plug flow primary digester (SP8, figure 9), before the pasteurization process to enable the sourcing of a mixed microbial culture that was rich in methanogenic bacteria to inoculate the laboratory reactors. Large particles were removed from the digestate by sieving it through two stainless steel sieves (first sieved at 2.0 mm and subsequently a 699 µm).

6.2.2 Feedstocks

The feedstocks used were ABP and cow slurry and these were supplied by the same company as the digestate. The feedstocks were collected once during Spring and were stored within small bottles and kept frozen until use. When required, feedstocks were defrosted, and were kept in the fridge and used within 1-3 days to feed the laboratory based reactors. The feedstock feeding mixture was prepared just before feeding by weighing 50% ABP and 50% cow slurry.

6.2.3 Laboratory rigs (PF reactor vs CSTR reactor)

The PF reactor was established with four reactors of 1 L each and a working volume of 800 mL, whilst the CSTR was one reactor of 1 L. The reactors were kept within a hot bath to keep the temperature constant (37°C ± 1°C) (Figure 49 A). The full scale AD plant

operations within a mesophilic at approximately 38°C and therefore this temperature was used to operate the laboratory reactors. To assess the reproducibility of the results, the systems were built in duplicates (A and B). All reactors and the gas flow meter were bespoke designed and built (Figure 49). The gas flow meter was based on a tip meter calibrated using a peristaltic pump Watson-Marlow SCI 323 (from Watson-Marlow Ltd, UK). LabView (National Instruments UK) was the software used for recording the gas volume produced from the reactors.

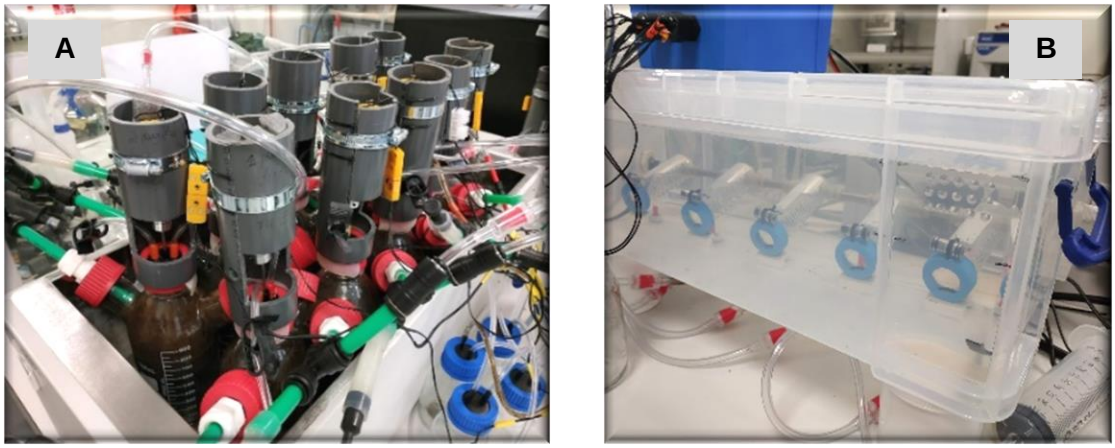

Figure 49: Reactors inside a controlled temperature hot bath (A), handmade tip meters (B)

At the beginning of the experiments and to investigate potential gas leakages, nitrogen was pumped using a peristaltic pump and gas flows were measured and compared. A gas leak detection method was based on the application of a surfactant (Snoop, Swagelok, US) on all the connection points as showed on Figure 50 to make sure reactors were fully sealed. An early attempt to mimic the gas mixing as per full scale reactor was performed however his was challenging to achieve in the small gas reactors and in order to avoid of leakages, each reactor was stirred by a rod driven by an electrical motor. The lab reactors had also a feeding tube and a sampling port to collect gas samples (Figure 51 A).

Figure 50: Detection for gas leakage

The multi-stage reactor (PF) tried to simulate the primary digester from the full scale AD plant. To mimic this reactor for lab-scale the headspace of each bottle was connected. The headspace from reactor 1 was connected to reactor 2, the headspace from reactor 2 was connected to reactor 3 and the headspace from reactor 3 was connected to reactor 4. The headspace from reactor 4 was then connected back to reactor 1 and the biogas produced was connected to one way valve to a 3M NaOH solution bottle (which objective was to remove the CO_2 and leaving only CH_4 to measure) (Figure 51 B) followed by a bespoke built gas tip meter to measure the volume of methane produced (Figure 49 B). Figure 51 A shows the main parts and assembly of the lab reactors.

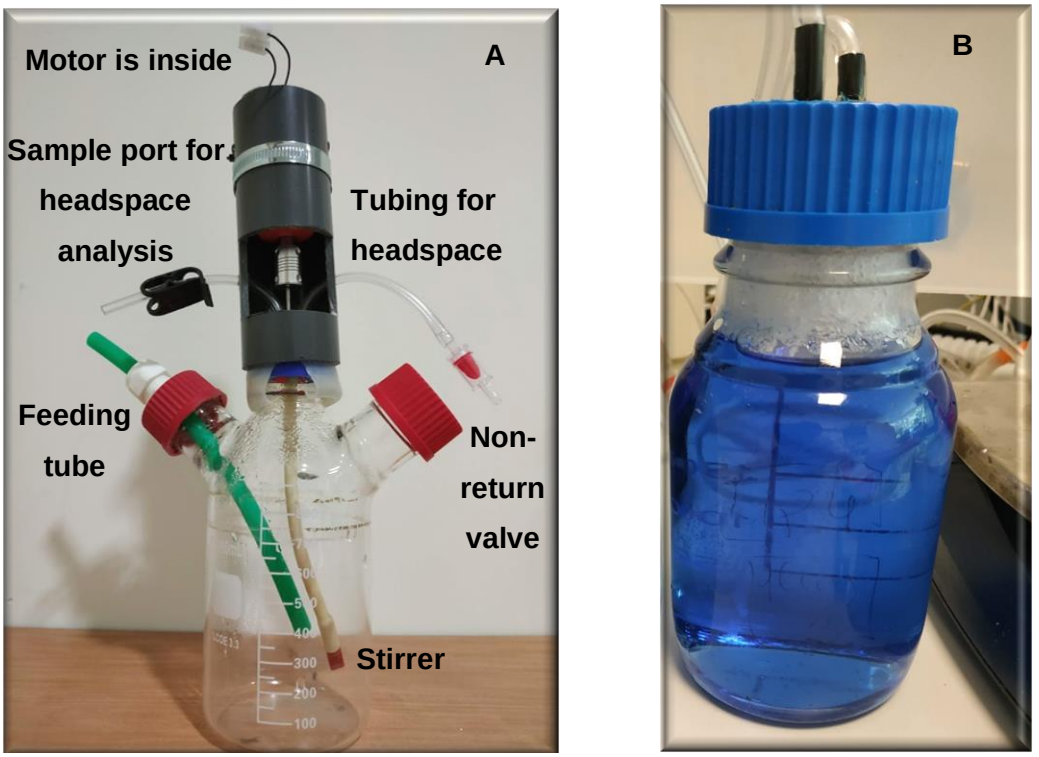

Figure 51: Representation of the structure for the lab reactors where it is possible to see the stirrer, the non-return valve for liquid, the feeding tube, the sample port for headspace analysis, the tubing for headspace (A); Bottle with 3M NaOH to stripped out CO_2 with CH_4 only being measured by the gas tip meter (B)

6.2.3.1 Reactor schematic

Figure 52 is a schematic representation of PF reactor (A) with gas recirculation and an internal, mechanical mixing vs a CSTR reactor (B) with just internal, mechanical mixing.

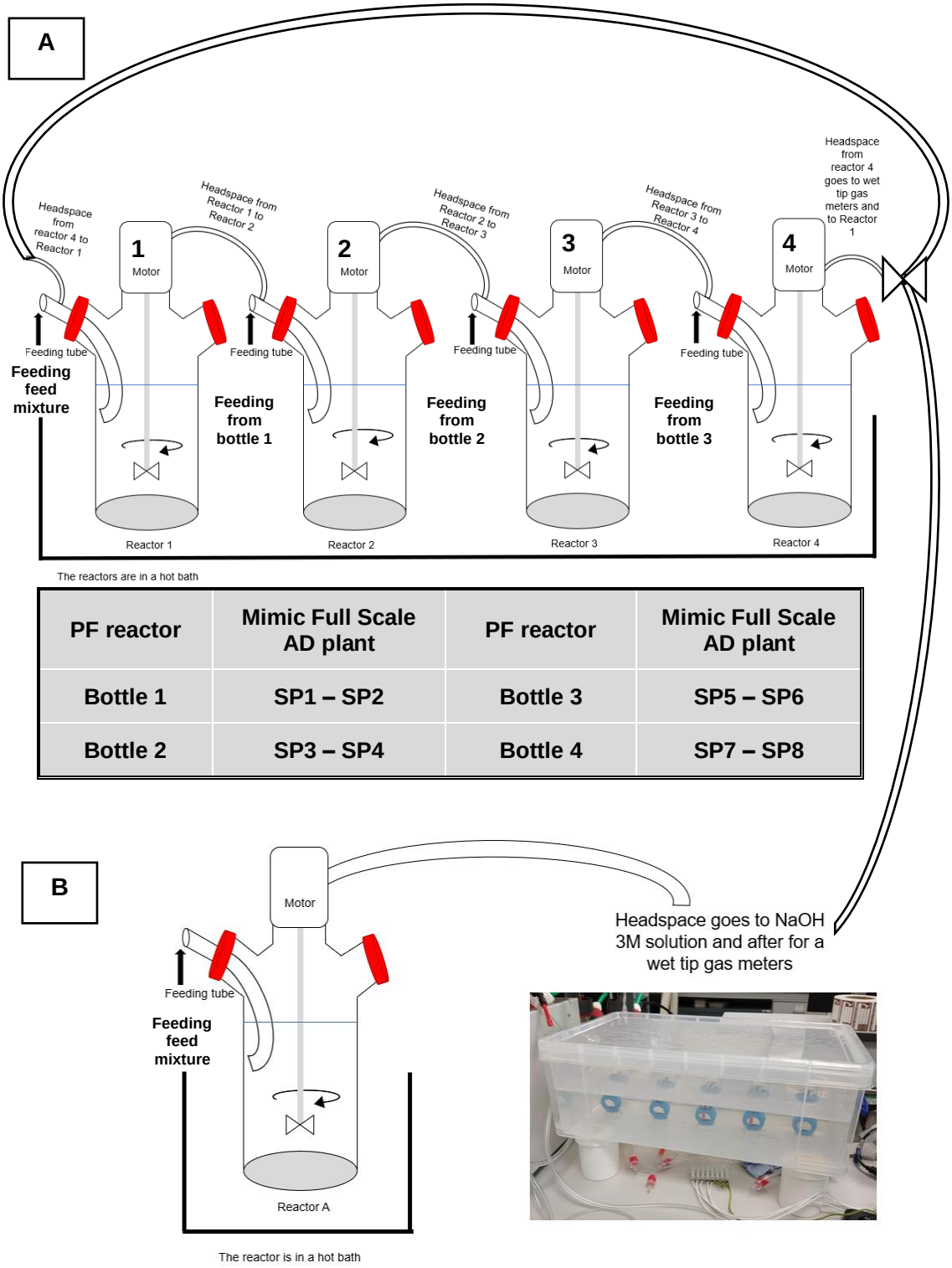

PF reactor	Mimic Full Scale AD plant	PF reactor	Mimic Full Scale AD plant
Bottle 1	SP1 – SP2	Bottle 3	SP5 – SP6
Bottle 2	SP3 – SP4	Bottle 4	SP7 – SP8

Figure 52: Schematic for PF reactor (A) and schematic for CSTR reactor (B)

6.2.3.2 Laboratory Reactors Feeding Procedure

The full scale AD plant has a total capacity for their primary digester of 3000 m^3, although the reactor runs only between 92 – 98% total volume capacity. Therefore, equal to 2850 m^3 working capacity. The full scale AD plant feedstock was approximately 22% dry matter and the OLR is 88 ton/day. The OLR for the lab reactors was established accordingly to the full scale plant and taking into consideration that the lab reactors working volumes of

3.2 L for the PF reactor and 0.8 L for the CSTR. Both reactors were operated at 33 days HRT. Feeding took place once a day over the weekdays during 1 to 33 day (OLR was 1.83 g VS/L reactor.day) and feeding was reduced to 3x a week from 34 - 115 day (OLR was 1.10 VS/L reactor.day). The OLR was low but was to mirror the full-scale AD operation (OLR was 1.86 VS/L reactor.day).

The reactors were fed using a bleed and feed method and this means that for PF, the first reactor was fed with 136 g of feedstock (50% ABP + 50% cow slurry), afterwards the second bottle was fed with the 136 g that were removed from the first reactor, subsequently the third reactor was fed with the 136 g that were removed from the second reactor, afterwards the fourth reactor was fed with the 136 g that were removed from the third reactor. Finally, 136 g from the fourth reactor was used for analysis or disposal. The CSTR reactor was fed with 34 g feedstock (50% ABP + 50% cow slurry) and 34 g were used for analysis or disposal.

6.2.4 GC-IMS Analysis

The method used in this chapter was developed in Chapter 3 and reported in Table 23. However, to confirm what was the best dilution range for reactor samples and to evaluate the temperature for headspace equilibrium, some extra investigations were performed. Table 32 correlated the samples used and what changes happened from the initial method. All samples were run in duplicate and between samples, a blank vial with nitrogen gas was placed. Sample “PF B – Reactor 1” and sample “PF B – Reactor 2” were used to decide the dilution range and the incubation temperature because “PF B – Reactor 1” had a higher input of feedstocks as compared to the CSTR reactor and it is still at beginning of the degradation process so more similar compounds as the feedstocks were expected. “PF B – Reactor 2” was expected to have a volatile compounds matrix more similar to the CSTR reactor.

Table 32: Changes to the GC-IMS method presented on Table 23

Initial method parameters summarise from the method presented in Table 23						
Column	**Addition of salt ($NAHSO_4$)**	**Dilution range**	**T Incubation [°C]**	**Incubation Time [min]**	**GC-Runtime [min]**	**Measurement Runtime [min]**
SE-54-CB1	No	Depend of each sample	45 °C	9 min	10 min 30 sec	10 min

Continuation Table 32: Changes to the GC-IMS method presented on Table 23

Sample	Dilution	Changes to the initial method	Results
ABP	10 ×	No changes	Presented on Fig. 52
Cow slurry	10 ×	No changes	Presented on Fig. 52
Feed mixture	10 ×	No changes	Presented on Fig. 52
PF B – Reactor 1	50 × 25 × 10 × ND	No changes	Presented on Fig. 53 A
PF B – Reactor 1	50 × 25 × 10 ×	Incubation temperature at 80 °C instead 45 °C	Presented on Fig. 53 B
PF B – Reactor 2	50 × 25 × 10 ×	No changes	Presented on Fig. 53 C
PF B – Reactor 2	10 × ND	Add 1 mL $NaHSO_4$ at 62%	Presented on Fig. 54
PF B – Reactor 2	10 × ND	Incubation temperature at 80 °C instead 45 °C and add 1 mL $NaHSO_4$ at 62%	Presented on Fig. 54

6.2.5 Other analysis

Table 33 summarises the analytical methods used for this chapter. VFAs were measured according to (Cruwys *et al.,* 2002) . TS and VS measurements were performed in triplicate and averaged.

Table 33: Analytical methodology used to support laboratory reactor performance

pH	Used a pH meter (Fisherbrand) with a probe which was calibrated to pH 7 and 4
TS	Sample dried at 105 ± 2°C (APHA, 2005), carried out in triplicate
VS	Sample ashed at 550 ± 25°C (APHA, 2005), carried out in triplicate
VFAs	Measure for acetic, propionic, iso- and n-butyric and iso- and n-valeric acids (between 0–1000 mg/L) and 2-ethylbutyric acid as an internal standard determined by GC-FID with an Elite 624 capillary column (mid polarity 6%-cyanopropylphenyl-94%dimethylpolysiloxane) 30m x 0.32mm, 1.80µm (Cruwys *et al.*, 2002)

6.3 RESULTS AND DISCUSSION

6.3.1 GC-IMS: Characterization of feedstocks

Figure 53 presents the spectra for the feedstocks where it is present the ABP sample, the cow slurry and the result obtained from mixing this two samples, the feed mixture. It is possible to see that the feed mixture presents a very similar profile as compared to the ABP sample. Although, it can also be seen that the mixture sample is more dilute than ABP samples with less intense peaks and there are some fingerprinting characteristics from the cow slurry.

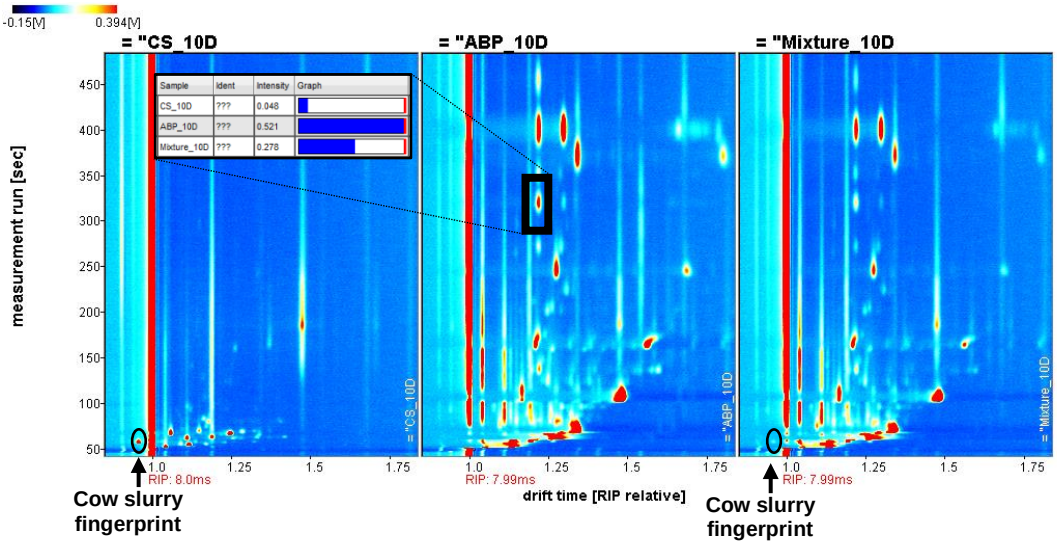

Figure 53: Spectrum for ABP, cow slurry and the feed mixture diluted 10 times each sample and an example where feed mixture had less intensity then the ABP peak

6.3.2 GC-IMS: Dilution effect and temperature for headspace equilibrium

Figure 54 presents the results from diluting samples from “PF B – reactor 1” with 50 ×, 25 ×, 10 ×, and ND dilution at 45°C as incubation temperature (Fig. 54 A) and diluted by 50 ×, 25 ×, and 10 × at 80°C (Fig 54 B). Looking at the results, as expected at 80°C saturates more the system than at 45°C. Nevertheless, at 45°C the analysis still presents most of the fingerprints as compared to 80°C and, for this reason 45°C was chosen the final incubation temperature. The final range of dilution chosen was a ND because even using a concentrated sample as “PF B – reactor 1”, the equipment still performed well and this could help for samples that are not so concentrated as “PF B – reactor 1” like “PF B – reactor 4” that represented the final stage of degradation and before the pasteurization process. Figure 54 C shows the dilution for the “PF B – reactor 2” where the main compound was ammonia and for this reason, the salt ($NaHSO_4$) was added to eliminate

the ammonia interference as explain in Chapter 5. The same chapter also explored the best range of dilution for samples with this type of profile and the adequate incubation temperature (Fig. 55 A). From the samples “PF B – reactor 1” and “PF B – reactor 2” it is possible to see a decrease in the amount of peaks present in the spectrum evidencing the occurrence of a degradation process (Figure 54 B).

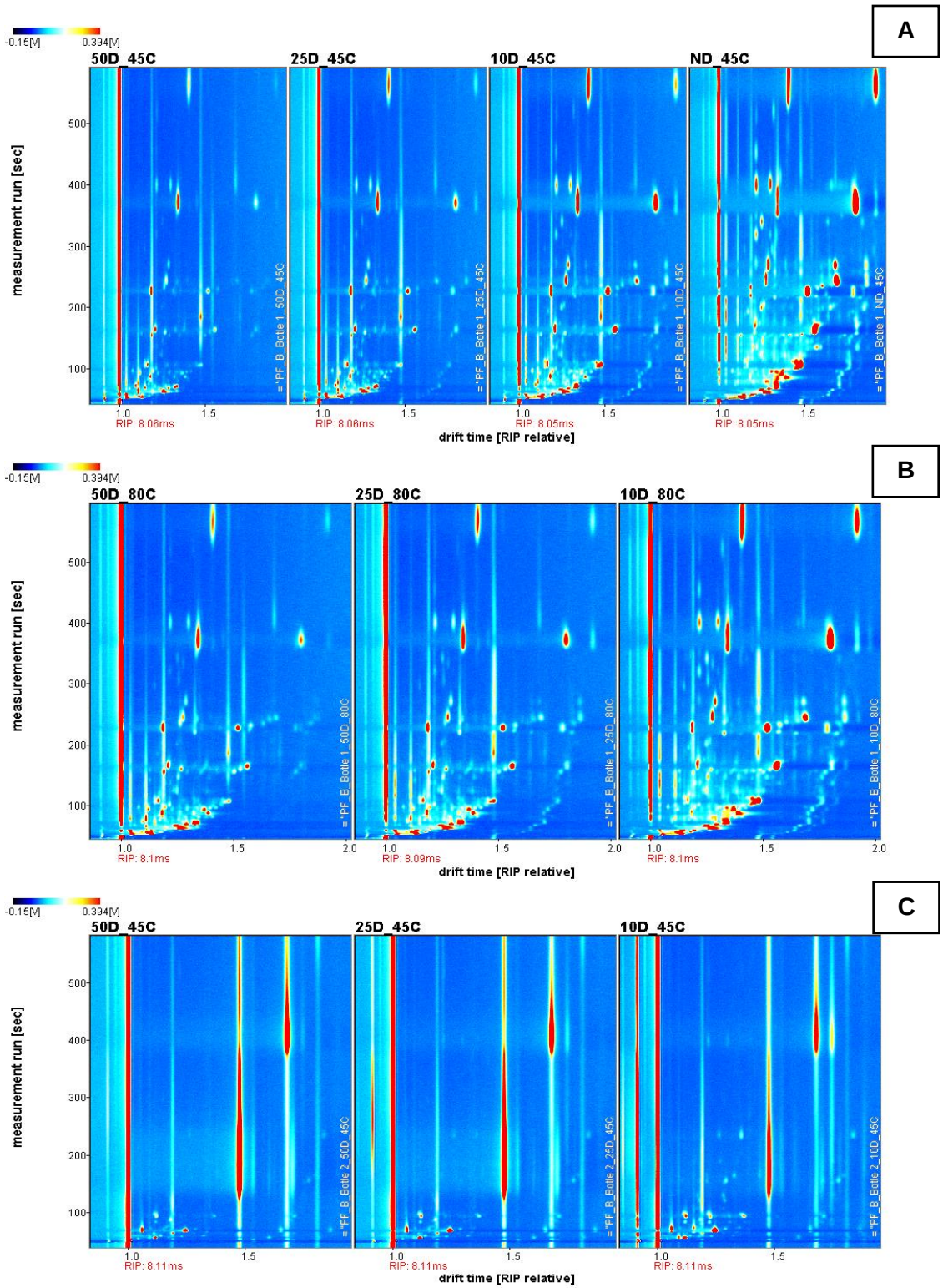

Figure 54: Spectrums for the “PF B – reactor 1” for several dilution with incubation temperature at 45 °C (A), at 80 °C (B), and the “PF B – reactor 2” at 45 °C (C)

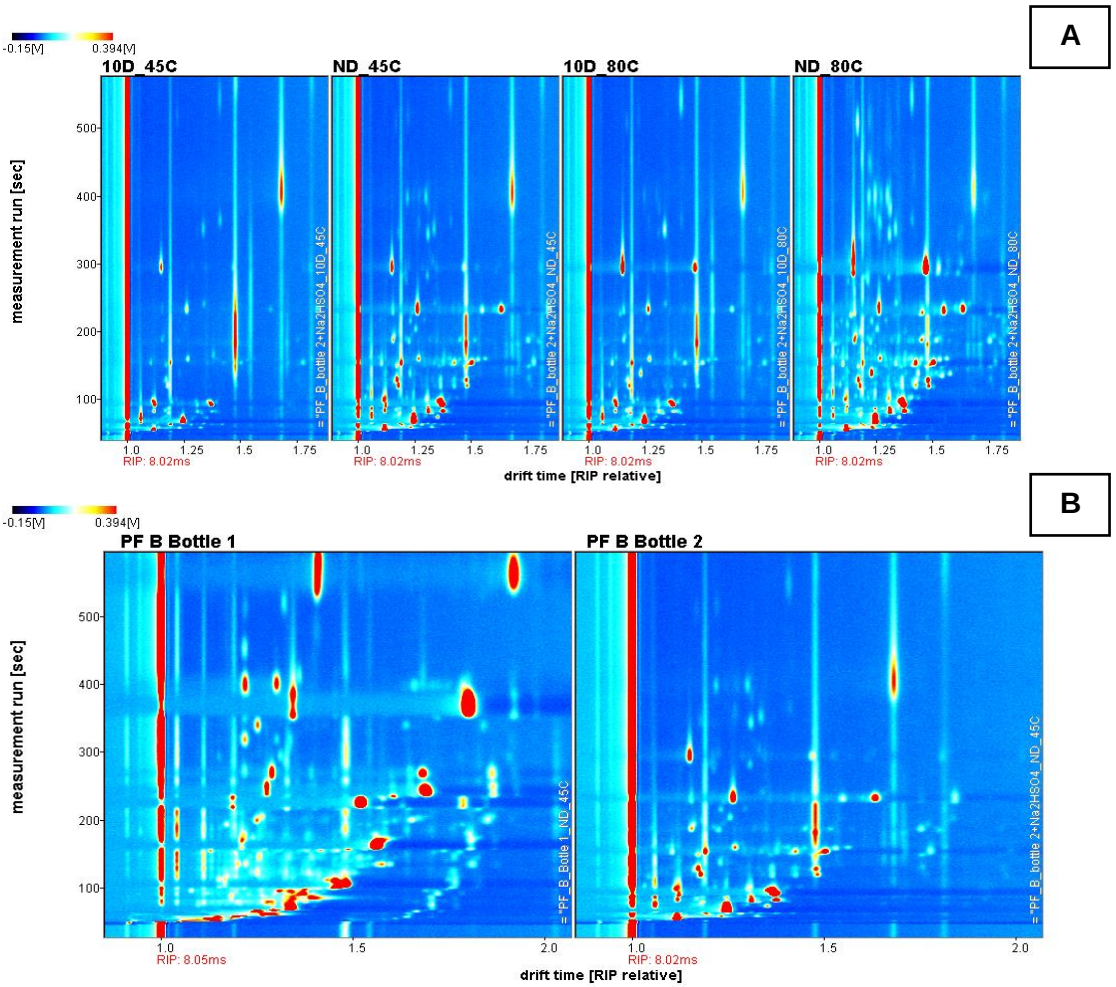

Figure 55: Spectra for the "PF B – reactor 2" for several dilution with incubation temperature at 45 °C and 80 °C (A) after adding the salt and comparing the "PF B – reactor 1" at 45 °C with ND with the "PF B – reactor 2" at 45 °C without any dilution and adding the salt (B)

In summary all the samples were to be measured at 45°C as incubation temperature, without any dilution for reactors 2, 3, 4 and CSTR and applied a 10 times for reactor 1 or no dilution but always adding 1 mL of $NaHSO_4$ to remove ammonia interference.

6.3.3 GC-IMS: Peaks identification

Using the information collected from previous chapters and from the GC×IMS Library Search, 14 compounds were identified from the reactor samples and they are presented in Table 34 with an organoleptic property collected from PubChem database (National Library of Medicine) (National Library of Medicine, 2020). For some compounds still would be necessary to run the standard to confirm the final results, nevertheless the results followed the data from GC-MS, excepted for butanoic acid, pyridine, ethyl pentanoate, propyl butanoate, 1-hexanol that follows the GC-IMS identification for Rt and dt. The functional group from the compounds identified were esters, monoterpenes, terpenes,

acids, alcohol, aromatic aldehyde, aromatics, and ketones. Acid compounds and aromatics are the most unpleasant odours presented in Table 34, while esters and ketones have similar odour to fruits and terpenes to plants.

Table 34: Compounds tentatively identified using GCxIMS Library Search

Sample	Compound	Functional Group	Organoleptic Properties
PF B – reactor 1	Hexanoic acid	**Acid**	Cheese, fatty, sour, sweat
PF B – reactor 1	Butanoic acid	**Acid**	Butter, cheese, fruit, rancid, sharp, sweat, acetic
PF B – reactor 2	Ethylbenzene	**Alkylbenzene**	Aromatic odour, pungent odour, sweet, gasoline-like odour
PF B – reactor 2	Pyridine	**Aromatic heterocycle**	Fishy, amine, sour, putrid, rancid, sickening
PF B – reactor 1	Benzaldehyde	**Aromatic aldehyde**	Bitter, burnt sugar, sharp, sweet, cherry, strong, almond
PF B – reactor 1	Ethyl pentanoate	**Ester**	Fruit, yeast, sweet, green, apple, fruity, tropical, pineapple
PF B – reactor 1	Propyl butanoate	**Ester**	Rancid, solvent, sweet, apricot, sweaty, fruity, pineapple
PF B – reactor 1	Propyl hexanoate	**Ester**	Fruit, sweet, juicy, green, fruity, tropical, pineapple
PF B – reactor 2	2-Butanone	**Ketone**	Camphor, ether, acetone, ethereal, fruity
PF B – reactor 2	2-Pentanone	**Ketone**	Fishy, ether, fruit, wine, sweet, ethereal, woody, potato, banana, fruity, alcohol
PF B – reactor 2	2-Heptanone	**Ketone**	Spicy, soap, cinnamon, sweet, herbal, woody, coconut, fruity
PF B – reactor 2	Cyclohexanone	**Cycle ketone**	Minty, acetone
PF B – reactor 1	1-Hexanol	**Organic alcohol**	Flower, oil, resin, alcoholic, sweet, ethereal, fusel, green, fruity
PF B – reactor 1	Gamma-terpinene	**Monoterpenes**	Bitter, gasoline, oily, turpentine, lemon, lime, herbal, woody, terpene, tropical
PF B – reactor 1	Beta-pinene	**Monoterpenes**	Pine, resin, turpentine, dry, hay, woody, green, resinous
PF B – reactor 1	Alpha-pinene	**Monoterpenes**	Camphor, fresh, pine, turpentine, sweet, woody, earthy
PF B – reactor 1	Limonene	**Terpene**	Citric, herbal, woody

Figure 56 A shows the identification of peaks using the GC×IMS Library Search for the compounds presented in “PF B – reactor 1” whilst in Figure 56 B is the identification for “PF B – reactor 2” and Figure 56 C the compound list for each peak.

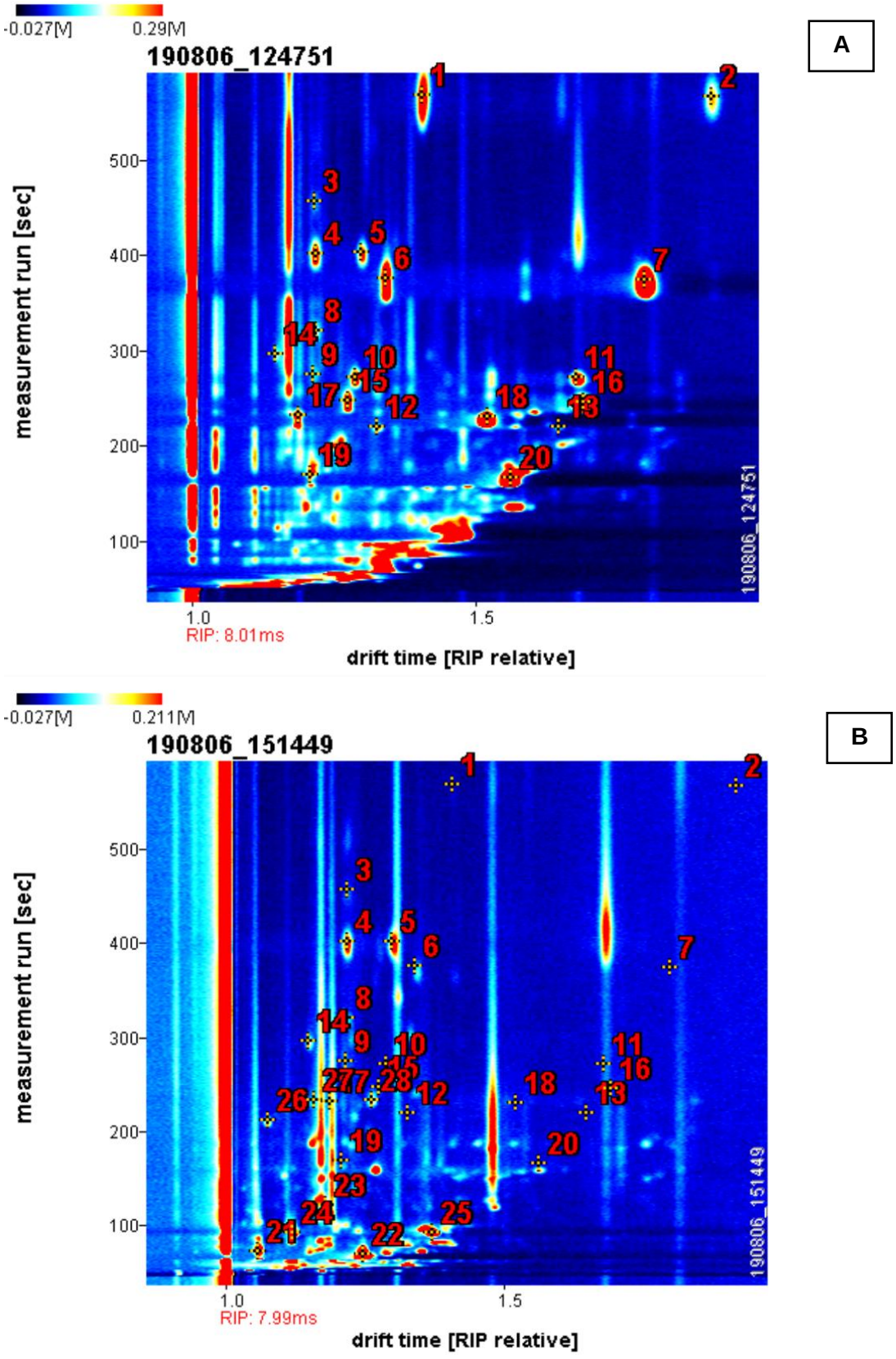

C

Count	Compound	RI	Rt (sec)	Dt (RIPrel)
1	Propyl hexanoate M	1102.7	567.748	1.4073
2	Propyl hexanoate D	1102.7	566.167	1.9175
3	γ-terpinene	1053.6	457.262	1.2189
4	Limonene M	1024.4	401.962	1.2196
5	Limonene D	1024.7	402.486	1.3010
6	Hexanoic acid M	1009.2	375.921	1.3424
7	Hexanoic acid D	1008.0	373.929	1.7987
8	β-pinene	970.9	321.379	1.2192
9	α-pinene M	930.7	274.408	1.2160
10	α-pinene D	928.7	272.236	1.2891
11	α-pinene T	928.1	271.613	1.6804
12	1-Hexanol M	873.5	219.849	1.3279
13	1-Hexanol D	874.3	220.559	1.6483
14	Benzaldehyde	950.0	296.068	1.1492
15	Ethyl pentanoate M	904.8	247.759	1.2759
16	Ethyl pentanoate D	902.3	245.316	1.6916
17	Propyl butyrate M	888.7	232.750	1.1885
18	Propyl butyrate D	886.3	230.656	1.5232
19	Butanoic acid M	804.7	170.027	1.2101
20	Butanoic acid D	798.9	166.370	1.5645
21	2-butanone M	604.2	73.103	1.0608
22	2-butanone D	591.1	70.195	1.2484
23	Pyridine	735.5	121.626	1.1803
24	2-pentanone M	683.6	93.381	1.1215
25	2-pentanone D	683.1	93.226	1.3719
26	Ethylbenzene	863.3	211.651	1.0777
27	Cyclohexanone	889.1	233.035	1.1594
28	2-heptanone	890.1	233.967	1.2639

Figure 56: Compounds identification for sample "PF – reactor 1" (A), "PF – reactor 2" (B), and the compound list

The information presented on PubChem database stated that the γ-terpinene is an antioxidant, a plant metabolite, a volatile oil component and a human xenobiotic metabolite and it can be found in products such as cleaning and furnishing care products, laundry and dishwashing products and personal care products. The reaction between the carboxy group of hexanoic acid with 1-propanol can make the propyl hexanoate and it has a role as a metabolite and it can be found in fruits (e.g. apple, apricot, grapes, passion fruit, starfruit, mountain papaya) or alcoholic beverages or cheeses. Limonene is an oil that can be extracted from citrus peels or a human metabolite from the degradation of perillic acid or derives from a hydride of a p-menthane. Hexanoic acid is the conjugate acid of a hexanoate and it is a straight-chain saturated fatty acid with six carbons with an unpleasant odour and it could outcome from the breakdown of either arachidonic acid or linoleic acid. It is a human metabolite and a plant metabolite founded in various plant and animal fats and oils. Beta-pinene and alpha-pinene are an essential oil and it is a substance formed in or necessary for metabolism for several plants and it can be found in lime peel oil, ginger, nutmeg, mace, bitter fennel, rosemary and sage. Benzaldehyde can be found in human as metabolite. Ethyl pentanoate can be present in alcoholic beverages or wines and several fruits (apple, banana, cherry, or guava). As propyl hexanoate, propyl butyrate can be made from the reaction between the carboxy group of butanoic acid with 1-propanol and it is present in many fruits like apple, apricot, banana, melon, papaya or cheeses such as the Camembert cheese. Butyric acid can be produced from the degradation of carbohydrates from bacteria and it can be found in rancid butter, parmesan cheese, vomit, or in esterified form in animal fats and plant oils. 2-Butanone as pyridine can be found in the environment from natural sources or manufactured, or human metabolite produce by oxidation of 2-butanol while 2-pentanone can be present in fruits (apple, pineapple), and soya oil. Ethylbenzene is a constituent of coal tar and petroleum or be manufactured or human metabolite from mandelic and phenylglyoxylic acids. Cyclohexanone can be manufactured or be a human metabolite obtained through oxidation of cyclohexane or 1-, 2-, and 3-hexanol, or dehydrogenation of phenol (National Library of Medicine, 2020). Terpenes like p-cymene or d-limonene characterize up to 90% of all VOCs in the biogas for AD plants that treat food wastes (Arrhenius *et al.*, 2016) while VFAs are significant intermediates and metabolites in biological processes and present for example in wastewater matrices (Cruwys *et al.*, 2002), the content of p-cymene and p-menthane will increase when the amount of α-pinene decreased or from other compounds such as 2-carene or 3-carene or γ-terpinene and toluene can be formed from aromatic amino acids by fermenting bacteria (Hylemon and Harder, 1998).

6.3.4 GC-IMS: Assessment of reactors' performance

Gallery plots were created for data analysis. The advantage of using this feature is to find similarities and differences between different compounds in different samples but it is worth noticing that the intensity scale of peaks are relative to the maximum in the range of that individual peak, consequently, cannot be directly comparable between different peaks in the plot. Figure 56 compares feedstocks and reactors from day 64. Cow slurry had in common with reactors samples the 2-butanone peak, while ABP had in common propyl hexanoate, ethyl pentanoate, limonene, γ-terpinene, β-pinene, α-pinene, hexanoic acid, and the butanoic acid peaks.

The PF – reactor 1 (A and B) is the most similar to the ABP sample with 8 compounds in common, mainly acids, terpenes and ester compounds. Only propyl hexanoate and hexanoic acid (dimer) had intensity in the reactors. In the PF compounds such as propyl hexanoate, γ-terpinene, hexanoic acid, β-pinene, α-pinene, 1-hexanol, propyl butanoate, and butanoic acid were degraded or convert to gas form or utilized by the bacteria through the system because they were present in the first stage but not anymore at last stage on reactor 4 and other compounds (ethyl pentanoate or 2-heptanone or limonene) had reduced the intensity. Benzaldehyde was produced during the process but was not present at last stage. Compounds such as 2-butanone, pyridine, 2-pentanone, ethylbenzene, cyclohexanone were still present within the last digestion stage. It is possible that the PF-reactors would have provided even greater performance if loaded with higher organic loads.

The CSTR reactors had a good performance as compounds as propyl hexanoate, 1-hexanol, α-pinene, hexanoic acid, benzaldehyde, were not detected while other compounds were reduced their intensity such as limonene, γ-terpinene, β-pinene, ethyl pentanoate, butanoic acid, were present in small amounts and compounds such as 2-butanone, pyridine, 2-pentanone, ethylbenzene, cyclohexanone, 2-heptanone were still present at last stage and they were a by-product from the process.

Analysing the data through time (from day 58 to day 107, Appendix 3 Figure 66 to Figure 72) all gallery plots showed the same profile and this explains that the reactors had a constant performance during the entire experiment in relation to VOCs. Besides VFAs, limonene could be another compound to use as indicator of the reactor performance if feedstocks contain the compound. In conclusion, the PF had a better performance especially for the degradation of terpenes as compared to the CSTR.

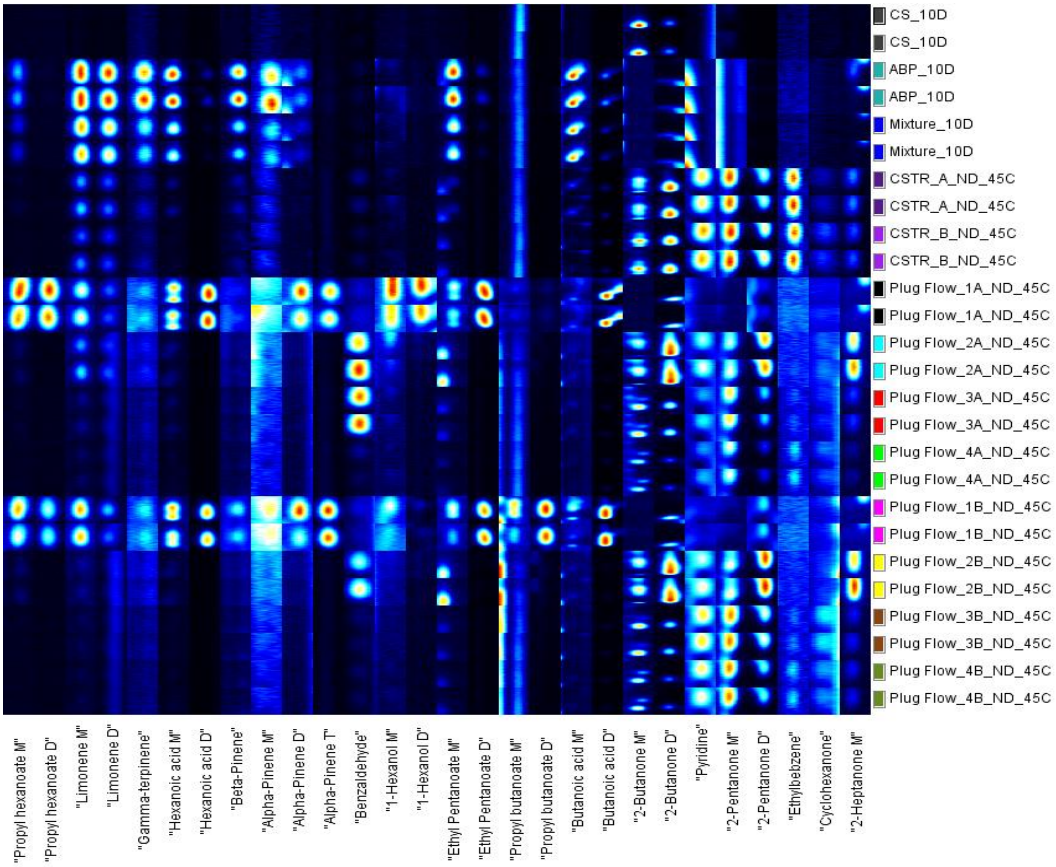

Figure 57: A gallery plot showing the peak selection and respective identification (monomer, dimer, trimer) for all feedstocks (cow slurry, ABP, and the mixture feed) and all reactors samples (CSTR A, CSTR B, PF A, PF B) for the day 64

Figure 58 shows the spectrum for PF A and CSTR A for the day 107 where it is possible to see clearly the changes that happened for the PF from reactor 1 to reactor 4 (Fig. 58 A) and from “PF – reactor 4” and CSTR A (Fig. 58 B)

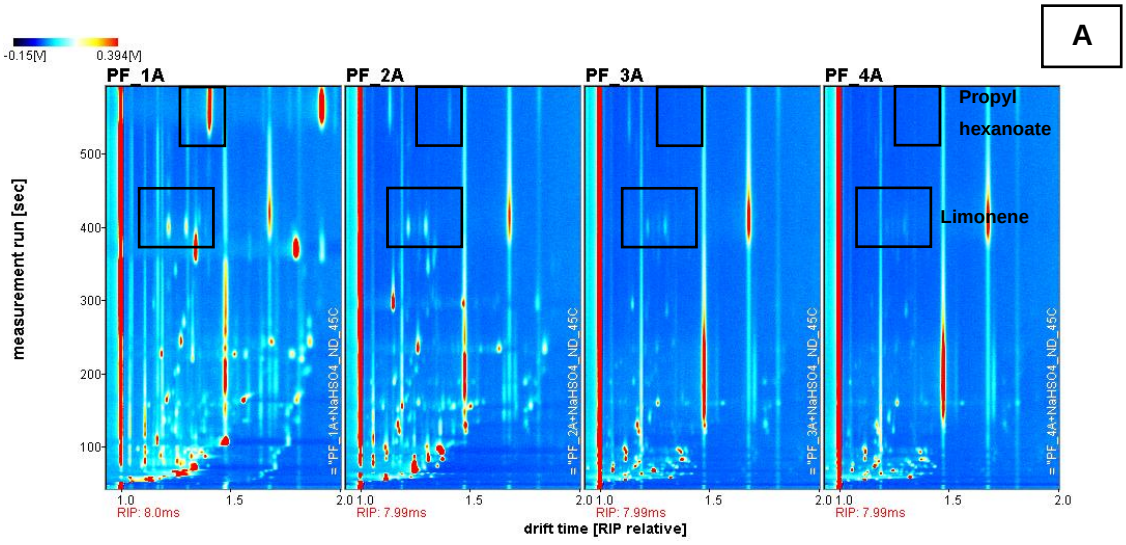

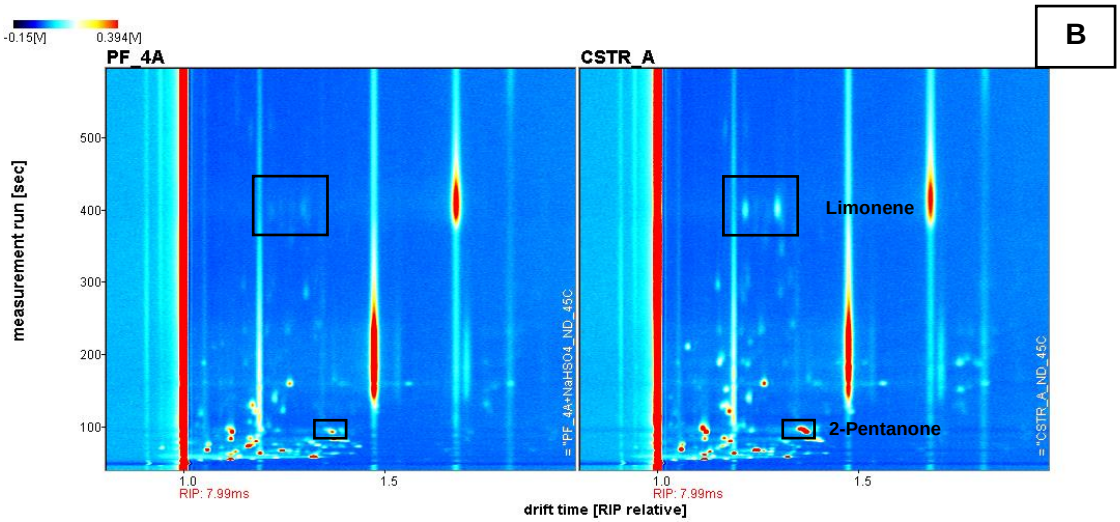

Figure 58: Spectrum for PF from reactor 1 to reactor 4 (A) and PF – reactor 4 and CSTR (B)

6.3.5 GC-IMS: Assessment of reactors' evolution over time for each reactor

Figures presented on appendix 4 (Figure 73 to 82) assess the progress of each reactor from day 58 until day 107 using GC-IMS as an analytical tool. For the CSTR A and CSTR B, the reactors kept constant the same profile just highlight in both reactors compounds such as limonene the intensity decreased from the beginning of the experiment until at end as well as for others terpenes or 2-heptanone, cyclohexanone, or benzaldehyde. Reactor 1, 2, 3, 4 (A and B) presented similar profiles, with a difference in the range of intensity for each of the peaks.

Table 35 presented the limonene concentration (µg/L) for monomer and dimer calculated using the LAV software and the Boltzmann function. Feedstocks (feeding mixture), one-stage reactors (CSTR A and CSTR B) and multi-stage reactors (plug flow A and plug flow B) samples from day 107 were analysed. The initial feedstock concentration was around 1500 µg/L while in contrast reactors samples were lower than 100 µg/L. Comparing the CSTR reactors with the plug flow, the plug flow (reactor 4) performed better but in general, both reactors decrease the initial volatile concentrations. In the plug flow reactors, it was possible to see a decrease in limonene concentration from reactor 1 to reactor 4. It was not possible to quantify ketones using this method because the amount was lower than the LOQ.

Table 35: Limonene concentration in different samples

	Baseline Volt	Intensity in RIP rel (Height [Area Min.]) Volt	Intensity in RIP rel (Height [Area Min.]) Volt	Monomer Concentration µg/L	Dimer Concentration µg/L
Feedstocks					
Feeding mixture (ABP + cow slurry)	0.050	0.558	0.728	1523.43	1581.98
Feeding mixture (ABP + cow slurry)	0.047	0.580	0.782	1641.12	1720.66
One-stage reactors					
CSTR_A	0.041	0.134	0.168	74.27	74.32
CSTR_A	0.036	0.145	0.173	75.27	74.77
CSTR_B	0.042	0.145	0.176	75.27	75.04
CSTR_B	0.037	0.147	0.165	75.45	74.06
Multi-stage reactors					
PF_1A+NaHSO4	0.039	0.321	0.268	94.69	83.94
PF_1A+NaHSO4	0.037	0.330	0.283	95.94	85.52
PF_2A+NaHSO4	0.040	0.170	0.186	77.59	75.94
PF_2A+NaHSO4	0.039	0.192	0.198	79.73	77.05
PF_3A+NaHSO4	0.039	0.072	0.093	69.01	68.05
PF_3A+NaHSO4	0.039	0.079	0.093	69.58	68.05
PF_4A+NaHSO4	0.039	0.039	0.057	66.38	65.29
PF_4A+NaHSO4	0.041	0.042	0.053	66.62	65.00
PF_1B+NaHSO4	0.041	0.216	0.193	82.17	76.58
PF_1B+NaHSO4	0.039	0.205	0.163	81.04	73.88
PF_2B+NaHSO4	0.040	0.074	0.126	69.17	70.72
PF_2B+NaHSO4	0.040	0.086	0.139	70.15	71.81
PF_3B+NaHSO4	0.041	0.051	0.065	67.32	65.89
PF_3B+NaHSO4	0.040	0.067	0.069	68.60	66.20
PF_4B+NaHSO4	0.040	0.043	0.045	66.70	64.41
PF_4B+NaHSO4	0.040	0.040	0.040	66.46	64.04

6.3.6 Integrating GC-IMS analysis with other chemical techniques

6.3.6.1 pH

Figure 59 (A, B, and C) present the pH for PF A, PF B, CSTR A, and CSTR B since the beginning of the study until the end. PF A for reactor 1 and PF B for reactor 1 after day 12, the pH starting go down and it could be related to accumulation of acids and this correlated with the data from GC-IMS, where was found on reactor 1 compounds such as butanoic acid or hexanoic acid. The pH in the others reactors was around 7.5 – 8.5 for PF A and 7.0 – 8.0 for PF B. The CSTR A and B had a similar performance with a pH around 7.5 – 8.0. The pH around 7.0 – 8.5 could be explained due the presence of compounds like ammonia. During days 19-26, the hot bath due to an electrical fault was off and resulted in the reduction of the pH for all reactors.

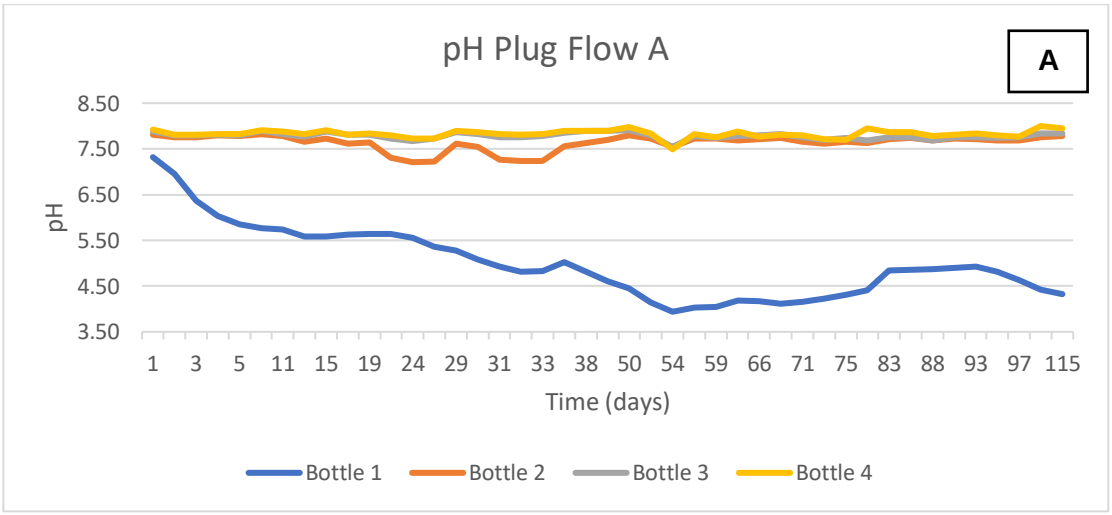

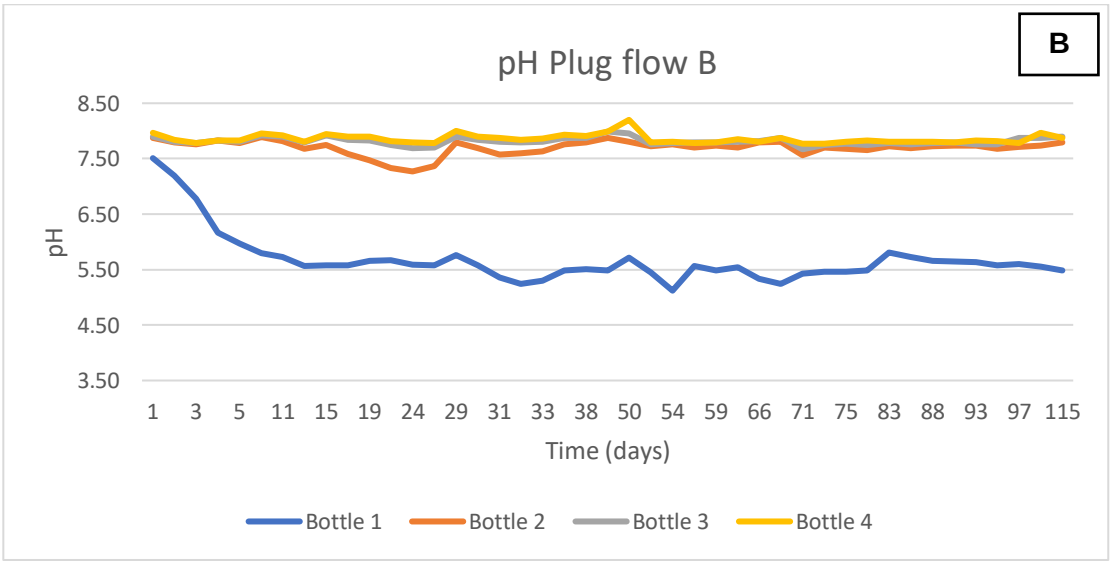

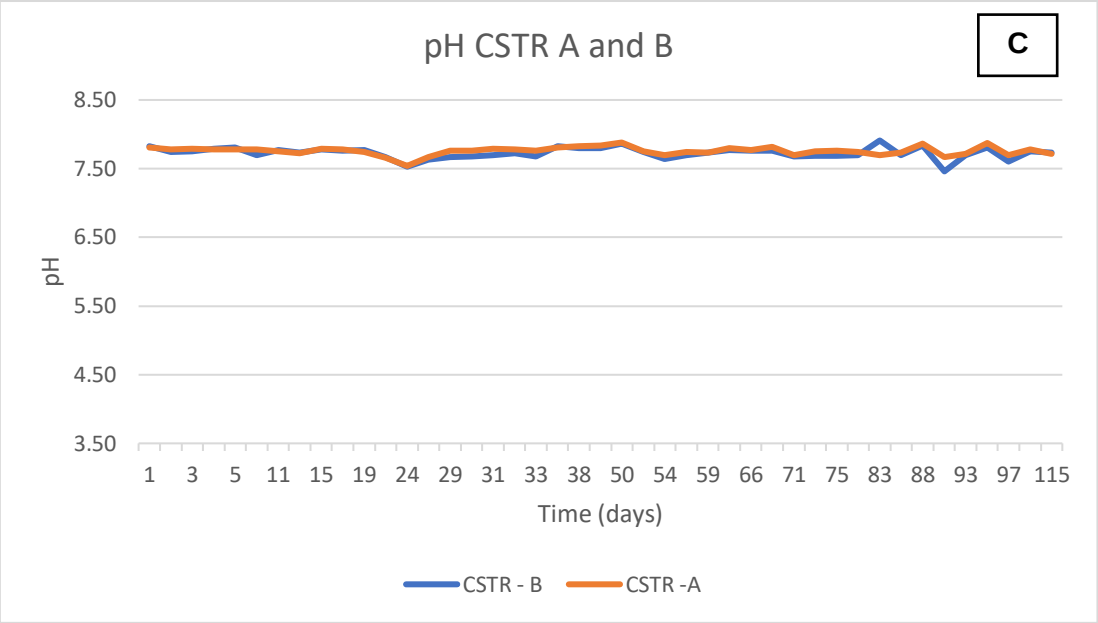

Figure 59: pH measurement for multi-stage reactor (A and B) and one-stage reactors (C) since day 1 to day 115

Based on the pH results, it is expected that the microbial population present in PF reactor 1 to be different from the others reactors. Reactor 1 is delivering an acidogenic phase, therefore is likely to have bacteria that can grow at low pH values and fermentative bacteria and the obligate hydrogen producing bacteria. The others reactors were at neutral pH values so it was expected a presence of bacteria that could develop methanogens (Alvarado *et al*., 2014; Sans *et al*., 1995).

When Sans *et al*. (1995) operated a plug flow reactor at mesophilic conditions, without sludge recirculation, they observed an increase of total VFA production and used the ammonia concentration as key indicator monitoring parameter of bacterial activity and reactor performance (Sans *et al*., 1995). Comparing the lab rig with the full AD plant there exist some differences particularly in the initial pH (SP 1 and reactor 1). This is related to the fact that the full AD plant recirculated digestate to the SP1 allowing the pH to be at neutral values and introduced some bacteria and archaea, whilst in the laboratory experiment that did not happened. In particular, the lab operation's objective was to observe if the pH would decrease and if that would help the degradation (conversion) of volatile organics.

6.3.6.2 VFAs

Table 36 presented the measurement for VFAs (acetic acid, propionic acid, butyric acid, 2-butyric acid, valeric acid, iso-valeric acid). VFAs were measured with less than 25.0

mg/L, excepted for acetic acid that had 40.0 mg/L for PF – reactor 4 and 44.3 mg/L for CSTR. It was possible to conclude the PF systems had a slight better performance than the CSTR, however in general both reactors performance very well with lower amount of VFAs detected.

Table 36. Summary of VFAs results

Acid label	Concentration (mg/L)	
	PF – reactor 4	CSTR
Acetic acid	40.0 mg/L	44.3 mg/L
Propionic acid	< 25.0 mg/L	< 25.0 mg/L
Butyric acid	< 25.0 mg/L	< 25.0 mg/L
2-Butyric acid	< 25.0 mg/L	< 25.0 mg/L
Valeric acid	< 25.0 mg/L	< 25.0 mg/L
Iso-Valeric acid	< 25.0 mg/L	< 25.0 mg/L

6.3.6.3 TS and VS

In this measurement the TS are the portion of a liquid or slurry that is left when the water is removed and that is the reason why the measurement is done at 105 °C and it can be correlated to organic and inorganic matter in the feedstock, liquid or slurry, while the VS is correlated to the organic matter of a feedstock, a liquid or a slurry (excluding the inorganic salts, ash) that is combusted at 550 °C. It is an easy measurement to conduct off-line and VS are typically associated with the digestible biomass that will be converted to biogas. Table 37 presented an example for TS and VS for feedstocks (ABP, cow slurry and the feed mixture) and final products (PF A and B for reactor 4 and CSTR A and B). The initial inoculum had a TS for 3.9 % and 2.7 % for VS. ABP presented the higher amount for TS and VS with values 14.1 % for TS and 12.8 % for VS. For cow slurry the values for TS was 3.3 % for TS and 2.4 % for VS. The feed mixture had values around 6.8 % for TS and 6.1 % for VS. The final products presented TS and VS lower than 3%, showing a reduction in TS and VS from initial feedstock. The VS was lower at the end of the recovery process for PF as compared to the CSTR by approximately 10 %.

Table 37. Example for TS and VS for several samples

Sample	TS (%) Mean	SD	VS (%) Mean	SD
Inoculum (SP8)	3.94	0.03	2.74	0.01
ABP	14.08	0.26	12.77	0.21
Cow slurry	3.26	0.04	2.36	0.03
Feed mixture (ABP + Cow Slurry)	6.84	0.24	6.13	0.11
PF A – reactor 4	2.20	0.03	1.41	0.01
PF B – reactor 4	2.00	0.01	1.23	0.01
CSTR A	2.48	0.05	1.74	0.09
CSTR B	2.55	0.02	1.75	0.02

6.3.6.4 Comparison between Lab-scale and full scale systems

A reasonably similar performance between lab-scale systems and full scale operation was found. The low OLR used was to enable a comparison with the full-scale operations. For example, limonene and ammonia were detected at full-scale and at lab-scale using GC-IMS. From data supplied from the company partner, between July 2016 to March 2017, their process was very stable and with a good buffering capacity. The pH had a little variation that could be a consequence from the food waste variability. In general, the pH remained within the operating range (between 7.4 - 7.8). The lab-scale values were similar to that (7.5-7.9), except for the first reactor from PF that was operating under acid conditions (<7.0). Such a low pH on the front end of the digestion was not experienced at full scale as some digestate is returned to the front of the process adding to the buffering capacity. This return of digestate was not performed at lab-scale.

The total VFAs were constantly lower than 80 mg/L for SP4 and second digestate, in the full AD plant. At lab-scale, the digestate samples (CSTR and PF-reactor 4) were lower than 50 mg/L for total VFAs. These values indicate that any volatiles present at the front end of the process were being converted to biogas efficiently and the process was stable. Besides VFAs, the ammonium nitrogen (NH_4^+-N) results support the process stability by having results lower than <3000 mg/kg for NH_4^+-N.

6.4 CONCLUSIONS

GC-IMS provides the possibility to correlate different reactors design in terms of VOCs degradation, pH, TS and VS and help assess bioprocesses performances. The GC-IMS method that was established was able to identify several compounds from different functional groups such as terpenes, acids, aromatics, ester, ketones, and alcohol. In the digestate, the p-cymene could come from compounds such as α-pinene, 2-carene, 3-carene or γ-terpinene.

Both reactors presented a good performance in general, however the PF (reactor 4 - last reactor) had a slight better performance than the CSTR, especially to degrade terpenes. The acid phase present in reactor 1 would likely inhibit methanogens in the first reactor but the pH was raised following the other plug flow reactors. The PF design and operation could enable a more effective degradation of certain compounds.

Whilst the CSTR reactors had a more neutral pH. It is possible that if a higher OLR was used to operate the lab reactors that the PF reactor could have shown further increased performance. In addition to identification of process performance and potential odours for feedstocks or digestates, these measurements could enable microbial pathways and degradation profiles in the various reactors to be evaluated and help establish an in-depth understanding of the bioprocesses performance. In addition, some of these compounds, more specifically the ones that are intermediates in PF reactors 1-3 could potentially be studied for potential recovery as they could provide significant economic value and contribute to biorefining concepts within a circular economy.

7. GC-IMS CHEMICAL FINGERPRINTING OF ENVIRONMENTAL SAMPLES

7.1 INTRODUCTION

Environmental Regulators are becoming increasingly aware of the potential risks associated with the storage and utilisation of complex organic matrices (Lin *et al.*, 2013; Saveyn and Eder, 2014; Wang, 2014). Cases of pollution incidents attributed to AD plants are now being reported in the literature (NRW, 2017; Studer *et al.*, 2017), and the agricultural utilisation of untreated organic wastes such as slurries, crop residues, FW, abattoir waste, farmyard manure as well as residues from a range of waste management processes also represent a potential source of pollution if not managed appropriately (Holm-Nielsen *et al.*, 2009; Li *et al.*, 2018). The work presented here related to the use of GC-IMS for chemical fingerprinting of AD process samples and environmental samples provided by a number of AD plants at times where acidental spills or pollution incidents in the close neighbourhood were taking place and also to be able to demonstrate the ability for the tool to recognise different chemical fingerprinting.

7.2 MATERIAL AND METHODS

The study presents four 'real world' case studies. In Case Studies 1, 2 and 3 the technique was applied to differentiate between a number of potential organic contaminants present on agricultural and industrial sites with the aim of identifying point sources of releases. In Case Study 4, GC-IMS was used to determine whether the technique could differentiate between different organic mixtures at different points within a treatment process with results potentially being applicable to process optimization as well as being able to identify specific materials if released to the environment.

Data generated by GC-IMS was in the form of a three-dimensional plot. Identifying visually minor differences in these plots across numerous samples, which may even relate to low concentrations of potential contaminants in environmental samples, is labour intensive and subject to human error. As such, the aim of this study was to demonstrate the application of Self Organising Maps (SOM) to support the clustering and therefore of similarity of fingerprints identified by GC-IMS. SOM is a type of artificial neural network, which can be trained using unsupervised learning to create low-dimensional views of high dimensional data (Céréghino and Park, 2009; Heikkinen *et al.*, 2011; Liukkonen *et al.*, 2013; Sharif *et al.*, 2015) for the analysis of environmental

samples. The function of differentiating between complex organic substrates commonly found in agricultural and industrial settings and the possibility of generating a “fingerprint” for each material then raises the potential to trace point source or diffuse contaminants to specific sources.

7.2.1 Samples

7.2.1.1 Description of Case Study 1

The site comprised of an AD plant located in a rural location designated as a Special Landscape Area. The site was mixed-use and included a dairy farm and a waste management business including AD and aggregate recycling operations. Adjacent land use was dominated by agricultural fields although occasional residential properties were located within 1 km of the site with a large village located approximately 2 km away. There were no major watercourses present near the site although there were many surface water drainage ditches, and the site geology comprised of a sandstone aquifer. The AD plant treated imported FW (Animal by Products), animal slurry from the dairy farm (S1 & S2), and maize silage. The animal slurry (S1 & S2) was piped to the plant and treated digestate (S5 &S6) was stored within an open lagoon. After a brown ‘organic’ liquid (S15 & S16) was identified escaping from the ground surface at the base of an embankment site operators required a rapid characterization of the liquid, in particular, to identify whether the material predominantly comprised of digestate (S5 & S6) or animal slurry (S1 & S2) as this would direct the remedial options required to limit environmental impact.

7.2.1.2 Description of Case Study 2

This case study was based on a ‘real world’ situation at an AD plant in a small industrial estate developed in a broadly rural setting with adjacent site uses including a poultry farm, a council-run gritting yard, and a waste transfer station. Residential properties and a drinking water reservoir were located within 1 km of the site. The main feedstocks utilised in the AD plant were maize (S31 & S32) and ryegrass silage (S39 & S40), FW, chicken litter, dairy waste, and glycerol, although only maize (S31 & S32) and ryegrass (S39 & S40) silage were stored on-site in significant volumes prior to digestion. The site also included a septic tank for sewage storage (S19 &S20).

An unidentified organic liquid contaminant was located within a site drainage trench (S21 & S22). Other samples were also analyzed to discount other potential sources (e.g. petrol

interceptor – S35 & S36) and to characterize clean and contaminated soils on site (S23 to S30). The site owner had previously identified deficiencies related to the site drainage systems, in particular for surface water and leachate drainage (S17 &S18), and therefore a sample was also recovered from an inspection chamber within the drainage system (S33 & S34).

7.2.1.3 Description of Case Study 3

The site comprised of an AD plant fed with maize silage, grass silage, animal slurry, and chicken litter. The plant was located adjacent to several commercial buildings including a small distillery and commercial premises that had been developed within the confines of an operational arable farm. The area surrounding the site was rural in nature. The nearest residential property was a farmhouse located approximately 100 m to the south of the AD plant. Maize silage was stored on-site in silage clamps with leachate generated within the clamps draining via below ground pipes to a collection tank (S47 & S48). Other potential sources of contamination located on the site included a storage pond (S49 & S50), holding surface water from other areas of the site, and a soakaway pond (S51 & S52). Digestate (S53 & S54) was stored in a number of lagoons located adjacent and to the north of the digesters. Shallow groundwater contaminated with organic material (S43 & S44) was found to be issuing from the surface of the site at one specific location, however, the source of contamination was unknown. Site operators suspected a problem with the site drainage infrastructure, and therefore samples were recovered from a number of points along the drainage system (such as drains (S55 & S56; S61 & S62), lagoon (S57 & S58; S59 & S60; S67 & S68), a spill tank (S65 & S66) and a pond (S63 & S64)).

7.2.1.4 Description of Case Study 4

In this case study, GC-IMS was used to differentiate between sewage sludge at different points within a sludge treatment process. As with previous case studies, results could be used to identify the origin of pollutants in the event of a release to the environment. In addition, this case study also demonstrated that the analytical technique could be used to influence operational process decisions and as such could be applied to other industrial sectors in which the processing of organic substrates was critical (e.g. waste treatment, food production).

The site comprised of a municipal wastewater treatment plant. Primary and secondary sewage sludge generated at the site is treated using AD following pre-treatment by

thermal hydrolysis. Sewage sludge was imported from other smaller satellite treatment plants for centralised treatment. Sludge samples were recovered from a sampling port prior to digestion (post thermal hydrolysis – S69, S70 & S71) and post AD (S72, S73 & S74).

7.2.1.5 Summary of Case Study Samples Recovered

A total of 36 samples from the four case study locations were analyzed (Table 38). Samples were divided into two for reproducibility testing except for Case Study 4 where samples were divided into three subsamples. Between receiving the sample and analysis some preparation steps were necessary. Most samples were diluted with deionized water to reduce contaminant concentrations to within the window of detection of the GC-IMS instrument. In case study 1 and 2 where liquid organic contaminants were interacting with site soils the influence of soil/liquid mixture was also investigated by creating a new sample where clean site soil was added to the liquid contaminant of interest (e.g. cow slurry, crop leachate) and compared with the results for the liquid sample alone.

Table 38. Summary of the samples label and their sample preparation

Case Study	Simplified Filename	Sample preparation	Type of sample
1	S1 & S2	Cow slurry (CS) diluted in a ratio of 1:2	50% CS + 50% DI water
1	S3 & S4	Digestate after pasteurization (DAP) diluted in a ratio of 1:2	50% DAP + 50% DI water
1	S5 & S6	Second digestate (SD) diluted in a ratio of 1:2	50% SD + 50% DI water
1	S7 & S8	Cow slurry diluted 1:2 and added to the soil	25% CS + 25% DI water + 50% clean soil
1	S9 & S10	Mix soil diluted 1:2	50% clean soil + 50% DI water
1	S11 & S12	Digestate after pasteurization diluted 1:2 and add to the soil	25% DAP + 25% DI water + 50% clean soil
1	S13 & S14	Second digestate diluted 1:2 and added to the soil	25% SD + 25% DI water + 50% clean soil
1	S15 & S16	No sample preparation was required	100% contaminated sample
2	S17 & S18	No sample preparation was required	100% combined leachate
2	S19 & S20	No sample preparation was required	100% sewage

Continuation Table 38. Summary of the samples label and their sample preparation

Case Study	Simplified Filename	Sample preparation	Type of sample
2	S21 & S22	Sample diluted in a ratio of 1:50, to confirm sewage was not present in the sample	100% diluted trench
2	S23 & S24	Leachate was add to the soil	50% combined leachate + 50% clean soil
2	S25 & S26	Sewage was added to the soil	50% sewage + 50% clean soil
2	S27 & S28	Mix soil with DI water	50% DI water + 50% clean soil
2	S29 & S30	Trench content added to the soil	50% trench + 50% clean soil
2	S31 & S32	No sample preparation was required	100% maize leachate
2	S33 & S34	No sample preparation was required	100% manhole S4
2	S35 & S36	No sample preparation was required	100% petrol interceptor
2	S37 & S38	No sample preparation was required	100% pond outlet
2	S39 & S40	No sample preparation was required	100% rye leachate
3	S41 & S42	No sample preparation was required	100% Clean Soil
3	S43 & S44	No sample preparation was required	100% rising water sample through the soil
3	S45 & S46	No sample preparation was required	100% Contaminated soil
3	S47 & S48	No sample preparation was required	100% spill tank underground
3	S49 & S50	No sample preparation was required	100% pond which is holding the dirty water
3	S51 & S52	No sample preparation was required	100% soak away pond
3	S53 & S54	No sample preparation was required	100% digestate
3	S55 & S56	No sample preparation was required	100% drain at the back of clamps
3	S57 & S58	No sample preparation was required	100% lagoon tank
3	S59 & S60	No sample preparation was required	100% top of the lagoon
3	S61 & S62	No sample preparation was required	100% spillway drain
3	S63 & S64	No sample preparation was required	100% pond
3	S65 & S66	No sample preparation was required	100% spill tank
3	S67 & S68	No sample preparation was required	100% soil from lagoon tank

Continuation Table38. Summary of the samples label and their sample preparation

Case Study	Simplified Filename	Sample preparation	Type of sample
4	S69, S70 & S71	Before treatment diluted in a ratio of 1:10	10% Before Treatment + 90% DI water
4	S72, S73 & S74	After treatment diluted in a ratio of 1:10	10% After Treatment (Digestate) + 90% DI water

7.2.2 Analytical method

All measurements were undertaken using the GC-IMS method using the experimental setup B5. A SOM was used as the data processing tool to produce a low dimensional representation of the larger original input space (Kohonen, 1982). The SOM used was coded within the MATLAB SOM toolbox (MathWorks®, UK) and the SOM specification was performed by a colleague. The said one dimensional SOM network was trained upon input vectors, which were selected from a user-specified region or window of the original GC-IMS data for the chosen samples.

This had the advantage of reducing the original data size of each liquid and soil sample which had over 20 x 10^6 data points to about 4.6 x 10^6 which represented circa 23% of the original sample population. The said selected region covered a “Retention Time” span of 0 to 600 seconds with the corresponding “Drift Time” range of between 6.2 milliseconds until 17 milliseconds. This chosen pocket of data is where the main changes in the contour characteristics occurred between the different samples.

A hard-limiting threshold of 0.12 which was derived based upon past knowledge to remove background noise and the uneven baseline, which was subsequently applied to convert these 4.6 x 10^6 data points into zeros and ones (values equal to or greater than 0.12 is 1, all else was 0) for all the sample sets. The conversion of the variable data from 0-4 Volts to a binary set (0 and 1), was defined in order to minimise the impact of potential dilutions in the environment (with clean effluents, rainfall or clean soils) by specifying that any value above 0.12 would correspond to a 1.

The results were a collection of large binary input vectors, each representing a single sample, which was used as the training vectors for the chosen SOM network. The binary plots of case study 1 were from 16 samples (S1 until S16), 24 samples for case study 2 (S17 until S40) and for case study 3, 28 samples (S41 until S68) were utilised all with a threshold of 0.12 and converted to binary sets. Fifteen neurons and 1000 iterations were

the constants used by all the 3 individual SOM networks. The number of neurons was found sufficient to provide the number of classifications required for all 3 case studies, and any further increase in the number of iterations did not yield any change in the classification.

7.3 RESULTS AND DISCUSSION

7.3.1 Case Study 1

In this case study, the aim was to identify the most likely source of contamination based on analysis of source materials including digestate (S3 & S4 and S5 & S6) and cow slurry (S1 & S2). Figure 60 A presents a gallery plot for all samples analysed. Comparing all samples, it was clear that cow slurry presented a different chemical signature from digestate or digestate after pasteurization and it was, therefore, possible to conclude the contaminated sample (S15 & S16) was more like cow slurry than digestates.

However, the contaminant sample exhibited a dilution effect because the intensity of the peaks were not as strong as in the cow slurry sample. The contamination sample was so dilute that it was exhibiting some similarities with clean site soil (Peak No. 2, Figure 60 A, S9 & S10). Figure 61 A is an excerpt from the instrument output that clearly identified the same peak (peak No.1) in both cow slurry (S1 & S2) and the contaminated sample (S15 & S16), whilst the peak was not present in either of the digestate samples (S3 & S4 and S5 & S6).

This work identified that the source of the contamination could be related to cow slurry (S1 & S2) or another matrix not sampled but it was not related to the digestate (S3 & S4 and S5 & S6). On this basis, the site operator did not emptied the digestate lagoon as the environmental release was not associated with this source. Based on these analyses, the operator was able to rapidly undertake an appropriate investigation and remedial works to stop the continued release of material.

7.3.2 Case Study 2

The aim of this case study was to identify the source of organic contamination identified within an on-site drainage trench (S21 & S22). Likely sources included sewage (S19 & S20, potentially from a septic tank), runoff/combine leachate from a maize crop and rye clamp (S17 & S18) or from a combination of both. Figure 60 B presents a LAV generated gallery plot for all 32 samples analysed for case study 2. Using peaks No. 2 until peak

No.18, it was possible to see that the results from the trench (S21 & S22) were very similar to those for combined Leachate (S17 & S18) and that the compounds that were present in Sewage (S19 & S20), (Peaks No. 30, 31 and 32, Figure 60 B) were not present in combined Leachate (S17 & S18) or Trench (S21 & S22).

The results therefore strongly suggested that the main source of contamination of water within the Trench (S21 & S22) was the combined leachate (S17 & S18). The result was common across both sub-samples of the original sample (i.e. was analytically repeatable). Differences across sample types (sewage, combine leachate and trench) also remained evident when liquid samples were mixed with clean site soils. Figure 61 B proved that Trench (S21 & S22) without any dilution and diluted 50 times did not have the same chemical signature as Sewage (S19 & S20). I was possible to categorically exclude Sewage (S19 & S20) as a source of contamination in the Trench (S21 & S22).

Clean soil with deionised water (S27 & S28) did not present any chemical signatures, such as petrol interceptor (S35 & S36) or pond outlet (S37 & S38). This suggested that no type of VOC contaminants were present in these samples. Manhole S4 sample (S33 & S34) had only 6 relevant peaks and peak No. 28 and 29 could be used as a fingerprint to differentiate it from other samples. Maize Leachate (S31 & S32) and Rye Leachate (S39 & S40) presented similar peaks to the Trench (S21 & S22). Defining a unique indicator was more challenging. However, for Rye Leachate (S39 & S40) peaks No 26 and 27 could be used as unique identifiers.

7.3.3 Case Study 3

The aim of this case study was to determine if GC-IMS could be used to identify the source of pollution within shallow groundwater that was rising to the surface of the site. This was particularly challenging due to the number of potential sources on-site, and the amount of dilution that was associated with the shallow groundwater. The first clear result was that there was a difference in the profiles for Clean Soil (S41 & S42) and Contaminated Soil (S45 & S46), which suggested that pollutants were indeed present within the Contaminated Soil sample (Fig. 60 C).

Profiles are shown in Figure 60 C for contaminated soil (S45 & S46), rising water sample (S43 & S44), spill tank underground (S47 & S48) and a pond with dirty water (S49 & S50) were similar, with a degree of difference brought from dilutions (rainwater / soil). Peaks between No. 1 to No.12 were common between these samples. Drain at the back of clamps (S55 & S56) and spill tank (S65 & S66) had almost the same profile (Fig. 60

C), which correlated with the function of a spill tank and the movement of material from the drain to the tank (i.e. it was the same material).

Digestate was stored on-site in significant volumes and as such, this was also sampled and analysed to determine whether this might be responsible, or partially responsible, for the contamination present within rising groundwater. However, as shown in Figure 60 C, digestate had a very specific profile and the peaks detected were not present in contaminated soil or water rising through the soil (Fig. 60 C). Peaks that can be used as a fingerprint for digestate included peaks No. 30, 31, 32 and 33. It was therefore concluded that digestate was not the source of contamination.

Figure 60 C also shows that profiles for soak away pond (S51 & S52), lagoon tank (S57 & S58), top of the lagoon (S59 & S60), spillway drain (S61 & S62), pond (S63 & S64) and the soil from lagoon tank (S67 & S68) were similar to clean soil (S41 & S42), which was not contaminated with volatile organic material. As such it was considered very unlikely that any of these sample points represented the source of contamination. This approach suggested the contamination was a result of a problem with the site drainage system, specifically the part that is associated with the collection of runoff from the clamps and then the movement and storage of this material in below-ground tanks.

7.3.4 Case Study 4

This case study attempted to further demonstrate how GC-IMS might be used to differentiate between complex organic mixtures (in this case sewage sludge) at different stages of a treatment process. Figure 60 D presented the results of samples recovered before and after treatment by AD. Results showed that the first peak was common in both samples. However, significant differences were clear between the two samples.

Peak No. 2 until 11 could be used as a fingerprint for sewage sludge prior to AD (S69, S70 & S71) and peaks No. 18 to 22 for digestate (S72, S73 & S74) after AD. With such clear differences evident between the two samples, these chemical signatures could readily be used for the identification of the origin of any unintended release from the process. Further research to identify individual compounds in each would provide powerful data that could inform the enhanced operation of the treatment process.

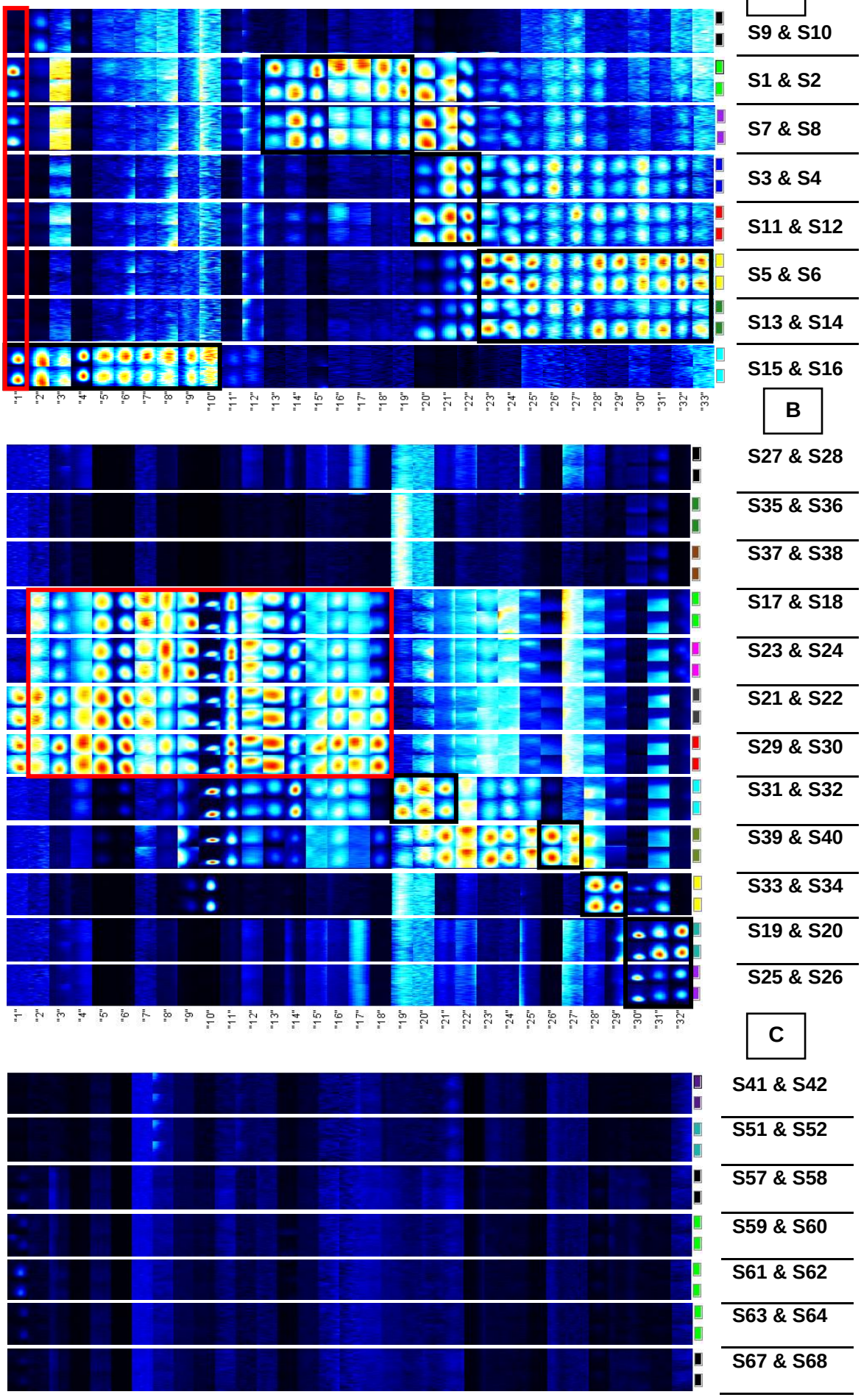
A
S9 & S10
S1 & S2
S7 & S8
S3 & S4
S11 & S12
S5 & S6
S13 & S14
S15 & S16
B
S27 & S28
S35 & S36
S37 & S38
S17 & S18
S23 & S24
S21 & S22
S29 & S30
S31 & S32
S39 & S40
S33 & S34
S19 & S20
S25 & S26
C
S41 & S42
S51 & S52
S57 & S58
S59 & S60
S61 & S62
S63 & S64
S67 & S68

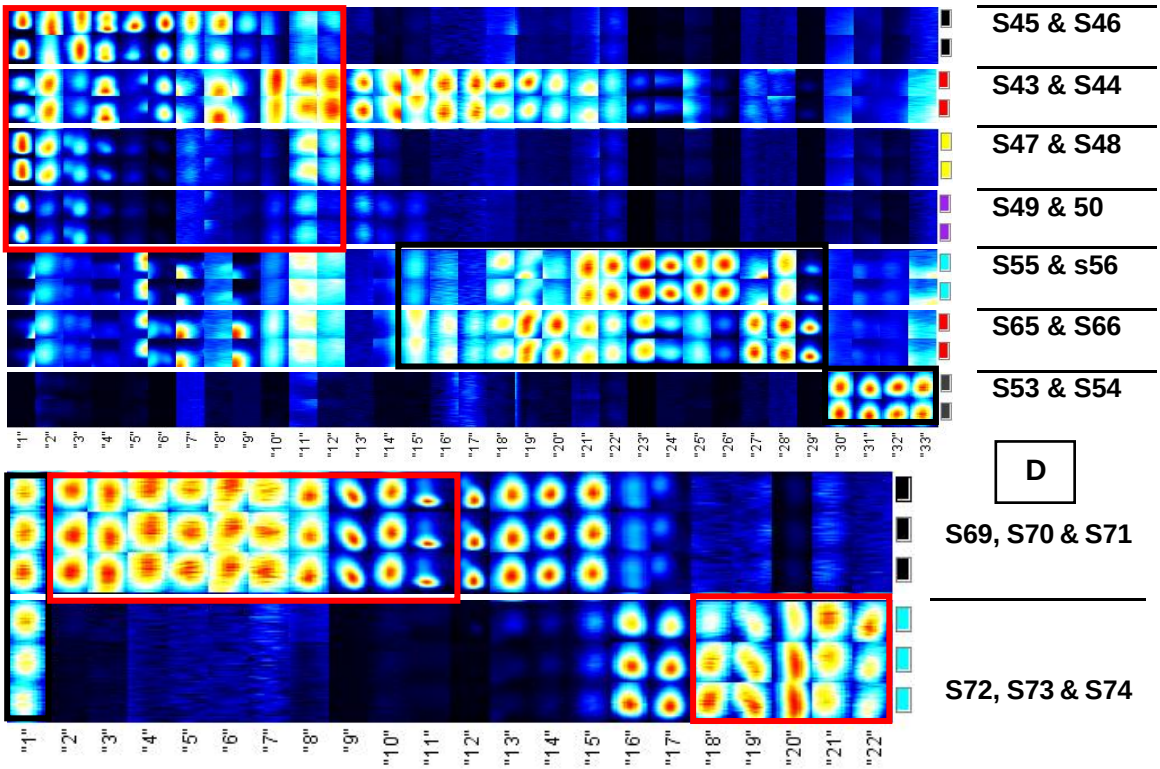

Figure 60: Gallery plot for case study 1 (A), gallery plot for case study 2 (B), gallery plot for case study 3 (C), gallery plot for case study 4 (D)

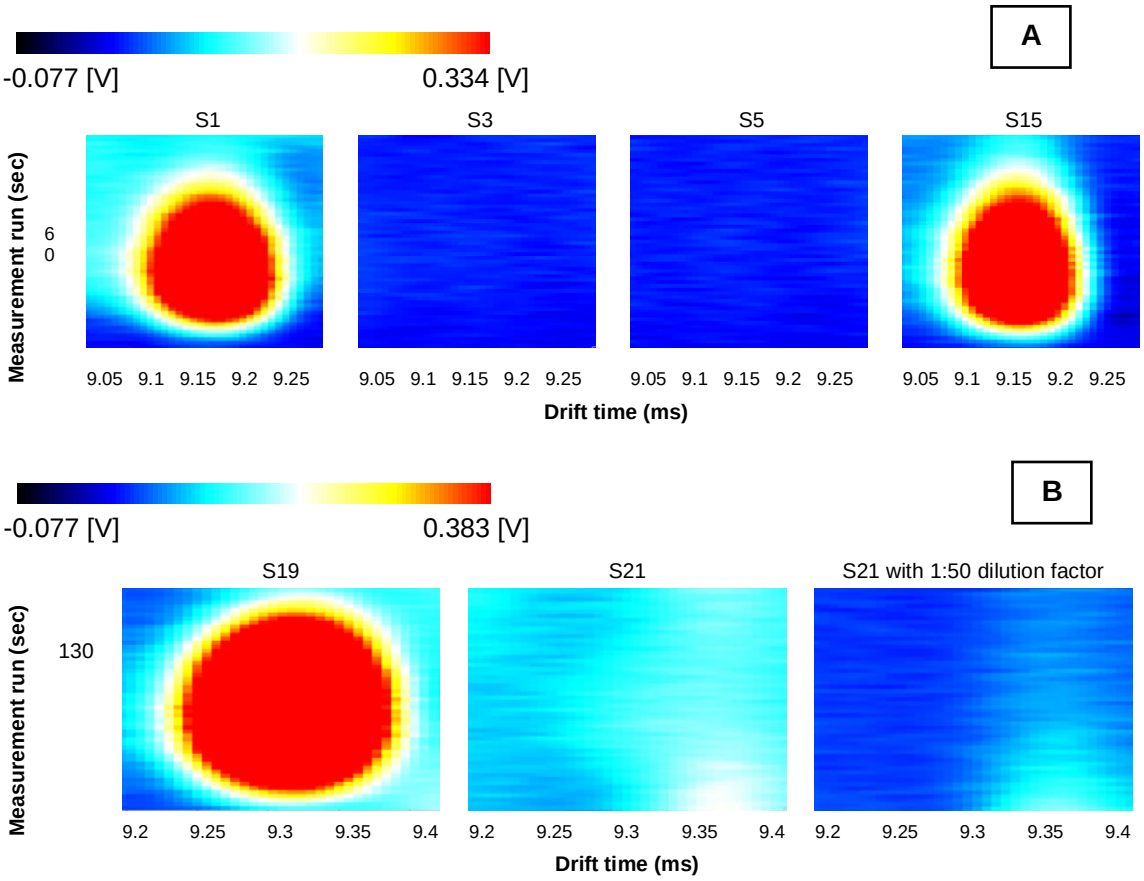

Figure 61: Confirmation the source of contamination (S15), in case study 1, was cow slurry (S1) (A), Confirmation sewage was not present in the trench sample and diluted trench sample (using 1:50 as dilution factor) (B).

7.3.5 SOM Results

Several chemometrics methods, such as PCA or PLS-R, were reviewd in the literature review, but SOM was employed instead in this work for visual image processing. The reason for choosing SOM over PCA was that the PCA given in the manufacturer's software package was a very basic tool, and other PCA toolboxes available did not support 2D data structures, and SOM implementation was simpler. Another reason for selecting SOM was the difficulties in transferring million data points to a Matlab tool (PCA) because SOM can convert data density more easily. SOM has shown to be a useful tool in image analysis, pattern recognition, chemical process monitoring, process control, and fault diagnosis as Nikhil *et al.* (2008) stated. (Nikhil et al., 2008)

Whilst in scenarios such as these case studies where contaminated samples would likely be generated from a site where only a narrow selection of organic pollutants exist, visualisation from the gallery plots could suffice to enable the identification of the source of pollution. However, if the analytical technique alone was applied to a larger number of samples in a regional or national context of environmental pollution, the ability of regulatory agencies' officers to identify the contaminants and specify potential sources rapidly and with a satisfactory degree of accuracy would be difficult.

In order to achieve this level of functionality, the paper evaluated the coupling of the SOM tool with GC-IMS, where it was hoped that pattern recognition and classification would help identify the source rapidly. Even in cases whereby the data may not be able to provide a conclusive outcome about the source of contamination present, it would likely be able to exclude some potential sources enabling faster and more effective investigative work to be targeted by not wasting efforts in non-relevant areas. Figure 62, 63, and 64 show the outputs of the SOMs developed for the first 3 case studies. It is worth confirming that each of the networks was trained separately and therefore the firing of neurons for each of the case studies is only relevant to that case study and should not be compared across case studies.

For case study 1 the contaminated samples (S15 & S16) were diluted at the site by rainwater and soil as the sample was collected from a pool of water in the soil. These were classified by neuron 1, which is closer to neurons 2 and 3 (clean soils and water – S9 & S10), followed by neurons 5 and 6 for cow slurry (S1 & S2), whilst other potential sources of contamination such as the digestates fired more distant neurons. This information was passed to the operator, who was able to identify that the contaminated sample was potentially coming from a pipe transporting cow slurry, which was situated

just below the digestate lagoon. If this information was not available to the plant operator, a first remediation action would have been to empty a very large digestate lagoon thinking that this was the source of pollution. Using the information generated, a minor intervention to decommission an old slurry transportation pipeline was instead identified as the correct course of action.

For case study 2, neuron 2 fired for the contaminated sample (trench – S21 & S22), which sits in between mixed leachate (S17 & S18) and mixed leachate with soil (S23 & S24), (both classified by neuron 1) and rye leachate (S39 & S40) (classified by neuron 3), and only afterwards by neuron 4, which classified maize leachate chemical characteristics. Passing this information to the operator, then the crop clamps were emptied, evaluated and appropriately leak proofed to prevent a future release of leachate to the environment.

For case study 3, the contaminated samples (raising water – S43 & S44) fired neurons 3 and 4, which were close to contaminated soil (S45 &S46) (neuron 5) and the underground spill tank (S47 & S48) (neuron 2) followed by the samples collected from the drain at the back of the clamps (S55 & S56) which carried leachate from the maize silage clamp. Passing this information to the operator, the drainage systems were re-engineered so that they did not lead to unwanted drainage to the spill tank and as a consequence avoiding the spill tank from leaking out and resulting in an ongoing pollution incident.

Case study 4 showed the effectiveness of GC-IMS in establishing the different chemical nature of the samples. Microbial degradation changes the chemical composition of a material. With samples sourced from environmental receptors, not only dilutions with soil and water will likely to play a role. Microbial degradation in soils and water streams for materials that may be stagnant for a few hrs or even days, will also likely to change the chemical nature of the various matrices. It would be of value for AD plants to catalogue a GC-IMS fingerprint of the various samples: a) feedstocks, intermediates and digestates; b) soils and water streams from around the site; c) land banks where digestate are spread; d) mixtures of these samples prepared in the laboratory. In addition material samples aging as well as forced degradations between feedstocks and digestates with site soils would also be useful. These would provide a wide characterisation of the various possible matrices. Any potential spillage or unintended release of material to the environment would then be easy to identify the source rapidly and effectively. Demonstrating environmental compliance is critical for AD plants as they operate based on meeting environmental permit conditions, however numerous other

industries and agriculture also discharge samples to the environment based on planned and incidental discharges. It is therefore important that AD plants protect their operations and environmental credentials by cataloguing their various samples matrices and related chemical characteristics.

An environmental regulator could utilise a GC-IMS based tool to establish the source of contaminants if a database was built of a wide range of possible pollutants. The analytical tool could travel to site for a quick diagnosis. The analysis would take minutes and decision making could be supported by an AI based clustering tool. The SOM network was appropriate for the number of samples that were part of these case studies, however it will likely to lose ability when the number of samples and characteristics increase. A tool such as deep learning could potentially provide the necessary function for a much wider/complex database (encompassing various sector type of potential discharges).

7.4 CONCLUSIONS

For the waste processing sites operators, the approach enabled rapid identification of the cause of the pollution, allowed timely remedial measures to be implemented, resulted in the improved engineering of the facilities, and ultimately demonstrates a pro-active approach to regulators in terms of pollution management. For regulators, in addition to enhanced environmental protection, the approach enabled an understanding of possible fragile components/stages in these facilities for which guidance could be improved for future design and operational improvements in AD plants. In a quest by the AD industry to demonstrate evidence of compliance, best practice and environmental protection, such a tool could be used by operators routinely for evidence gathering and for protection against potential claims or liabilities for other contamination not attributable to their plants. The development of a more globalised tool with a greater number of organic pollutants fingerprinted using GC-IMS and classified by a robust artificial intelligence (AI), the SOM, based tool in readiness of any future environmental pollution incidents would only require the time of sample collection for contaminated samples. Their analysis as well as their validation on the AI-based classifier, all of which could be achieved in less than 30 minutes. This globalised tool could enable the regulators to act more promptly in terms of stopping pollution incidents, but also allow the identification of sources of both point source and diffused pollution for a fairer approach to penalties.

Case Study 1: Samples		Firing Neuron (1 Dimension – Total of 15) After 1000 Iterations
		N1 N2 N3 N4 N5 N6 N7 N8 N9 N10 N11 N12 N13 N14 N15
50% cow slurry (CS) + 50% DI water	S1	
50% cow slurry (CS) + 50% DI water	S2	
50% digestate after pasteurization (DAP) + 50% DI water	S3	
50% digestate after pasteurization (DAP) + 50% DI water	S4	
50% second digestate (SD) + 50% DI water	S5	
50% second digestate (SD) + 50% DI water	S6	
25% CS + 25% DI water + 50% clean soil	S7	
25% CS + 25% DI water + 50% clean soil	S8	
50% clean soil + 50% DI water	S9	
50% clean soil + 50% DI water	S10	
25% DAP + 25% DI water + 50% clean soil	S11	
25% DAP + 25% DI water + 50% clean soil	S12	
25% SD + 25% DI water + 50% clean soil	S13	
25% SD + 25% DI water + 50% clean soil	S14	
100% contaminated sample	S15	
100% contaminated sample	S16	

Figure 62 SOM results for case study 1

Case Study 2: Samples		Firing Neuron (1 Dimension – Total of 15) After 1000 Iterations														
		N1	N2	N3	N4	N5	N6	N7	N8	N9	N10	N11	N12	N13	N14	N15
100% leachate	S17	•														
100% leachate	S18	•														
100% sewage	S19									•						
100% sewage	S20													•		
100% trench	S21		•													
100% trench	S22		•													
50% leachate + 50% clean soil	S23	•														
50% leachate + 50% clean soil	S24	•														
50% sewage + 50% clean soil	S25										•					
50% sewage + 50% clean soil	S26											•				
50% deionised water (DI) + 50% clean soil	S27								•							
50% deionised water (DI) + 50% clean soil	S28							•								
50% trench + 50% clean soil	S29		•													
50% trench + 50% clean soil	S30		•													
100% maize leachate	S31				•											
100% maize leachate	S32				•											
100% manhole S4	S33						•									
100% manhole S4	S34						•									
100% petrol interceptor	S35					•										
100% petrol interceptor	S36					•										
100% pond outlet	S37					•										
100% pond outlet	S38					•										
100% rye leachate	S39			•												
100% rye leachate	S40			•												

Figure 63 SOM results for case study 2

Case Study 3: Samples		Firing Neuron (1Dimension – Total of 15) After 1000 Iterations														
		N1	N2	N3	N4	N5	N6	N7	N8	N9	N10	N11	N12	N13	N14	N15
100% Clean Soil	S41						•									
100% Clean Soil	S42						•									
100% rising water sample through soil	S43			•												
100% rising water sample through soil	S44				•											
100% Contaminated soil	S45					•										
100% Contaminated soil	S46					•										
100% spill tank underground	S47								•							
100% spill tank underground	S48								•							
100% pond which is holding the dirty water	S49							•								
100% pond which is holding the dirty water	S50							•								
100% soak away pond	S51						•									
100% soak away pond	S52						•									
100% digestate	S53										•					
100% digestate	S54										•					
100% drain at the back of clamps	S55	•														
100% drain at the back of clamps	S56	•														
100% lagoon tank	S57														•	
100% lagoon tank	S58															•
100% top of the lagoon	S59													•		
100% top of the lagoon	S60												•			
100% spillway drain	S61												•			
100% spillway drain	S62												•			
100% pond	S63												•			
100% pond	S64												•			
100% spill tank	S65		•													
100% spill tank	S66		•													
100% soil from lagoon tank	S67											•				
100% soil from lagoon tank	S68											•				

Figure 64 SOM results for case study 3

8. OVERALL CONCLUSIONS AND FURTHER WORK

This research focused on important areas to promote the optimisation and environmental performance of AD. These included developing an analytical methodology for measuring VOCs i.e. typically associated with malodours and related to product intermediates within the AD process that could identify process operational concerns (e.g. VFAs and ammonia). The work evaluated the utilisation of GC-IMS as an aider to establish the efficiency of various AD designs and operations. The GC-IMS was also evaluated as a tool to identify the source of industrial and environmental contaminants in order to support rapid site remedial actions and support regulatory compliance; and at the same time was able to identify other sources of diffused pollution. The main conclusions from each chapter is presented underneath.

8.1 METHODOLOGY DEVELOPMENT FOR GC-IMS

As GC-IMS had not been used within the AD and biogas industry previously except for siloxane measurements in the biogas, methodological steps were developed to identify and quantify volatile compounds present within various matrices relevant to AD plants. The aim of the work was to identify the robustness and applicability of such as tool as a rapid and cost-effective method to optimise plant efficiencies and environmental performance. The GC-IMS was found to be able to analyse a broad AD matrices and type of samples i.e. gas, liquid or solid samples. The GC-IMS methodology took into consideration parameters such as headspace equilibrium time, the appropriate column type for targeted compounds, the column temperature, the flows for the carrier and drift gas, the dilution effect of samples (in order to avoid concentration overloads and enable minimum detection), optimal run times, and the appropriate use of blanks and of standards.

As stated in the introduction, a very polar column, such as a Nukol, would retain better polar molecules including alcohols, acids, ethers, esters, amines, and thiols. This aspect could explain the reason why no amines or mercaptans were discovered throughout the experiment. The column employed was a non-polar variety instead a polar type. Results found that placing one blank (fill with nitrogen gas) between samples was important to identify compound carryover and avoided cross-contamination between samples. Ketones were used to normalize the NIST library. AD samples are very complex and for that reason difficult to measure, so the method was designed to measure VOCs that are already in the gas phase and for that reason, an incubation temperature of 45°C was chosen. The method was able to be applied for a wide range of samples from feedstocks

to final products (digestates) with dilutions range from (no dilution; 1:10, 1:100). The equipment performance was evaluated by a repeatability study and an intermediate precision study, which established values lower than 5% in the repeatability study and lower than 7% in the intermediate precision study.

8.2 IDENTIFICATION AND QUANTIFICATION OF VOLATILE CHEMICALS USING GC-IMS

Merging an automated sampling with a GC separation and IMS detection provided a very efficient and robust VOCs profiling and fingerprinting of samples. The identification of compounds by GC-IMS was based on a dual separation of compounds that happened on the GC column and in drift region of the IMS. Therefore, each compound can be identified by two parameters the Rt and the dt. The dt is typically reported as K_0 or $1/K_0$. Different compounds were successfully identified using standards from different groups such as ketones, terpenes, aromatics, besides ammonia. Identification using the GC-IMS was performed for several chemicals, which were also identified by GC-MS. GC-IMS showed some limitations comparing with GC-MS where compounds with retention time above 4-methylphenol were not identified and this could be related to the fact that the maximum temperature that the analyser column operated was 80°C, whilst the GC-MS column went up to 200 – 300°C. GC-MS data showed that for an AD plant operating on food wastes and animal slurry, food waste as the feedstock was mostly constituted by ester from acids (e.g. propyl butyrate, ethyl valerate and limonene). Whilst the cow slurry highest intensity peak was 4-metylphenol and for digestate it was p-cymene.

Terpene compounds such as p-cymene or limonene were found within the digestate and biogas as reported by Arrhenius. An initial quantification was estimated using a 2^{nd} order polynomial equation for ammonia hydroxide, limonene, acetic acid, propionic acid, butyric acid, and several ketones. Limits of detection and quantification (LOD and LOQ) were calculated for VFAs using a linear equation getting values lower than 13 mg/L for LOD and 40 mg/L for LOQ. For ketones and limonene a Boltzmann function for calibration was explored with the nominal concentration found to be similar to the concentration calculated using the Boltzmann equation.

8.3 INFLUENCE OF AMMONIA ON GC-IMS MONITORING

One of the biggest challenges for the method development for AD related samples was the impact of ammonia particularly for digestate samples. The ammonia influence was studied on several compounds and it was observed that ammonia influenced the

ionization of terpenes and ketones by proton transfer while for aromatics by charge transfer. For ketones and terpenes ammonia created adduct products, whilst for aromatics the effect was different and did not create adduct products. This could be related to the fact that aromatics have an aromatic ring or could potentially be ionized differently. To avoid the ionization problem of ammonia and as part of the sample preparation, a salt ($NaHSO_4$) concentration was introduced. This salt was found not to affect the ionization of the targeted compounds: terpenes, ketones, aromatics. The $NaHSO_4$ proved to be effective in removing ammonia interference when the ammonia concentration was below 2.5 g/L. However, when the saturation point was achieved, the salt was no longer effective. A dilution of the sample should therefore be undertaken. Another advantage of introducing the salt in the sample was that the carry-over of ammonia stopped occurring and an improved method was achieved. If measurements of ammonia are required and are to be based on GC-IMS measurements, effective dilutions without salt addition would need to take place with an extended cleaning cycle to avoid ammonia carry over.

8.4 ONE-STAGE AND MULTI-STAGE REACTORS PERFORMANCE

The performance of one-stage reactor (the CSTR) compared with a multi-stage reactor (the plug-flow – simulated using 4 CSTRs in series) was studied when were fed with food waste and cow slurry. Cow slurry had in common with reactors samples the 2-butanone peak, whilst the PF – reactor 1 (A and B) was the most similar to the ABP sample with 8 compounds in common, mainly acids, terpenes and ester compounds. The PF reactor system proved to deliver a good performance. In the PF reactor compounds such as propyl hexanoate, γ-terpinene, hexanoic acid, β-pinene, α-pinene, 1-hexanol, propyl butanoate, and butanoic acid were degraded or converted to gas form or utilized by the microbial consortium because they were present in the first stage but no longer in the last stage i.e. reactor 4. For other compounds such as ethyl pentanoate or 2-heptanone or limonene, degradation reduced their intensity through the conversion process. Limonene reduced from 1500 µg/L in the feed mixture to less than 100 µg/L in all reactors. Benzaldehyde was produced during the process but was not present during the last reactor; however, compounds such as 2-butanone, pyridine, 2-pentanone, ethylbenzene, cyclohexanone were still present within the last stage of process.

The CSTR reactor delivered as well a good performance where compounds reduced their intensity such as limonene, γ-terpinene, β-pinene, ethyl pentanoate, butanoic acid, propyl hexanoate, hexanoic acid, benzaldeyde, and 1-hexanol, were present in small amounts and compounds such as α-pinene, propoyl butanoate, 2-butanone, pyridine, 2-

pentanone, ethylbenzene, cyclohexanone, 2-heptanone were still present at last stage and they were a by-product from the process. Another step in the process would be important to add to improve the degradation efficiency and to avoid the release of these compounds to the environment.

The duplicate reactors performed similarly with a good performance. The PF reactor system delivered a better performance especially for the degradation of terpenes as compared to the CSTR. It is possible that the advantage of the PF system over the one CSTR stage reactor would have been more beneficial in the case of reactors operating at a higher OLR. The GC-IMS tool could detect differences between feedstocks and final products and identified non degraded compounds and did help established the conversion performance of the two reactor systems. In addition to VFAs, limonene could be another indicator compound of the reactor performance for digesters that receive food wastes for treatment. However, it would be important to study if non-degraded terpenes would likely indicate a lack of treatment or if they could just be volatilised to the biogas (instead of being converted).

8.5 ENVIRONMENTAL SAMPLE CHEMICAL FINGERPRINT

The GC-IMS methodology developed has also been applied as a screening tool for a fast fingerprint analysis of environmental samples to distinguish between several potential organic pollutants. Such use of the GC-IMS tool could solve environmental problems promptly i.e. in hrs to one day; and avoid major pollution incidents. GC-IMS was the tool that determined that leachate was the main cause of contamination of the soil of two sites, and cow slurry in another. However, each GC-IMS analytical run created a complex and multi-dimensional data and comparing the data by direct visualization presented difficulties. Using just manual visualization, a complete interpretation of the GC-IMS results was a challenge for plot image processing. Using an artificial neural network, SOM as a classification tool helped to improve the data processing for GC-IMS results. The benefit would be even greater, if the contaminated sample had to be mapped across numerous potential equivalents. The use of such an automated classification tool would then become essential.

8.6 IMPORTANCE OF WORK CARRIED OUT AND STATEMENT OF CONTRIBUTION TO KNOWLEDGE

This PhD fits under the low carbon, energy, and the environment area namely, sustainable energy, food and farming, climate change, and resource efficiency topics.

Therefore, it is expected that this research will have an impact in the society and, in particular within the AD sector and associated fields of biotechnology, bioenergy and biorefining. Societies are looking for more sustainable options to replace fossil fuels and decrease the carbon footprint. This research addresses specific challenges in the AD and biogas industry as it monitors, quantifies and manages compounds over time (including odours) enabling an improved plant performance. Even GC-MS can detect more odours compounds as compared to GC-IMS, it is still beneficial to develop GC-IMS for a wider spread of compounds application. As was presented in Fig. 6, in the last ten years, publications under the topic GC-IMS had an increase.

A GC-IMS analyser can be a valuable tool for monitoring parameters in a short period of time, it can benefit and give advantages to the AD plants to understand how they should control their process *in-situ* and real-time. This methodology can change the way how AD plants and other plants could be monitored and operated, not just in the UK but internationally. As referred in the introduction, odours can have serious impacts to local communities close to waste management facilities such as AD plants, so having an analytical tool such as GC-IMS that allows understanding and control of this problem could bring benefits to local communities and plant operators. It is a novel application for GC-IMS, but this was found to be able to measure compounds (especially for odorous compounds) at lower concentrations and it could identify important intermediates and degradation performance. Even in the case of samples rich in ammonia, which would interfere in the ionization, a methodology was established that enabled the use of such as an analytical tool without introducing errors.

Another important contribution from this research was demonstrated in the ability of GC-IMS to be used for environmental samples fingerprinting. Distinguishing between several potential organic pollutants and avoiding pollution, fees or even prosecution and loss of permit to operate the plant. It was the first time that the instrument was applied for that purpose. Table 39 summarizes the five objectives for this research and where they were achieved within this thesis.

Table 39. Research objectives

OBJECTIVE	TASK IDENTIFICATION	ACHIEVEMENT OF THAT OBJECTIVE
Objective 1	Critical literature review (different methodologies to measure VOCs)	Chapter 2
Objective 2	Develop and test a methodology on GC-IMS for fingerprinting of chemical characteristics	Chapters 3, 4, 5 and 7

Objective 3	Identification and quantification of compounds using GC-IMS and investigate LOD and LOQ	Chapters 3, 4
Objective 4	Investigate the "fate" of VOCs in AD systems	Chapter 6
Objective 5	Monitoring process performance changes in different reactor configurations	Chapter 6

8.7 FURTHER WORK

Monitoring and control of AD plants is important to enable optimal operating conditions, ability to vary types of feedstocks and loading, enable robustness in treatment with greater solids conversion, enhanced biogas yields and avoidance of process inefficiencies, incidents related to potential leakages and complaints from neighbours due to odorous emissions. Real-time and multi-parameter monitoring including for difficult compounds and for some in very low concentrations will significantly help to overcome challenges in operation and environmental compliance. Improved environmental and financial performances are therefore expected, with the added benefit of these plants becoming more neighbour friendly. The GC-IMS analytical tool developed has showed great promise in delivering these improvements. The GC-IMS methodology developed has demonstrated ability to enable the establishment of the fate of volatiles through the biological process, a robust measurement of intermediates and final compounds, and the identification of the type and load of odorous compounds within the various samples as well as a useful technique for the establishment of contaminants and their sources when associated with a pattern modelling technique. Further work would however be beneficial to optimise the technique and test further its full scope for integration with biotechnology processes. Some of the recommendations for further work are explained below.

8.7.1 Methodology development for GC-IMS

The SE-54 column used in this work is a generic column that was able to provide a wide arrange of analytes of worth consideration for this work. Other columns could also be investigated in order to enable detection or improved accuracy of other compounds and more specific columns in the case of interest in defined compounds. For example, in the case of wanting to target the monitoring of VFAs, a wax or a Carbowax or FFAP (Free Fatty Acid Phase) columns or others with a very polar phase would likely to be more beneficial in order to avoid derivatization of the sample. Other columns would likely enable the separation of different compounds and further optimisation of the methodologies may then be required when other columns are used and for measuring

other compounds. The current methodology relied on the usage of ketones as external standards and used once a day to enable measurement robustness and to support identification. The use of an internal standard could however enable improved accuracy, precision and robustness in the measurements; nevertheless, potential impacts and interferences would need to be evaluated in detail. If the tool was to be adopted for industrial analytical regular use, a cocktail mix of compounds of interest or from several functional groups could be tested post column regeneration.

8.7.2 Identification and quantification of volatile chemicals using GC-IMS

An accurate identification of compounds can be done by other analytical tools such as GC-MS or by using standards. For further developments, it would be important to extend the identification using analytical standards for the compounds identified currently only by the GC×IMS Library Search. To increase the database, it would be interesting to identify more compounds from other functional groups such as alcohols, alkanes, ethers, esters alkenes, mercaptans, or phenol by running these standards.

The methodology for quantification of compounds by GC-IMS is not a consensual topic. Therefore, it would be important to continue to evaluate quantification methodologies and establish the most appropriate one. This would allow to establish calibrations using for example just the dimer only or a combination of monomer/dimer or explore alternative chemometrics or statistical software to integrate the peaks. The manufacturer suggests using an exponential, logarithm or a Boltzmann equation to create the calibration curves and their technical note identifies the Boltzmann equation as the most suitable. The objective would be to find the best fit for the data and create a suitable mathematical equation and for this reason this approach should be consider in the future. To improve the calibrations an in depth evaluation of a selection of most suitable internal standards would be recommended.

8.7.3 Influence of ammonia on GC-IMS based monitoring

Whilst the addition of salt ($NaHSO_4$) was effective for samples rich in ammonia with a concentration lower than 2.5 g/L for functional groups such as terpenes, aromatics and ketones. The impact of ammonia on VFAs was only briefly evaluated and further work is still required. For other functional groups such as amines, alcohols and organic acids, there is still a need to conduct further evaluations as for some of these volatilisation may then be reduced by the addition of the salt. Other salts such as monosodium phosphate (NaH_2PO_4) or ammonium chloride (NH_4Cl) or ammonium sulphate ($(NH_4)_2SO_4$) or other

acids such as phosphoric acid (H_3PO_4) would aid volatilisation and should be further investigated for potential additions to halt the ionisation effect that ammonia has on specific compounds.

8.7.4 One-stage and multi-stage reactors performance

The present research compared the performance of a one-stage with a multi-stage reactor system and in general, both systems had a good performance to degrade food waste and cow slurry. The volatile compounds were measured using liquid samples from the reactors and the decrease in concentration from feedstock to digestate could be an outcome from an effective degradation. Some of these volatiles could have also not have been degraded, but have only been driven to the gas phase. One aspect that could be important to study in the future would be the compounds in the gas phase. This is particularly important for establishing and for reducing the levels of pollutants in the gas phase by enhancing degradation pathways to avoid pollutants in the exhaust gases from engines or reduce issues related to biogas upgrading for injection into the gas grid. Another aspect that may be worthwhile to consider is to remove limonene from feedstocks to avoid the product such as p-cymene, ethylbenzene, cyclohexanone that are produced through the degradation of limonene. This research was focused on food waste and cow slurry, however it would be interesting to study other types of organic materials such as energy crops, straw, sewage, sewage sludges and biopolymers.

8.7.5 Environmental samples fingerprinting

The GC-IMS analytical technique was successfully used to detect volatile compounds fingerprints for samples sourced from environmental receptors and for potential contaminant matrices. The detection was fast (approx. 10 mins per sample). For this objective, and considering only a relatively narrow sample range (adequate for an AD plant), the GC-IMS tool and the methodology devised together with the SOM classification tool was able to identify and compare between various spectra and was able to identify close similarities and indicate the potential source of contamination successfully that enabled remediation steps to be undertaken at the plants.

If the tool was to deliver a globalised environmental contaminant monitoring tool with all sorts of samples from a variety of industries, agriculture, road run-offs and others being able to be recognised by the diagnostic tool and used by environmental regulators, further work would be required. The work would likely entail a significant increase in diversity of samples analysed by GC-IMS associated with a more effective globalised

pattern recognition tool such as Deep Learning with a possibility for sub-classification AI based tools to be utilised. The benefits of such an approach would be a rapid fingerprinting of environmental contaminants and from a variety of matrices that would facilitate the identification of sources of environmental pollutants by regulators enabling the halting of discharges or accidental spillages of contaminants, ultimate improving environmental protection. For samples with a high degree of dilution e.g. in the case of water courses, an analyte concentration may be required with techniques such as SPME. For samples that may have been stagnant within soils for some time, degradation profiles may need to be considered as the chemical profile of the source of contamination may have been altered. If a full identification of the various volatile compounds and quantification were required, further work would need to be conducted by undertaking a series of analytical runs to match NIST labelled compounds and followed by a detailed calibration procedure.

8.7.6 Ways forward to integrate GC-IMS within AD, biogas and biorefining sectors and environmental protection

All the work performed was using an off-line operational system with dilutions prepared by the operator. It would be of great value to extend the specification of the GC-IMS analyser to be able to cope with real-time characterisation and identification, where accurate dilutions and a flowcell mechanism could be integrated. Although G.A.S has implemented a real-time system for GC-IMS-ODOR and GC-IMS-SILOX for a very narrow application with relevance to AD and biogas system; this work demonstrated that GC-IMS could be established as a multi-parameter monitoring tool for AD systems and even for environmental pollutant detection. For AD and biogas applications, the monitor could be placed at each AD plant and could integrate SCADA and supervisory monitoring and control systems with alarms and control actions taken to support plant optimisation and regulatory compliance. For aspects around environmental pollutant detection, portable units could be driven next to the pollution incident and support a rapid determination of the type and source of pollutant. The GC-IMS tool could enable the identification of bioprocess performance, odours, biogas and digestate quality. In more novel biorefining technological concepts, the GC-IMS could enable microbial pathways and degradation profiles in the various bioprocesses to be evaluated and would help establish an in-depth understanding of the bioprocesses performance, extraction or product refining quality enabling the design, operation, quality and regulatory verifications of biotechnology concepts within a circular economy.

9. REFERENCES

Aatamila, M., Verkasalo, P.K., Korhonen, M.J., Suominen, A.L., Hirvonen, M.-R., Viluksela, M.K., Nevalainen, A., 2011. Odour annoyance and physical symptoms among residents living near waste treatment centres. Environ. Res. 111, 164–170. https://doi.org/10.1016/j.envres.2010.11.008

ADBA, 2017. Anaerobic Digestion Market Report 2017.

ADBA, 2012. The Practical Guide to AD: First Edition.

Agapiou, A., Schmid, A., Amann, A., Mochalski, P.P., Schmid, A., Amann, A., 2013. Potential Applications of Volatile Organic Compounds in Safety and Security, in: Volatile Biomarkers. Elsevier, pp. 514–558. https://doi.org/10.1016/B978-0-44-462613-4.00024-6

Agency, S.E., 2015. PPC Technical Guidance Note 38 Anaerobic Digestion.

Aggarwal, P., Baker, J., Boyd, M.T., Coyle, S., Probert, C., Chapman, E.A., 2020. Optimisation of Urine Sample Preparation for Headspace-Solid Phase Microextraction Gas Chromatography-Mass Spectrometry: Altering Sample pH, Sulphuric Acid Concentration and Phase Ratio. Metabolites 10, 482. https://doi.org/10.3390/metabo10120482

Agler, M.T., Wrenn, B.A., Zinder, S.H., Angenent, L.T., 2011. Waste to bioproduct conversion with undefined mixed cultures: the carboxylate platform. Trends Biotechnol. 29, 70–78. https://doi.org/10.1016/j.tibtech.2010.11.006

Alvarado, A., Montanez-Hernandez, L.E., Palacio-Molina, S.L., Oropeza-Navarro, R., Luevanos-Escareno, M.P., Balagurusamy, N., 2014. Microbial trophic interactions and mcrA gene expression in monitoring of anaerobic digesters. Front. Microbiol. 5, 1–14. https://doi.org/10.3389/fmicb.2014.00597

Alvarenga, P., Mourinha, C., Farto, M., Santos, T., Palma, P., Sengo, J., Morais, M.-C., Cunha-Queda, C., 2015. Sewage sludge, compost and other representative organic wastes as agricultural soil amendments: Benefits versus limiting factors. Waste Manag. 40, 44–52. https://doi.org/10.1016/j.wasman.2015.01.027

Angenent, L.T., Karim, K., Al-Dahhan, M.H., Wrenn, B.A., Domíguez-Espinosa, R., 2004. Production of bioenergy and biochemicals from industrial and agricultural wastewater. Trends Biotechnol. 22, 477–485. https://doi.org/10.1016/j.tibtech.2004.07.001

Aouadi, B., Zaukuu, J.L.Z., Vitális, F., Bodor, Z., Fehér, O., Gillay, Z., Bazar, G., Kovacs, Z., 2020. Historical evolution and food control achievements of near infrared spectroscopy, electronic nose, and electronic tongue—critical overview. Sensors (Switzerland) 20, 1–42. https://doi.org/10.3390/s20195479

Appels, L., Baeyens, J., Degrève, J., Dewil, R., 2008. Principles and potential of the anaerobic digestion of waste-activated sludge. Prog. Energy Combust. Sci. 34, 755–781. https://doi.org/10.1016/j.pecs.2008.06.002

Arce, L., Valcarcel, M., 2013. The Role of Ion Mobility Spectrometry to Support the Food Protected Designation of Origin, in: Comprehensive Analytical Chemistry. Copyright © 2013 Elsevier B.V. All rights reserved., pp. 221–249. https://doi.org/10.1016/B978-0-444-59562-1.00009-8

Armenta, S., Alcala, M., Blanco, M., 2011. A review of recent, unconventional applications of ion mobility spectrometry (IMS). Anal. Chim. Acta 703, 114–123. https://doi.org/10.1016/j.aca.2011.07.021

Armenta, S., Blanco, M., 2011. Pros and cons of benzodiazepines screening in human saliva by ion mobility spectrometry. Anal. Bioanal. Chem. 401, 1935–1948. https://doi.org/10.1007/s00216-011-5267-x

Armenta, S., Esteve-Turrillas, A., Alcala, M., 2020. Analysis of hazardous chemicals by “stand alone” drift tube ion mobility spectrometry: A review. Anal. Methods. https://doi.org/10.1039/C9AY02268F

Armenta, S., Guardia, M. de la, Alcala, M., Blanco, M., Perez-Alfonso, C., Galipienso, N., 2014. Ion mobility spectrometry evaluation of cocaine occupational exposure in forensic laboratories. Talanta 130, 251–258. https://doi.org/10.1016/j.talanta.2014.06.044

Arrhenius, K., Engelbrektsson, J., Yaghooby, H., 2016. Development of Analytical Methods to Gain Insight into the Role of Terpenes in Biogas Plants. J. Anal. Bioanal. Tech. 7. https://doi.org/10.4172/2155-9872.1000324

Arroyo-Manzanares, N., García-Nicolás, M., Castell, A., Campillo, N., Viñas, P., López-García, I., Hernández-Córdoba, M., 2019. Untargeted headspace gas chromatography – Ion mobility spectrometry analysis for detection of adulterated honey. Talanta 205, 120123. https://doi.org/10.1016/j.talanta.2019.120123

Arroyo-Manzanares, N., Martín-Gómez, A., Jurado-Campos, N., Garrido-Delgado, R., Arce, C., Arce, L., 2018. Target vs spectral fingerprint data analysis of Iberian ham samples for avoiding labelling fraud using headspace – gas chromatography–ion mobility spectrometry. Food Chem. 246, 65–73. https://doi.org/10.1016/j.foodchem.2017.11.008

Babushok, V.I., Linstrom, P.J., Zenkevich, I.G., 2011. Retention Indices for Frequently Reported Compounds of Plant Essential Oils. J. Phys. Chem. Ref. Data 40, 043101. https://doi.org/10.1063/1.3653552

Baumbach, J.I., 2009. Ion mobility spectrometry coupled with multi-capillary columns for metabolic profiling of human breath. J. Breath Res. 3, 034001. https://doi.org/10.1088/1752-7155/3/3/034001

Baumbach, J.I., 2008. Ion mobility spectrometry in scientific literature and in the International Journal for Ion Mobility Spectrometry (1998–2007). Int. J. Ion Mobil. Spectrom. 11, 3–11. https://doi.org/10.1007/s12127-008-0009-2

Baumbach, J.I., 2006. Process analysis using ion mobility spectrometry. Anal. Bioanal. Chem. 384, 1059–1070. https://doi.org/10.1007/s00216-005-3397-8

Baumbach, J.I., Sielemann, S., Xie, Z., Schmidt, H., 2003. Detection of the gasoline components methyl tert-butyl ether, benzene, toluene, and m-xylene using ion mobility spectrometers with a radioactive and UV ionization source. Anal. Chem. 75, 1483–1490. https://doi.org/10.1021/ac020342i

Bhardwaja, S.K., Dwivedia, K., Agarwal, D.D., 2016. A Review: GC Method Development and validation. Int. J. Anal. Bioanal. Chem. 6, 1–7.

Blanes-Vidal, V., Hansen, M.N., Adamsen, A.P.S., Feilberg, A., Petersen, S.O., Jensen, B.B., 2009a. Characterization of odor released during handling of swine slurry: Part II. Effect of production type, storage and physicochemical characteristics of the slurry. Atmos. Environ. 43, 3006–3014. https://doi.org/10.1016/j.atmosenv.2009.01.046

Blanes-Vidal, V., Hansen, M.N., Adamsen, A.P.S., Feilberg, A., Petersen, S.O., Jensen, B.B., 2009b. Characterization of odor released during handling of swine slurry: Part I. Relationship between odorants and perceived odor concentrations. Atmos. Environ. 43, 2997–3005. https://doi.org/10.1016/j.atmosenv.2008.10.016

Blazy, V., de Guardia, A., Benoist, J.C., Daumoin, M., Guiziou, F., Lemasle, M., Wolbert, D., Barrington, S., 2015. Correlation of chemical composition and odor concentration for emissions from pig slaughterhouse sludge composting and storage. Chem. Eng. J. 276, 398–409. https://doi.org/10.1016/j.cej.2015.04.031

Bockreis, A., Steinberg, I., 2005. Measurement of odour with focus on sampling techniques. Waste Manag. 25, 859–863. https://doi.org/10.1016/j.wasman.2005.07.013

Bödeker, B., Vautz, W., Baumbach, J.I., 2008. Peak comparison in MCC/IMS-data—searching for potential biomarkers in human breath data. Int. J. Ion Mobil. Spectrom. 11, 89–93. https://doi.org/10.1007/s12127-008-0013-6

Boe, K., Batstone, D.J., Steyer, J.P., Angelidaki, I., 2010. State indicators for monitoring the anaerobic digestion process. Water Res. 44, 5973–5980. https://doi.org/10.1016/j.watres.2010.07.043

Boe, K., Steyer, J.P., Angelidaki, I., 2008. Monitoring and control of the biogas process based on propionate concentration using online VFA measurement. Water Sci. Technol. 57, 661–666.

https://doi.org/10.2166/wst.2008.046

Bonetta, Si., Ferretti, E., Bonetta, Sa, Fezia, G., Carraro, E., 2011. Microbiological contamination of digested products from anaerobic co-digestion of bovine manure and agricultural by-products. Lett. Appl. Microbiol. 53, 552–557. https://doi.org/10.1111/j.1472-765X.2011.03148.x

Borsdorf, H., Mayer, T., Zarejousheghani, M., Eiceman, G.A., 2011. Recent Developments in Ion Mobility Spectrometry. Appl. Spectrosc. Rev. 46, 472–521. https://doi.org/10.1080/05704928.2011.582658

Burlachenko, J., Kruglenko, I., Snopok, B., Persaud, K., 2016. Sample handling for electronic nose technology: State of the art and future trends. TrAC - Trends Anal. Chem. 82, 222–236. https://doi.org/10.1016/j.trac.2016.06.007

Camlin, 2020. BioSpec VOC [WWW Document]. URL https://www.camlingroup.com/product/biospecvoc/ (accessed 6.7.20).

Cavanna, D., Zanardi, S., Dall'Asta, C., Suman, M., 2019. Ion mobility spectrometry coupled to gas chromatography: A rapid tool to assess eggs freshness. Food Chem. 271, 691–696. https://doi.org/10.1016/j.foodchem.2018.07.204

Céréghino, R., Park, Y.-S., 2009. Review of the Self-Organizing Map (SOM) approach in water resources: Commentary. Environ. Model. Softw. 24, 945–947. https://doi.org/10.1016/j.envsoft.2009.01.008

Charnier, C., Latrille, E., Jimenez, J., Lemoine, M., Boulet, J.-C., Miroux, J., Steyer, J.-P., 2017. Fast characterization of solid organic waste content with near infrared spectroscopy in anaerobic digestion. Waste Manag. 59, 140–148. https://doi.org/10.1016/j.wasman.2016.10.029

Chen, C., Jiang, D., Li, H., 2019. UV photoionization ion mobility spectrometry: Fundamentals and applications. Anal. Chim. Acta 1077, 1–13. https://doi.org/10.1016/j.aca.2019.05.018

Chen, T., Chen, X., Lu, D., Chen, B., 2018. Detection of Adulteration in Canola Oil by Using GC-IMS and Chemometric Analysis. Int. J. Anal. Chem. 2018, 1–8. https://doi.org/10.1155/2018/3160265

Chen, Y., Cheng, J.J., Creamer, K.S., 2008. Inhibition of anaerobic digestion process: A review. Bioresour. Technol. 99, 4044–4064. https://doi.org/10.1016/j.biortech.2007.01.057

Cheng, S., Li, H.H., Jiang, D., Chen, C., Zhang, T., Li, Y., Wang, H., Zhou, Q., Li, H.H., Tan, M., 2017. Sensitive detection of trimethylamine based on dopant-assisted positive photoionization ion mobility spectrometry. Talanta 162, 398–402. https://doi.org/10.1016/j.talanta.2016.10.056

Chouinard, C.D., Wei, M.S., Beekman, C.R., Kemperman, R.H.J., Yost, R.A., 2016. Ion Mobility in Clinical Analysis: Current Progress and Future Perspectives. Clin. Chem. 62, 124–133. https://doi.org/10.1373/clinchem.2015.238840

Churchill, A., 2006. Measurement of fragrance perception, in: Pybus, D., Sell, C. (Eds.), The Chemistry of Fragrances from Perfume to Consumer 2nd Edition. Royal Society of Chemistry, Cambridge, pp. 151–167. https://doi.org/10.1039/9781847555342-00151

Clarivate, 2020. Web of Science [WWW Document]. URL http://apps.webofknowledge.com/RAMore.do?product=UA&search_mode=GeneralSearch&SID=F6QT72yCVrFplcWRTCn&qid=19&ra_mode=more&ra_name=PublicationYear&colName=&viewType=raMore (accessed 2.7.20).

Contreras, M. del M., Jurado-Campos, N., Arce, L., Arroyo-Manzanares, N., 2019. A robustness study of calibration models for olive oil classification: Targeted and non-targeted fingerprint approaches based on GC-IMS. Food Chem. 288, 315–324. https://doi.org/10.1016/j.foodchem.2019.02.104

Contreras, M. del M., Jurado-Campos, N., Sánchez-Carnerero Callado, C., Arroyo-Manzanares, N., Fernández, L., Casano, S., Marco, S., Arce, L., Ferreiro-Vera, C., 2018. Thermal desorption-ion mobility spectrometry: A rapid sensor for the detection of cannabinoids and discrimination of Cannabis sativa L. chemotypes. Sensors Actuators B Chem. 273, 1413–1424. https://doi.org/10.1016/j.snb.2018.07.031

Cook, S.M., Skerlos, S.J., Raskin, L., Love, N.G., 2017. A stability assessment tool for anaerobic codigestion. Water Res. 112, 19–28. https://doi.org/10.1016/j.watres.2017.01.027

Creaser, C.S., Griffiths, J.R., Bramwell, C.J., Noreen, S., Hill, C.A., Thomas, C.L.P., 2004. Ion mobility spectrometry: a review. Part 1. Structural analysis by mobility measurement. Analyst 129, 984. https://doi.org/10.1039/b404531a

Criado-García, L., Arce, L., 2016. Extraction of toxic compounds from saliva by magnetic-stirring-assisted micro-solid-phase extraction step followed by headspace-gas chromatography-ion mobility spectrometry. Anal. Bioanal. Chem. 408, 6813–6822. https://doi.org/10.1007/s00216-016-9808-1

Criado-García, L., Garrido-Delgado, R., Arce, L., López, F., Peón, R., Valcárcel, M., 2015. Simultaneous determination of benzene and phenol in heat transfer fluid by head-space gas chromatography hyphenated with ion mobility spectrometry. Talanta 144, 944–952. https://doi.org/10.1016/j.talanta.2015.07.053

Cruwys, J.., Dinsdale, R.., Hawkes, F.., Hawkes, D.., 2002. Development of a static headspace gas chromatographic procedure for the routine analysis of volatile fatty acids in wastewaters. J. Chromatogr. A 945, 195–209. https://doi.org/10.1016/S0021-9673(01)01514-X

Cumeras, R., Figueras, E., Davis, C.E., Baumbach, J.I., Gràcia, I., 2015a. Review on Ion Mobility Spectrometry. Part 1: current instrumentation. Analyst 140, 1376–1390. https://doi.org/10.1039/C4AN01100G

Cumeras, R., Figueras, E., Davis, C.E., Baumbach, J.I., Gràcia, I., 2015b. Review on Ion Mobility Spectrometry. Part 2: hyphenated methods and effects of experimental parameters. Analyst 140, 1391–1410. https://doi.org/10.1039/C4AN01101E

Cumeras, R., Figueras, E., Davis, C.E., Baumbach, J.I., Gràcia, I., 2015c. Review on Ion Mobility Spectrometry. Part 2: hyphenated methods and effects of experimental parameters. Analyst 140, 1391–1410. https://doi.org/10.1039/C4AN01101E

Davoli, E., Gangai, M.L., Morselli, L., Tonelli, D., 2003. Characterisation of odorants emissions from landfills by SPME and GC/MS. Chemosphere 51, 357–368. https://doi.org/10.1016/S0045-6535(02)00845-7

Denawaka, C.J., Fowlis, I.A., Dean, J.R., 2014. Evaluation and application of static headspace–multicapillary column-gas chromatography–ion mobility spectrometry for complex sample analysis. J. Chromatogr. A 1338, 136–148. https://doi.org/10.1016/j.chroma.2014.02.047

EBA, 2017. Statistical Report 2017 [WWW Document]. Annu. Rep. URL https://www.fuelseurope.eu/publication/statistical-report-2017/

Edwards, J., Othman, M., Burn, S., 2015. A review of policy drivers and barriers for the use of anaerobic digestion in Europe, the United States and Australia. Renew. Sustain. Energy Rev. 52, 815–828. https://doi.org/10.1016/j.rser.2015.07.112

Eiceman, G.A., Karpas, Z., Herbert H. Hill, J., 2016. Ion Mobility Spectrometry 3rd ed. CRC Press Taylor & Francis Group.

Environment Agency, 2007. Review of odour character and thresholds.

EPA, 2019. Technical Overview of Volatile Organic Compounds [WWW Document]. URL https://www.epa.gov/indoor-air-quality-iaq/technical-overview-volatile-organic-compounds#definition (accessed 12.5.19).

Esteves, S., Miltner, M., Fletch, S., 2012. Review and Guide for Monitoring Anaerobic Digestion and Biogas Plants for the Optimisation of Biogas and Biomethane Production 2, 72.

European Union, 2014. 2030 climate & energy framework [WWW Document]. URL https://ec.europa.eu/clima/policies/strategies/2030_en (accessed 7.18.20).

Ewing, R., 2001. A critical review of ion mobility spectrometry for the detection of explosives and explosive related compounds. Talanta 54, 515–529. https://doi.org/10.1016/S0039-9140(00)00565-8

Fang, J.J., Yang, N., Cen, D.Y., Shao, L.M., He, P.J., 2012. Odor compounds from different sources of landfill: Characterization and source identification. Waste Manag. 32, 1401–1410. https://doi.org/10.1016/j.wasman.2012.02.013

Fatemi, M.H., 2002. Simultaneous modeling of the Kovats retention indices on OV-1 and SE-54 stationary phases using artificial neural networks. J. Chromatogr. A 955, 273–280. https://doi.org/10.1016/S0021-9673(02)00169-3

Fernández, R., Dinsdale, R.M., Guwy, A.J., Premier, G.C., 2016. Critical analysis of methods for the measurement of volatile fatty acids. Crit. Rev. Environ. Sci. Technol. 46, 209–234. https://doi.org/10.1080/10643389.2015.1073493

G.A.S, n.d. Exemplary list of compounds, detection limits.

Gaik, U., Sillanpää, M., Witkiewicz, Z., Puton, J., 2017. Nitrogen oxides as dopants for the detection of aromatic compounds with ion mobility spectrometry. Anal. Bioanal. Chem. 409, 3223–3231. https://doi.org/10.1007/s00216-017-0265-2

Gallego, E., Roca, F.J., Perales, J.F., Sánchez, G., Esplugas, P., 2012. Characterization and determination of the odorous charge in the indoor air of a waste treatment facility through the evaluation of volatile organic compounds (VOCs) using TD–GC/MS. Waste Manag. 32, 2469–2481. https://doi.org/10.1016/j.wasman.2012.07.010

Gallegos, J., Arce, C., Jordano, R., Arce, L., Medina, L.M., 2017. Target identification of volatile metabolites to allow the differentiation of lactic acid bacteria by gas chromatography-ion mobility spectrometry. Food Chem. 220, 362–370. https://doi.org/10.1016/j.foodchem.2016.10.022

Gao, H., Niu, W., Hong, Y., Xu, B., Shen, C., Huang, C., Jiang, H., Chu, Y., 2014. Negative photoionization chloride ion attachment ion mobility spectrometry for the detection of organic acids. RSC Adv. 4, 63977–63984. https://doi.org/10.1039/C4RA10763B

Garrido-Delgado, R., Arce, L., Valcárcel, M., 2012. Multi-capillary column-ion mobility spectrometry: a potential screening system to differentiate virgin olive oils. Anal. Bioanal. Chem. 402, 489–498. https://doi.org/10.1007/s00216-011-5328-1

Garrido-Delgado, R., Dobao-Prieto, M.D.M., Arce, L., Valcárcel, M., 2015. Determination of volatile compounds by GC–IMS to assign the quality of virgin olive oil. Food Chem. 187, 572–579. https://doi.org/10.1016/j.foodchem.2015.04.082

Garrido-Delgado, R., Mercader-Trejo, F., Sielemann, S., de Bruyn, W., Arce, L., Valcárcel, M., 2011. Direct classification of olive oils by using two types of ion mobility spectrometers. Anal. Chim. Acta 696, 108–115. https://doi.org/10.1016/j.aca.2011.03.007

Gerhardt, N., Birkenmeier, M., Sanders, D., Rohn, S., Weller, P., 2017. Resolution-optimized headspace gas chromatography-ion mobility spectrometry (HS-GC-IMS) for non-targeted olive oil profiling. Anal. Bioanal. Chem. 409, 3933–3942. https://doi.org/10.1007/s00216-017-0338-2

Heikkinen, M., Poutiainen, H., Liukkonen, M., Heikkinen, T., Hiltunen, Y., 2011. Subtraction analysis based on self-organizing maps for an industrial wastewater treatment process. Math. Comput. Simul. 82, 450–459. https://doi.org/10.1016/j.matcom.2010.10.021

Hill, H.H., Siems, W.F., St. Louis, R.H., McMinn, D.G., 2004. Ion Mobility Spectrometry, in: Detection Technologies for Chemical Warfare Agents and Toxic Vapors. CRC Press, pp. 113–133. https://doi.org/10.1201/9780203485705.ch6

Hjorth, M., Nielsen, a. M., Nyord, T., Hansen, M.N., Nissen, P., Sommer, S.G., 2009. Nutrient value, odour emission and energy production of manure as influenced by anaerobic digestion and separation. Agron. Sustain. Dev. 29, 329–338. https://doi.org/10.1051/agro:2008047

Hobbs, P.J., Misselbrook, T.H., Pain, B.F., 1998. Emission rates of odorous compounds from pig slurries. J. Sci. Food Agric. 77, 341–348. https://doi.org/10.1002/(SICI)1097-0010(199807)77:3<341::AID-

JSFA45>3.0.CO;2-9

Holm-Nielsen, J.B., Al Seadi, T., Oleskowicz-Popiel, P., 2009. The future of anaerobic digestion and biogas utilization. Bioresour. Technol. 100, 5478–5484. https://doi.org/10.1016/j.biortech.2008.12.046

Holubar, P., Zani, L., Hagar, M., Fröschl, W., Radak, Z., Braun, R., 2000. Modelling of anaerobic digestion using self-organizing maps and artificial neural networks. Water Sci. Technol. 41, 149–156. https://doi.org/10.2166/wst.2000.0259

Horttanainen, M., Deviatkin, I., Havukainen, J., 2017. Nitrogen release from mechanically dewatered sewage sludge during thermal drying and potential for recovery. J. Clean. Prod. 142, 1819–1826. https://doi.org/10.1016/j.jclepro.2016.11.102

Hu, X., Wang, R., Guo, J., Ge, K., Li, G., Fu, F., Ding, S., Shan, Y., 2019. Changes in the volatile components of candied kumquats in different processing methodologies with headspace-gas chromatography-ion mobility spectrometry. Molecules 24. https://doi.org/10.3390/molecules24173053

Hylemon, P.B., Harder, J., 1998. Biotransformation of monoterpenes, bile acids, and other isoprenoids in anaerobic ecosystems. FEMS Microbiol. Rev. 22, 475–488. https://doi.org/10.1016/S0168-6445(98)00027-8

Jafari, M.T., Khayamian, T., 2008. Direct determination of ammoniacal nitrogen in water samples using corona discharge ion mobility spectrometry. Talanta 76, 1189–1193. https://doi.org/10.1016/j.talanta.2008.05.028

Jafari, M.T., Saraji, M., Kermani, M., 2018. Sol-gel electrospinning preparation of hybrid carbon silica nanofibers for extracting organophosphorus pesticides prior to analyzing them by gas chromatography-ion mobility spectrometry. J. Chromatogr. A 1558, 1–13. https://doi.org/10.1016/j.chroma.2018.05.014

Jafari, M.T., Saraji, M., Sherafatmand, H., 2011. Electrospray ionization-ion mobility spectrometry as a detection system for three-phase hollow fiber microextraction technique and simultaneous determination of trimipramine and desipramine in urine and plasma samples. Anal. Bioanal. Chem. 399, 3555–3564. https://doi.org/10.1007/s00216-011-4730-z

Jiang, D., Wang, X., Chen, C., Wang, W., Guo, L., Lv, Y., Li, E., Li, H., 2018. Dopant-assisted photoionization positive ion mobility spectrometry coupled with time-resolved purge introduction for online quantitative monitoring of intraoperative end-tidal propofol. Anal. Chim. Acta 1032, 83–90. https://doi.org/10.1016/j.aca.2018.06.047

Jin, X., Li, X., Zhao, N., Angelidaki, I., Zhang, Y., 2017. Bio-electrolytic sensor for rapid monitoring of volatile fatty acids in anaerobic digestion process. Water Res. 111, 74–80. https://doi.org/10.1016/j.watres.2016.12.045

Jünger, M., Bödeker, B., Baumbach, J.I., 2010. Peak assignment in multi-capillary column–ion mobility spectrometry using comparative studies with gas chromatography–mass spectrometry for VOC analysis. Anal. Bioanal. Chem. 396, 471–482. https://doi.org/10.1007/s00216-009-3168-z

Jünger, M., Vautz, W., Kuhns, M., Hofmann, L., Ulbricht, S., Baumbach, J.I., Quintel, M., Perl, T., 2012. Ion mobility spectrometry for microbial volatile organic compounds: a new identification tool for human pathogenic bacteria. Appl. Microbiol. Biotechnol. 93, 2603–2614. https://doi.org/10.1007/s00253-012-3924-4

Kanu, A.B., Hill, H.H., 2008. Ion mobility spectrometry detection for gas chromatography. J. Chromatogr. A 1177, 12–27. https://doi.org/10.1016/j.chroma.2007.10.110

Kleeberg, K.K., Liu, Y., Jans, M., Schlegelmilch, M., Streese, J., Stegmann, R., 2005. Development of a simple and sensitive method for the characterization of odorous waste gas emissions by means of solid-phase microextraction (SPME) and GC–MS/olfactometry. Waste Manag. 25, 872–879. https://doi.org/10.1016/j.wasman.2005.07.003

Kohonen, T., 1998. The self-organizing map. Neurocomputing 21, 1–6. https://doi.org/10.1016/S0925-2312(98)00030-7

Kohonen, T., 1982. Self-Organized Formation of Topologically Correct Feature Maps. Biol. Cybern. 43, 59–69.

Lee, J., Kim, J., Oh, J.I., Lee, S.R., Kwon, E.E., 2017. Quantification and speciation of volatile fatty acids in the aqueous phase. Environ. Pollut. 230, 81–86. https://doi.org/10.1016/j.envpol.2017.06.042

Li, F., Xie, Z., Schmidt, H., Sielemann, S., Baumbach, J.., 2002. Ion mobility spectrometer for online monitoring of trace compounds. Spectrochim. Acta Part B At. Spectrosc. 57, 1563–1574. https://doi.org/10.1016/S0584-8547(02)00110-6

Li, H., Jiang, D., Liu, W., Yang, Y., Zhang, Y., Jin, C., Sun, S., 2020. Comparison of fermentation behaviors and properties of raspberry wines by spontaneous and controlled alcoholic fermentations. Food Res. Int. 128, 108801. https://doi.org/10.1016/j.foodres.2019.108801

Li, J., Yuan, H., Yao, Y., Hua, J., Yang, Y., Dong, C., Deng, Y., Wang, J., Li, H., Jiang, Y., Zhou, Q., 2019. Rapid volatiles fingerprinting by dopant-assisted positive photoionization ion mobility spectrometry for discrimination and characterization of Green Tea aromas. Talanta 191, 39–45. https://doi.org/10.1016/j.talanta.2018.08.039

Li, L., Peng, X., Wang, X., Wu, D., 2018. Anaerobic digestion of food waste: A review focusing on process stability. Bioresour. Technol. 248, 20–28. https://doi.org/10.1016/j.biortech.2017.07.012

Li, X., Cui, W., Wang, W., Wang, Y., Gong, Z., Xu, Z., 2019. Analysis of the volatile compounds associated with pickling of ginger using headspace gas chromatography - ion mobility spectrometry. Flavour Fragr. J. 34, 485–492. https://doi.org/10.1002/ffj.3530

Liedtke, S., Seifert, L., Ahlmann, N., Hariharan, C., Franzke, J., Vautz, W., 2018. Coupling laser desorption with gas chromatography and ion mobility spectrometry for improved olive oil characterisation. Food Chem. 255, 323–331. https://doi.org/10.1016/j.foodchem.2018.01.193

Lin, C.S.K., Pfaltzgraff, L.A., Herrero-Davila, L., Mubofu, E.B., Abderrahim, S., Clark, J.H., Koutinas, A.A., Kopsahelis, N., Stamatelatou, K., Dickson, F., Thankappan, S., Mohamed, Z., Brocklesby, R., Luque, R., 2013. Food waste as a valuable resource for the production of chemicals, materials and fuels. Current situation and global perspective. Energy Environ. Sci. 6, 426. https://doi.org/10.1039/c2ee23440h

Littarru, P., 2007. Environmental odours assessment from waste treatment plants: Dynamic olfactometry in combination with sensorial analysers “electronic noses.” Waste Manag. 27, 302–309. https://doi.org/10.1016/j.wasman.2006.03.011

Liukkonen, M., Laakso, I., Hiltunen, Y., 2013. Advanced monitoring platform for industrial wastewater treatment: Multivariable approach using the self-organizing map. Environ. Model. Softw. 48, 193–201. https://doi.org/10.1016/j.envsoft.2013.07.005

Lützhøft, H.C.H., Boe, K., Fang, C., Angelidaki, I., 2014. Comparison of VFA titration procedures used for monitoring the biogas process. Water Res. 54, 262–272. https://doi.org/10.1016/j.watres.2014.02.001

Mao, C., Feng, Y., Wang, X., Ren, G., 2015. Review on research achievements of biogas from anaerobic digestion. Renew. Sustain. Energy Rev. 45, 540–555. https://doi.org/10.1016/j.rser.2015.02.032

Márquez-Sillero, I., Aguilera-Herrador, E., Cárdenas, S., Valcárcel, M., 2011a. Ion-mobility spectrometry for environmental analysis. TrAC - Trends Anal. Chem. 30, 677–690. https://doi.org/10.1016/j.trac.2010.12.007

Márquez-Sillero, I., Cárdenas, S., Sielemann, S., Valcárcel, M., 2014. On-line headspace-multicapillary column-ion mobility spectrometry hyphenation as a tool for the determination of off-flavours in foods. J. Chromatogr. A 1333, 99–105. https://doi.org/10.1016/j.chroma.2014.01.062

Márquez-Sillero, I., Cárdenas, S., Valcárcel, M., 2012. Headspace–multicapillary column–ion mobility

spectrometry for the direct analysis of 2,4,6-trichloroanisole in wine and cork samples. J. Chromatogr. A 1265, 149–154. https://doi.org/10.1016/j.chroma.2012.09.087

Márquez-Sillero, I., Cárdenas, S., Valcárcel, M., 2011b. Direct determination of 2,4,6-tricholoroanisole in wines by single-drop ionic liquid microextraction coupled with multicapillary column separation and ion mobility spectrometry detection. J. Chromatogr. A 1218, 7574–7580. https://doi.org/10.1016/j.chroma.2011.06.032

Martín-Gómez, A., Arroyo-Manzanares, N., Rodríguez-Estévez, V., Arce, L., 2019. Use of a non-destructive sampling method for characterization of Iberian cured ham breed and feeding regime using GC-IMS. Meat Sci. 152, 146–154. https://doi.org/10.1016/j.meatsci.2019.02.018

Masár, M., Hradski, J., Nováková, M., Szucs, R., Sabo, M., Matejčík, Š., 2020. Online coupling of microchip electrophoresis with ion mobility spectrometry for direct analysis of complex liquid samples. Sensors Actuators B Chem. 302, 127183. https://doi.org/10.1016/j.snb.2019.127183

Mata-Alvarez, J., 2003. Biomethanization of the organic fraction of municipal solid wastes Edited by.

Mata-Alvarez, J., Macé, S., Llabrés, P., 2000. Anaerobic digestion of organic solid wastes. An overview of research achievements and perspectives. Bioresour. Technol. 74, 3–16. https://doi.org/10.1016/S0960-8524(00)00023-7

Materić, D., Bruhn, D., Turner, C., Morgan, G., Mason, N., Gauci, V., 2015. Methods in Plant Foliar Volatile Organic Compounds Research. Appl. Plant Sci. 3, 1500044. https://doi.org/10.3732/apps.1500044

Matz, G., Schröder, W., Ollesch, T., 2005. New methods for fast on-site measurement of odorous compounds. Waste Manag. 25, 864–871. https://doi.org/10.1016/j.wasman.2005.07.014

Matz, L., Tornatore, P.S., Hill, H.H., 2001. Evaluation of suspected interferents for TNT detection by ion mobility spectrometry. Talanta 54, 171–179. https://doi.org/10.1016/S0039-9140(00)00663-9

Mesquita, D.P., Quintelas, C., Amaral, A.L., Ferreira, E.C., 2017. Monitoring biological wastewater treatment processes: recent advances in spectroscopy applications. Rev. Environ. Sci. Bio/Technology 16, 395–424. https://doi.org/10.1007/s11157-017-9439-9

Mochalski, P., Wiesenhofer, H., Allers, M., Zimmermann, S., Güntner, A.T., Pineau, N.J., Lederer, W., Agapiou, A., Mayhew, C.A., Ruzsanyi, V., 2018. Monitoring of selected skin- and breath-borne volatile organic compounds emitted from the human body using gas chromatography ion mobility spectrometry (GC-IMS). J. Chromatogr. B 1076, 29–34. https://doi.org/10.1016/j.jchromb.2018.01.013

Namsree, P., Suvajittanont, W., Puttanlek, C., Uttapap, D., Rungsardthong, V., 2012. Anaerobic digestion of pineapple pulp and peel in a plug-flow reactor. J. Environ. Manage. 110, 40–47. https://doi.org/10.1016/j.jenvman.2012.05.017

National Library of Medicine, 2020. PubChem database [WWW Document]. Natl. Libr. Med. URL https://pubchem.ncbi.nlm.nih.gov/ (accessed 5.15.20).

Neri, G., Lacquaniti, A., Rizzo, G., Donato, N., Latino, M., Buemi, M., 2012. Real-time monitoring of breath ammonia during haemodialysis: Use of ion mobility spectrometry (IMS) and cavity ring-down spectroscopy (CRDS) techniques. Nephrol. Dial. Transplant. 27, 2945–2952. https://doi.org/10.1093/ndt/gfr738

Nguyen, D., Gadhamshetty, V., Nitayavardhana, S., Khanal, S.K., 2015. Automatic process control in anaerobic digestion technology: A critical review. Bioresour. Technol. 193, 513–522. https://doi.org/10.1016/j.biortech.2015.06.080

Nicell, J.A., 2009. Assessment and regulation of odour impacts. Atmos. Environ. 43, 196–206. https://doi.org/10.1016/j.atmosenv.2008.09.033

Nikhil, Koskinen, P.E.P., Visa, A., Kaksonen, A.H., Puhakka, J.A., Yli-Harja, O., 2008. Clustering hybrid regression: A novel computational approach to study and model biohydrogen production through dark fermentation. Bioprocess Biosyst. Eng. 31, 631–640. https://doi.org/10.1007/s00449-008-0213-9

Nimmermark, S., 2011. Influence of odour concentration and individual odour thresholds on the hedonic tone of odour from animal production. Biosyst. Eng. 108, 211–219. https://doi.org/10.1016/j.biosystemseng.2010.12.003

NIST Chemistry WebBook, 2018. NIST Standard Reference Database Number 69 [WWW Document]. https://doi.org/10.18434/T4D303

NRW, 2017. Ceredigion river pollution update 07/06/17 [WWW Document]. URL https://naturalresources.wales/about-us/news-and-events/news/nrw-investigates-ceredigion-river-pollution/?lang=en (accessed 3.10.18).

Omelianski, V.L., 1922. Aroma-Producing Microörganisms. J. Bacteriol. 8, 393–419.

Orellana-Silla, A., Armenta, S., de la Guardia, M., Mercader, J. V., Esteve-Turrillas, A., 2018. Development of immunosorbents for the analysis of forchlorfenuron in fruit juices by ion mobility spectrometry. Anal. Bioanal. Chem. 410, 5961–5967. https://doi.org/10.1007/s00216-018-1213-5

Othman, A., Goggin, K.A., Tahir, N.I., Brodrick, E., Singh, R., Sambanthamurthi, R., Parveez, G.K.A.A., Davies, A.N., Murad, A.J., Muhammad, N.H., Ramli, U.S., Murphy, D.J., 2019. Use of headspace–gas chromatography–ion mobility spectrometry to detect volatile fingerprints of palm fibre oil and sludge palm oil in samples of crude palm oil. BMC Res. Notes 12, 229. https://doi.org/10.1186/s13104-019-4263-7

Page, L.H., Ni, J.-Q., Zhang, H., Heber, A.J., Mosier, N.S., Liu, X., Joo, H.-S., Ndegwa, P.M., Harrison, J.H., 2015. Reduction of volatile fatty acids and odor offensiveness by anaerobic digestion and solid separation of dairy manure during manure storage. J. Environ. Manage. 152, 91–98. https://doi.org/10.1016/j.jenvman.2015.01.024

Parchami, R., Kamalabadi, M., Alizadeh, N., 2017. Determination of biogenic amines in canned fish samples using head-space solid phase microextraction based on nanostructured polypyrrole fiber coupled to modified ionization region ion mobility spectrometry. J. Chromatogr. A 1481, 37–43. https://doi.org/10.1016/j.chroma.2016.12.046

Pawliszyn, J., 2012. Handbook of Solid Phase Microextraction, 1st editio. ed. Waltham, Md. : Elsevier. https://doi.org/10.1016/C2011-0-04297-7

Perl, T., Bödeker, B., Jünger, M., Nolte, J., Vautz, W., 2010. Alignment of retention time obtained from multicapillary column gas chromatography used for VOC analysis with ion mobility spectrometry. Anal. Bioanal. Chem. 397, 2385–2394. https://doi.org/10.1007/s00216-010-3798-1

Persaud, K.C., 2017. Towards bionic noses. Sens. Rev. 37, 165–171. https://doi.org/10.1108/SR-10-2016-0238

Przybylko, A.R.M., Thomas, C.L.P., Anstice, P.J., Fielden, P.R., Brokenshire, J., Irons, F., 1995. The determination of aqueous ammonia by ion mobility spectrometry. Anal. Chim. Acta 311, 77–83. https://doi.org/10.1016/0003-2670(95)00177-2

Pu, D., Zhang, H., Zhang, Y., Sun, B., Ren, F., Chen, H., He, J., 2019. Characterization of the aroma release and perception of white bread during oral processing by gas chromatography-ion mobility spectrometry and temporal dominance of sensations analysis. Food Res. Int. 123, 612–622. https://doi.org/10.1016/j.foodres.2019.05.016

Puton, J., Nousiainen, M., Sillanpää, M., 2008. Ion mobility spectrometers with doped gases. Talanta 76, 978–987. https://doi.org/10.1016/j.talanta.2008.05.031

Qamaruz-Zaman, N., Milke, M.W., 2012. VFA and ammonia from residential food waste as indicators of odor potential. Waste Manag. 32, 2426–2430. https://doi.org/10.1016/j.wasman.2012.06.023

Rahman, M.M., Abd El-Aty, A.M., Choi, J.-H., Shin, H.-C., Shin, S.C., Shim, J.-H., 2015. Basic Overview on Gas Chromatography Columns, in: Analytical Separation Science. Wiley-VCH Verlag GmbH & Co. KGaA, Weinheim, Germany, pp. 823–834. https://doi.org/10.1002/9783527678129.assep024

Rajagopal, R., Massé, D.I., Singh, G., 2013. A critical review on inhibition of anaerobic digestion process by excess ammonia. Bioresour. Technol. 143, 632–641. https://doi.org/10.1016/j.biortech.2013.06.030

Ramachandran, A., Rustum, R., Adeloye, A.J., 2019. Anaerobic digestion process modeling using Kohonen self-organising maps. Heliyon 5, e01511. https://doi.org/10.1016/j.heliyon.2019.e01511

Ramírez-Guízar, S., Sykes, H., Perry, J.D., Schwalbe, E.C., Stanforth, S.P., Perez-Perez, M.C.I., Dean, J.R., 2017. A chromatographic approach to distinguish Gram-positive from Gram-negative bacteria using exogenous volatile organic compound metabolites. J. Chromatogr. A 1501, 79–88. https://doi.org/10.1016/j.chroma.2017.04.015

Ranau, R., Kleeberg, K.K., Schlegelmilch, M., Streese, J., Stegmann, R., Steinhart, H., 2005. Analytical determination of the suitability of different processes for the treatment of odorous waste gas. Waste Manag. 25, 908–916. https://doi.org/10.1016/j.wasman.2005.07.004

Raposo, F., Borja, R., Cacho, J.A., Mumme, J., Orupõld, K., Esteves, S., Noguerol-Arias, J., Picard, S., Nielfa, A., Scherer, P., Wierinck, I., Aymerich, E., Cavinato, C., Rodriguez, D.C., García-Mancha, N., Lens, P.N.T., Fernández-Cegrí, V., 2013. First international comparative study of volatile fatty acids in aqueous samples by chromatographic techniques: Evaluating sources of error. TrAC Trends Anal. Chem. 51, 127–143. https://doi.org/10.1016/j.trac.2013.07.007

Rappert, S., Müller, R., 2005. Odor compounds in waste gas emissions from agricultural operations and food industries. Waste Manag. 25, 887–907. https://doi.org/10.1016/j.wasman.2005.07.008

Reed, J.P., Devlin, D., Esteves, S., Dinsdale, R., Guwy, A.J., 2011. Performance parameter prediction for sewage sludge digesters using reflectance FT-NIR spectroscopy. Water Res. 45, 2463–2472. https://doi.org/10.1016/j.watres.2011.01.027

Reed, J.P., Devlin, D., Esteves, S.R.R., Dinsdale, R., Guwy, A.J., 2013. Integration of NIRS and PCA techniques for the process monitoring of a sewage sludge anaerobic digester. Bioresour. Technol. 133, 398–404. https://doi.org/10.1016/j.biortech.2013.01.083

Reyes-Garcés, N., Gómez-Ríos, G.A., Souza Silva, É.A., Pawliszyn, J., 2013. Coupling needle trap devices with gas chromatography–ion mobility spectrometry detection as a simple approach for on-site quantitative analysis. J. Chromatogr. A 1300, 193–198. https://doi.org/10.1016/j.chroma.2013.05.042

Rister, A.L., Dodds, E.D., 2020. Steroid analysis by ion mobility spectrometry. Steroids 153, 108531. https://doi.org/10.1016/j.steroids.2019.108531

Rodríguez-Maecker, R., Vyhmeister, E., Meisen, S., Rosales Martinez, A., Kuklya, A., Telgheder, U., 2017. Identification of terpenes and essential oils by means of static headspace gas chromatography-ion mobility spectrometry. Anal. Bioanal. Chem. 409, 6595–6603. https://doi.org/10.1007/s00216-017-0613-2

Rodríguez-Navas, C., Forteza, R., Cerdà, V., 2012. Use of thermal desorption–gas chromatography–mass spectrometry (TD–GC–MS) on identification of odorant emission focus by volatile organic compounds characterisation. Chemosphere 89, 1426–1436. https://doi.org/10.1016/j.chemosphere.2012.06.013

Rouessac, F., Rouessac, A., 2007. Chemical Analysis Modern Instrumentation Methods and Techniques, John Wiley & Sons, Ltd.

Rudnicka, J., Mochalski, P., Agapiou, A., Statheropoulos, M., Amann, A., Buszewski, B., 2010. Application of ion mobility spectrometry for the detection of human urine. Anal. Bioanal. Chem. 398, 2031–2038. https://doi.org/10.1007/s00216-010-4147-0

Ruzsanyi, V., Baumbach, J.I., Sielemann, S., Litterst, P., Westhoff, M., Freitag, L., 2005. Detection of human metabolites using multi-capillary columns coupled to ion mobility spectrometers. J. Chromatogr. A 1084, 145–151. https://doi.org/10.1016/j.chroma.2005.01.055

Ruzsanyi, V., Mochalski, P., Schmid, A., Wiesenhofer, H., Klieber, M., Hinterhuber, H., Amann, A., 2012. Ion mobility spectrometry for detection of skin volatiles. J. Chromatogr. B Anal. Technol. Biomed. Life

Sci. 911, 84–92. https://doi.org/10.1016/j.jchromb.2012.10.028

Safaei, Z., Eiceman, G.A., Puton, J., Stone, J.A., Nasirikheirabadi, M., Anttalainen, O., Sillanpää, M., 2019. Differential Mobility Spectrometry of Ketones in Air at Extreme Levels of Moisture. Sci. Rep. 9, 5593. https://doi.org/10.1038/s41598-019-41485-7

Sans, C., Mata-Alvarez, J., Cecchi, F., Pavan, P., Bassetti, A., 1995. Volatile fatty acids production by mesophilic fermentation of mechanically-sorted urban organic wastes in a plug-flow reactor. Bioresour. Technol. 51, 89–96. https://doi.org/10.1016/0960-8524(95)95866-Z

Satoh, T., Kishi, S., Nagashima, H., Tachikawa, M., Kanamori-Kataoka, M., Nakagawa, T., Kitagawa, N., Tokita, K., Yamamoto, S., Seto, Y., 2015. Ion mobility spectrometric analysis of vaporous chemical warfare agents by the instrument with corona discharge ionization ammonia dopant ambient temperature operation. Anal. Chim. Acta 865, 39–52. https://doi.org/10.1016/j.aca.2015.02.004

Saveyn, H., Eder, P., 2014. End-of-waste criteria for biodegradable waste subjected to biological treatment (compost & digestate): Technical proposals. https://doi.org/10.2791/6295

Schiffman, S.S., Bennett, J.L., Raymer, J.H., 2001. Quantification of odors and odorants from swine operations in North Carolina. Agric. For. Meteorol. 108, 213–240. https://doi.org/10.1016/S0168-1923(01)00239-8

Schlegelmilch, M., Streese, J., Biedermann, W., Herold, T., Stegmann, R., 2005a. Odour control at biowaste composting facilities. Waste Manag. 25, 917–927. https://doi.org/10.1016/j.wasman.2005.07.011

Schlegelmilch, M., Streese, J., Stegmann, R., 2005b. Odour management and treatment technologies: An overview. Waste Manag. 25, 928–939. https://doi.org/10.1016/j.wasman.2005.07.006

Schulz-Bohm, K., Martín-Sánchez, L., Garbeva, P., 2017. Microbial volatiles: Small molecules with an important role in intra- and inter-kingdom interactions. Front. Microbiol. 8, 1–10. https://doi.org/10.3389/fmicb.2017.02484

Sciex, A., 2012. Speed Your Selection With This One-Stop Resource. Speed Your Sel. with this One-Stop Resour. 1–268.

Sferopoulos, R., 2009. A Review of Chemical Warfare Agent (CWA) Detector Technologies and Commercial-Off-The-Shelf Items. Aust. Gov. Dep. Def. 98.

Shahraki, H., Tabrizchi, M., Farrokhpor, H., 2018. Detection of explosives using negative ion mobility spectrometry in air based on dopant-assisted thermal ionization. J. Hazard. Mater. 357, 1–9. https://doi.org/10.1016/j.jhazmat.2018.05.054

Sharif, S.M., Kusin, F.M., Asha'ari, Z.H., Aris, A.Z., 2015. Characterization of Water Quality Conditions in the Klang River Basin, Malaysia Using Self Organizing Map and K-means Algorithm. Procedia Environ. Sci. 30, 73–78. https://doi.org/10.1016/j.proenv.2015.10.013

Sigma, 2019. Supelco Analytical Nukol™ Fused Silica Capillary GC Column [WWW Document]. URL https://www.sigmaaldrich.com/catalog/product/supelco/24131?lang=en&region=GB (accessed 12.6.19).

Sigma Aldrich, 2019. SE-54 Column [WWW Document]. URL https://www.sigmaaldrich.com/catalog/product/supelco/24001?lang=en&region=GB (accessed 12.6.19).

Sigurnjak, I., Vaneeckhaute, C., Michels, E., Ryckaert, B., Ghekiere, G., Tack, F.M.G., Meers, E., 2017. Fertilizer performance of liquid fraction of digestate as synthetic nitrogen substitute in silage maize cultivation for three consecutive years. Sci. Total Environ. 599–600, 1885–1894. https://doi.org/10.1016/j.scitotenv.2017.05.120

Singhania, R.R., Patel, A.K., Christophe, G., Fontanille, P., Larroche, C., 2013. Biological upgrading of volatile fatty acids, key intermediates for the valorization of biowaste through dark anaerobic fermentation. Bioresour. Technol. 145, 166–174. https://doi.org/10.1016/j.biortech.2012.12.137

Sironi, S., Capelli, L., Céntola, P., Del Rosso, R., Il Grande, M., 2007. Continuous monitoring of odours from a composting plant using electronic noses. Waste Manag. 27, 389–397. https://doi.org/10.1016/j.wasman.2006.01.029

Sironi, S., Capelli, L., Céntola, P., Del Rosso, R., Pierucci, S., 2010. Odour impact assessment by means of dynamic olfactometry, dispersion modelling and social participation. Atmos. Environ. 44, 354–360. https://doi.org/10.1016/j.atmosenv.2009.10.029

Sonnberg, S., Armenta, S., Garrigues, S., de la Guardia, M., 2015. Detection of tetrahydrocannabinol residues on hands by ion-mobility spectrometry (IMS). Correlation of IMS data with saliva analysis. Anal. Bioanal. Chem. 407, 5999–6008. https://doi.org/10.1007/s00216-015-8784-1

Sorribes-Soriano, A., de la Guardia, M., Esteve-Turrillas, A., Armenta, S., 2018a. Trace analysis by ion mobility spectrometry: From conventional to smart sample preconcentration methods. A review. Anal. Chim. Acta 1026, 37–50. https://doi.org/10.1016/j.aca.2018.03.059

Sorribes-Soriano, A., Esteve-Turrillas, A., Armenta, S., de la Guardia, M., Herrero-Martínez, J.M., 2017. Cocaine abuse determination by ion mobility spectrometry using molecular imprinting. J. Chromatogr. A 1481, 23–30. https://doi.org/10.1016/j.chroma.2016.12.041

Sorribes-Soriano, A., Esteve-Turrillas, A., Armenta, S., Montoya, A., Herrero-Martínez, J.M., de la Guardia, M., 2018b. Magnetic molecularly imprinted polymers for the selective determination of cocaine by ion mobility spectrometry. J. Chromatogr. A 1545, 22–31. https://doi.org/10.1016/j.chroma.2018.02.055

Sorribes-Soriano, A., Esteve-Turrillas, F.A., Armenta, S., Amorós, P., Herrero-Martínez, J.M., 2019. Amphetamine-type stimulants analysis in oral fluid based on molecularly imprinting extraction. Anal. Chim. Acta 1052, 73–83. https://doi.org/10.1016/j.aca.2018.11.046

Stenmark, Å., Jensen, C., Quested, T., Moates, G., 2016. Estimates of European food waste levels, IVL-report C 186. https://doi.org/10.13140/RG.2.1.4658.4721

Studer, I., Boeker, C., Geist, J., 2017. Physicochemical and microbiological indicators of surface water body contamination with different sources of digestate from biogas plants. Ecol. Indic. 77, 314–322. https://doi.org/10.1016/j.ecolind.2017.02.025

Sundberg, C., Yu, D., Franke-Whittle, I., Kauppi, S., Smårs, S., Insam, H., Romantschuk, M., Jönsson, H., 2013. Effects of pH and microbial composition on odour in food waste composting. Waste Manag. 33, 204–211. https://doi.org/10.1016/j.wasman.2012.09.017

Szymańska, E., Brodrick, E., Williams, M., Davies, A.N., van Manen, H.-J., Buydens, L.M.C., 2015. Data Size Reduction Strategy for the Classification of Breath and Air Samples Using Multicapillary Column-Ion Mobility Spectrometry. Anal. Chem. 87, 869–875. https://doi.org/10.1021/ac503857y

Szymańska, E., Davies, A.N., Buydens, L.M.C.C., 2016. Chemometrics for ion mobility spectrometry data: recent advances and future prospects. Analyst 141, 5689–5708. https://doi.org/10.1039/C6AN01008C

Takuwa, Y., Matsumoto, T., Oshita, K., Takaoka, M., Morisawa, S., Takeda, N., 2009. Characterization of trace constituents in landfill gas and a comparison of sites in Asia. J. Mater. Cycles Waste Manag. 11, 305–311. https://doi.org/10.1007/s10163-009-0257-1

Talaiekhozani, A., Bagheri, M., Goli, A., Talaei Khoozani, M.R., 2016. An overview of principles of odor production, emission, and control methods in wastewater collection and treatment systems. J. Environ. Manage. 170, 186–206. https://doi.org/10.1016/j.jenvman.2016.01.021

Tao, B., Donnelly, J., Oliveira, I., Anthony, R., Wilson, V., Esteves, S.R., 2017. Enhancement of microbial density and methane production in advanced anaerobic digestion of secondary sewage sludge by continuous removal of ammonia. Bioresour. Technol. 232, 380–388. https://doi.org/10.1016/j.biortech.2017.02.066

Taylor, C., Lough, F., Stanforth, S.P., Schwalbe, E.C., Fowlis, I.A., Dean, J.R., 2017. Analysis of Listeria using exogenous volatile organic compound metabolites and their detection by static headspace–

multi-capillary column–gas chromatography–ion mobility spectrometry (SHS–MCC–GC–IMS). Anal. Bioanal. Chem. 409, 4247–4256. https://doi.org/10.1007/s00216-017-0375-x

The Danish Environmental Protection Agency, 2013. Evaluation of health hazards by exposure to d-Limonene and proposal of a health-based quality criterion for ambient air.

The European Parliament and the Council of the European Union, 2004. Directive 2004/42/CE of the European Parliament and of the Council of 21 April 2004 on the limitation of emissions of volatile organic compounds due to the use of organic solvents in certain paints and varnishes and vehicle refinishing products and amendi. Off. J. Eur. Union 87–96. https://doi.org/http://eur-lex.europa.eu/LexUriServ/LexUriServ.do?uri=OJ:L:2004:143:0087:0096:EN:PDF

Thompson, R., Perry, J.D., Stanforth, S.P., Dean, J.R., 2018. Rapid detection of hydrogen sulfide produced by pathogenic bacteria in focused growth media using SHS-MCC-GC-IMS. Microchem. J. 140, 232–240. https://doi.org/10.1016/j.microc.2018.04.026

Tian, H., Wen, H., Yang, X., Li, S., Li, J., 2021. Exploring the effects of anthocyanins on volatile organic metabolites of alzheimer's disease model mice based on HS-GC-IMS and HS-SPME-GC–MS. Microchem. J. 162, 105848. https://doi.org/10.1016/j.microc.2020.105848

Tipler, A., 2013. An introduction to headspace sampling in gas chromatography fundamentals and theory. Chromatogr. Res. Technol. Manag. PerkinElmer,.

Toledo-Cervantes, A., Serejo, M.L., Blanco, S., Pérez, R., Lebrero, R., Muñoz, R., 2016. Photosynthetic biogas upgrading to bio-methane: Boosting nutrient recovery via biomass productivity control. Algal Res. 17, 46–52. https://doi.org/10.1016/j.algal.2016.04.017

Tran, P.D., Van de Walle, D., De Clercq, N., De Winne, A., Kadow, D., Lieberei, R., Messens, K., Tran, D.N., Dewettinck, K., Van Durme, J., 2015. Assessing cocoa aroma quality by multiple analytical approaches. Food Res. Int. 77, 657–669. https://doi.org/10.1016/j.foodres.2015.09.019

Valadbeigi, Y., Ilbeigi, V., Michalczuk, B., Sabo, M., Matejcik, S., 2019. Study of Atmospheric Pressure Chemical Ionization Mechanism in Corona Discharge Ion Source with and without NH 3 Dopant by Ion Mobility Spectrometry combined with Mass Spectrometry: A Theoretical and Experimental Study. J. Phys. Chem. A 123, 313–322. https://doi.org/10.1021/acs.jpca.8b11417

Vásquez Quintero, A., Molina-Lopez, F., Smits, E.C.P., Danesh, E., Van Den Brand, J., Persaud, K., Oprea, A., Barsan, N., Weimar, U., De Rooij, N.F., Briand, D., 2016. Smart RFID label with a printed multisensor platform for environmental monitoring. Flex. Print. Electron. 1, 1–12. https://doi.org/10.1088/2058-8585/1/2/025003

Vautz, W., Baumbach, J.I., Jung, J., 2006a. Beer Fermentation Control Using Ion Mobility Spectrometry - Results of a Pilot Study. J. Inst. Brew. 112, 157–164. https://doi.org/10.1002/j.2050-0416.2006.tb00245.x

Vautz, W., Baumbach, J.I., Uhde, E., 2006b. Detection of emissions from surfaces using ion mobility spectrometry. Anal. Bioanal. Chem. 384, 980–986. https://doi.org/10.1007/s00216-005-0240-1

Vautz, W., Bödeker, B., Baumbach, J.I., Bader, S., Westhoff, M., Perl, T., 2009. An implementable approach to obtain reproducible reduced ion mobility. Int. J. Ion Mobil. Spectrom. 12, 47–57. https://doi.org/10.1007/s12127-009-0018-9

Vautz, W., Franzke, J., Zampolli, S., Elmi, I., Liedtke, S., 2018a. On the potential of ion mobility spectrometry coupled to GC pre-separation – A tutorial. Anal. Chim. Acta 1024, 52–64. https://doi.org/10.1016/j.aca.2018.02.052

Vautz, W., Hariharan, C., Weigend, M., 2018b. Smell the change: On the potential of gas-chromatographic ion mobility spectrometry in ecosystem monitoring. Ecol. Evol. 8, 4370–4377. https://doi.org/10.1002/ece3.3990

Vera, L., Companioni, E., Meacham, A., Gygax, H., 2016. Real time monitoring of VOC and odours based

on GC-IMS at wastewater treatment plants. Chem. Eng. Trans. 54, 79–84. https://doi.org/10.3303/CET1654014

Verbeeck, K., Buelens, L.C., Galvita, V. V., Marin, G.B., Van Geem, K.M., Rabaey, K., 2018. Upgrading the value of anaerobic digestion via chemical production from grid injected biomethane. Energy Environ. Sci. 11, 1788–1802. https://doi.org/10.1039/C8EE01059E

Wallace, P., Harris, G., Frederickson, J., Howell, G., 2011. Biofertiliser management : best practice for agronomic benefit & odour control. Wrap.

Wang, J., 2014. Decentralized Biogas Technology of Anaerobic Digestion and Farm Ecosystem: Opportunities and Challenges. Front. Energy Res. 2, 1–12. https://doi.org/10.3389/fenrg.2014.00010

Wang, S., Chen, H., Sun, B., 2020. Recent progress in food flavor analysis using gas chromatography–ion mobility spectrometry (GC–IMS). Food Chem. 126158. https://doi.org/10.1016/j.foodchem.2019.126158

Waraksa, E., Perycz, U., Namieśnik, J., Sillanpää, M., Dymerski, T., Wójtowicz, M., Puton, J., 2016. Dopants and gas modifiers in ion mobility spectrometry. TrAC Trends Anal. Chem. 82, 237–249. https://doi.org/10.1016/j.trac.2016.06.009

Ward, A.J., Bruni, E., Lykkegaard, M.K., Feilberg, A., Adamsen, A.P.S., Jensen, A.P., Poulsen, A.K., 2011. Real time monitoring of a biogas digester with gas chromatography, near-infrared spectroscopy, and membrane-inlet mass spectrometry. Bioresour. Technol. 102, 4098–4103. https://doi.org/10.1016/j.biortech.2010.12.052

Williams, J., Williams, H., Dinsdale, R., Guwy, A., Esteves, S., 2013. Monitoring methanogenic population dynamics in a full-scale anaerobic digester to facilitate operational management. Bioresour. Technol. 140, 234–242. https://doi.org/10.1016/j.biortech.2013.04.089

WRAP, 2016. Digestate and compost in agriculture 2392. https://doi.org/10.13140/RG.2.1.2298.1366

WRAP, 2012. Using quality anaerobic digestate to benefit crops 1–12. https://doi.org/Summer 2012

Yang, X., Jiao, R., Zhu, X., Zhao, S., Liao, G., Yu, J., Wang, D., 2019. Profiling and characterization of odorous volatile compounds from the industrial fermentation of erythromycin. Environ. Pollut. 255, 113130. https://doi.org/10.1016/j.envpol.2019.113130

Yanini, A., Esteve-Turrillas, A., de la Guardia, M., Armenta, S., 2018. Ion mobility spectrometry and high resolution mass-spectrometry as methodologies for rapid identification of the last generation of new psychoactive substances. J. Chromatogr. A 1574, 91–100. https://doi.org/10.1016/j.chroma.2018.09.006

Yenigün, O., Demirel, B., 2013. Ammonia inhibition in anaerobic digestion: A review. Process Biochem. 48, 901–911. https://doi.org/10.1016/j.procbio.2013.04.012

Zellner, B. d'Acampora, Bicchi, C., Dugo, P., Rubiolo, P., Dugo, G., Mondello, L., 2008. Linear retention indices in gas chromatographic analysis: a review. Flavour Fragr. J. 23, 297–314. https://doi.org/10.1002/ffj.1887

Zhang, C., Su, H., Baeyens, J., Tan, T., 2014. Reviewing the anaerobic digestion of food waste for biogas production. Renew. Sustain. Energy Rev. 38, 383–392. https://doi.org/10.1016/j.rser.2014.05.038

Zhang, L., Shuai, Q., Li, P., Zhang, Q., Ma, F., Zhang, W., Ding, X., 2016. Ion mobility spectrometry fingerprints: A rapid detection technology for adulteration of sesame oil. Food Chem. 192, 60–66. https://doi.org/10.1016/j.foodchem.2015.06.096

Zhang, Y., Yue, D., Liu, J., He, L., Nie, Y., 2012. Effect of organic compositions of aerobically pretreated municipal solid waste on non-methane organic compound emissions during anaerobic degradation. Waste Manag. 32, 1116–1121. https://doi.org/10.1016/j.wasman.2012.01.005

Zolotov, Y.A., 2006. Ion mobility spectrometry. J. Anal. Chem. 61, 519–519. https://doi.org/10.1134/S1061934806060013

APPENDICES

APPENDIX 1: PUBLICATIONS FROM THIS RESEARCH

Presentations in international conferences

Oliveira, A., Chong, A., Patterson, T., Reed, J., Kumi, P. & Esteves, S. R., 2019. Development of a Novel Multi-Parameter Monitoring Tool for Odour Management and Environmental Compliance of Anaerobic Digestion Technology. Conference. ODOURS 19 – International conference on odours, University of Aveiro, Portugal.

Presentations in Postgraduate Researchers Presentation Day

Oliveira, A., 2019. Development of a novel multi-parameter monitoring tool for odour management and environmental compliance of anaerobic digestion technology presented at 7th Annual Postgraduate Research's Presentation Day, USW, UK

Presentations in 3 Minute Thesis Competition

Oliveira, A., 2018. Development of a novel multi-parameter monitoring tool for optimisation of anaerobic digestion technology performance for improved energy production, odour management and environmental compliance" presented at 6th Annual Postgraduate Research's Presentation Day, USW, UK winning an honourable place

Oliveira, A., 2018. Development of a novel multi-parameter monitoring tool for optimisation of anaerobic digestion technology" presented at 2018 KESS 2 Annual Event St Fagans National Museum of History, UK

Posters

Oliveira, A., Patterson, T., Reed, J., & Esteves, S. R,. 2018. Development of a novel multi-parameter monitoring tool for optimisation of anaerobic digestion. Poster at KESS 2 Poster Presentation event, USW, UK

Oliveira, A., Reed, J., Patterson, T., Chong, A. & Esteves, S. R. 2019. Development of a novel multi-parameter monitoring tool using GC-IMS for chemical fingerprinting in

anaerobic digestion. Poster at the 16th IWA World Conference on Anaerobic Digestion, University of Delft, Netherlands.

Darke, M., Donnelly, J., Henley, A., Savvas, S., Kumi, P., Oliveira, A., Patterson, T., Reed, J., Chong, Z., Wilson, V., Matthews, R., Vergara, L. & Esteves, S. R., 2019. Ultrasound to Maximise Anaerobic Digestion of Thermally hydrolysed Sewage Sludge. Poster at the 16th IWA World Conference on Anaerobic Digestion, University of Delft, Netherlands.

APPENDIX 2: CALIBRATION CURVES

Figure 65 presents a second order polynomial calibration curve for ammonium hydroxide (A), limonene (B), 2-butanone (C), 2-pentanone (D), 2-hexanone (E), 2-heptanone (F), 2-octanone (G), 2-nonanone (H), acetic acid (I), propionic acid (J), and butyric acid (L).

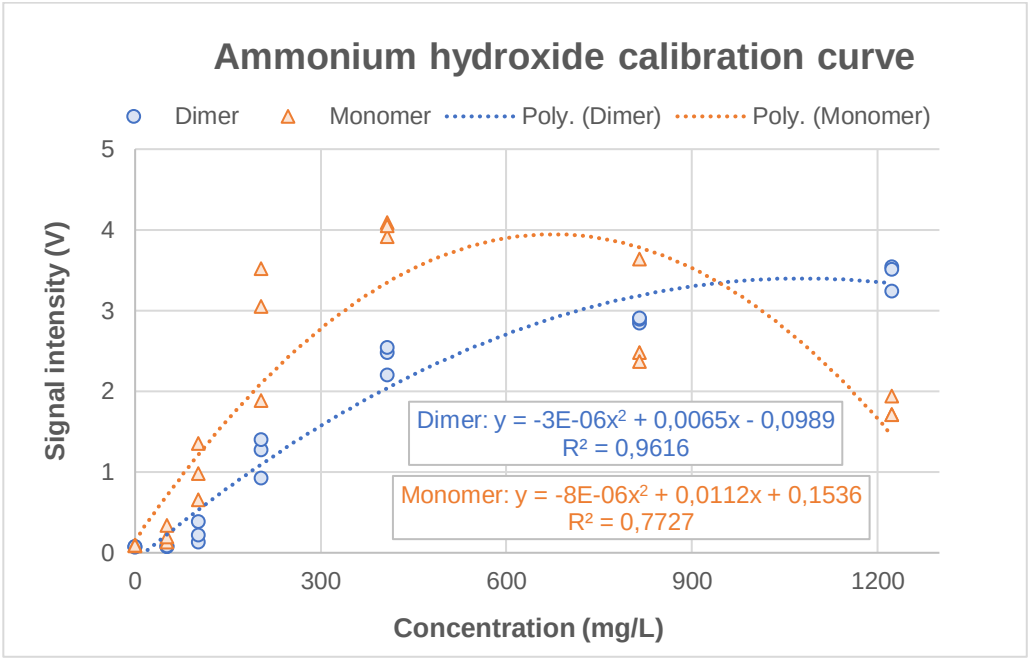

A

B

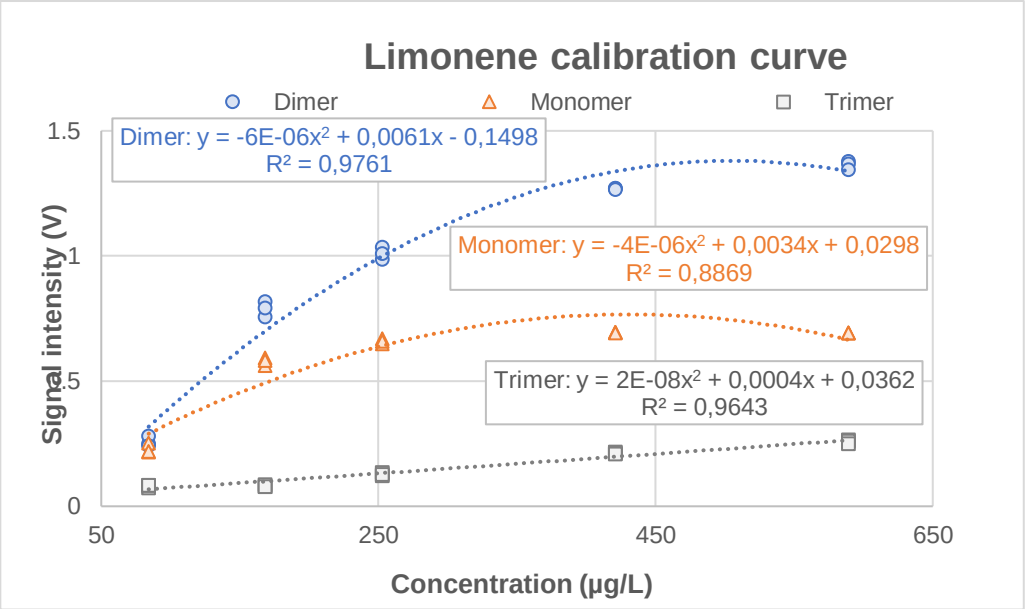
Limonene calibration curve
Dimer
Monomer
Trimer
Dimer: y = -6E-06x² + 0,0061x - 0,1498
R² = 0,9761
Monomer: y = -4E-06x² + 0,0034x + 0,0298
R² = 0,8869
Trimer: y = 2E-08x² + 0,0004x + 0,0362
R² = 0,9643
Signal intensity (V)
Concentration (µg/L)
0
0,5
1
1,5
50
250
450
650

C

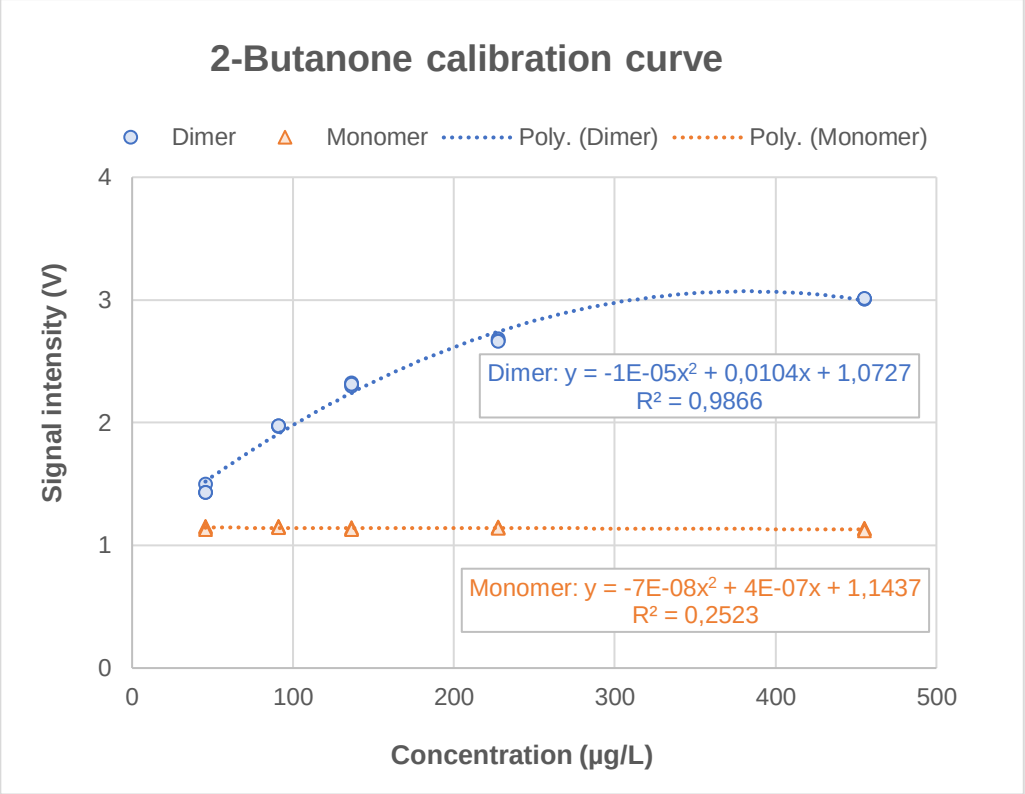
2-Butanone calibration curve
Dimer
Monomer
Poly. (Dimer)
Poly. (Monomer)
Dimer: y = -1E-05x² + 0,0104x + 1,0727
R² = 0,9866
Monomer: y = -7E-08x² + 4E-07x + 1,1437
R² = 0,2523
Signal intensity (V)
Concentration (µg/L)
0
1
2
3
4
0
100
200
300
400
500

D

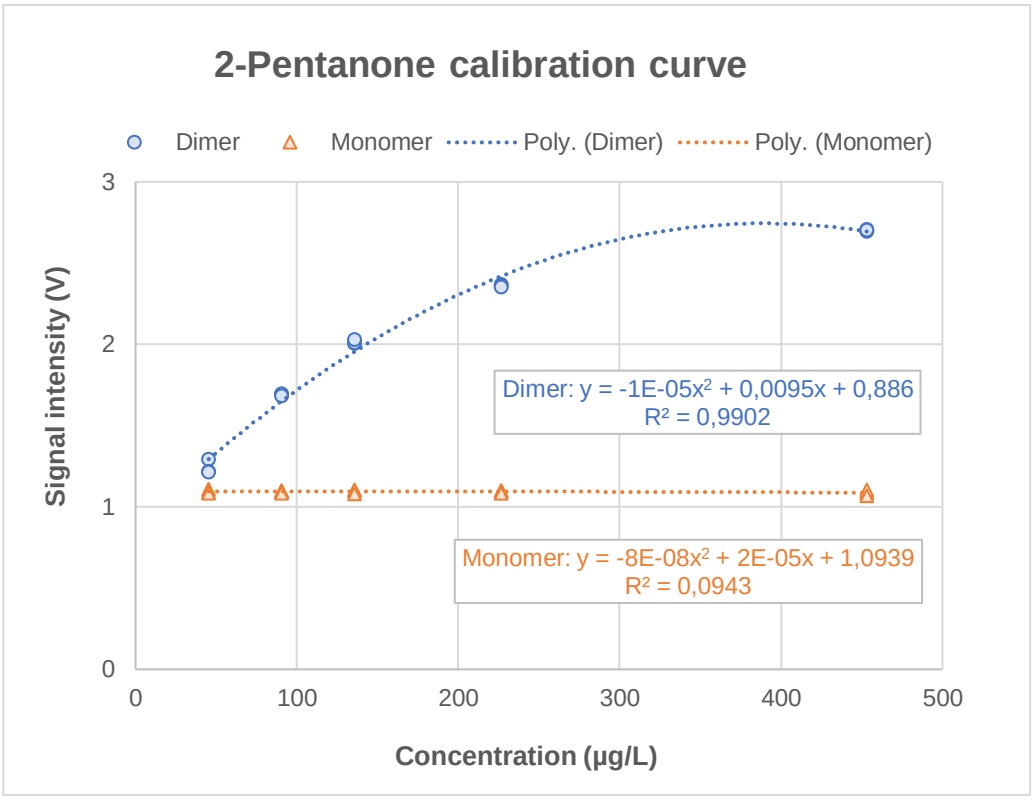
2-Pentanone calibration curve
Dimer
Monomer
Poly. (Dimer)
Poly. (Monomer)
Signal intensity (V)
Concentration (µg/L)
Dimer: y = -1E-05x² + 0,0095x + 0,886
R² = 0,9902
Monomer: y = -8E-08x² + 2E-05x + 1,0939
R² = 0,0943
0
1
2
3
0
100
200
300
400
500

E

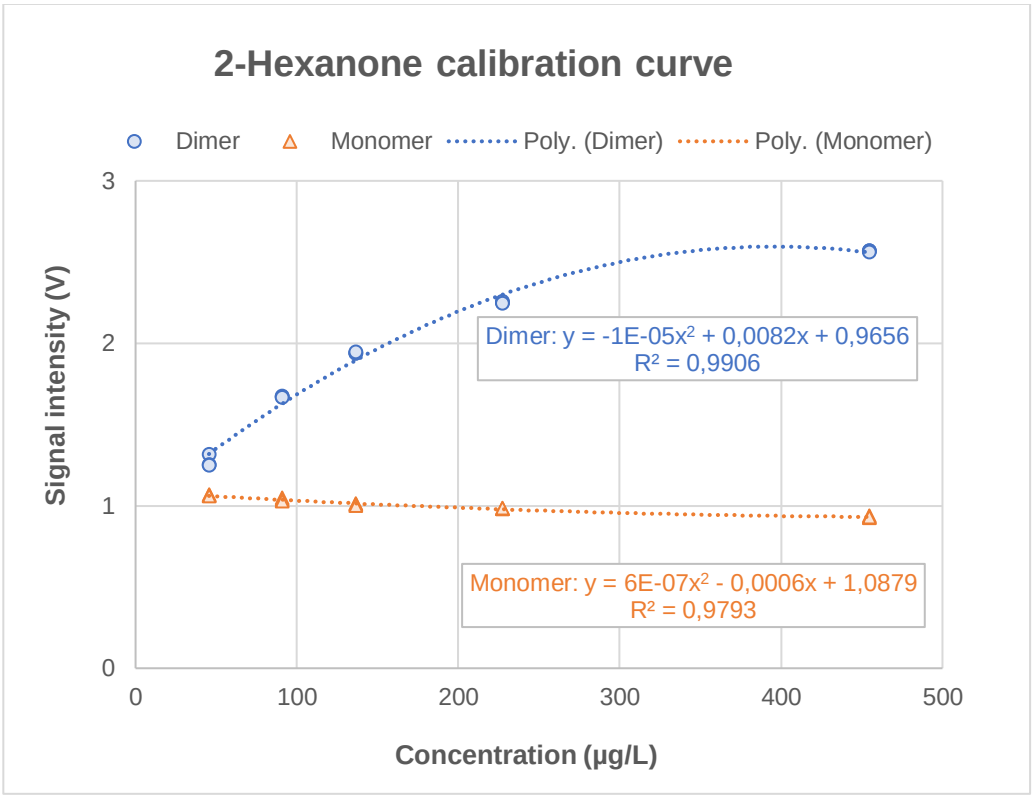
2-Hexanone calibration curve
Dimer
Monomer
Poly. (Dimer)
Poly. (Monomer)
Signal intensity (V)
Concentration (µg/L)
Dimer: y = -1E-05x² + 0,0082x + 0,9656
R² = 0,9906
Monomer: y = 6E-07x² - 0,0006x + 1,0879
R² = 0,9793
0
1
2
3
0
100
200
300
400
500

F

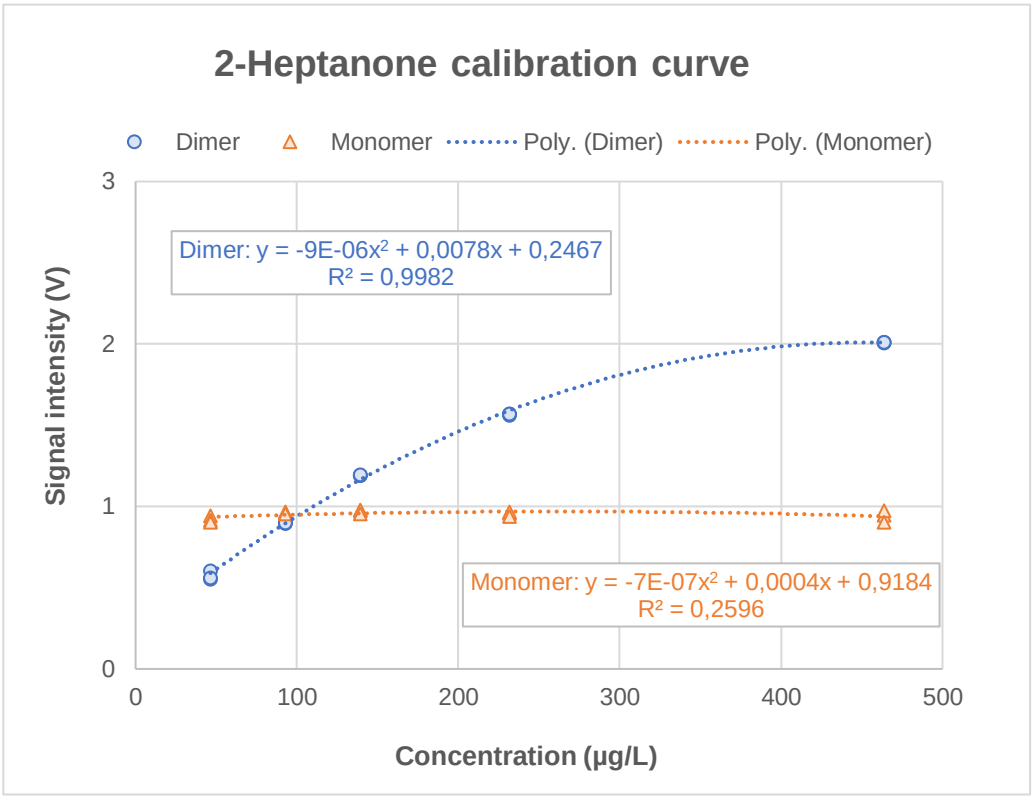
2-Heptanone calibration curve
Dimer
Monomer
Poly. (Dimer)
Poly. (Monomer)
Dimer: y = -9E-06x² + 0,0078x + 0,2467
R² = 0,9982
Monomer: y = -7E-07x² + 0,0004x + 0,9184
R² = 0,2596
Signal intensity (V)
Concentration (µg/L)
0
1
2
3
0
100
200
300
400
500

G

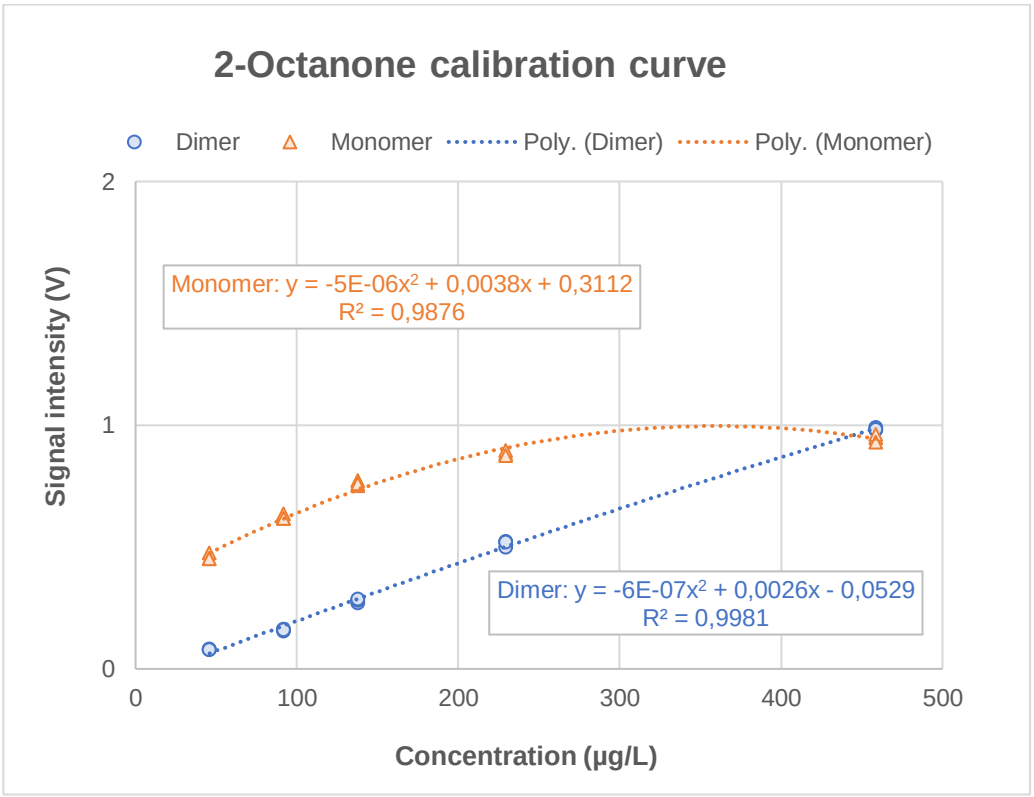
2-Octanone calibration curve
Dimer
Monomer
Poly. (Dimer)
Poly. (Monomer)
Monomer: y = -5E-06x² + 0,0038x + 0,3112
R² = 0,9876
Dimer: y = -6E-07x² + 0,0026x - 0,0529
R² = 0,9981
Signal intensity (V)
Concentration (µg/L)
0
1
2
0
100
200
300
400
500

H

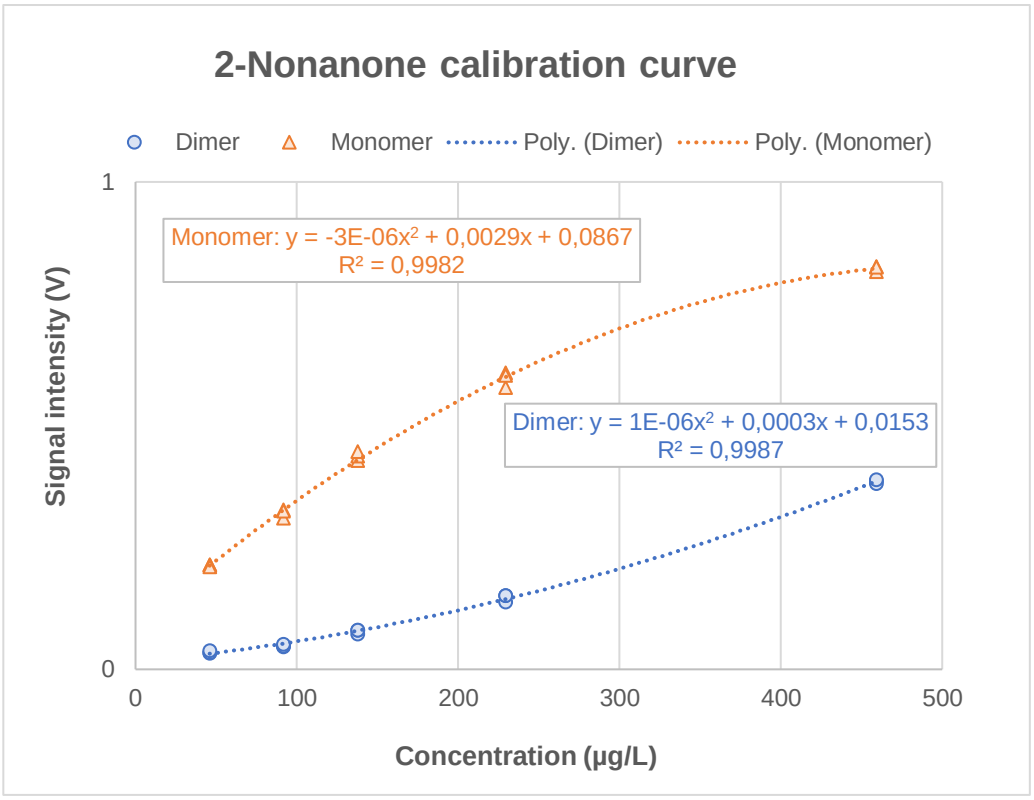
2-Nonanone calibration curve
Dimer
Monomer
Poly. (Dimer)
Poly. (Monomer)
Monomer: y = -3E-06x² + 0,0029x + 0,0867
R² = 0,9982
Dimer: y = 1E-06x² + 0,0003x + 0,0153
R² = 0,9987
Signal intensity (V)
Concentration (µg/L)
0
1
0
100
200
300
400
500

I

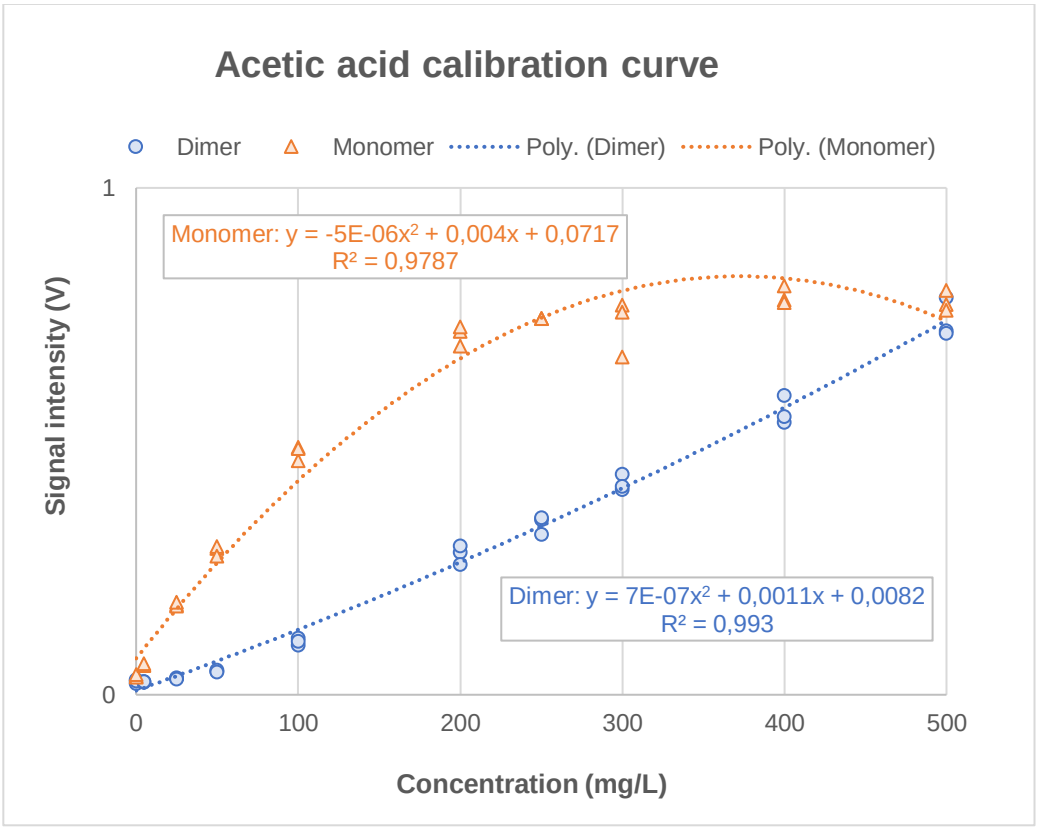
Acetic acid calibration curve
Dimer
Monomer
Poly. (Dimer)
Poly. (Monomer)
Monomer: y = -5E-06x² + 0,004x + 0,0717
R² = 0,9787
Dimer: y = 7E-07x² + 0,0011x + 0,0082
R² = 0,993
Signal intensity (V)
Concentration (mg/L)
0
1
0
100
200
300
400
500

J

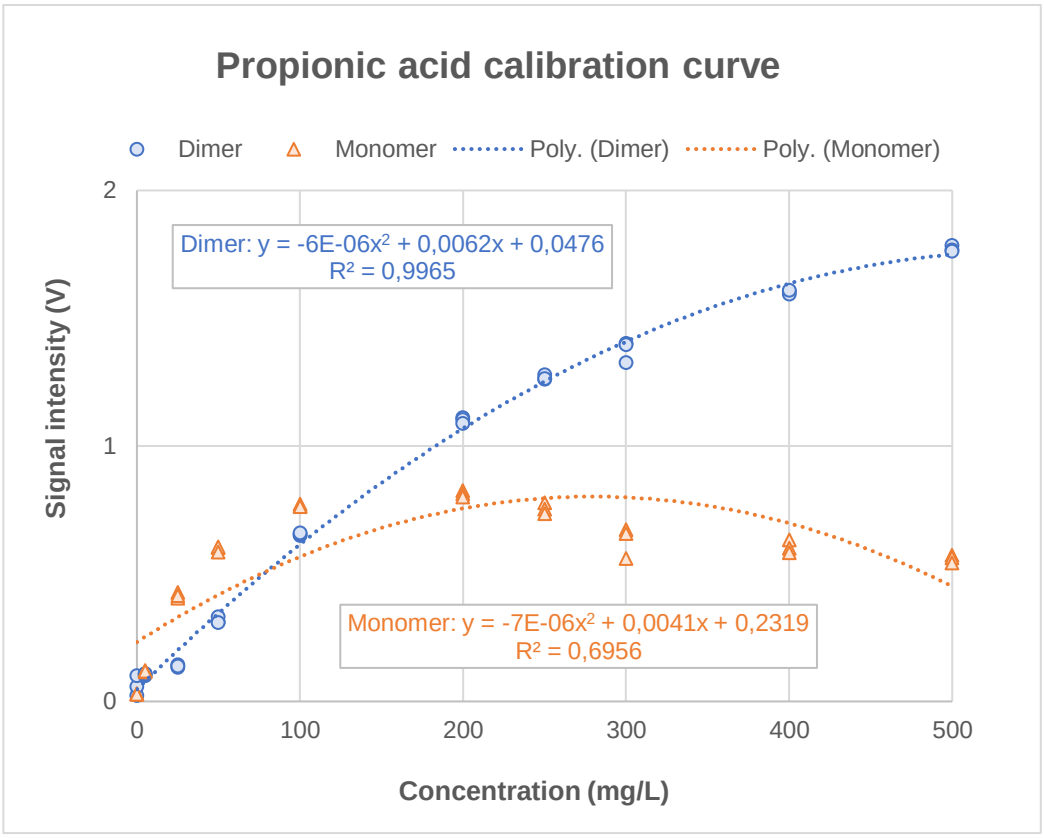

L

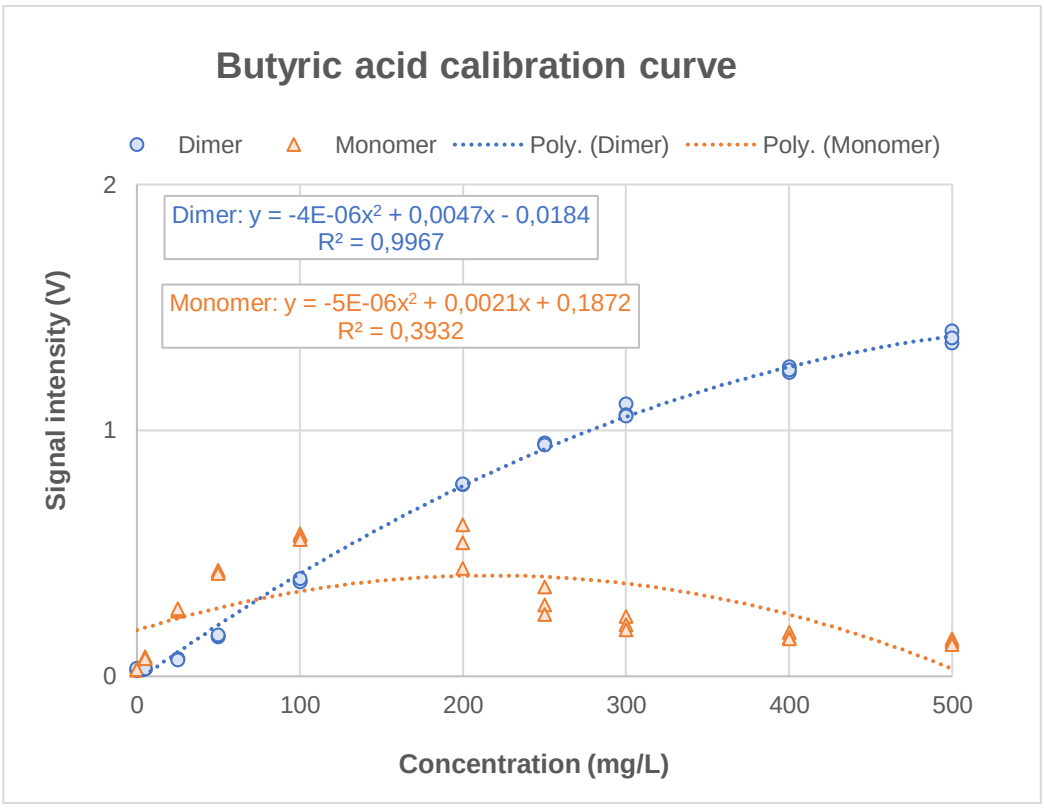

Figure 65: Second order polynomial calibration curve for several compounds such as ammonium hydroxide (A), limonene (B), 2-butanone (C), 2-pentanone (D), 2-hexanone (E), 2-heptanone (F), 2-octanone (G), 2-nonanone (H), acetic acid (I), propionic acid (J), butyric acid (L)

APPENDIX 3: CHAPTER 6 GALLERY PLOTS (REACTOR COMPARISON)

Figure 66 to 72 present the gallery plots for all reactor samples (CSTR and PF) A and B, based on the day of the measurement (analysis done day 58 until day 107).

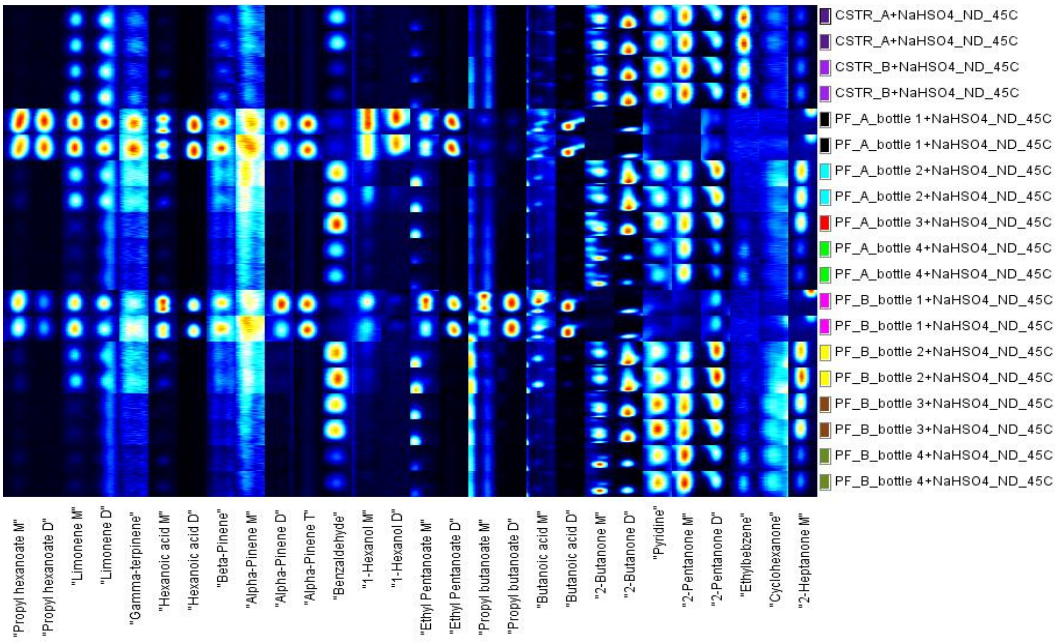

Figure 66: A gallery plot showing the peak selection and respective identification (monomer, dimer, trimer) for all reactors samples (CSTR A, CSTR B, PF A, PF B) for the day 58

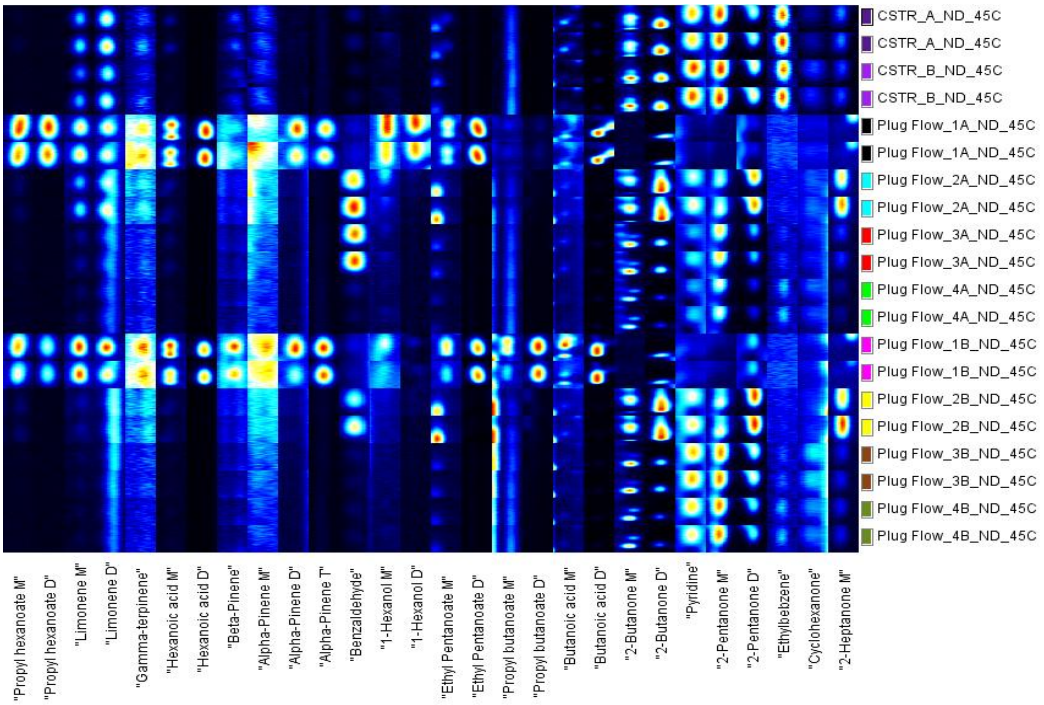

Figure 67: A gallery plot showing the peak selection and respective identification (monomer, dimer, trimer) for all reactors samples (CSTR A, CSTR B, PF A, PF B) for the day 64

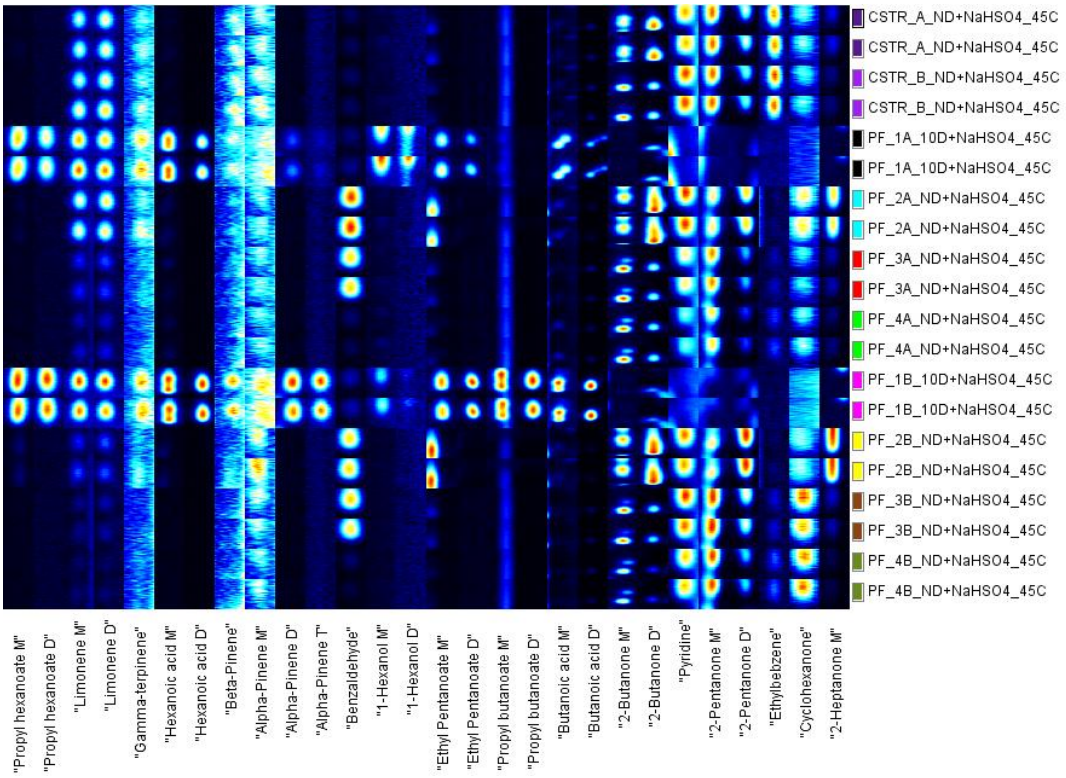

Figure 68: A gallery plot showing the peak selection and respective identification (monomer, dimer, trimer) for all reactors samples (CSTR A, CSTR B, PF A, PF B) for the day 71

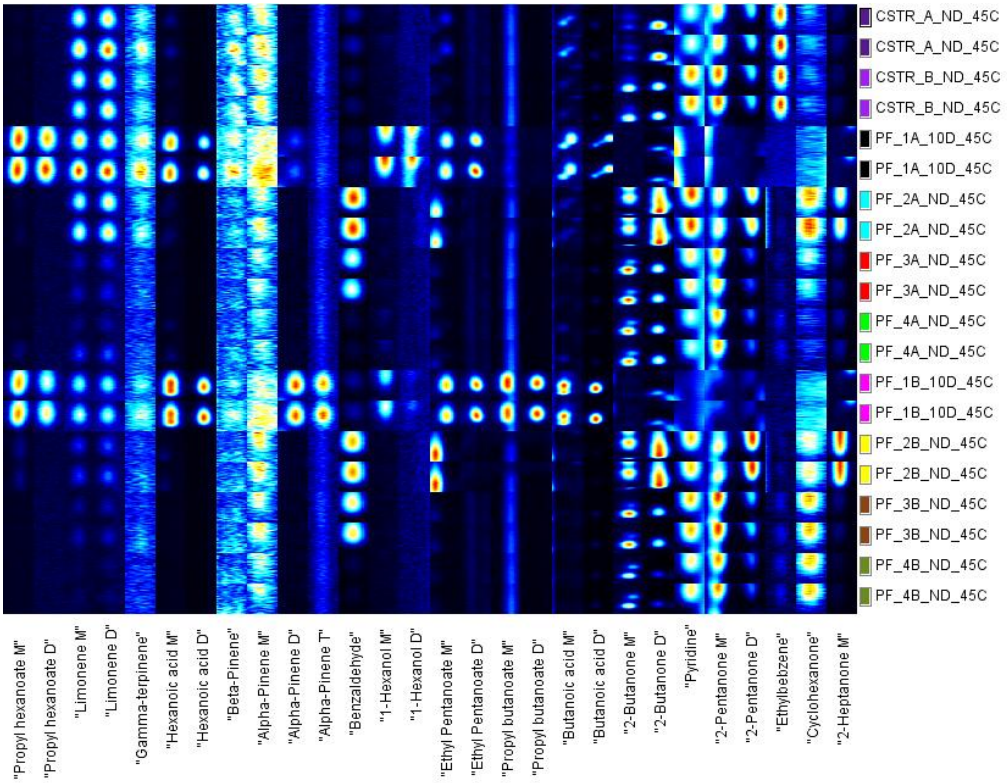

Figure 69: A gallery plot showing the peak selection and respective identification (monomer, dimer, trimer) for all reactors samples (CSTR A, CSTR B, PF A, PF B) for the day 80

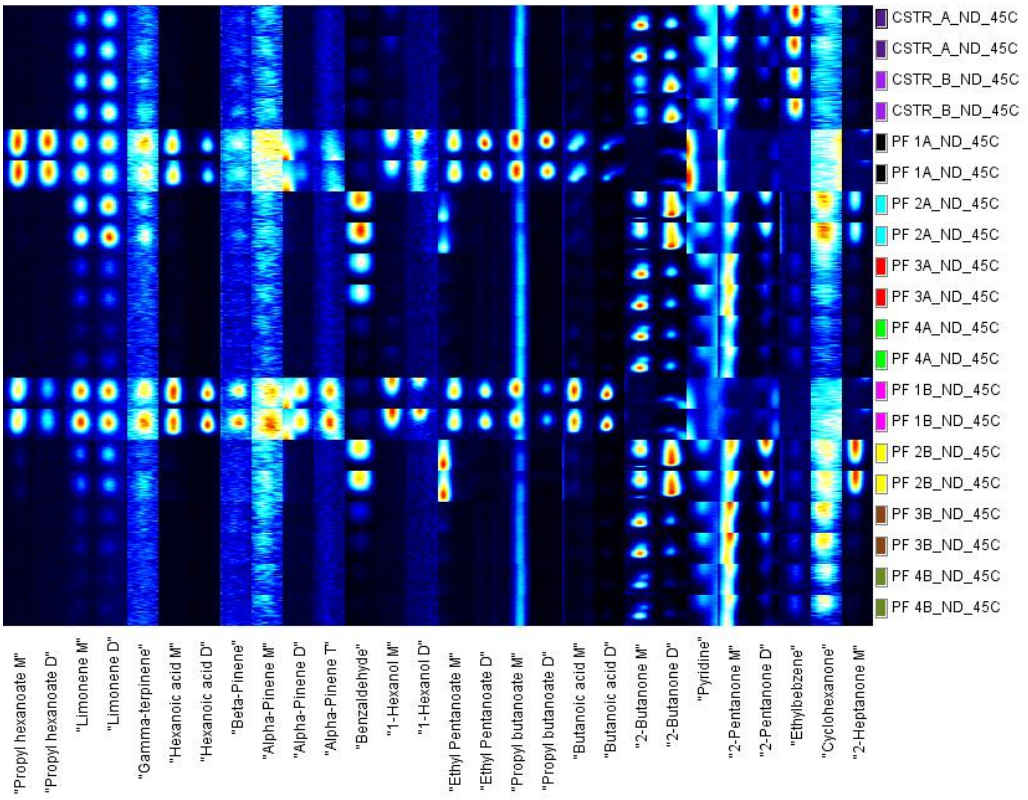

Figure 70: A gallery plot showing the peak selection and respective identification (monomer, dimer, trimer) for all reactors samples (CSTR A, CSTR B, PF A, PF B) for the day 86

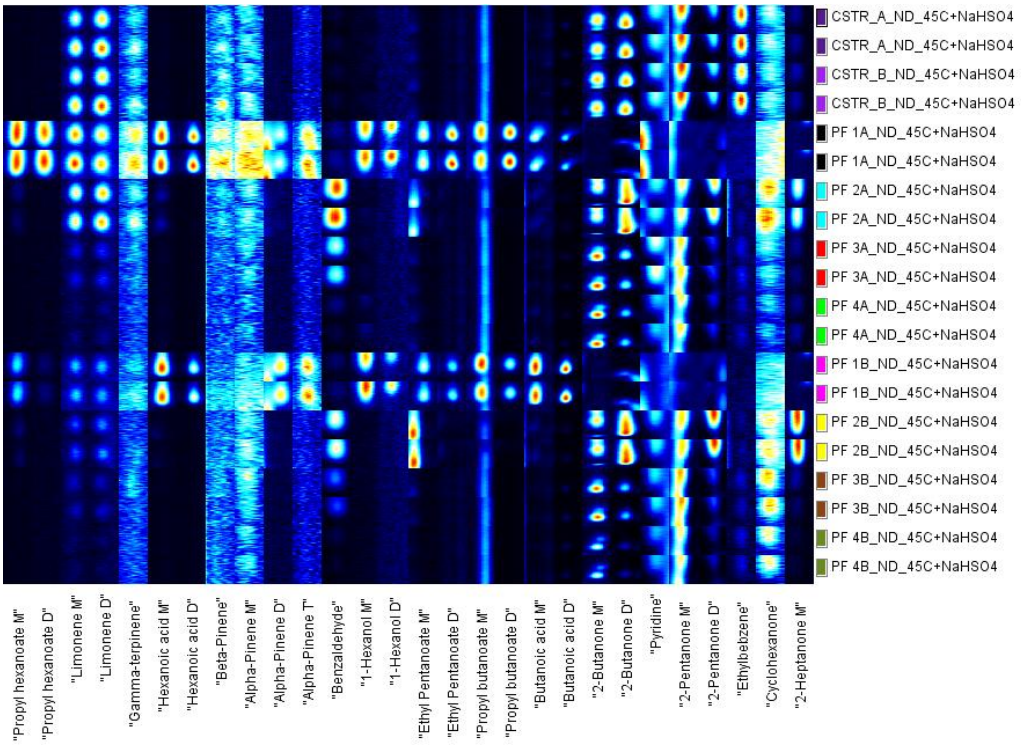

Figure 71: A gallery plot showing the peak selection and respective identification (monomer, dimer, trimer) for all reactors samples (CSTR A, CSTR B, PF A, PF B) for the day 93

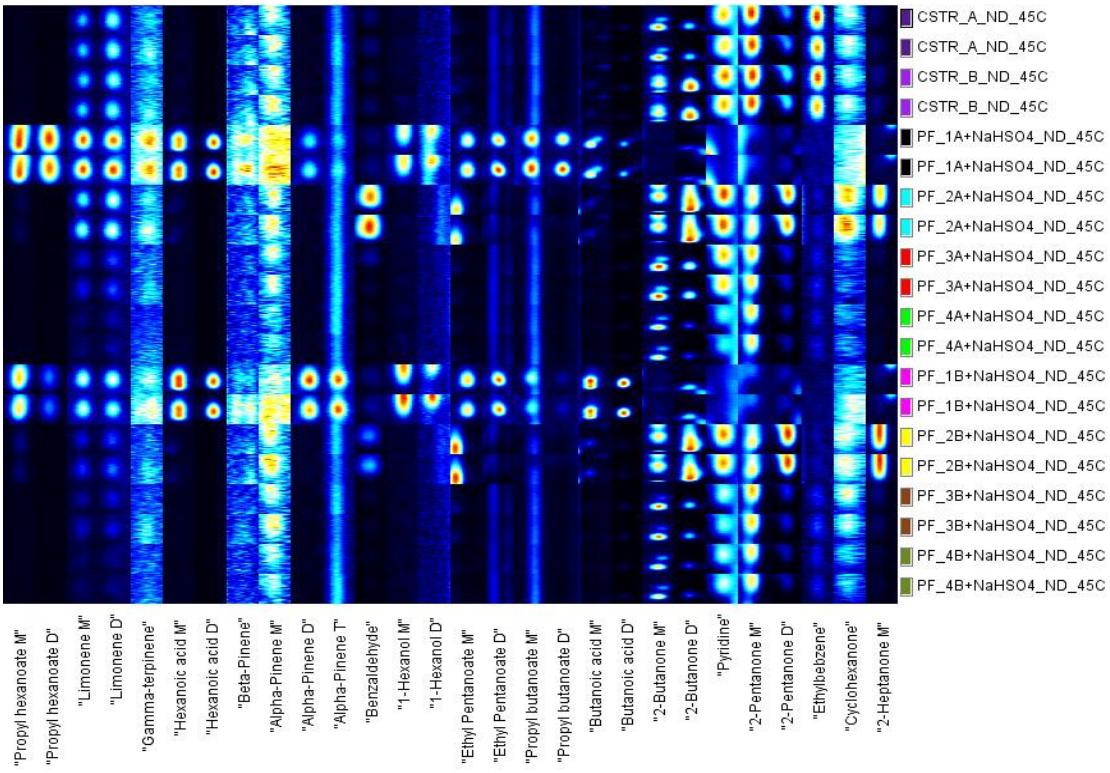

Figure 72: A gallery plot showing the peak selection and respective identification (monomer, dimer, trimer) for all reactors samples (CSTR A, CSTR B, PF A, PF B) for the day 107

APPENDIX 4: CHAPTER 6 GALLERY PLOTS (OPERATIONAL TIMELINE COMPARISON)

Figure 73 to 82 present a comparative study using the gallery plots based on each reactor over time (from day 58 until day 107).

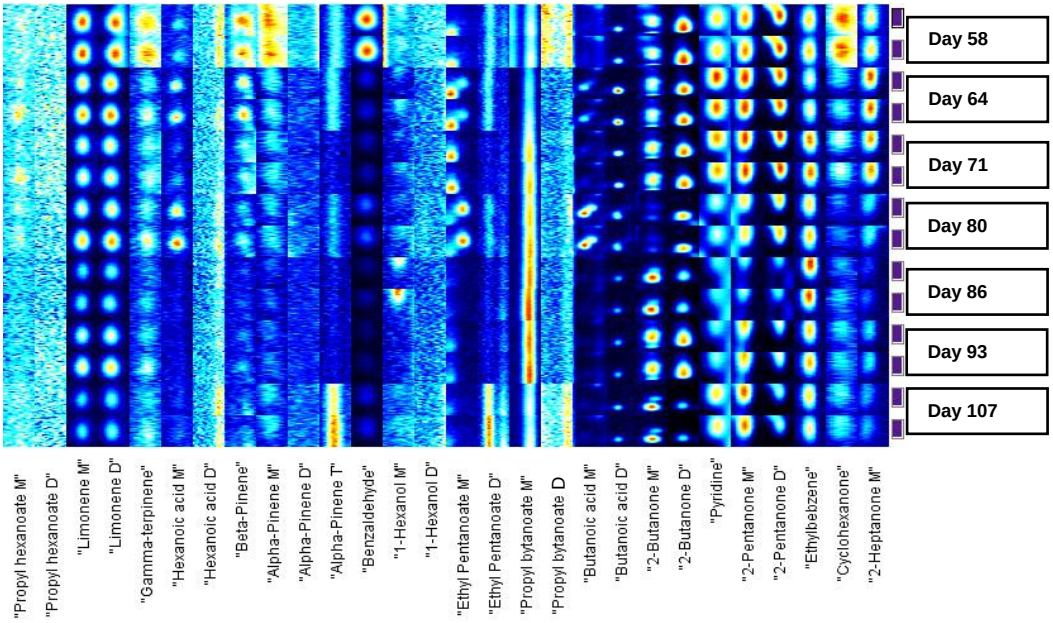

Figure 73: Reactors evolution during day 58 until day 107 for the CSTR A sample

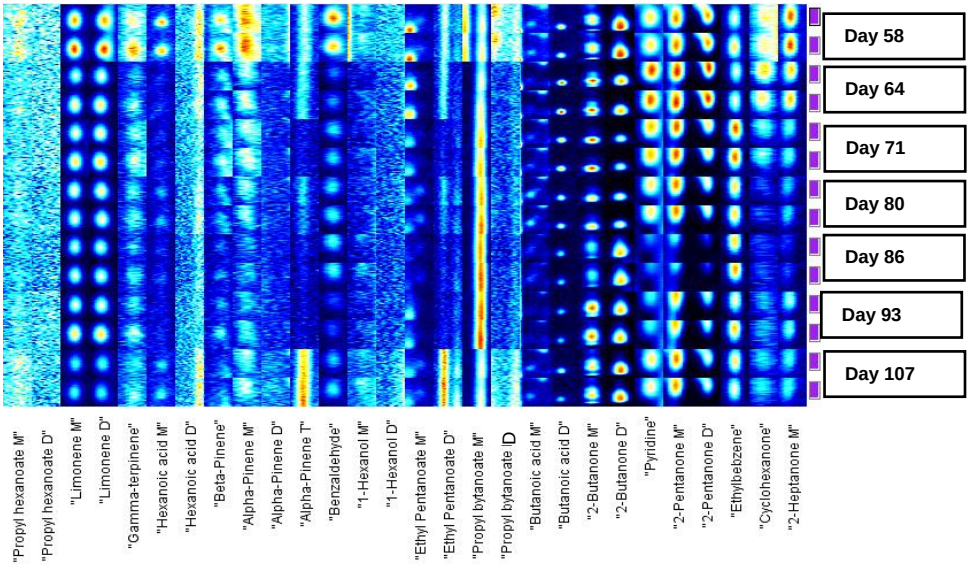

Figure 74: Reactors evolution during day 58 until day 107 for the CSTR B sample

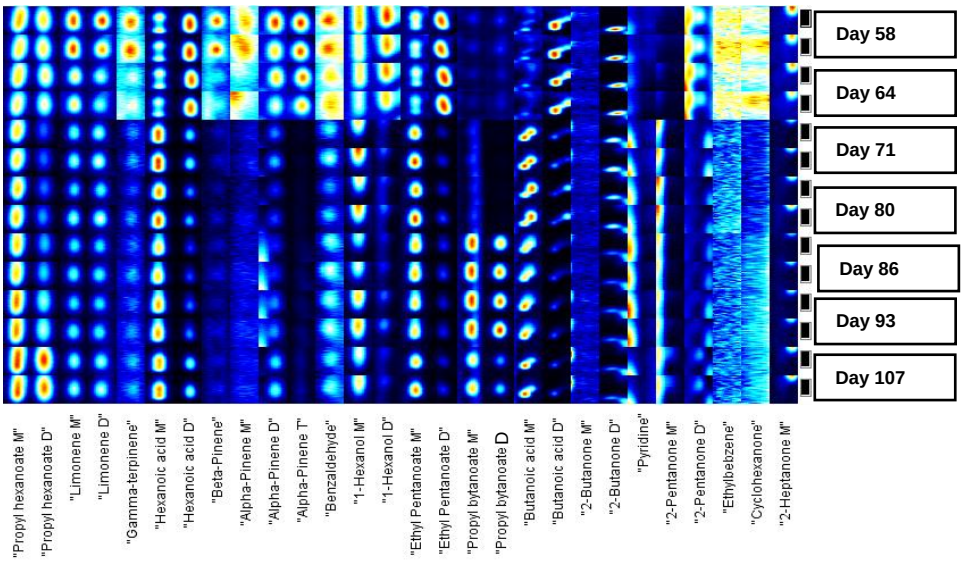

Figure 75: Reactors evolution during day 58 until day 107 for the PF – reactor 1A sample

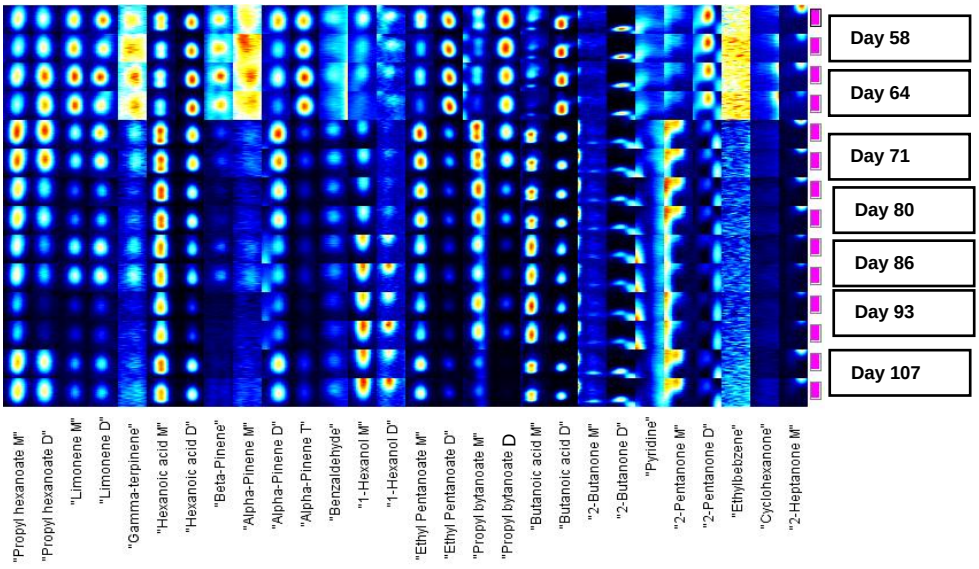

Figure 76: Reactors evolution during day 58 until day 107 for the PF – reactor 1B sample

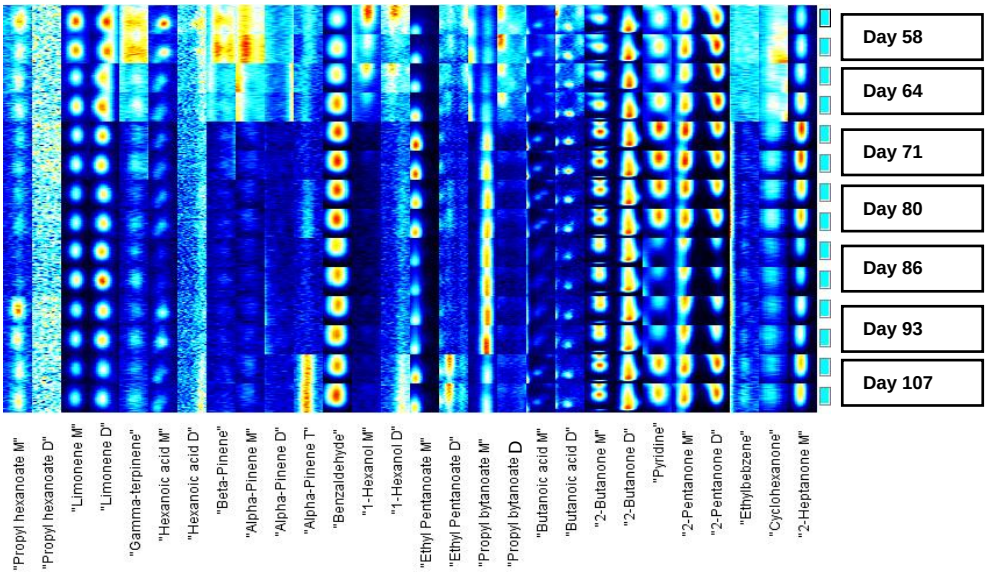

Figure 77: Reactors evolution during day 58 until day 107 for the PF – reactor 2A sample

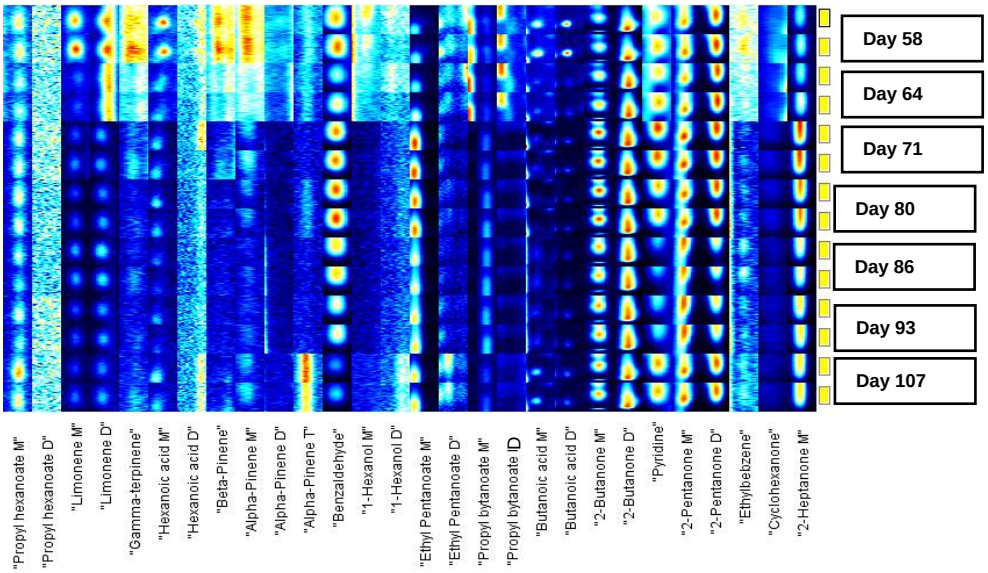

Figure 78: Reactors evolution during day 58 until day 107 for the PF – reactor 2B sample

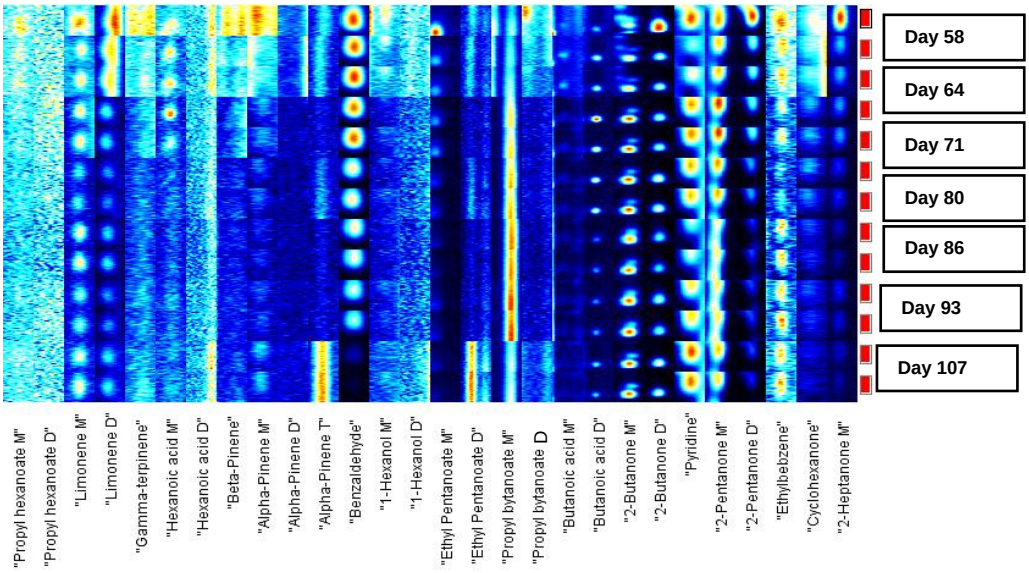

Figure 79: Reactors evolution during day 58 until day 107 for the PF – reactor 3A sample

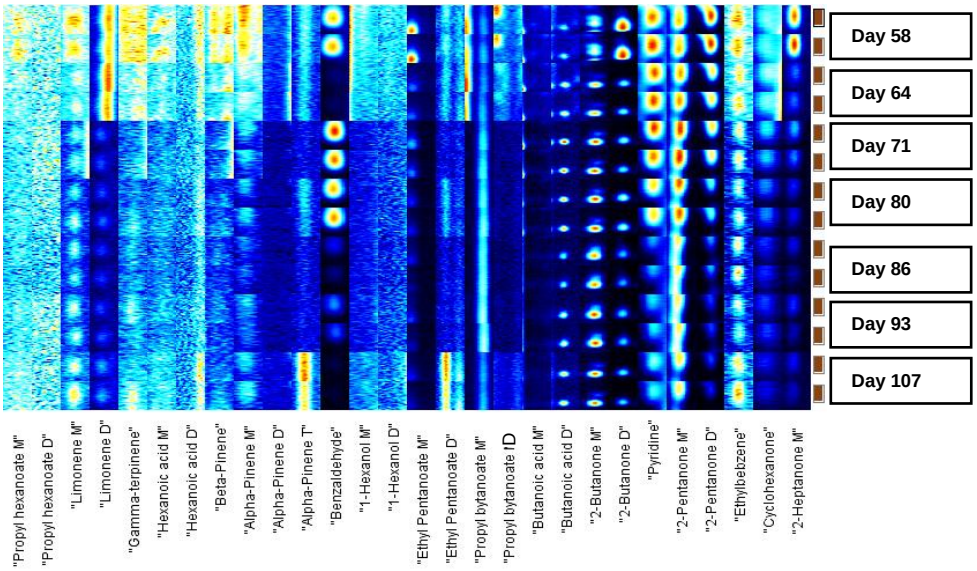

Figure 80: Reactors evolution during day 58 until day 107 for the PF – reactor 3B sample

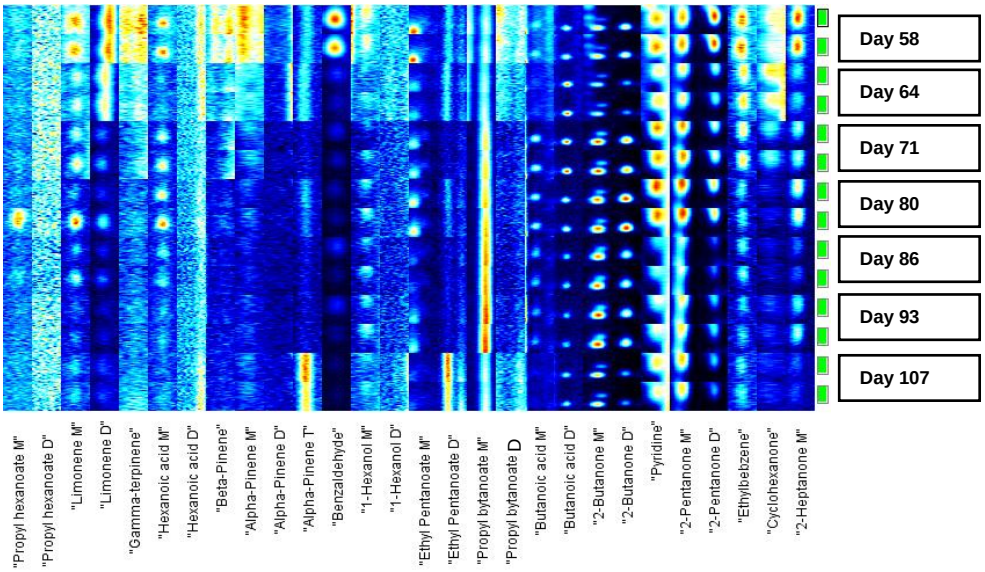

Figure 81: Reactors evolution during day 58 until day 107 for the PF – reactor 4A sample

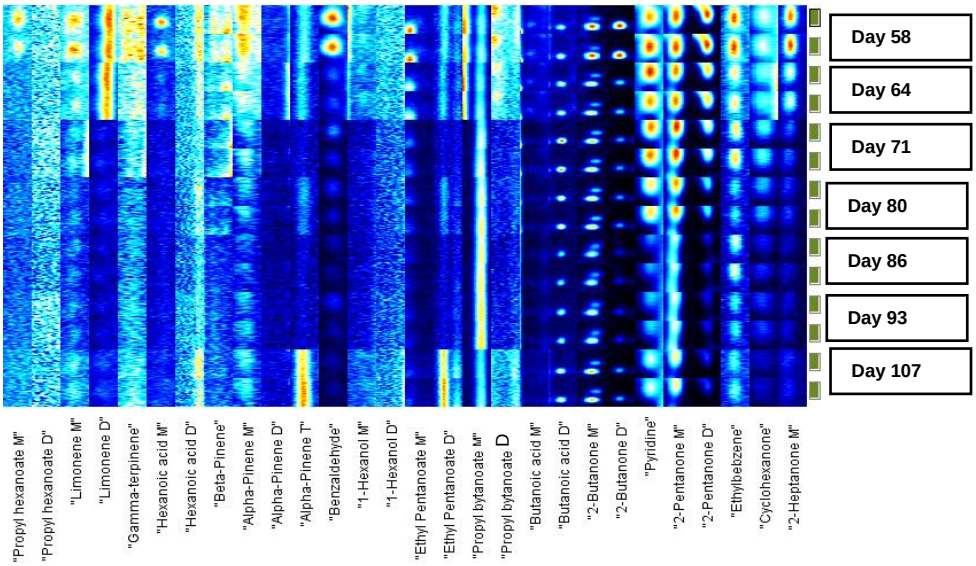

Figure 82: Reactors evolution during day 58 until day 107 for the PF – reactor 4B sample

APPENDIX 5: SUMMARY TABLE FOR GC-IMS METHODOLOGY

Table 40 provides recommendations related to the methodology for the GC-IMS to be applied to AD related samples.

Table 40. Methodology and recommendations for the use of FlavourSpec® in AD applications

Generic recommendations		**Sample treatment**	**Method**
Sample type	Headspace	Setup sample volume (from 100 µL to 1000 µL) Incubation temperatures from ambient temperature to 80 °C (to avoid condensation on the injector port). Incubation temperature and time for each sample/study should be evaluated	Column type should be studied according to target compounds e.g. specific, generic , a polar or non-polar column.
Blanks	The blank is a vial fill with nitrogen gas and placed between samples		
Salt	To acidify the sample it is possible to add a volume of $NaHSO_4$ (62%, w/v), normally 1 mL		

Matrix	**Sample type**	**Pre-treatment**	**Sample preparation**	**Method**
Solid	Headspace between solid and gas phase	If the objective is to remove ammonia interference add an acidifying salt (e.g. $NaHSO_4$) or an acid that would help to decrease the pH	Weigh the sample and introduce it on the vial (vial volume is maximum of 20 mL), typically samples weighed around 1 – 3 g.	Parameters to control during measurement: column temperature; headspace temperature; IMS temperature; flows for carrier and drift gas showed be
Liquid	Headspace between liquid and gas phase		Weigh or pipette the sample. Dilute between 50 to 10 times with deionised water or another adequate solvent. Start the analysis with the more diluted sample and build up to the more concentrate sample	

Gas	Gas headspace	Diluted with nitrogen if sample is too concentrated. Sample could be collected in a sampling bag or with a syringe	Sample collected with a syringe and injected into inject port or fill a vial with gas of interest	studied for each study / project

Method for generic VOCs detection (setup for autosampler, GC-IMS, and flows for drift and carrier gas)

Column	Sample type	Sample Volume [µL]	T Incubation [°C]	Incubation Time [min]	T Syringe [°C]	GC-Runtime [min]
SE-54-CB1	Headspace	100 µL	45 °C	9 min	80 °C	10 min 30 sec

T1 IMS [°C]	T 2 Column [°C]	T 3 Injection Port [°C]	RIP Voltage	Av	Trigger-D [µs]	Measurement Runtime [min]
45 °C	40 °C	80 °C	+	6	100	10 min

Time	EPC1 [mL/min]	EPC2 [mL/min]	Recording
00:00.000	150	5	Starting recording
02:00.000	150	5	|
10:00.000	150	50	|
10:00.020	150	50	Stop recording

Method for measuring VFAs detection (setup for autosampler, GC-IMS, and flows for drift and carrier gas)

Column	Sample type	Sample Volume [µL]	T Incubation [°C]	Incubation Time [min]	T Syringe [°C]	GC-Runtime [min]
SE-54	Headspace	500 µL	60 °C	20 min	80 °C	20 min 30 sec

T1 IMS [°C]	T 2 Column [°C]	T 3 Injection Port [°C]	Measurement Runtime [min]
45 °C	40 °C	80 °C	20 min

Time	EPC1 [mL/min]	EPC2 [mL/min]	Recording
00:00.000	150	2	Starting recording
5:00.000	150	2	Recording
15:00.000	150	50	Recording
20:00.000	150	50	Recording
20:00.020	150	50	Recording
20:00.040	150	50	Stop recording